Transition-Metal-Catalyzed C−C and C−Heteroatom Bonds Formation: Stereoselective Access to Functionalized Heterocycles

A Thesis Submitted

in Partial Fulfilment of the Requirements

for the Degree of

DOCTOR OF PHILOSOPHY

by

Prabhat Kumar Maharana

Roll No. 196122020

Department of Chemistry
Indian Institute of Technology Guwahati
Guwahati 781039
March 2025

Dedicated To

My Family

INDIAN INSTITUTE OF TECHNOLOGY GUWAHATI

Department of Chemistry

STATEMENT

I hereby declare that the matter embodied in this thesis is the result of investigations carried out by me in the Department of Chemistry, Indian Institute of Technology Guwahati, Guwahati, India under the supervision of Prof. Tharmalingam Punniyamurthy.

In keeping with the general practice of reporting scientific observations, due acknowledgement has been made wherever the work described is based on the findings of other investigators.

Guwahati
March 2025

Prabhat Kumar Maharana

INDIAN INSTITUTE OF TECHNOLOGY GUWAHATI

Department of Chemistry

CERTIFICATE

This is to certify that Mr. Prabhat Kumar Maharana has been working under my supervision since July 2019. I am forwarding his thesis entitled "*Transition-Metal-Catalyzed C−C and C−Heteroatom Bonds Formation: Stereoselective Access to Functionalized Heterocycles*" being submitted for the Ph.D. degree of this institute. I certify that he has fulfilled all the requirements according to the rules of this institute, and regarding the investigations embodied in his thesis and this work has not been submitted elsewhere for a degree.

Guwahati
March 2025

Prof. Tharmalingam Punniyamurthy
Supervisor

ACKNOWLEDGEMENT

I am bereft of words to thank my mentor and supervisor, **Prof. Tharmalingam Punniyamurthy** for introducing me to the fascinating world of synthetic chemistry and affording me the privilege and freedom to execute this research work. I truly owe him a great debt for his devotion to chemistry, valuable guidance, unwavering motivation, constant support and inspiration. Thank you, Sir! for always challenging and assisting me to accomplish this goal. I will be forever grateful of the invaluable opportunities you have provided me and the doors you have opened for me. Besides my supervisor, I would like to acknowledge my doctoral committee members, **Prof. G. Krishnamoorthy, Prof. A. S. Achalkumar**, Department of Chemistry, **Prof. Vishal Trivedi**, Department of Biosciences and Bioengineering and **Prof. Vijay S. Moholkar,** Department of Chemical Engineering for their valuable suggestions and comments during all assessments in the entire period of my doctoral thesis.

I am delighted to convey my heartfelt gratitude to my dear labmates Dr. Vijay Murugan, Dr. Sourav Pradhan, Dr. Pinaki Bhusan De, Dr. Tanumay Sarkar, Dr. Bijay Ketan Das, Dr. Manmath Mishra, Dr. Sonbidya Banerjee, Dr. Pallab Karjee, Dr. Kangkan Talukdar, Dr. Subhasish Roy, Dr. Sandeep Kumar, Dr. S. Vivek Kumar, Dr. Tariq. A. Shah, Dr. Dinesh Kumar Nayak, Dr. R. Arunachalam, Dr. Muthuraja Perumal, Dr. V. Tamilthendral, Mr. Shubhajit Basak, Mr. Bijoy Debnath, Ms. Subhradeep Kar, Ms. Tripti Paul, Mr. Santu Mandal, Mr. Hemanga Bhattacharyya, Mr. Kshitiz Verma, Mr. Sharajit Saha, Mr. Maniya Vadakanamala Nanjegowda, Ms. Swati Samantaray, Mr. Madhab Barman, Ms. Anita Sahoo, Mr. Sajal Roy, Ms. Priya Patra, Ms. Ravina Yadav, Mr. Vishwanath Kumar, Mr. Utsab Das, Ms. Nirali Namdev, Mr. Oishik Sarkar, Ms. Sonali Dabas, Mr. Subhankar Dolai, Ms. Swagata Maity and Mr. Nicky jones Lyngdoh Marshillong for their moral support and valuable encouragement whenever I approached them and for friendly relationship.

I wish to express my sincerest appreciation to all the faculty members, Department of Chemistry, staff of Central Instruments Facility and the non-teaching staff of Department of Chemistry for their valuable support during my Ph.D. tenure.

It gives me immense pleasure to gratefully acknowledge DST for INSPIRE Research Fellowship. I also would like to thank Department of Chemistry, Central Instrument Facility (CIF), IIT Guwahati, North East Centre for Biological Sciences and Healthcare Engineering (NECBH) for providing the instrument facility and DST for providing the X-ray facility.

It gives me enormous pleasure to convey my courteous gesture to my Ph.D. batch mates (July, 2019), research scholars in the chemistry department and B.Sc., M.Sc. friends for their support and cherished moments spent with them.

I always cherish my friendship with Ms. Subhradeep Kar, Mr. Debasish Satapathy, Mr. Sujit Kumar Gouda, Mr. Abinash Sahu, Mr. Ruturaj Mahapatro and Mr. Akshay Kumar Sahu, for their help in my tough times.

To my respected teachers: Amulya Achary sir, Prof. Panchanana Gouda, Late Prof. Ilarani Pattnaik, Prof. Laxmidhar Rout for their significant contribution in shaping me as a student and chemist. I owe a lot to you all!

Finally, I wholeheartedly express my deepest regards to my beloved parents (**Mrs. Kuni Maharana** & **Mr. Kalu Charan Maharana**), brother (**Mr. Sagar Maharana**), sister-in-law (**Mrs. Nibedita Maharana**) and Nephew (**Master Vaibhav Maharana**) for their tireless patience, limitless sacrifices, sincere encouragement and inspiration. Thank you for believing in my vision and providing me the wings of freedom and opportunity to chase my dreams. It was incredibly very tedious without your blessings and moral support. I owe a lot to your love, affection, care and blessings.

Last but not the least my words are insufficient to thank the almighty God (Lord Jagannath) and I surrender myself to Him, for showering His blessings upon me for making me able to sew up this thesis work.

May God bless you all!

Prabhat Kumar Maharana

List of Abbreviations

Ar	aryl
Ac	acetyl
Å	angstrom (10^{-8} cm)
APIs	Active pharmaceutical ingredients
BHT	butylated hydroxytoluene
Bn	benzyl
Boc	*tert*-butoxycarbonyl
Cbz	benzyloxycarbonyl
Cp*	1,2,3,4,5-pentamethylcyclopentadiene
CCDC	Cambridge crystallographic data center
p-cymene	4-isopropyltoluene
DG	directing group
DMSO	dimethylsulfoxide
DME	Dimethoxyethane
DMF	N,N-Dimethylmethanamide
dppf	1,1'-bis(diphenylphosphino)ferrocene
DIPEA	N,N-diisopropylethylamine
EDG	electron donating group
equiv	equivalent
ee	enantiomeric excess
Et	ethyl
ESI	electrospray ionization
EWG	electron wthdrawing group
FT-IR	Fourier transform infrared spectroscopy
FG	functional group
HFIP	hexafluoroisopropanol
Het	heterocyclic
HMPA	hexamethylphosphoramide
HRMS	high-resolution mass spectrometry
HPLC	high-performance liquid chromatography
Hz	hertz

^{i}Pr	isopropyl
m/z	mass to charge ratio
mp	melting point
MS	molecular sieves
MHz	megahertz
Mes	mesityl
nm	nanometer
NMR	nuclear magnetic resonance
Ns	nosyl
NHC	N-Heterocyclic carbene
^{n}Pr	propyl
^{n}Bu	butyl
Me	methyl
ORTEP	oak ridge thermal ellipsoid plot
R_f	retardation factor
rt	room temperature
pym	pyrimidyl
PTSA	p-toluenesulfonic acid
PIDA	Phenyliodine(III) diacetate
PG	protecting group
TFE	2,2,2-trifluoroethanol
TBS	*tert*-butyldimethylsilyl
TFA	trifluoroacetic acid
TMEDA	tetramethylethylenediamine
TEMPO	2,2,6,6-tetramethylpiperidin-1-oxyl
THF	tetrahydrofuran
TLC	thin layer chromatography
TM	transition metal
Ts	tosyl
^{t}Bu	tert-butyl
μL	Microliter

Abstract

The thesis is divided into four chapters. The first chapter describes a general introduction on the synthesis of heterocycles utilizing transition-metal (TM) catalyzed ring opening cyclization of strained three-membered rings and cascade C−H functionalization/annulation strategy. The second chapter illustrates on a highly stereospecific synthesis of tetrahydro-[1,3,4]-oxadiazines *via* a Co-catalyzed C−N and C−O bonds formations of oxiranes with diaziridines. The third chapter focuses on a regiodivergent Cu-catalyzed cross-dimerization of oxaziridines with aziridines to synthesize functionally diverse [1,2,4]/[1,2,5]-oxadiazines. The fourth chapter deals with a Rh-catalyzed cascade C−H functionalization/annulation of benzamides with maleimides to furnish succinimide tethered isoquinoline-1,3-diones.

Chapter I. Strained Rings and Cascade C−H Functionalization/Annulation Strategy for Heterocycle Synthesis

Heterocyclic motifs constitute the key structural skeleton of a plethora of bioactive natural products, pharmaceuticals and functional materials. In this direction, cycloaddition/annulation reactions of strained three-membered rings have exemplified the disconnection approach towards synthesis of complex molecular frameworks. Similarly, transition-metal-catalyzed auxiliary assisted cascade C−H functionalization/annulation transformations have gained the significant momentum due to their ability to generate functionalized heterocycles. Utilizing simple substrates, these step/atom-economic strategies offer a high degree of regio/stereo controls. This chapter covers the strategies based on transition-metal catalyzed cycloaddition involving strained three-membered rings and cascade C−H functionalization/annulation methods in synthesizing functionalized heterocycles (Scheme 1).

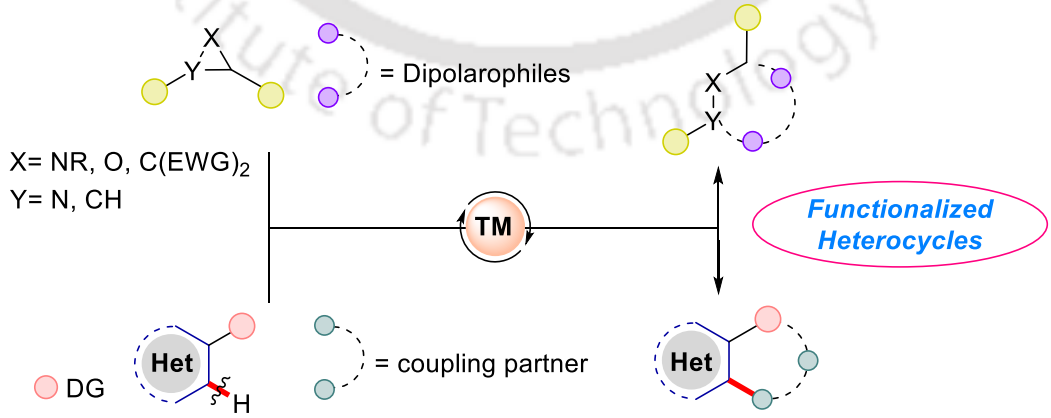

Scheme 1. TM-Catalyzed Strategies for Heterocycle Synthesis

Chapter II. Co-Catalyzed C−N/C−O Bonds Formation of Oxiranes with Diaziridines

[1,3,4]-oxadiazine frameworks play a crucial role as structural subunits in the pharmaceuticals. Despite the advances made, it is worthwhile to devise possible retrosynthetic pathways to synthesize them with an enhanced efficiency and flexibility. In this line, strained bicyclic diaziridines are known for their unique reactivity to generate azomethine imine ylide using Lewis acids which undergo further (3+n)-cycloaddition to generate nitrogen rich heterocycles. Similarly, oxiranes are staple three-atom building blocks and are frequently encountered in several ring opening and cycloaddition reactions. In this regard, selective activation of these two saturated strained rings under Lewis acid catalysis for synthesis of [1,3,4]-oxadiazines is fascinating from step/atom-economic stand point. Herein, we established a stereospecific synthesis of functionalized [1,3,4]-oxadiazines *via* C−N and C−O bonds formation of oxiranes with diaziridines utilizing Co-catalysis (Scheme 2).

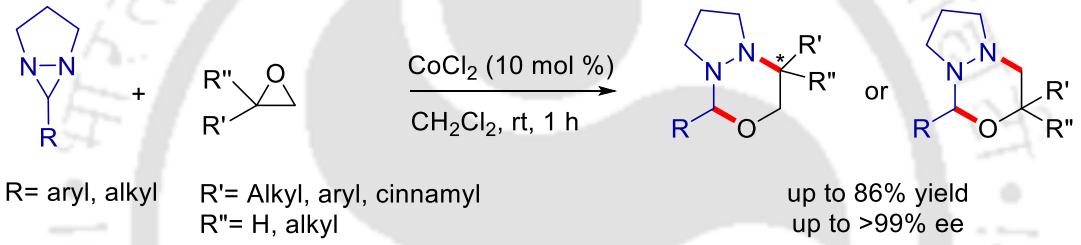

J. Org. Chem. **2023**, *88*, 9447.

Scheme 2. Synthesis of [1,3,4]-Oxadiazines using Diaziridines and Oxiranes

Chapter III. Cu-Catalyzed Cross-Dimerization of Oxaziridines with Aziridines

Saturated heterocyclic structures, owing to their superior conformational flexibility, offer enhanced physicochemical profiles. In this array, [1,2,4]- and [1,2,5]-oxadiazines, as privileged heterocyclic scaffolds have found manifold utilities in pharmaceuticals. Considering their practicality, development of efficient synthetic strategies utilizing saturated strained three-membered rings is highly sought after. In this context, strain release driven cross-dimerization reaction involving oxaziridines and aziridines can deliver an attractive tool to synthesize oxadiazines. This chapter focuses on a Cu-catalyzed cycloaddition of oxaziridines with aziridines to access [1,2,4]/[1,2,5]-oxadiazines (Scheme 3). This substituent controlled regiodivergent transformation is step/atom-economic, broad substrate scope with functional group tolerance and post-synthetic transformations are important practical features.

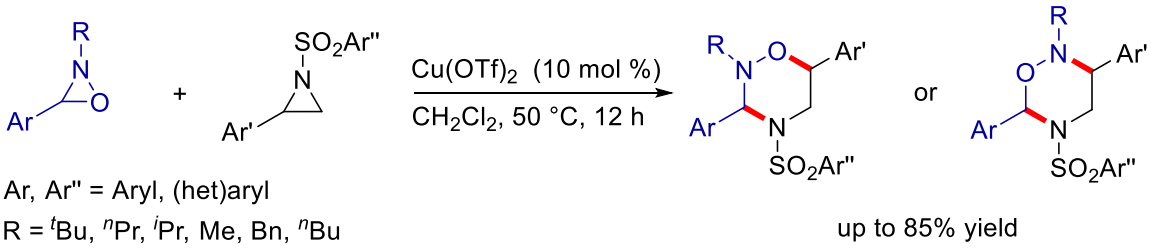

Scheme 3. Divergent Access to [1,2,4]/[1,2,5]-Oxadiazines

Chapter IV. Rh-Catalyzed C−H Functionalization/Annulation of Arylamides with Maleimides

Isoquinoline-1,3-diones stand out as pervasive structural motifs owing to their significant bio-activity and multifarious utility in medicinal science. The development of efficient strategies for their synthesis utilizing simple starting precursors is thus highly noteworthy. In this regard, transition-metal-catalyzed DG-assisted cascade C−H functionalization/annulation reactions have strengthened chemists tool box in the ability to synthesize cyclic scaffolds. Further, arylamides, being ubiquitous and inexpensive, are synthetically appealing precursors for generating *N*-heterocycles. Besides, the utilization of maleimides as a staple coupling partner for installing succinimides is highly appealing. The present chapter describes a cascade C−H functionalization/annulation to afford succinimide tethered isoquinoline-1,3-diones using arylamides and maleimides as the coupling partner (Scheme 4).

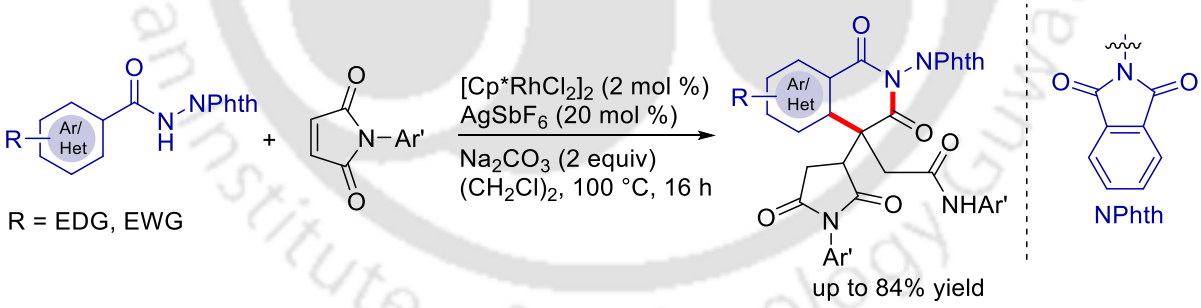

Chem. Commun. **2025**. https://doi.org/10.1039/D5CC02963E.

Scheme 4. Cascade C−H Functionalization/Annulation to Access Isoquinoline-1,3-diones

Contents

Chapter I

Strained Rings and Cascade C–H Functionalization/Annulation Strategy for Heterocycles Synthesis

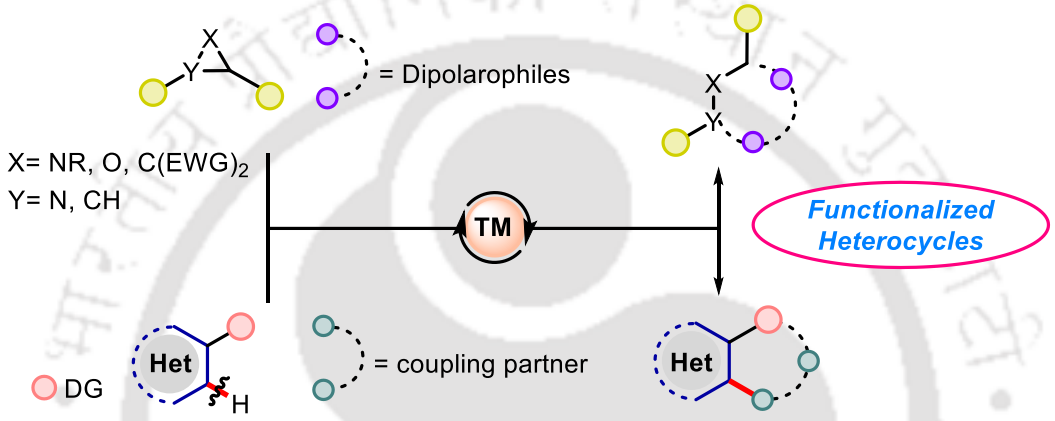

Strained Rings and Cascade C–H Functionalization/Annulation Strategy for Heterocycles Synthesis

Heterocyclic structures are integral core structural scaffolds in a wide range of pharmaceuticals and natural products (Figure 1).[1] In this regard, inception of saturated heterocycles of three-dimensional (3D) character have widened skeletal diversity in the design and synthesis of active pharmaceutical ingredients (APIs), which are increasingly important in medicinal science.[2] Further, increasing saturation in heterocycles enhances the structural diversity, resulting in improved physicochemical profiles and better receptor/ligand complimentarity.[3] Expediently, incorporating multiple heteroatoms into the saturated heterocycles intuitively improve their ability to interact with multiple targets inside the biological system, making them valuable in target-oriented drug design.[4] Similarly, fused heterocycles owing to their unique structural aspects, exhibit significant potencies in agrochemicals, biochemistry and materials. Additionally, these scaffolds are used as vital intermediates, ligands and catalysts in synthetic organic chemistry.[5]

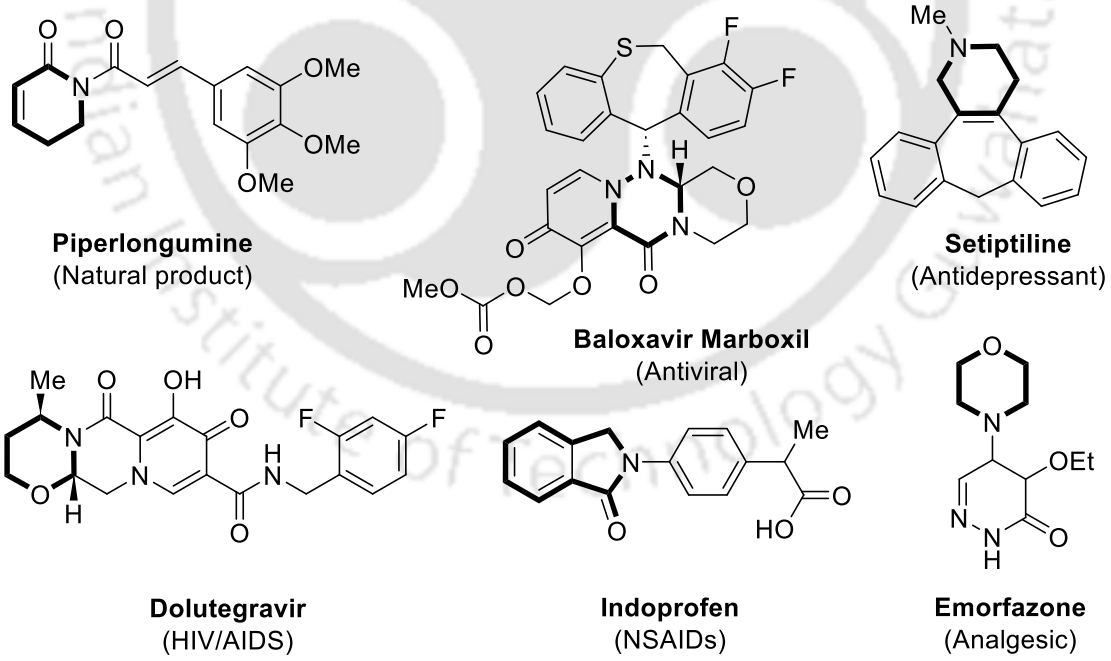

Figure 1. Representative Examples of Bioactive Heterocycles.

In view of the profound relevance, development of sustainable synthetic strategies for the rapid construction of heterocycles utilizing simple precursors with step/atom-economy is desirable. In this context, emergence of strained three-membered carbo-/heterocycles as staple

coupling partners has bolstered the synthetic feedstock to generate functionalized heterocycles *via* ring opening cyclization or cycloaddition process. This strategy can be realized by suitably coupling various dipolarophiles with strained three-membered rings *via* Lewis acid catalyzed (3+n)-cycloaddition reactions.[6] Additionally, potential lengthy pre-functionalization can be averted by the introduction of transition-metal-catalyzed DG-assisted cascade C−H functionalization/annulation strategy for efficient assembly of fused heterocycles.[7] In this section, the methods for the transition metal catalyzed cycloaddition reactions using strained three-membered rings and C−H activation-initiated cascade transformation for synthesizing heterocyclic architectures are presented.

1.1 State-of-the Art for Synthesis of Heterocycles using Strained Rings

Transition-metal-catalyzed strain-driven ring opening functionalization of three-membered rings offers an alluring alternative to conventional synthetic strategies. Intrinsic reactivity associated with these rings positions them as a versatile three-atom synthons to synthesize heterocycles following ring expansion strategy. Although, kinetically inert, vicinal installation of donor/acceptor substituents makes them undergo ring cleavage under Lewis acid catalysis to yield 1,3-dipolar synthons. Later, trapping of these reactive zwitterionic species by appropriate dipolarophiles leads to the *de novo* synthesis of complex heterocycles (Scheme 1).[6]

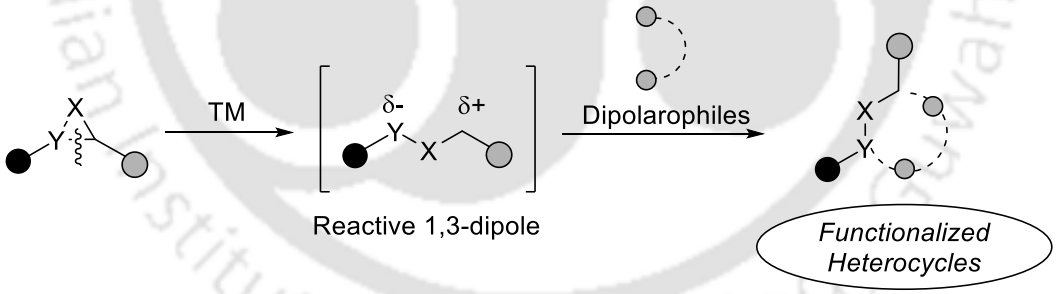

Scheme 1. Strategies for Ring Opening/Cyclization or Cycloaddition of Strained Rings

1.1.1 Using Donor-Acceptor Cyclopropanes

In recent times, donor-acceptor cyclopropanes have attracted a lot of research interest from synthetic community owing to their ability to undergo ring opening/cyclization or cycloaddition with heteroatom containing dipolarophiles to afford heterocyclic scaffolds. The presence of vicinal donor-acceptor entities leads them to undergo reaction even under mild conditions, thus making them indispensable building blocks in sustainable molecular synthesis.

Kerr and co-workers presented a homo (3+2)-cycloaddition of nitrones with donor-acceptor cyclopropanes using $Yb(OTf)_3$ as the Lewis acid to afford diverse oxazine scaffolds in good to excellent yields (Scheme 2).[8] A practical utility of this methodology was exhibited in the preparation of FR-900482 skeleton.

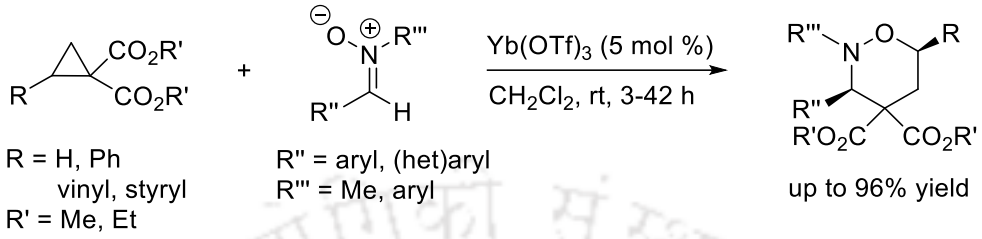

Scheme 2. Yb-Catalyzed Tetrahydro-1,2-oxazine Synthesis

Charette group reported a Lewis acid catalyzed cycloaddition of aromatic azomethine ylides with donor-acceptor cyclopropanes (Scheme 3).[9] This diastereoselective protocol was tolerated to quinolinium ylides and cyclopropane diesters giving access tricyclic dihydroquinoline derivatives in moderate to good yields.

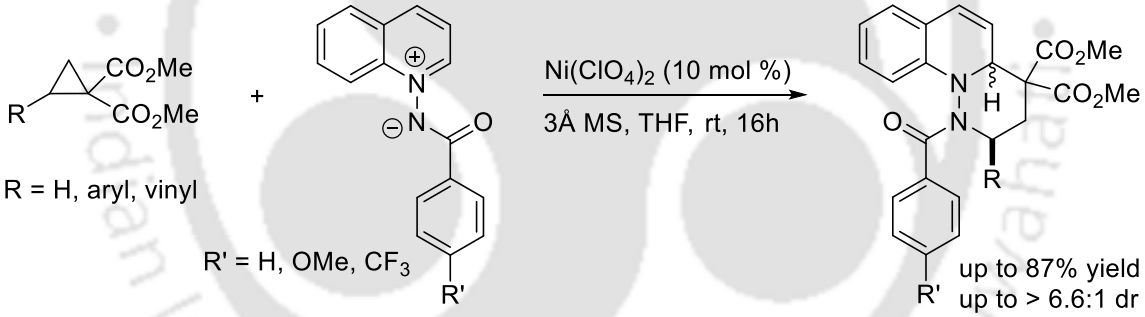

Scheme 3. Ni-Catalyzed Dihydro-quinoline Synthesis

A $TiCl_4$-promoted (3+3)-cycloaddition of donor-acceptor cyclopropanes with diverse azides has been reported to achieve diversely functionalized triazines in moderate to good yields (Scheme 4).[10] The products could be further transformed into biologically significant azetidines by subsequent thermolysis.

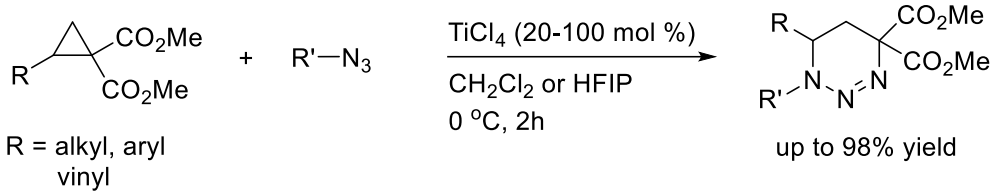

Scheme 4. Ti-Catalyzed Triazines Synthesis

Werz group reported a synergestic dirhodium(II)-Lewis acid catalyzed (3+3)-annulation of carbonyl ylides with donor-acceptor cyclopropanes to achieve pyran scaffolds in good yields and diastereoselectivity (Scheme 5).[11] Enantioenriched cyclopropanes afforded the respective inversion products in high enantiomeric excess. A strong solvent effect was observed to affect the stereochemical outcome, suggesting the involvement of different reactive species in the mechanistic cycle.

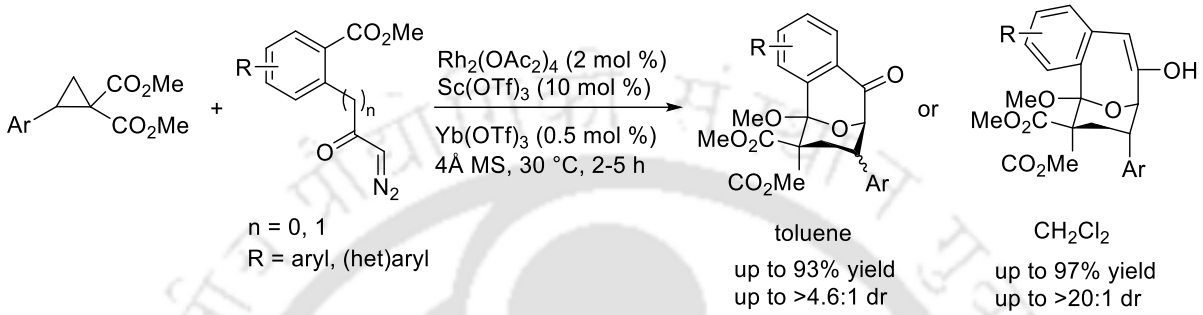

Scheme 5. Rh-Sc-Synergistic Catalysis for Pyran Synthesis

1.1.2 Using Aziridines

Being the smallest aza-heterocycles, aziridines have proven as versatile three-atom synthons for obtaining larger N-heterocycles through tandem cyclization or cycloaddition process. In presence of Lewis acids, the innate ring strain associated with them makes them susceptible to act as masked 1,3-dipolar components *via* preferential C−N/C−C bond cleavage thereby making them valuable reactants in accessing N-heterocycles.

Contextually, Zhang group described a robust $Y(OTf)_3$-catalyzed C−C bond cleavage of donor-acceptor aziridines and their (3+2)-dipolar cycloaddition with electron-rich olefins *via* an azomethine ylide to afford substituted pyrrolidines in high regio- and diastereoselectivity (Scheme 6).[12]

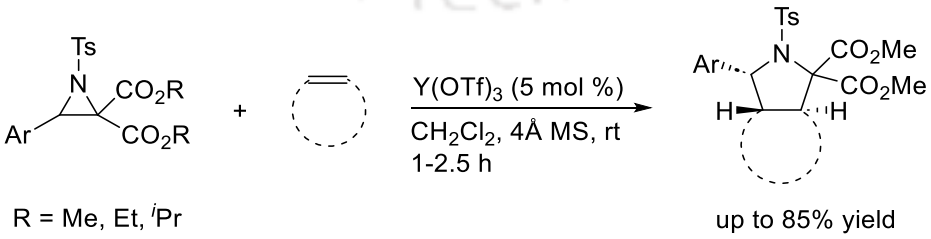

Scheme 6. Y-Catalyzed Pyrrolidine Synthesis

Xu group described a gold and ytterbium relay catalysis for the respective cycloisomerization and diastereoselective (3+2)-cycloaddition of alkynyl alcohols and amides with aziridines under mild reaction conditions to generate diverse nitrogen-embedded spiro heterocycles from readily accessible starting materials (Scheme 7).[13]

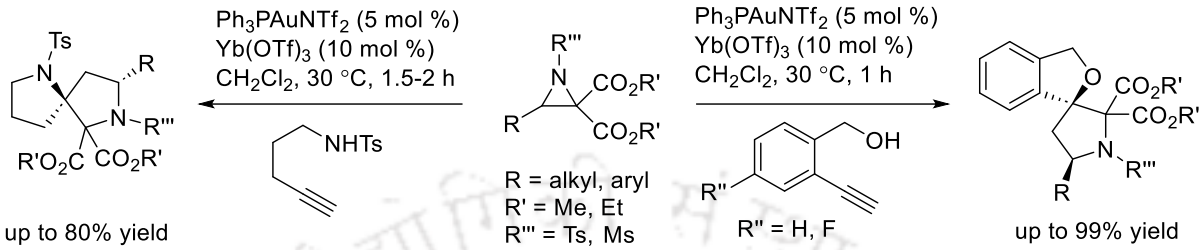

Scheme 7. Au-Yb-Catalyzed Diverse Spiro-N-heterocycles Synthesis

Zhao and co-workers reported a formal cross-dimerization of sulfonylated aziridines and cyclopropenones to afford synthetically valuable dihydropyridinones using Pd-Lewis acid cooperative catalysis (Scheme 8).[14] Gratifyingly, enantiopure aziridines reacted efficiently to afford the optically pure ring-expansion products in >99% ee.

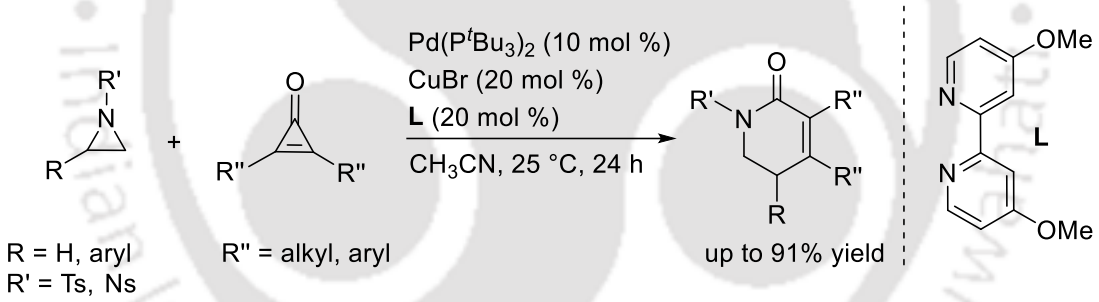

Scheme 8. Pd-Cu-Cooperative Catalysis for Dihydropyridinone Synthesis

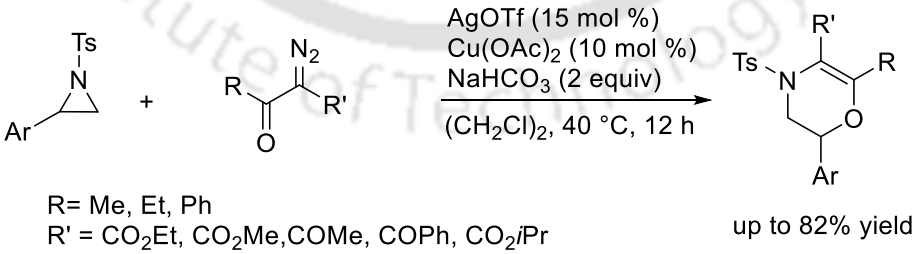

Scheme 9. Ag-Cu-Catalyzed Oxazine Synthesis

An efficient strategy has been developed for the (3+3)-cycloaddition of α-diazocarbonyls and *N*-tosylaziridines generating polysubstituted oxazines through synergetic AgOTf/$Cu(OAc)_2$

catalysis (Scheme 9).[15] A series of both electronically as well as sterically diverse substituents were well tolerated under the protocol.

1.1.3 Using Oxiranes

Oxiranes are versatile synthons for accessing oxygen containing heterocycles. The innate ring strain embodied within its structure makes them prone to undergo stereoselective ring cleavage in presence of carbo/heteroatom dipolarophiles to furnish functionalized heterocycles.

A transannulation strategy towards the synthesis functionalized dihydro-2*H*-1,4-oxazines was developed by Chen and co-workers under Rh-catalysis (Scheme 10).[16] A diverse set of *N*-sulfonyl-1,2,3-triazoles and substituted styrene oxides were coupled to afford functionalized oxazines in moderate yields. The reaction proceeds *via* α-imino rhodium(II)carbene species followed by oxirane ring opening/cyclization sequence.

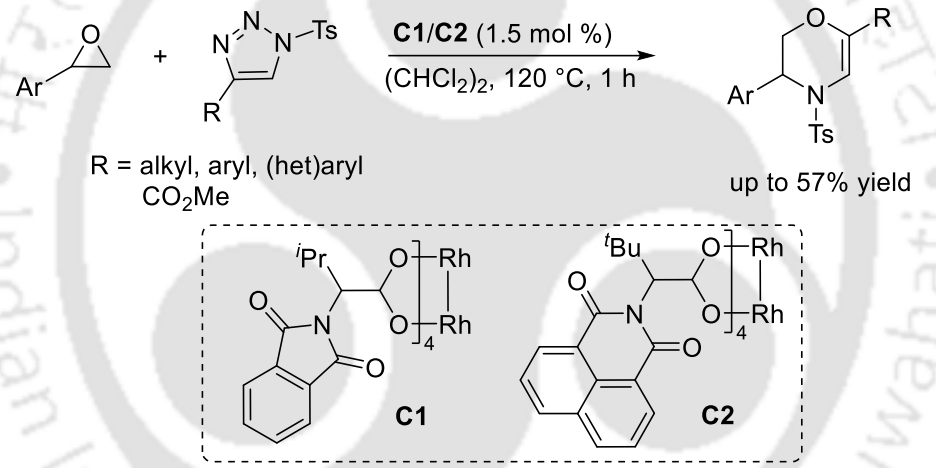

Scheme 10. Rh-Catalyzed Transannulation

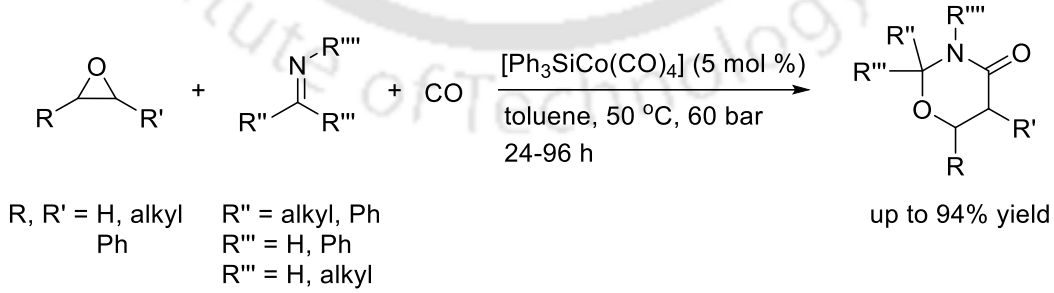

Scheme 11. Co-Catalyzed Multi-Component (3+2+1)-Cycloaddition

Co-catalyzed multi-component (3+2+1)-cycloaddition strategy involving readily available oxiranes, CO gas and imines was disclosed for assembly of 1,3-oxazinan-4-ones in high yields

(Scheme 11).[17] Tolerance to a broad range of imines and oxiranes under mild conditions with high atom economy showcases the practicality of the protocol.

Guo reported a highly diastereoselective dearomative (3+2)-cycloaddition of donor-acceptor oxiranes with benzazoles. This methodology starts with a Sc-catalysed chemoselective C−C bond cleavage of oxiranes to give benzazolo [3,2-c] oxazoles in good yields (Scheme 12).[18]

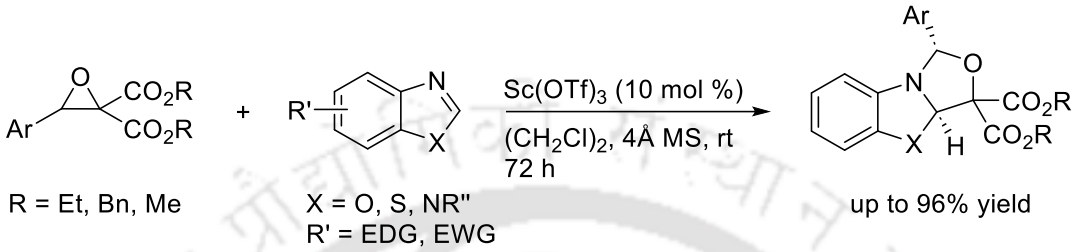

Scheme 12. Sc-Catalyzed Benzo-Fused Heterocycle Synthesis

1.1.4 Using Diaziridines

Diaziridines are known for their unique reactivity under thermal or Lewis acid catalysis to form azomethine imine ylide intermediate. These *in situ* generated intermediates can combine with suitable dipolar species to furnish nitrogen rich heterocycles. Notably, bicyclic diaziridines possessing both nitrogen atoms at the ring junction are valuable in affording fused heterocycles.

Trushkov group carried out a Ni(II)-catalyzed (3+3)-annulation of donor-acceptor cyclopropanes with diaziridine to afford perhydropyridazines under mild conditions (Scheme 13).[19] Gratifyingly, bicyclic diaziridines having aliphatic as well as aromatic substituents and monocyclic diaziridines proved viable in delivering the desired heterocycles in good yield and diastereoselecitivities.

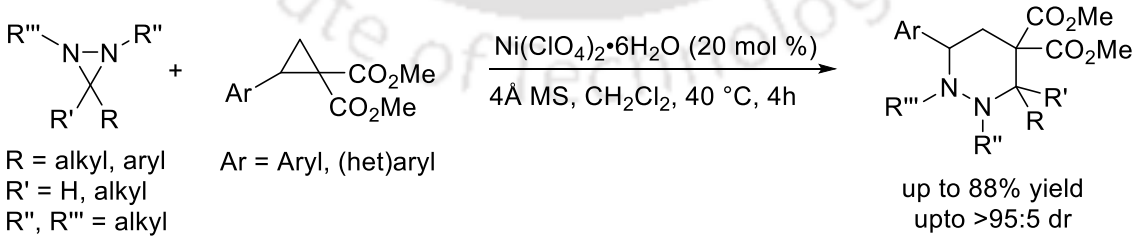

Scheme 13. (3+3)-Cycloaddition of Diaziridines with Donor-Acceptor Cyclopropane

Feng and co-workers have accomplished a highly enantioselective 1,3-dipolar cycloaddition in presence of Sc(III)-N,N′-dioxide chiral complex utilizing diaziridines and chalcones as the coupling partners (Scheme 14).[20] This protocol can accommodate diverse electron donating

and withdrawing substituents on both the substrates to furnish 1,5-diazabicylo[3.3.0]octane in high diastereo and enantioselectivities.

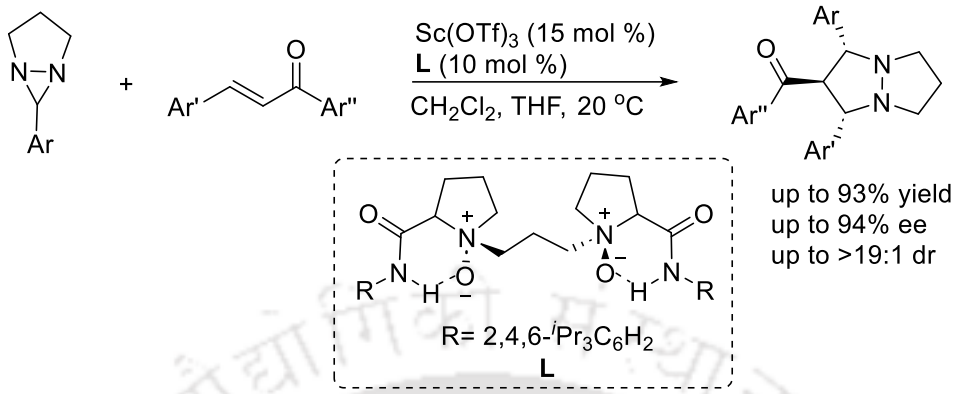

Scheme 14. (3+2)-Cycloaddition of Diaziridines with Chalcones

Our group reported a Fe(III)-catalyzed (3+3)-annulation of aziridines with diaziridines to furnish fused [1,2,4]-triazines. This protocol provides a potential route for the annulation of two different three-membered rings in synthesizing N-heterocycles (Scheme 15).[21] The use of cost-effective iron catalysis, quick reaction time, broad functional group tolerance and high stereospecificity are the important practical features.

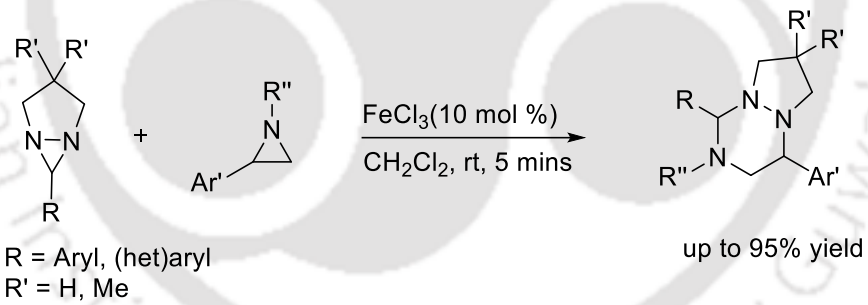

Scheme 15. (3+3)-Cycloaddition of Diaziridines with Aziridines

Feng and co-workers developed a σ-bond cross-exchange strategy utilizing diaziridines and bicyclobutanes to access medicinally important azabicyclo[3.1.1]heptane derivatives in good yields (Scheme 16).[22] Under $Sc(OTf)_3$ catalysis, a high level of cross-redistribution selectivity was observed with broad substrate scope.

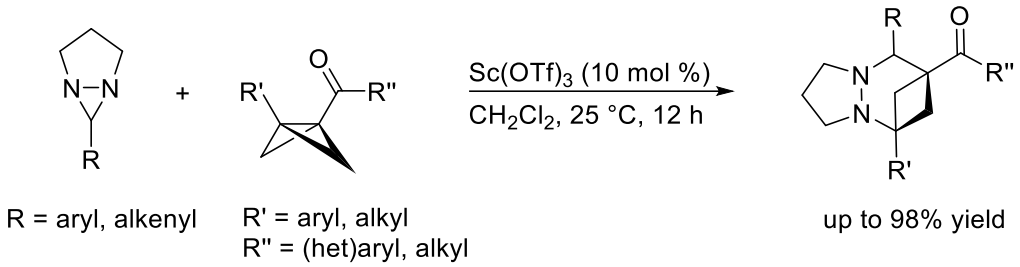

Scheme 16. (3+3)-Cycloaddition of Diaziridines with Bicyclobutanes

1.1.5 Using Oxaziridines

Oxaziridines are intriguing strained ring systems possessing both nitrogen and oxygen atoms in its core to offer a wide variety of dipolar synthons *via* regioselective C−O, C−N and N−O bond cleavage which undergo cycloaddition to yield varied classes of heterocycles.

A (3+2)-cycloaddition of oxaziridines with alkenes was reported by Troisi and co-workers towards the synthesis of isoxazolidines. The reaction proceeds *via* exclusive C−O bond cleavage in oxaziridines under reflux in toluene (Scheme 17).[23] The reaction tolerated both aryl as well as heteroaryl derived oxaziridines and electronically diverse styrenes in delivering the intended heterocycles in up to 95% yield.

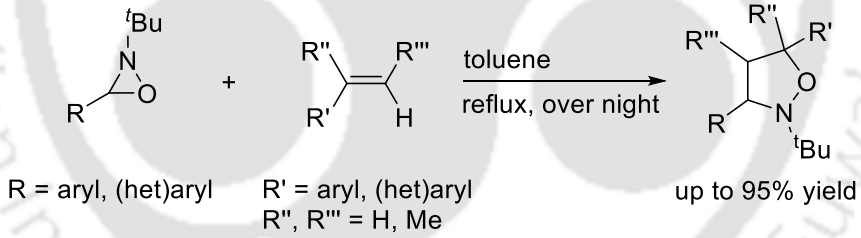

Scheme 17. (3+2)-Cycloaddition of Oxaziridines with Alkenes

Yoon group accomplished a highly stereoselective 1,3-dipolar cycloaddition of N-sulfonyl oxaziridines with dipolarphiles to achieve heterocycles (Scheme 18).[24] Mechanistically, in presence of a bulkier scandium catalytic complex, oxaziridines undergo preferential C−N bond cleavage to generate carbonyl imine intermediate, which combines with dipolarophiles to access intricate heterocycles.

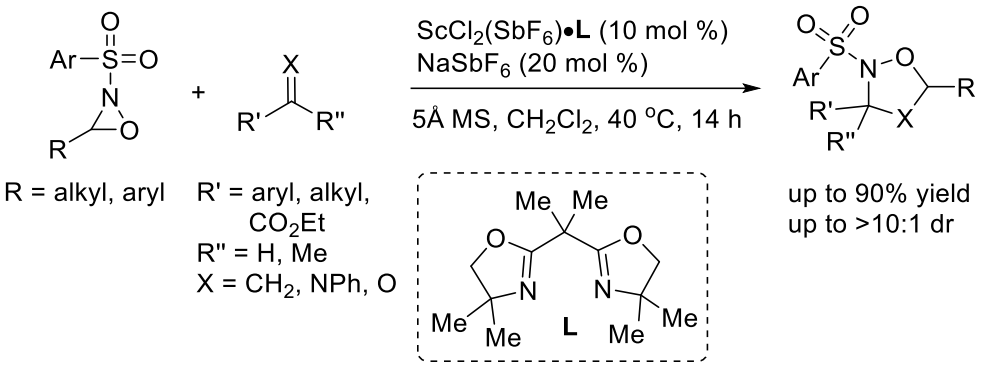

Scheme 18. Sc(III)-Catalyzed 1,3-Dipolar Cycloaddition *via* Carbonyl Imine Intermediate

1.2 Cascade C−H Functionalization/Annulation for Heterocycle Synthesis

Transition-metal-catalyzed DG assisted cascade C−H functionalization/annulation has emerged as a powerful step/atom-economic tool towards heterocycle synthesis. These one-pot cascade transformations involve the cleavage and reconstruction of multiple bonds which pave the way for molecular complexity, thus streamlining modern synthetic endeavours. In presence of transition-metal, suitably placed DGs in the molecule undergo coordination and C−H activation to form metallacycle intermediate, later, subsequent functionalization and annulation affords fused heterocycles (Scheme 19).[7]

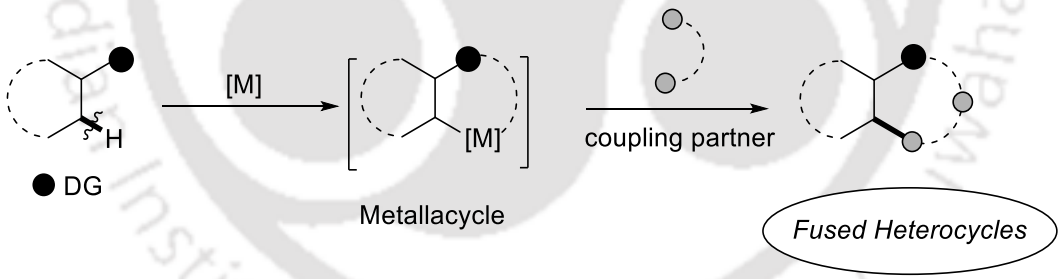

Scheme 19. Cascade C–H Functionalization/Annulation to Access Fused Heterocycles

Glorius group reported an oxidant-free Rh(III)-catalyzed annulation towards the construction of tetrahydroisoquinolone cores in good yields (Scheme 20).[25] Mechanistically, the authors have outlined the important role of DG as an internal oxidant in regenerating the active Rh-catalyst, thus obviating the need of a toxic stoichiometric oxidant.

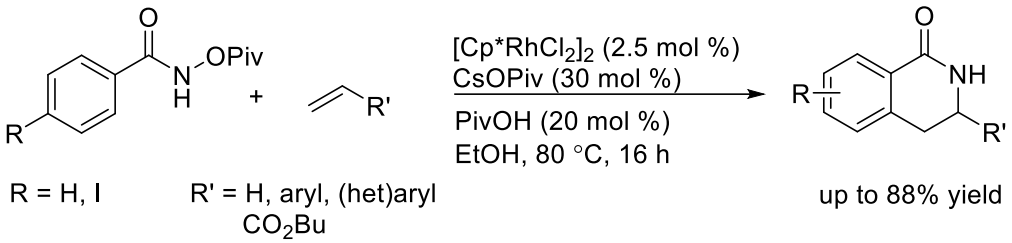

Scheme 20. Rh-Catalyzed Tetrahydroisoquinolone Synthesis

Ackermann and co-workers reported a Co(II)-catalyzed C−H/N−H functionalization of benzamides to access isoindoline-1-one using electron deficient alkenes (Scheme 21).[26] This oxidative annulation strategy utilizes a removable bidentate 8-aminoquinoline auxiliary to regioselectively install alkene onto the benzamides and subsequently the alkenylated intermediate upon hydroamination furnishes the desired heterocycles.

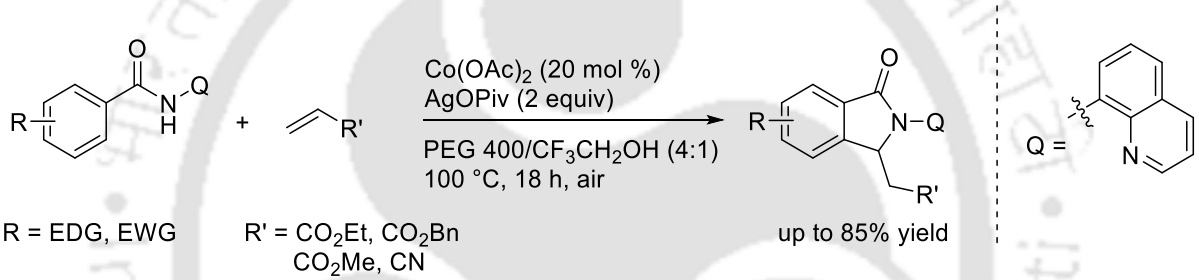

Scheme 21. Co-Catalyzed Isoindolin-1-one Synthesis

A modular approach towards the synthesis of 1,2-benzothiazines was demonstrated by Bolm group employing a Rh-catalyzed C−H activation/annulation strategy (Scheme 22).[27] A broad range of S-aryl sulfoximines and diazo compounds proved viable in delivering the heterocycles in high yield. This domino strategy is highly regioselective, scalable, and generates green by-products.

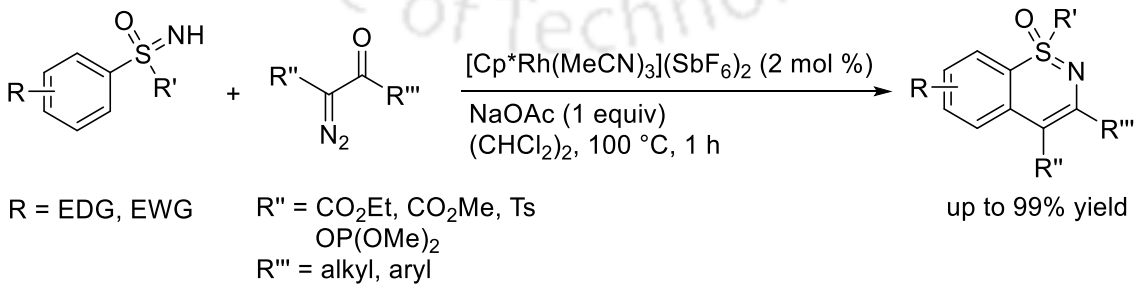

Scheme 22. Rh-Catalyzed 1,2-Benzothiazine Synthesis

A tandem Rh(III)-catalyzed C−H activation and Brønsted acid catalyzed dehydrative annulative sequence using indoles and enaldiazo compounds was developed to produce functionalized carbazoles with good functional group tolerance (Scheme 23).[28] Interestingly, the authors have extended the same strategy towards the synthesis of indoles utilizing pyrroles as the coupling partner.

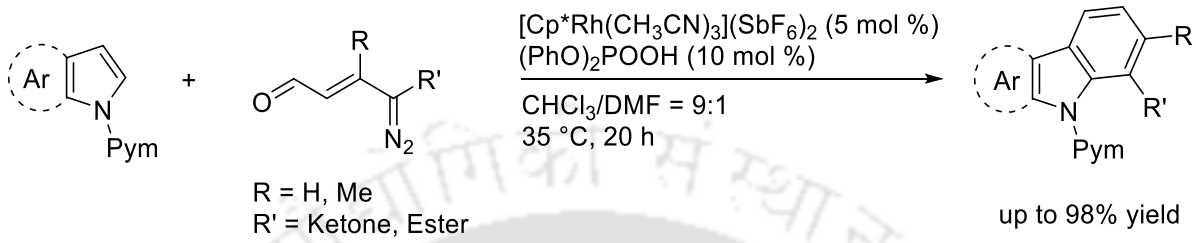

Scheme 23. Synthesis of Carbazoles and Indoles

Loh group disclosed a redox neutral (4+1)-annulation of benzamides under Rh(III)-catalysis using α,α-difluoromethylene alkyne as an efficient one-carbon synthon (Scheme 24).[29] This regiospecific strategy lays forth a straight-forward way for the construction of isoindolin-1-one derivatives with a quaternary carbon center in moderate to good yield.

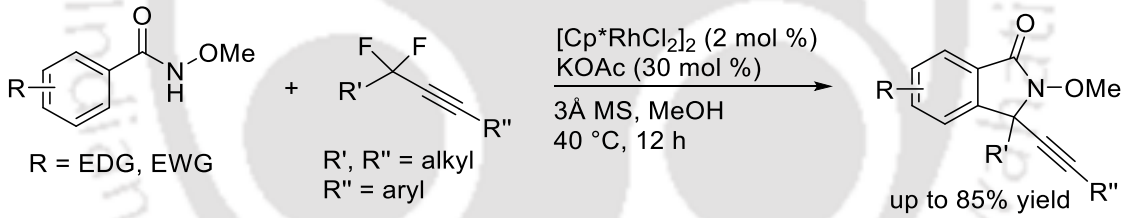

Scheme 24. Rh-Catalyzed Isoindolin-1-one Synthesis

Zhou group carried out an oxidative annulation of benzoic acids with unsymmetrical internal alkynes to afford isocoumarins with broad substrate scope (Scheme 25).[30] The reaction achieved good regiocontrol under Ir(III)-catalyst using silver salt as an external oxidant.

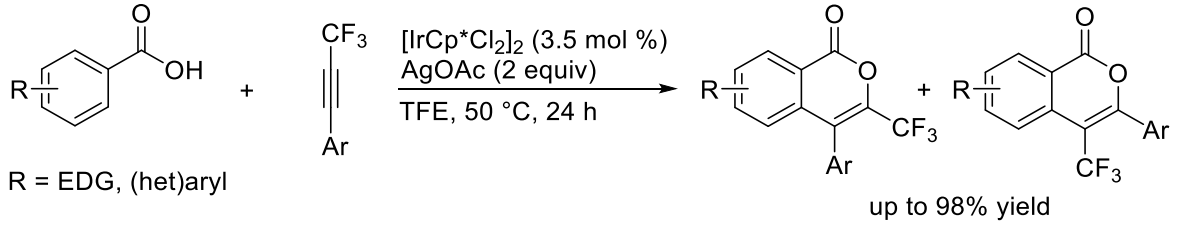

Scheme 25. Ir-Catalyzed Isocoumarin Synthesis

1.3 Objective of the Thesis

Strained three-membered carbo-/heterocyclic scaffolds have exemplified enormous potential in the field of heterocycle synthesis *via* ring-opening functionalization. In a similar manner, transition-metal-catalyzed cascade transformations involving C−H functionalization/annulation have strengthened the synthetic arsenal in light of generating fused heterocycles. The above discussed strategies resulted in good yield with strong functional group tolerance. Despite the progress, there still exists synthetic voids that can lead the way for further research in this evolving field.

- Considering the ample importance of atom/step-economy in sustainable synthesis, divergent strategies can be developed under mild conditions utilizing strained rings.
- The ring opening cyclization or cycloaddition reactions of strained three-membered rings were extensively studied utilizing acyclic or π-bonded dipolarophiles, whilst formal cycloaddition of two different strained rings is challenging and requires much attention.
- Compared to mono-heteroatomic strained rings, strategies encompassing diaziridines and oxaziridines are limited. In this line, development of synthetic strategies using these two strained ring systems can help accessing N,O-rich heterocycles.
- Viewing the significance of chiral heterocycles in medicinal domain, optically pure three-membered rings can be utilized as valuable precursors to synthesize such scaffolds in a stereospecific manner.
- From synthetic perspective, it would be valuable to achieve control over the regioselective bond breaking in oxaziridine to engage them in cycloaddition, synthesizing diverse scaffolds.
- Use of stoichiometric oxidants in transition-metal-catalyzed C−H functionalization poses a drawback from sustainability perspective; thus, development of oxidant-free approach is desirable.
- C−H activation prompted multiple cascade transformations have attracted a great deal of research interest due to their ability to form multiple bonds in step economic manner. In this line, easily accessible maleimides and benzamides can be utilized to achieve the goal.

1.4 References

1. (a) Vitaku, E.; Smith, D. T.; Njardarson, J. T. *J. Med. Chem.* **2014**, *57*, 10257. (b) Taylor, R. D.; MacCoss, M.; Lawson, A. D. G. Rings in Drugs: Miniperspective. *J. Med. Chem.* **2014**, *57*, 5845. (c) Fukui, N.; Maki, T.; Ban, K.; Kijima, A.; Shibahara, S.; Okamoto, K.; Kamiya, S.; Yasukata, T.; Tsuritani, T. *Org. Process Res. Dev.* **2024**, *28*, 2128. (d) Marshall, C. M.; Federice, J. G.; Bell, C. N.; Cox, P. B.; Njardarson, J. T. *J. Med. Chem.* **2024**, *67*, 11622.
2. (a) Lovering, F.; Bikker, J.; Humblet, C. *J. Med. Chem.* **2009**, *52*, 6752. (b) Lovering, F. *Med. chem. Comm.* **2013**, *4*, 515. (c) Kombo, D. C.; Tallapragada, K.; Jain, R.; Chewning, J.; Mazurov, A. A.; Speake, J. D.; Hauser, T. A.; Toler, S. *J. Chem. Inf. Model.* **2013**, *53*, 327. (d) Aldeghi, M.; Malhotra, S.; Selwood, D. L.; Chan, A. W. E. **2014**, *83*, 450. (e) Liu, D.-H.; Pflüger, P. M.; Outlaw, A.; Lückemeier, L.; Zhang, F.; Regan, C.; Rashidi Nodeh, H.; Cernak, T.; Ma, J.; Glorius, F. *J. Am. Chem. Soc.* **2024**, *146*, 11866.
3. (a) Cox, B.; Booker-Milburn, K. I.; Elliott, L. D.; Robertson-Ralph, M.; Zdorichenko, V. *ACS Med. Chem. Lett.* **2019**, *10*, 1512. (b) Bauer, M. R.; Di Fruscia, P.; Lucas, S. C. C.; Michaelides, I. N.; Nelson, J. E.; Storer, R. I.; Whitehurst, B. C. *RSC Med. Chem.* **2021**, *12*, 448. (c) Ma, J.; Chen, S.; Bellotti, P.; Wagener, T.; Daniliuc, C.; Houk, K. N.; Glorius, F. *Nat. Catal.* **2022**, *5*, 405.
4. (a) Marson, C. M. Saturated Heterocycles with Applications in Medicinal Chemistry. In *Advances in Heterocyclic Chemistry*; Elsevier, 2017; pp 13-33. (b) Qadir, T.; Amin, A.; Sharma, P. K.; Jeelani, I.; Abe, H. *Open Med. Chem. J.* **2022**, *16*, 1.
5. (a) Kumar, S.; Bawa, S.; Gupta, H. *Mini Rev. Med. Chem.* **2009**, *9*, 1648. (b) Bollini, M.; Casal, J. J.; Alvarez, D. E.; Boiani, L.; González, M.; Cerecetto, H.; Bruno, A. M. *Bioorg. Med. Chem.* **2009**, *17*, 1437. (c) Ning, J.; Tian, Z.; Wang, B.; Ge, G.; An, Y.; Hou, J.; Wang, C.; Zhao, X.; Li, Y.; Tian, X.; Yu, Z.; Huo, X.; Sun, C.; Feng, L.; Cui, J.; Ma, X. *Mater. Chem. Front.* **2018**, *2*, 2013. (d) Hao, Y.; Guo, J.; Wang, Z.; Liu, Y.; Li, Y.; Ma, D.; Wang, Q. *J. Agric. Food Chem.* **2020**, *68*, 5586. (e) Nifant'ev, I. E.; Ivchenko, P. V.; Vinogradov, A. A. *Coord. Chem. Rev.* **2021**, *426*, 213515.
6. (a) Stanković, S.; D'hooghe, M.; Catak, S.; Eum, H.; Waroquier, M.; Van Speybroeck, V.; De Kimpe, N.; Ha, H.-J. *Chem. Soc. Rev.* **2012**, *41*, 643. (b) Xu, X.; Doyle, M. P. *Acc. Chem. Res.* **2014**, *47*, 1396. (c) Cavitt, M. A.; Phun, L. H.; France, S. *Chem. Soc.*

Rev. **2014**, *43*, 804. (d) Fumagalli, G.; Stanton, S.; Bower, J. F. *Chem. Rev.* **2017**, *117*, 9404. (e) Pirenne, V.; Muriel, B.; Waser, J. *Chem. Rev.* **2021**, *121*, 227.

7. (a) Dutta, C.; Choudhury, J. *RSC Adv.* **2018**, *8*, 27881. (b) Wang, C.; Chen, F.; Qian, P.; Cheng, J. *Org. Biomol. Chem.* **2021**, *19*, 1705. (c) Qiu, M.; Fu, X.; Fu, P.; Huang, J. *Org. Biomol. Chem.* **2022**, *20*, 1339. (d) Tang, X.; Ding, S.; Song, L.; Van der Eycken., E. V. *Chem. Rec.* **2023**, *23*, 1.
8. Young, I. S.; Kerr, M. A. *Angew. Chem. Int. Ed.* **2003**, *42*, 3023.
9. Perreault, C.; Goudreau, S. R.; Zimmer, L. E.; Charette, A. B. *Org. Lett*. **2008**, *10*, 689.
10. Zhang, H.-H.; Luo, Y.-C.; Wang, H.-P.; Chen, W.; Xu, P.-F. *Org. Lett*. **2014**, *16*, 4896.
11. Petzold, M.; Jones, P. G.; Werz, D. B. *Angew. Chem. Int. Ed.* **2019**, *58*, 6225.
12. Li, L.; Wu, X.; Zhang, J. *Chem. Commun*. **2011**, *47*, 5049.
13. Wang, B.; Liang, M.; Tang, J.; Deng, Y.; Zhao, J.; Sun, H.; Tung, C.-H.; Jia, J.; Xu, Z. *Org. Lett*. **2016**, *18*, 4614.
14. Li, R.; Li, B.; Zhang, H.; Ju, C.-W.; Qin, Y.; Xue, X.-S.; Zhao, D. *Nat. Chem.* **2021**, *13*, 1006.
15. Fang, S.; Zhao, Y.; Li, H.; Zheng, Y.; Lian, P.; Wan, X. *Org. Lett.* **2019**, *21*, 2356.
16. Ma, X.; Pan, S.; Wang, H.; Chen, W. *Org. Lett.* **2014**, *16*, 4554.
17. Liu, L.; Sun, H. *Angew. Chem. Int. Ed.* **2014**, *53*, 9865.
18. Zhang, S.-S.; Wang, D.-C.; Xie, M.-S.; Qu, G.-R.; Guo, H.-M. *Org. Lett.* **2018**, *20*, 8026.
19. Chagarovskiy, A. O.; Vasin, V. S.; Kuznetsov, V. V.; Ivanova, O. A.; Rybakov, V. B.; Shumsky, A. N.; Makhova, N. N.; Trushkov, I. V. *Angew. Chem. Int. Ed.* **2018**, *57*, 10338.
20. Hu, H.; Xu, J.; Wang, F.; Dong, S.; Liu, X.; Feng, X. *Org. Lett.* **2020**, *22*, 93.
21. Sarkar, T.; Talukdar, K.; Roy, S.; Punniyamurthy, T. *Chem. Commun.* **2020**, *56*, 3381.
22. He, H.-X.; Wu, F.; Zhang, X.; Feng, J.-J. *Angew. Chem. Int. Ed.* **2025**, *64*, e202416741.
23. Fabio, M.; Ronzini, L.; Troisi, L. *Tetrahedron* **2007**, *63*, 12896.
24. Partridge, K. M.; Guzei, I. A.; Yoon, T. P. *Angew. Chem. Int. Ed.* **2010**, *49*, 930.
25. Rakshit, S.; Grohmann, C.; Besset, T.; Glorius, F. *J. Am. Chem. Soc.* **2011**, *133*, 2350.
26. Ma, W.; Ackermann, L. *ACS Catal.* **2015**, *5*, 2822.
27. Cheng, Y.; Bolm, C. *Angew. Chem. Int. Ed.* **2015**, *54*, 12349.
28. Wu, J.-Q.; Yang, Z.; Zhang, S.-S.; Jiang, C.-Y.; Li, Q.; Huang, Z.-S.; Wang, H. *ACS Catal.* **2015**, *5*, 6453.

29. Wang, C.-Q.; Ye, L.; Feng, C.; Loh, T.-P. *J. Am. Chem. Soc.* **2017**, *139*, 1762.

30. Liu, G.; Kuang, G.; Zhang, X.; Lu, N.; Fu, Y.; Peng, Y.; Zhou, Y. *Org. Lett.* **2019**, *21*, 3043.

Chapter II

Co-Catalyzed C–N/C–O Bonds Formation of Oxiranes with Diaziridines

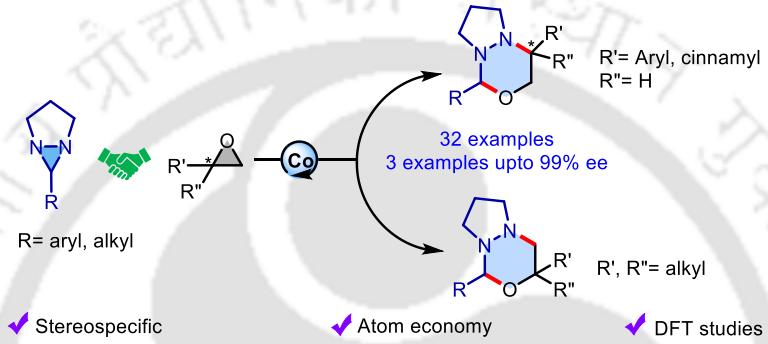

J. Org. Chem. **2023**, *88*, 9447.

Co-Catalyzed C–N/C–O Bonds Formation of Oxiranes with Diaziridines

[1,3,4]-Oxadiazines are versatile scaffolds that exhibit persistent utility as potential anticancer and antibiotic agents (Figure 1). Their utility as significant pesticides and antiviral drugs, such as in case of indoxacarb, that displays inhibitory activity against lepidopteran larvae while oxadin, that restricts the in vitro replication of herpex simplex virus, is highly noteworthy.[1] Considering manifold utilities in the field of medicine and drug discovery, efficient synthesis of such heterocyclic scaffolds in a stereospecific approach in an atom- and step-economic[2] manner would be valuable. Further, considering the notable reactivity of strained ring systems as primary three-atom synthon, their utility as chief building blocks for C−C/C−heteroatom bond formation can certainly lead to generation of a plethora of privileged carbo-/heterocyclic motifs.[3] In this domain, oxiranes, the smallest oxygen containing heterocyclic unit, have been widely used as prerequisites for synthesising diverse O-heterocycles.[4,5] In addition, diaziridines, under thermal as well as Lewis acidic conditions are known to undergo heterolytic cleavage *in situ* to generate an azomethine imine intermediate, that in turn can be exploited for obtaining potent cyclic scaffolds.[6] Subsequently, channelling the innate potential of strained ring systems as powerful alternatives for unsaturated coupling partners can open up innumerable avenues for the synthetic chemist. This chapter, thereby, focuses on a Co(II)-catalysed C−N/C−O bond formation of oxiranes with diaziridines to furnish tetrahydro-[1,3,4]-oxadiazines as a single diastereomer. The key features include the use of benign and cost-effective Co-catalysis,[7] the compatibility of a library of electronically divergent substrates and the highly stereospecific reactivity that yields enantiopure sp^3-rich heterocycles in up to >96% ee.

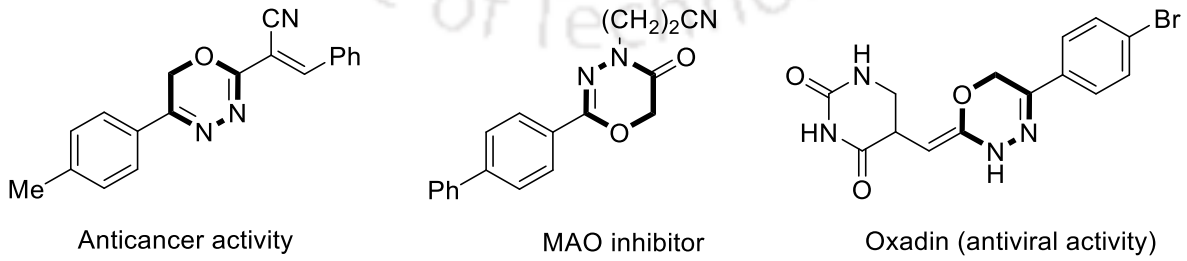

Figure 1. Representative examples of biologically active oxadiazines.

2.1 Literature

2.1.1 NHC-Catalysed (4+2)-Cycloaddition

Ye and co-workers reported an enantioselective (4+2)-cycloaddition of ketenes with N-benzoyldiazenes using chiral NHCs to obtain oxadiazine motifs in good yields and excellent enantiomeric excess (Scheme 1).[8] The observed switchable enantioselectivities make this protocol potent enough for obtaining enantiopure oxadiazine cores.

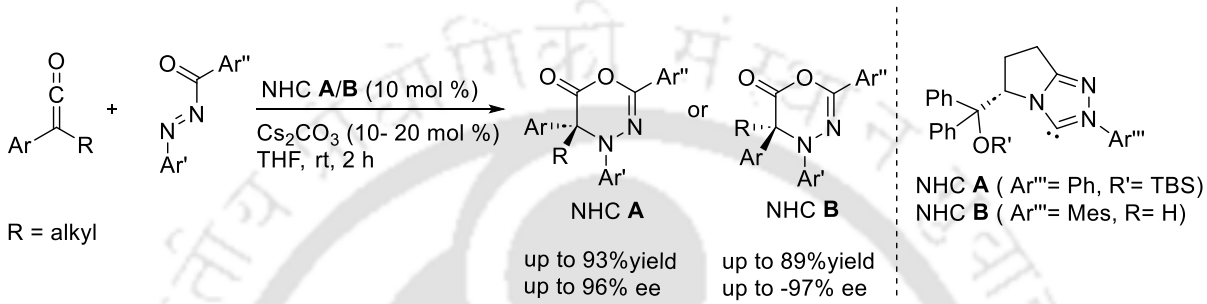

Scheme 1. NHC-Catalysed (4+2)-Cycloaddition of Ketenes with N-Benzoyldiazenes

2.1.2 Sc-Catalysed (3+3)-Cycloaddition

Luo and co-workers presented a formal (3+3)-cycloaddition strategy for the synthesis of 1,3,4-oxadiazines in up to 96% ee (Scheme 2).[9] The protocol exhibited broad substrate scope and a synergistic activation of both diaziridine as well as quinone was found to be crucial to enable the cycloaddition.

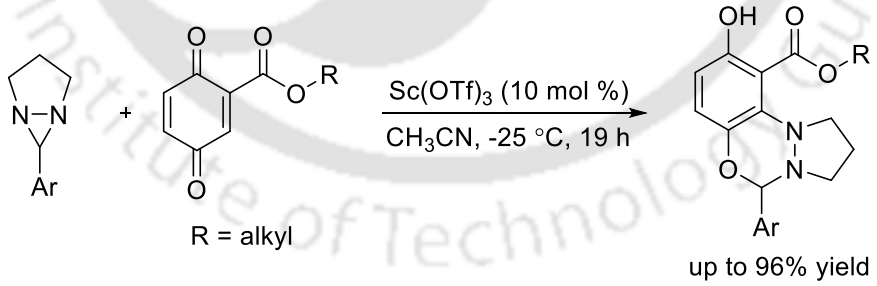

Scheme 2. Sc-Catalysed Formal (3+3)-Cycloaddition of Diaziridines with Quinones

2.1.3 Co-Catalysed Cascade Ring-opening/Cyclization

Our group described a Co-catalysed cascade ring-opening/cyclization of epoxides with hydrazones to afford oxadiazine cores under aerobic conditions (Scheme 3).[10] The catalyst has been reported to play a dual role, both as a Lewis acid as well as a redox catalyst. Enantiopure oxadiazines were obtained in up to >99% ee.

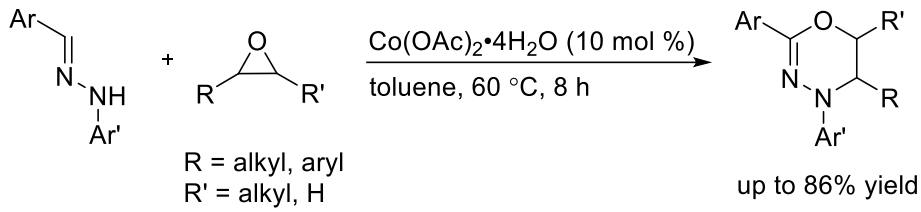

Scheme 3. Co-Catalysed Cascade C−N/C−O Bond Formation of Styrene Oxides with Hydrazones

2.1.4 Diastereoselective Synthesis of Bridgehead Dihydro-Oxadiazines

Trofimov and co-workers reported an acid-mediated diastereoselective synthesis of bridgehead dihydro-oxadiazines (Scheme 4).[11] Diverse 7-methylene-6,8-dioxabicyclo[3.2.1]octanes were efficiently coupled with hydrazine to yield the bridged heterocycle in moderate to good yield.

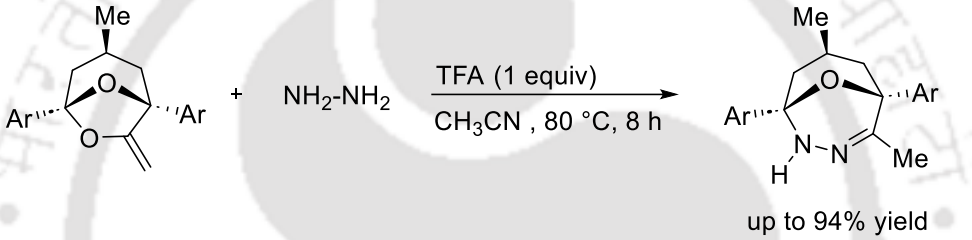

Scheme 4. TFA mediated cyclization

2.1.5 NHC-Catalyzed Enantioselective Aza-Diels-Alder Reaction

A highly enantioselective aza-Diels-Alder reaction of oxodiazenes with α-chloroaldehydes was demonstrated utilizing chiral-NHC catalyst to afford oxadiazines in high yields (Scheme 5).[12] This (4+2)-cycloaddition showed good functional group tolerance on both the substrates in delivering the intended heterocycles in high enantioselectivities (ee >99%).

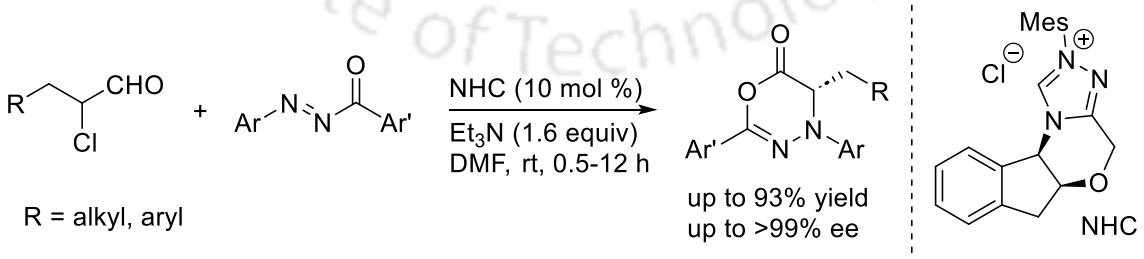

Scheme 5. Asymmetric aza-Diels-Alder reaction

2.1.6 Organocatalytic α-Amination/Michael-Lactonization Cascade

Smith and co-workers unveiled a highly enantioselective isothiourea catalyzed cascade α-amination/Michael-lactonization of carboxylic acids with N-aryl-N-aroyldiazenes to afford oxadiazines in good yield (Scheme 6).[13]

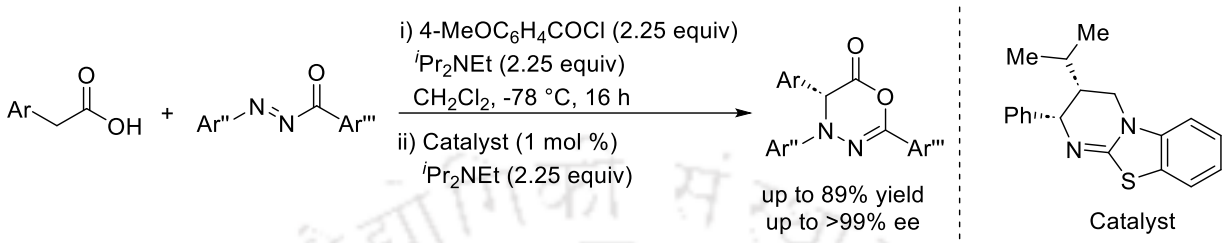

Scheme 6. Organocatalytic cascade synthesis

2.1.7 Ring Expansion of Cyclic Azomethine Imines

A base mediated strategy towards ring expansion of C,N-cyclic-N′-acyl azomethine imines with sulfonium salts was disclosed (Scheme 7).[14] Under mild conditions, *in situ* generated sulfonium ylide couple with cyclic azomethine imine to afford tricyclic oxadizines *via* aziridinium cation intermediate.

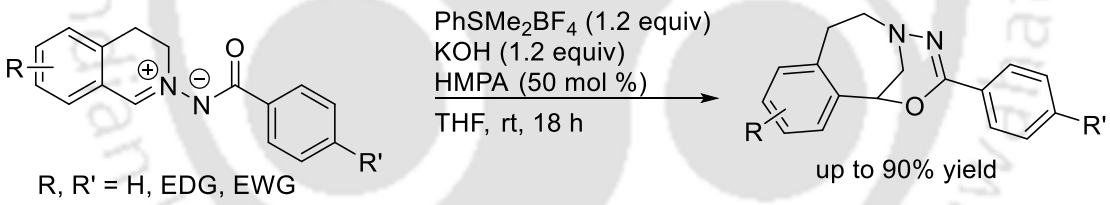

Scheme 7. Base mediated ring enlargement of C,N-cyclic-N′-acyl azomethine imines.

2.1.8 Brønsted Base Catalyzed (3+3)-Cycloaddition

A base catalyzed highly diastereoselective (3+3)-cycloaddition involving *p*-quinols and azomethine imine ylides was developed to synthesize tricyclic oxadiazines (Scheme 8).[15] This reaction was carried out in mild conditions and supported varieties of functional groups in delivering the cycloadduct in moderate to good yield.

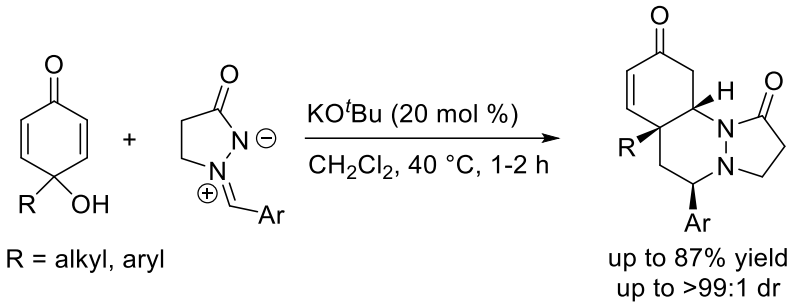

Scheme 8. (3+3)-Cycloaddition of *p*-quinols with azomethine imine ylide

2.1.9 Hemin Catalyzed Oxidative (3+3)-Cycloaddition

Zhong and co-workers performed a (3+3)-cycloaddition involving phenol and hydrozones under hemin/H_2O_2 catalysis to seamlessly generate functionalized benzo fused oxadiazines in good yield (Scheme 9).[16] Bio-inspired catalysis, chemoselective oxidation and step/atom economy are the highlighted features.

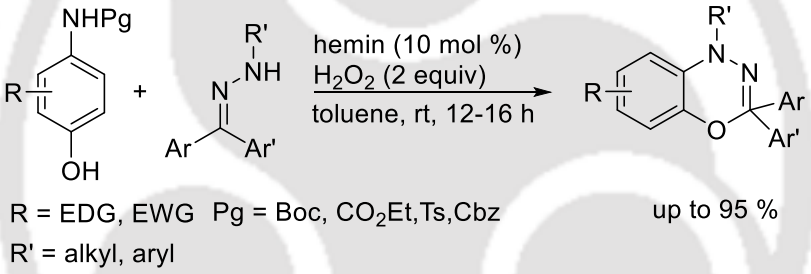

Scheme 9. Bio-catalytic (3+3)-cycloaddition

2.2 Present Study

This chapter describes a stereospecific C−N/C−O bond formation of oxiranes with diaziridines utilizing cobalt catalysis to furnish tetrahydro-[1,3,4]-oxadiazines in a diastereoselective manner. Our optimization studies began by taking 6-phenyl-1,5-diazabicyclo[3.1.0]hexane **1a** and 2-phenyloxirane **2a** as the representative substrates (Table 1). An initial approach towards performing the cycloaddition under catalyst-free conditions remained futile, thereby directing us for the screening of a series of 3d-transition-metal halides such as $FeCl_3$, $NiCl_2$, $CoCl_2$•$6H_2O$, $CuCl_2$, and $MnCl_2$•$4H_2O$ at room temperature (entries 1-7). Delightedly, **3aa** was produced in 36% yield when **1a** and **2a** were stirred in CH_2Cl_2 in presence of 10 mol % $CoCl_2$•$6H_2O$, while other metal chlorides demonstrated inferior outcomes. Further screening of a series of cobalt catalysts depicted a significant increase in yield to 82% with $CoCl_2$, while the use of metal triflates as well as Bronsted acids remained comparatively ineffective (entries

8-16). In case of solvents, CH_2Cl_2 proved to be the solvent of choice, while $(CH_2Cl)_2$, CH_3CN, THF, DMSO, DMF, and CH_3OH produced <70% of the desired cycloadduct (entries 17-22).

Table 1. Optimization of the Reaction Conditions[a]

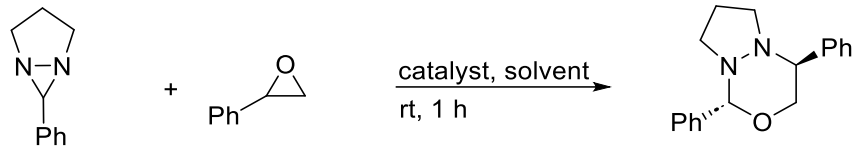

Entry	Catalyst (10 mol %)	Solvent	Yield [**3aa**, (%)][b]
1[c]	none	CH_2Cl_2	n.r.
2	$FeCl_3$	CH_2Cl_2	16
3	$NiCl_2$	CH_2Cl_2	20
4	$CuCl_2$	CH_2Cl_2	trace
5	$MnCl_2•4H_2O$	CH_2Cl_2	trace
6	$CoCl_2•6H_2O$	CH_2Cl_2	36
7[d]	$CoCl_2•6H_2O$	CH_2Cl_2	40
8	**$CoCl_2$**	**CH_2Cl_2**	**82**
9	$Co(OAc)_2$	CH_2Cl_2	trace
10	$Co(acac)_2$	CH_2Cl_2	n.r.
11	$Cu(OTf)_2$	CH_2Cl_2	15
12	$Sc(OTf)_3$	CH_2Cl_2	46
13	$Yb(OTf)_3$	CH_2Cl_2	10
14	$Zn(OTf)_2$	CH_2Cl_2	25
15	PTSA	CH_2Cl_2	trace
16	CF_3SO_3H	CH_2Cl_2	n.r.
17	$CoCl_2$	$(CH_2Cl)_2$	70
18	$CoCl_2$	CH_3CN	n.r.
19	$CoCl_2$	THF	trace
20	$CoCl_2$	DMSO	n.r.
21	$CoCl_2$	DMF	20
22	$CoCl_2$	MeOH	trace

[a]Reaction conditions: **1a** (0.2 mmol), **2a** (0.2 mmol), catalyst (10 mol %), solvent (2 mL), 1 h, rt. [b]Isolated yield. [c]At 40 °C. [d]4 Å MS used. n.r. = no reaction.

Table 2. Scope of Diaziridines[a,b]

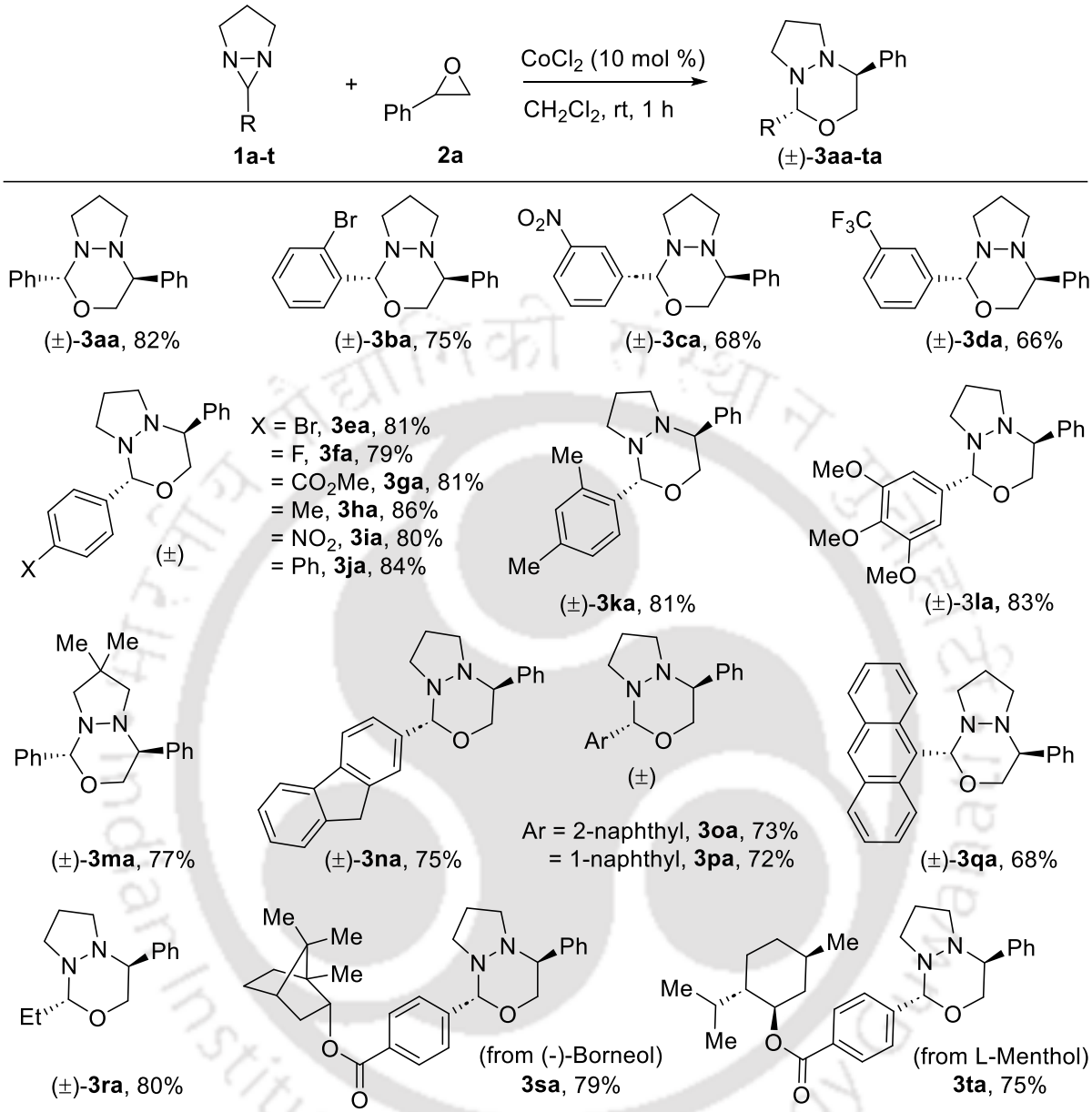

[a]Reaction conditions: **1a-t** (0.2 mmol), **2a** (0.2 mmol), $CoCl_2$ (10 mol %), CH_2Cl_2 (2 mL), 1 h, rt. [b]Isolated yield.

Having the optimised conditions, the generality of the protocol was investigated using a series diaziridines **1a-t** with **2a** as the standard substrate (Table 2). A variation of diverse substituents on the aryl ring of the diaziridine revealed that 2-bromo substituted diaziridine **1b** produced **3ba** in 75% yield. Likewise, substituents at the 3-position of the aryl ring such as nitro **1c** and trifluoromethyl **1d** afforded **3ca** and **3da** in 68% and 66% yields respectively. Diaziridines bearing substitution at the 4-position *viz*., bromo **1e**, fluoro **1f**, ester **1g**, methyl **1h**, nitro **1i**, and phenyl **1j** reacted to yield **3ea-ja** in 79-86%. Intriguingly, 2,4-dimethyl diaziridine **1k**, 3,4,5-

trimethoxy **1l**, and 3,3-dimethyl **1m** reacted to produce the corresponding cycloadducts **3ka-3ma** in 77-83% yields. Polycyclic 2-fluorenyl substituted **1n** and diaziridines tethered with π-extended aryl moieties 2-naphthyl **1o**, 1-naphthyl **1p**, and anthracenyl **1q** delivered the target products **3na-qa** in 68-75% yields. Aliphatic diaziridine **1r** as well as diaziridines derived from naturally occurring terpenoids such as (-)-borneol **1s** and L-menthol **1t** successfully participated affording **3ra-3ta** in 75-80% yields.

Table 3. Scope of Oxiranes[a,b]

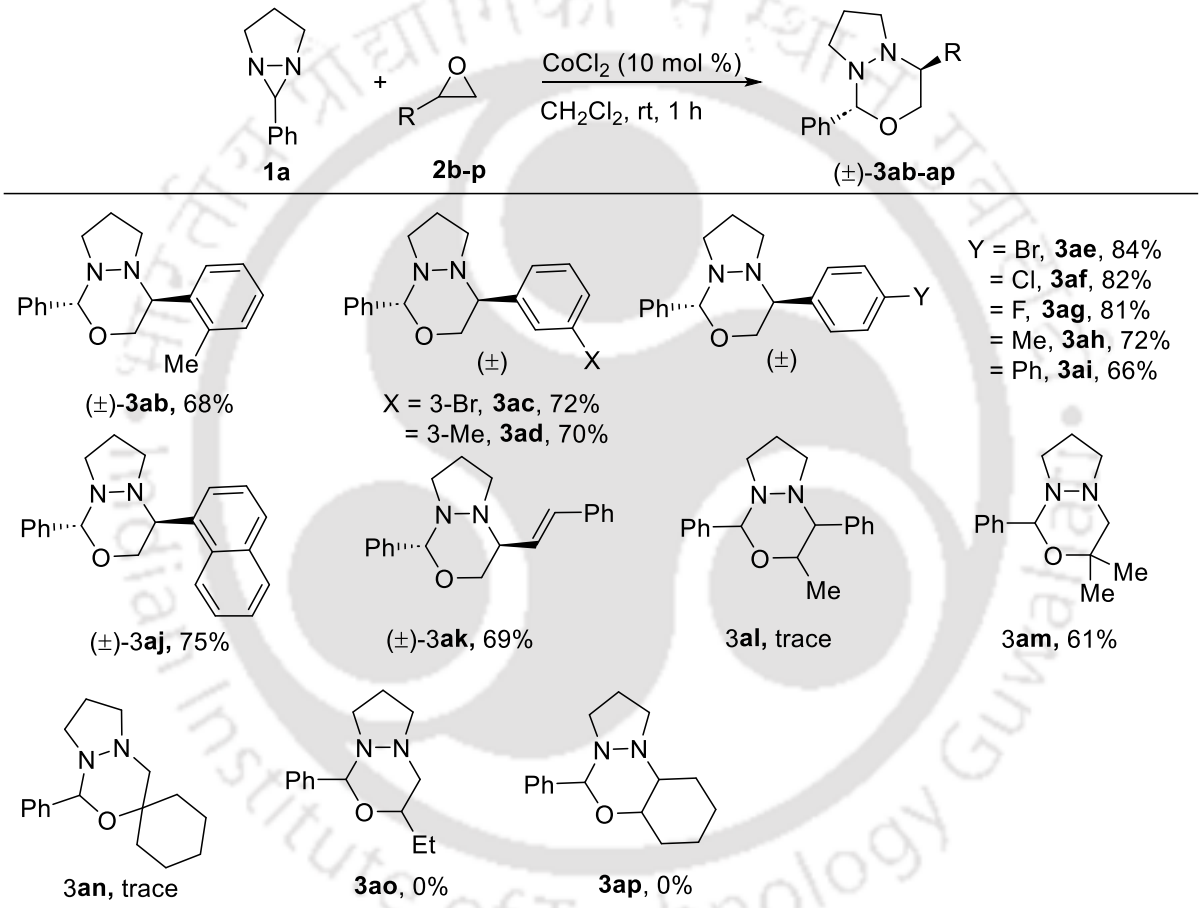

[a]Reaction conditions: **1a** (0.2 mmol), **2b-p** (0.2 mmol), $CoCl_2$ (10 mol %), CH_2Cl_2 (2 mL), 1 h, rt. [b]Isolated yield.

The scope of the protocol was extended to the coupling of a series of oxiranes **2b-p** using **1a** as the standard substrate (Table 3). Oxirane **2b** bearing methyl substituent on the 2-position of the aryl ring produced **3ab** in 68% yield. Similarly, oxiranes bearing substitution at the 3-position of the aryl ring *viz*., 3-bromo **2c** and 3-methyl **2d** afforded **3ac** and **3ad** in 72% and 70% yields, respectively. Further, the reaction of 4-substituted oxiranes encompassing both

electron-donating as well as -withdrawing groups, such as bromo **2e**, chloro **2f**, fluoro **2g**, methyl **2h**, and phenyl **2i**, occurred efficiently to produce **3ae-ai** in 66-84% yields. The structure of **3af** was confirmed by X-ray analysis. Pertinently, 1-naphthyl substituted 2j and styryl substituted **2k** oxiranes afforded **3aj** and **3ak** in 75% and 69% yields, respectively. However, a 2,3-disubstituted oxirane **2l**, produced the cycloadduct **3al** in a trace amount. Additionally, 2,2-disubstituted isobutylene oxide **2m** furnished **3am** in 61% yield, while spirocyclic 1-oxaspiro[2.5]octane **2n** resulted in a trace amount of **3an**. However, in contrast, 2-ethyloxirane **2o** and 7-oxabicyclo[4.1.0]- heptane **2p** remained unsuccessful substrates.

To shed light into the stereoselectivity of the reaction pathway, the reaction of diaziridines was studied with 2-phenyloxirane (*R*)-**2a′** as the standard example (Table 4). For example, 3-nitro substituted diaziridine **1c** furnished **3ca′** in 66% yield with >99% ee while, diaziridine bearing 4-methyl **1h** delivered **3ha′** in 84% yield with >98% ee. X-ray analysis confirmed the absolute configuration of **3ha′**. Moreover, the reaction of oxirane (*S*)-**2i′** with diaziridine **1a** afforded **3ai′** in 62% yield with >96% ee. These outcomes validate the protocol is stereospecific to furnish tetrahydro-[1,3,4]-oxadiazines in good yields and excellent enantiomeric excess. Further, to reveal the enantioselectivity of the described protocol, the reaction of diaziridine **1c** was carried out with oxirane (±)-**2a** using chiral Co(Salen) **C1** and **C2** as the representative

Table 4. Enantiospecific Synthesis[a,b]

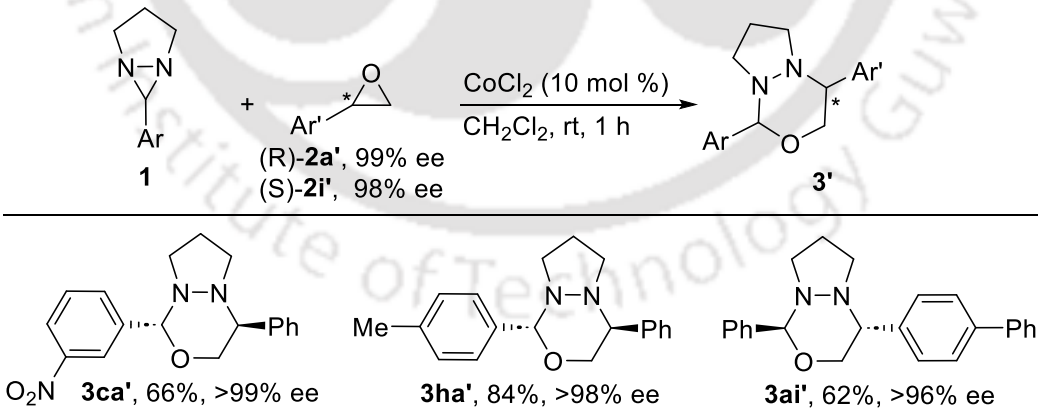

[a]Reaction conditions: **1** (0.2 mmol), (R/S)-**2'** (0.2 mmol), $CoCl_2$ (10 mol %), CH_2Cl_2 (2 mL), 1 h, rt. [b]Isolated yield. [c]Absolute stereochemistry of compound **3ha'** was confirmed *via* single crystal X-ray analysis, while the stereochemical outcome of **3ca'** and **3ai'** are assigned by analogy.

Table 5. Enantioselective Synthesis[a,b]

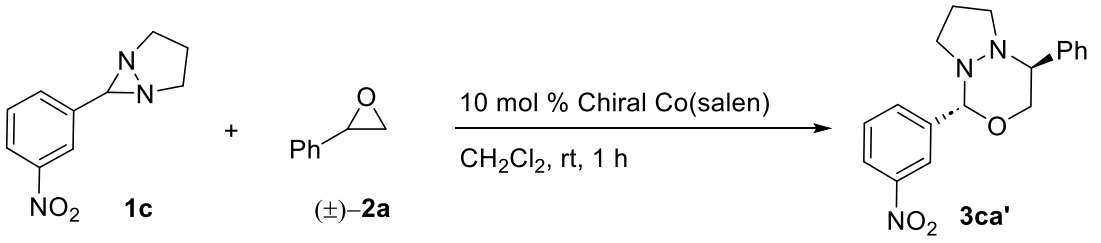

Chiral Co(Salen) (10 mol %)	Yield (3ca′, %)	ee (%)
C1	65	>28
C2	59	>46

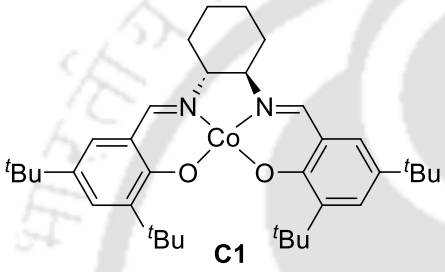

$[\alpha]^{28.5}_{D}$ = - 210 (c = 0.01, $CHCl_3$)

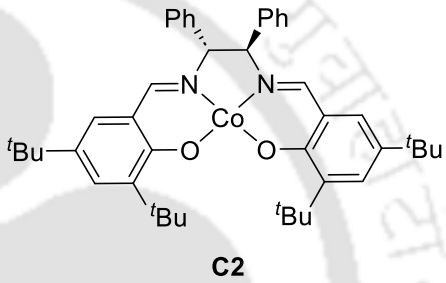

$[\alpha]^{28.5}_{D}$ = 560 (c = 0.01, $CHCl_3$)

[a]Reaction conditions: **1c** (0.2 mmol), (±)-**2a** (0.2 mmol), Co(Salen) **C1**/**C2** (10 mol %), CH_2Cl_2 (2 mL), 1 h, rt. [b]Isolated yield.

examples (Table 5). The reaction occurred to produce the cycloadduct **3ca′** in 28 and 46% ee, respectively.

To get some insight into the reaction pathway, control experiments using 2,6-di-*tert*-butyl-4-methylphenol (BHT) and 2,2,6,6-tetramethyl-1-piperidinyloxy (TEMPO) were performed. However, no significant decrement in yield was observed in the presence of radical scavengers, thus, precluding the possibility of a radical pathway (Scheme 10a). Again, epimerization of **3aa** in the presence of AcOH failed to deliver **3′aa**, which confirms the relative thermodynamic preference of the *trans*-isomer over the *cis*-isomer (Scheme 10b).

On basis of these pmechanistic studies and literature precedents,[6] a plausible mechanism is depicted, wherein, the initial coordination of $CoCl_2$ with styrene oxide generates intermediate **I** (Scheme 11). Similarly, in the presence of $CoCl_2$, heterolytic C-N bond cleavage of diaziridine **1** may generate the azomethine imine intermediate **A**, which then stereospecifically opens **I** to give intermediate **II**. Intramolecular cyclization of **II** leads to the formation of **3** with absolute

trans-selectivity, while, the formation of the cis-isomer is disfavoured owing to the unfavourable steric interactions. To further provide an account for the observed diastereoselectivity, density functional theory (DFT) calculations were performed. Figure 2 showcases the obtained energy profile for the formation of both the diastereomers

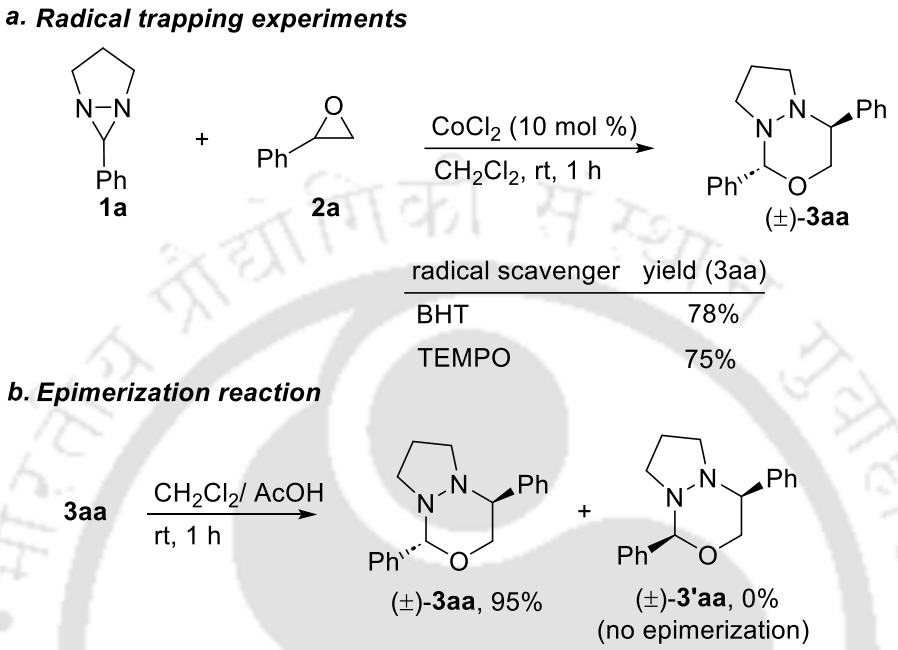

Scheme 10. Preliminary Mechanistic Investigations

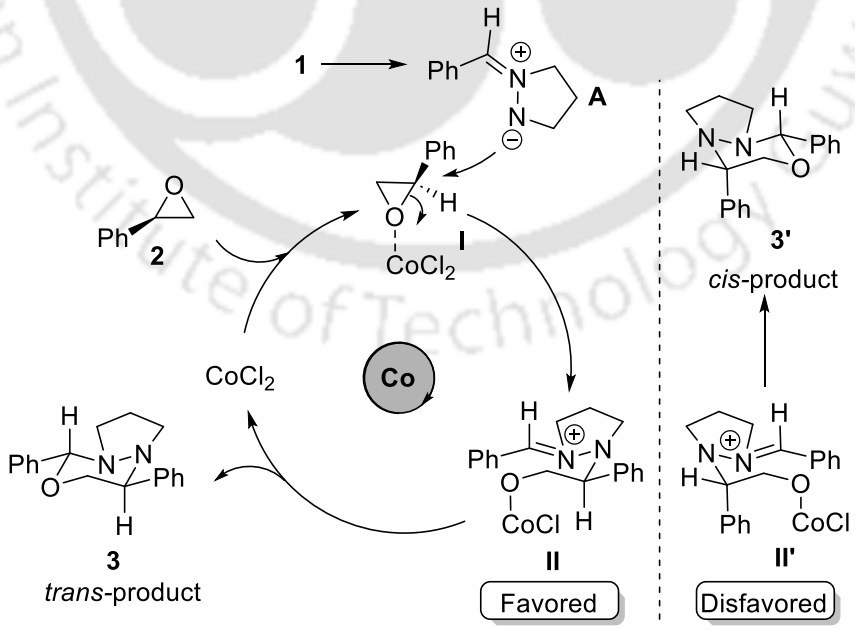

Scheme 11. Plausible Mechanism

calculated at 298 K in gas phase. Initially, chelation of oxirane **2a** with $CoCl_2$ generates the active species **Int-I** following an exergonic pathway (ΔG_{298} = -5.4 kcal/mol). Later, stereospecific ring opening of **Int-I** by **A** affords **Int-II** and **Int-II′** *via* two different reaction pathways involving distinct transition states **TS-I** (*Re*-face of **A**) and **TS-I′** (*Si*-face of **A**) with activation energies of 14.3 and 18.6 kcal/mol respectively. Later, cyclization of **Int-II** affords the *trans*-product **3** *via* TS-II, which involves an activation barrier of 20.5 kcal/mol. The formation of **3′** from **Int-II′** *via* **TS-II′** requires a comparatively higher activation energy of 23.3 kcal/mol. Thus, owing to lower activation energies, the formation of the trans-product is more favoured, which is also in good agreement with the experimental findings from DFT studies.

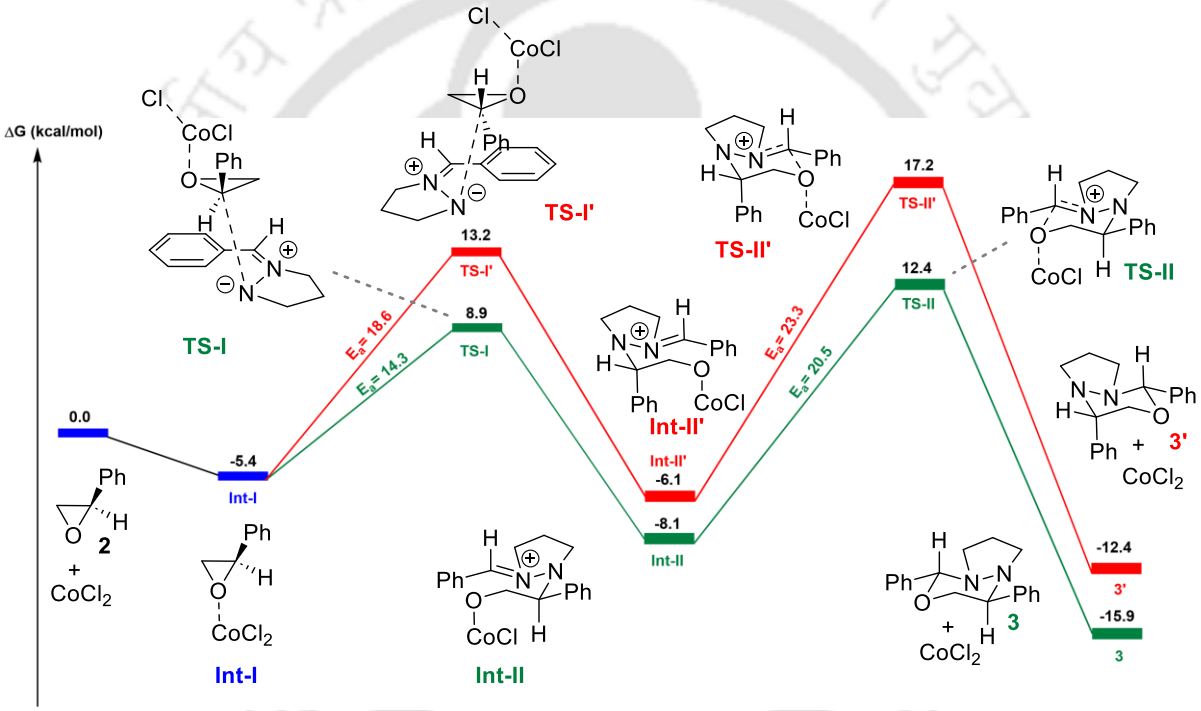

Figure 2. Reaction energetic for the formation of *cis* and *trans* diastereomer. Relative energies (ΔG_{298}) are in kcal/mol.

Post-synthetic transformations were accomplished to highlight the synthetic utility of the protocol. A scale-up synthesis was first performed on a 5 mmol scale taking **1e** and **2a** as the representative examples to afford the target heterocycle **3ea** in 70% yield (Scheme 12). Further, a Pd-catalysed Suzuki coupling reaction of **3ea** produced the coupled product **4** in 81% yield. In addition, a borylation reaction using B_2Pin_2 produced the desired product 5 in 75% yield. The aforementioned reactions, thus, showcase the efficacy of the stated protocol.

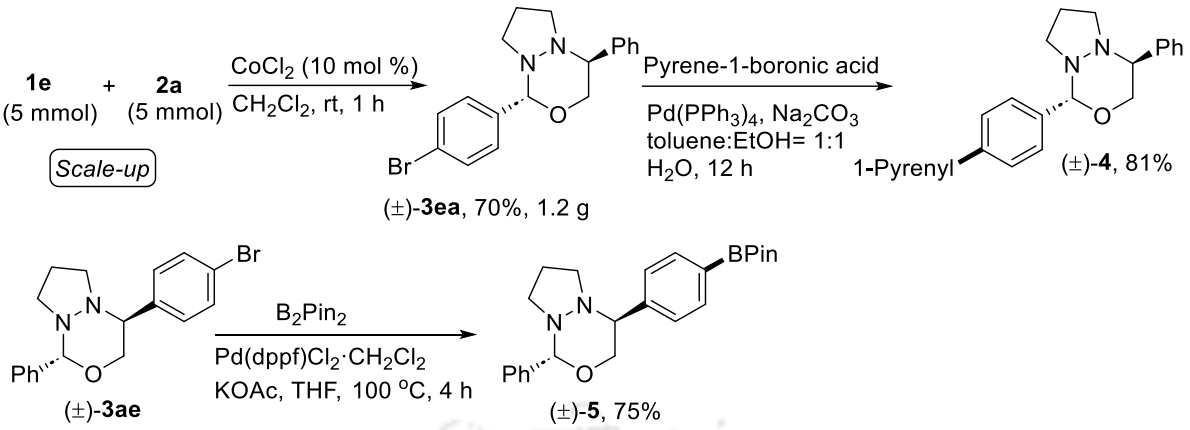

Scheme 12. Synthetic Utilities.

In conclusion, a stereospecific Co(II)-catalyzed C−N/C−O bonds formations of diaziridine with oxirane was accomplished under mild conditions. The protocol tolerates a broad spectrum of substrates in delivering the intended [1,3,4]-oxadiazine cores in good yield. Step/atom economic transformation, high diastereoselectivity and natural product modifications are the important practical features.

2.3 Experimental Section

General Information. (*R*)-(+)-2-Phenyloxirane (98%), $CoCl_2$ (97%), $CoCl_2$•$6H_2O$ (98%), $Co(OAc)_2$ (>99%), $Sc(OTf)_3$ (99%), $Cu(OTf)_2$ (98%), $Yb(OTf)_3$ (>99%), $Co(acac)_2$ (97%), $MnCl_2$•$4H_2O$ (>99%), $NiCl_2$ (>99.9%), $CuCl_2$ (97%), $Pd(dppf)Cl_2$•CH_2Cl_2 (>99%), *m*CPBA (≤77%), $Pd(PPh_3)_4$ (99%), AD-mix-α, BHT (99%), TEMPO (98%) and styrenes purchased from Aldrich and used as received. $FeCl_3$ (96%) purchased from Rankem used as received. Diaziridines[7] and styrene oxides[17] were prepared according to reported procedure. SRL silica gel G/GF 254 plates were used for analytical TLC and SRL silica gel (100-200 mesh) was used for column chromatography. NMR (^1H, $^{13}C\{^1H\}$, ^{19}F and NOESY) spectra were recorded on Brucker 400, 500 and 600 MHz spectrometer using $CDCl_3$ as solvent and Me_4Si as an internal standard. Chemical shifts (δ) and spin-spin coupling constant (*J*) are reported in ppm and in Hz, respectively, and other data are reported as follows: s = singlet, d = doublet, t = triplet, m = multiplet, q = quartet, dd = doublet of doublet. Melting points were determined using a Büchi B-540 apparatus and are uncorrected. FT-IR spectra were collected on Perkin Elmer IR spectrometer. Q-Tof ESI-MS (model HAB 273) was used for recording mass spectra. Optical rotation was determined using Rudolph autopol I automatic polarimeter. HPLC analysis was carried out using Waters-2489 with Daicel Chiralcel OJ-H column utilizing *iso*-propanol and hexane as eluent. Single crystal X-ray data of **3af** was determined using Bruker SMART

APEX-II CCD diffractometer, which is equipped with 1.75 kW sealed-tube Mo-Kα irradiation and the crystal structure was solved by direct method using SHELXL-14 (Göttingen, Germany) and refined with full-matrix least squares on F^2 using SHELXL-14, while the single crystal X-ray data of **3ha'** was determined using Bruker SMART APEX-II CCD diffractometer, which is equipped with 1.75 kW sealed-tube Mo-Kα irradiation and the crystal structure was solved by direct method using SHELXL-19 (Göttingen, Germany) and refined with full-matrix least squares on F^2 using SHELXL-19.

General Procedure for the Synthesis of Tetrahydro-[1,3,4]-oxadiazines. Diaziridine **1** (0.2 mmol, 1.0 equiv), oxirane **2** (0.2 mmol, 1.0 equiv) and $CoCl_2$ (3 mg, 0.02 mmol, 0.1 equiv) were stirred for 1 h in CH_2Cl_2 (2.0 mL, 0.1 M) at room temperature (25 ^oC). The reaction mixture was diluted using CH_2Cl_2 (5 mL) and passed through a short pad of celite using CH_2Cl_2 (10 mL). Evaporation of the solvent gave a residue that was purified on silica gel column chromatography using ethyl acetate and hexane as eluent to afford [1,3,4]-oxadiazine motifs.

General Procedure for the Enantiospecific Synthesis of Tetrahydro-[1,3,4]-oxadiazines. A mixture of diaziridine **1** (0.2 mmol, 1.0 equiv), enantioenriched oxirane (0.2 mmol, 1.0 equiv) and $CoCl_2$ (3 mg, 0.02 mmol, 0.1 equiv) was stirred for 1 h in CH_2Cl_2 (2.0 mL, 0.1 M) at room temperature (25 ^oC). The purification was performed as above in general procedure. The enantiomeric excess was determined using chiral HPLC.

Enantioselective Synthesis of 3ca′. 6-(3-Nitrophenyl)-1,5-diazabicyclo[3.1.0]hexane **1c** (41 mg, 0.2 mmol, 1.0 equiv), 2-phenyloxirane **2a** (24 mg, 0.2 mmol, 1.0 equiv) and chiral Co(Salen) **C1**/**C2** (0.02 mmol, 0.1 equiv) were stirred for 1 h in CH_2Cl_2 (2.0 mL, 0.1 M) at room temperature. The reaction mixture was diluted using CH_2Cl_2 (5 mL) and passed through a short pad of celite using CH_2Cl_2 (10 mL). Evaporation of the solvent gave a residue that was purified on silica gel column chromatography using ethyl acetate and hexane as eluent to afford 1-(3-nitrophenyl)-4-phenyltetrahydro-1H,6H-pyrazolo **3ca′** whose *ee* was determined using chiral HPLC with Daicel Chiralcel OJ-H column using hexane and *iso*-propanol (9:1).

Epimerization Reaction.[18] Acetic acid (6 μL, 0.1 mmol, 1.0 equiv) was added to a stirring solution of **3a** (28 mg, 0.1 mmol, 1.0 equiv) in CH_2Cl_2 (1 mL, 0.1 M) and the stirring was continued for 6 h at room temperature. The reaction mixture was quenched using saturated aqueous $NaHCO_3$ (10 mL) and extracted with CH_2Cl_2 (3 × 10 mL). Drying (Na_2SO_4) and evaporation of the solvent gave a residue that was purified on silica gel column chromatography using ethyl acetate and hexane as an eluent to give **3aa** in 95% yield (27 mg).

Scale-up Synthesis of 3ea. 6-(4-Bromophenyl)-1,5-diazabicyclo[3.1.0]hexane **1e** (1.2 g , 5 mmol, 1.0 equiv), styrene oxide **2a** (600 mg, 5 mmol, 1.0 equiv) and $CoCl_2$ (65 mg, 0.5 mmol, 0.1 equiv) were stirred for 1 h in CH_2Cl_2 (50 mL, 0.1 M) at room temperature. The reaction mixture was then diluted with CH_2Cl_2 (20 mL) and passed through a short pad of celite using CH_2Cl_2 (100 mL). Evaporation of the solvent gave a residue that was purified on silica gel column chromatography using ethyl acetate and hexane as an eluent to yield **3ea** in 70% yield (1.2 g).

Synthesis of 4. Compound **3ea** (72 mg, 0.2 mmol, 1.0 equiv), boronic acid (50 mg, 0.2 mmol, 1.0 equiv), $Pd(PPh_3)_4$ (7 mg, 0.006 mmol, 0.03 equiv), Na_2CO_3 (22 mg, 0.2 mmol, 1.0 equiv) and H_2O (50 µL) were stirred in toluene: EtOH (1:1, 2 mL) at 100 °C in an oil bath for 12 h under N_2 atmosphere. The reaction mixture was cooled to room temperature and passed through a short pad of celite using CH_2Cl_2 (10 mL). Evaporation of the solvent gave a residue that was purified on silica gel column chromatography to give **4** in 81% yield (78 mg).

Synthesis of 5.[19] Compound **3ae** (72 mg, 0.2 mmol, 1.0 equiv), bis(pinacolato)diboron (50 mg, 0.2 mmol, 1.0 equiv), KOAc (40 mg, 0.4 mmol, 2.0 equiv) and $Pd(dppf)Cl_2$•CH_2Cl_2 (8 mg, 0.01 mmol, 0.05 equiv) were stirred in THF (3 mL) at 100 ºC for 4 h in a pressure tube. After completion, the reaction mixture was cooled to room temperature and passed through a short pad of celite using CH_2Cl_2 (15 ml). Evaporation of the solvent gave a residue that was purified on silica gel column chromatography using hexane and ethyl acetate as an eluent to give **5** in 75% yield (61 mg).

2.4 Characterization Data of the Products

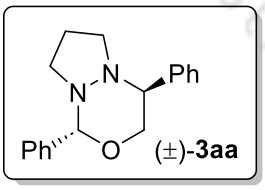

1,4-Diphenyltetrahydro-1H,6H-pyrazolo[1,2-c][1,3,4]oxadiazine

3aa. Analytical TLC on silica gel, 1:24 ethyl acetate/hexane R_f = 0.48; colorless solid; mp 101-102 ºC; yield 82% (46 mg); ^{1}H NMR (500 MHz, $CDCl_3$) δ 7.49-7.47 (m, 2H), 7.36-7.34 (m, 2H), 7.29-7.22 (m, 6H), 4.94 (s, 1H), 3.96-3.91 (m, 1H), 3.69-3.64 (m, 2H), 2.92-2.88 (m, 1H), 2.67-2.62 (m, 1H), 2.41-2.31 (m, 2H), 1.79-1.71 (m, 2H); ^{13}C{^{1}H} NMR (125 MHz, $CDCl_3$) δ 138.26, 138.23, 129.0, 128.6, 128.4, 128.2, 128.1, 127.6, 95.5, 72.2, 66.5, 51.5, 46.8, 22.0; FT-IR (KBr) 2963, 2852, 1493, 1453, 1365, 1313, 1118, 1075, 1039 cm^{-1}; HRMS (ESI) m/z $[M+H]^+$ calcd for $C_{18}H_{21}N_2O$: 281.1648, found: 281.1645.

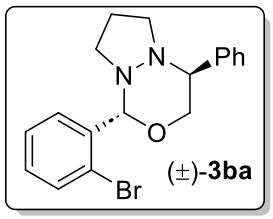

1-(2-Bromophenyl)-4-phenyltetrahydro-1H,6H-pyrazolo[1,2-c][1,3,4]oxadiazine 3ba. Analytical TLC on silica gel, 1:9 ethyl acetate/hexane R_f = 0.50; colorless liquid; yield 75% (54 mg); ^{1}H NMR (500 MHz, $CDCl_3$) δ 7.72 (d, *J* = 7.5 Hz, 1H), 7.50 (d, *J* = 8.0 Hz, 1H), 7.38-7.36 (m, 2H), 7.30-7.22 (m, 4H), 7.15-7.12 (m, 1H), 5.37 (s, 1H), 3.92-3.89 (m, 1H), 3.72-3.67 (m, 1H), 3.64-3.62 (m, 1H), 2.93-2.88 (m, 1H), 2.67-2.62 (m, 1H), 2.54-2.49 (m, 1H), 2.34-2.29 (m, 1H), 1.77-1.71 (m, 2H); ^{13}C{^{1}H} NMR (150 MHz, $CDCl_3$) δ 137.9, 137.1, 132.7, 130.44, 130.40, 128.6, 128.29, 128.23, 127.8, 123.4, 93.8, 72.1, 67.9, 51.6, 47.0, 21.7; FT-IR (neat) 2960, 2852, 1492, 1452, 1114, 1075, 1035, 752 cm^{-1}; HRMS (ESI) m/z $[M+H]^+$ calcd for $C_{18}H_{20}BrN_2O$: 359.0754, found: 359.0753.

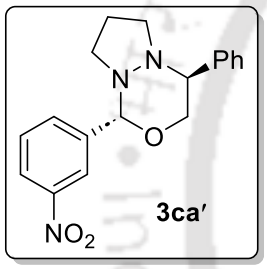

(1*R*,4*S*)-1-(3-Nitrophenyl)-4-phenyltetrahydro-1H,6H-pyrazolo[1,2-c][1,3,4]oxadiazine 3ca'. Analytical TLC on silica gel, 1:19 ethyl acetate/hexane R_f = 0.48; yellow solid; mp 142-143 °C; yield 66% (43 mg); ^{1}H NMR (400 MHz, $CDCl_3$) δ 8.36-8.35 (m, 1H), 8.14-8.12 (m, 1H), 7.82 (d, *J* = 7.6, 1H), 7.47 (t, *J* = 8.0 Hz, 1H), 7.35-7.33 (m, 2H), 7.29-7.20 (m, 3H), 5.13 (s, 1H), 3.97-3.91 (m, 1H), 3.70-3.64 (m, 2H), 2.92-2.86 (m, 1H), 2.67-2.62 (m, 1H), 2.44-2.38 (m, 1H), 2.35-2.29 (m, 1H), 1.87-1.70 (m, 2H); ^{13}C{^{1}H} NMR (100 MHz, $CDCl_3$) δ 148.3, 140.3, 137.8, 133.7, 129.4, 128.7, 128.2, 128.1, 123.9, 122.7, 93.2, 72.2, 65.2, 51.3, 45.9, 22.1; FT-IR (KBr) 2961, 2853, 1531, 1492, 1349, 1112, 1077, 1060 cm^{-1}; HRMS (ESI) m/z $[M+H]^+$ calcd for $C_{18}H_{20}N_3O_3$: 326.1499, found: 326.1506; $[\alpha]_D^{21.5}$ = +110 (c = 0.05, $CHCl_3$); HPLC: >99% *ee* [CHIRALCEL OJ-H, hexane/^{i}PrOH = 90:10, flow rate: 1 mL /min, λ = 254 nm, t_R = 15.13 min (minor), 20.62 min (major)].

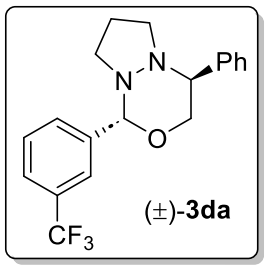

4-Phenyl-1-(3-(trifluoromethyl)phenyl)tetrahydro-1H,6H-pyrazolo[1,2-c][1,3,4]oxadiazine 3da. Analytical TLC on silica gel, 1:19 ethyl acetate/hexane R_f = 0.43; colorless solid; mp 85-86 ºC; yield 66% (46 mg); ^{1}H NMR (500 MHz, $CDCl_3$) δ 7.86 (s, 1H), 7.76 (d, *J* = 7.5 Hz, 1H), 7.63 (d, *J* = 7.5 Hz, 1H), 7.52-7.49 (m, 1H), 7.45-7.43 (m, 2H), 7.37-7.30 (m, 3H), 5.15 (s, 1H), 4.06-4.01 (m, 1H), 3.79-3.73 (m, 2H), 3.01-2.97 (m, 1H), 2.75-2.71 (m, 1H), 2.52-2.47 (m,1H), 2.43-2.38 (m, 1H), 1.91-1.82 (m, 2H); ^{13}C{^{1}H} NMR (125 MHz, $CDCl_3$) δ 139.2, 138.0, 131.3 (q, J_{C-F} = 32.2 Hz), 131.1, 128.9, 128.7, 128.2, 127.5, 127.4 (q, J_{C-F} = 270.6 Hz), 125.9 (q, J_{C-F} = 3.6 Hz), 124.6 (q, J_{C-F} = 3.7 Hz), 94.1, 72.2, 65.7, 51.4, 46.2, 22.1;^{19}F NMR (377 MHz, $CDCl_3$) δ -62.4; FT-IR (KBr) 2961, 2854, 1493, 1452, 1326, 1273, 1165, 1126, 1072 cm^{-1}; HRMS (ESI) m/z $[M+H]^+$ calcd for $C_{19}H_{20}F_3N_2O$: 349.1522, found: 349.1523.

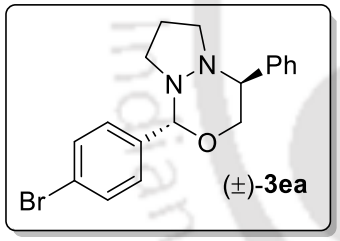

1-(4-Bromophenyl)-4-phenyltetrahydro-1H,6H-pyrazolo[1,2-c][1,3,4]oxadiazine 3ea. Analytical TLC on silica gel, 1:19 ethyl acetate/hexane R_f = 0.42; colorless solid; mp 115-116 ºC ; yield 81% (58 mg); ^{1}H NMR (500 MHz, $CDCl_3$) δ 7.45 (d, *J* = 8 Hz, 2H), 7.37-7.34 (m, 4H), 7.29-7.22 (m, 3H), 4.93 (s, 1H), 3.95-3.90 (m, 1H), 3.68-3.63 (m, 2H), 2.92-2.87 (m, 1H), 2.66-2.61 (m, 1H), 2.41-2.36 (m, 1H), 2.33-2.28 (m, 1H), 1.81-1.72 (m, 2H); ^{13}C{^{1}H} NMR (125 MHz, $CDCl_3$) δ 138.1, 137.3, 131.6, 129.3, 128.7, 128.26, 128.25, 123.0, 94.5, 72.2, 66.1, 51.5, 46.5, 22.0; FT-IR (KBr) 2961, 2852, 1594, 1488, 1452, 1361, 1113, 1068, 1012 cm^{-1}; HRMS (ESI) m/z $[M+H]^+$ calcd for $C_{18}H_{20}BrN_2O$: 359.0754, found: 359.0740.

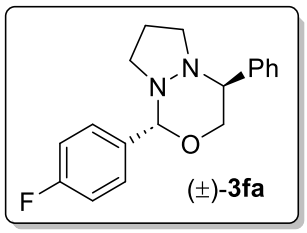

1-(4-Fluorophenyl)-4-phenyltetrahydro-1H,6H-pyrazolo[1,2-c][1,3,4]oxadiazine 3fa. Analytical TLC on silica gel, 1:24 ethyl acetate/hexane R_f = 0.45; colorless solid; mp 101-102 °C; yield 79% (47 mg); ^{1}H NMR (400 MHz, $CDCl_3$) δ 7.55-7.51 (m, 2H), 7.43-7.41 (m, 2H), 7.37-7.30 (m, 3H), 7.08-7.04 (m, 2H), 4.98 (s, 1H), 4.03-3.96 (m, 1H), 3.76-3.69 (m, 2H), 3.00-2.94 (m, 1H), 2.72-2.66 (m, 1H), 2.48-2.35 (m, 2H), 1.88-1.78(m, 2H); ^{13}C{^{1}H} NMR (100 MHz, $CDCl_3$) δ 164.4 (d, $J_{C\text{-}F}$ = 245.5 Hz), 138.0, 134.2 (d, $J_{C\text{-}F}$ = 3.2 Hz), 129.4 (d, $J_{C\text{-}F}$ = 8.2 Hz), 128.7, 128.2, 115.5 (d, $J_{C\text{-}F}$ = 21.3 Hz), 94.8, 72.2, 66.5, 51.5, 46.9, 21.9; ^{19}F NMR (471 MHz, $CDCl_3$) δ -112.8; FT-IR (KBr) 2957, 2853, 1609, 1492, 1453, 1362, 1225, 1117, 1076 cm^{-1}; HRMS (ESI) m/z $[M+H]^+$ calcd for $C_{18}H_{20}FN_2O$: 299.1554, found: 299.1555.

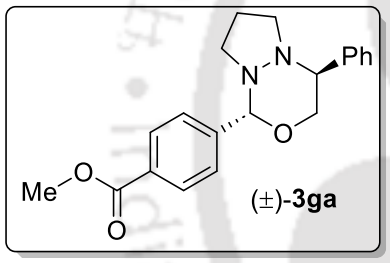

Methyl 4-(4-phenyltetrahydro-1H,6H-pyrazolo[1,2-c][1,3,4]oxadiazin-1-yl)benzoate 3ga. Analytical TLC on silica gel, 1:19 ethyl acetate/hexane R_f = 0.45; colorless solid; mp 134-135 °C; yield 81% (55 mg); ^{1}H NMR (400 MHz, $CDCl_3$) δ 8.00 (d, J = 8.4 Hz, 2H), 7.57 (d, J = 8 Hz, 2H), 7.37-7.35 (m, 2H), 7.31-7.22 (m, 3H), 5.07 (s, 1H), 3.99-3.92 (m, 1H), 3.85 (s, 3H), 3.71-3.65 (m, 2H), 2.93-2.88 (m, 1H), 2.67-2.61 (m, 1H), 2.44-2.38 (m, 1H), 2.36-2.30 (m, 1H), 1.85-1.71 (m, 2H); ^{13}C{^{1}H} NMR (100 MHz, $CDCl_3$) δ 166.9, 142.9, 138.0, 130.7, 129.8, 128.7, 128.2, 127.6, 94.4, 72.2, 65.7, 52.3, 51.4, 46.2, 22.1; FT-IR (KBr) 2968, 2842, 1725, 1451,1276, 1112, 1075 cm^{-1}; HRMS (ESI) m/z $[M+H]^+$ calcd for $C_{20}H_{23}N_2O_3$: 339.1703, found: 339.1703.

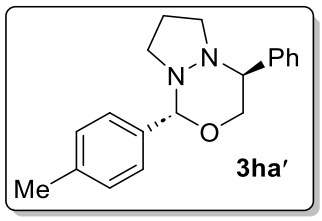

(1*R*,4*S*)-4-Phenyl-1-(*p*-tolyl)tetrahydro-1H,6H-pyrazolo[1,2-c][1,3,4]oxadiazine 3ha'. Analytical TLC on silica gel, 1:24 ethyl acetate/hexane R_f = 0.48;

colorless solid; mp 110-111 °C; yield 84% (49 mg); ^{1}H NMR (500 MHz, $CDCl_3$) δ 7.36-7.34 (m, 4H), 7.27-7.20 (m, 3H), 7.10 (d, *J* = 8.0 Hz, 2H), 4.89 (s, 1H), 3.94-3.89 (m, 1H), 3.68-3.63 (m, 2H), 2.91-2.87 (m, 1H), 2.66-2.62 (m, 1H), 2.40-2.27 (m, 5H), 1.80-1.67 (m, 2H); ^{13}C{^{1}H} NMR (100 MHz, $CDCl_3$) δ 138.8, 138.2, 135.3, 129.1, 128.6, 128.2, 128.1, 127.5, 95.5, 72.2, 66.7, 51.5, 46.9, 21.9, 21.3; FT-IR (KBr) 2961, 2850, 1493, 1452, 1362, 1177, 1075, 1059, 1038 cm^{-1}; HRMS (ESI) m/z $[M+H]^+$ calcd for $C_{19}H_{23}N_2O$: 295.1805, found: 295.1804; $[\alpha]_D^{21.5}$ = +144 (c = 0.05, $CHCl_3$); HPLC: >98% *ee* [CHIRALCEL OJ-H, hexane/^{i}PrOH = 90:10, flow rate: 1 mL /min, λ = 254 nm, t_R = 6.84 min (minor), 13.13 min (major)].

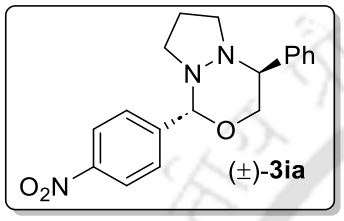

1-(4-Nitrophenyl)-4-phenyltetrahydro-1H,6H-pyrazolo[1,2-c][1,3,4]oxadiazine 3ia. Analytical TLC on silica gel, 1:19 ethyl acetate/hexane R_f = 0.42; yellow solid; mp 142-143 °C; yield 80% (52 mg); ^{1}H NMR (500 MHz, $CDCl_3$) δ 8.25 (d, *J* = 8.5 Hz, 2H), 7.75 (d, *J* = 8.5 Hz, 2H), 7.43-7.42 (m, 2H), 7.37-7.30 (m, 3H), 5.24 (s, 1H), 4.06-4.01 (m, 1H), 3.78-3.73 (m, 2H), 3.00-2.95 (m, 1H), 2.75-2.70 (m, 1H), 2.53-2.48 (m, 1H), 2.42-2.37 (m, 1H), 1.95-1.81 (m, 2H); ^{13}C{^{1}H} NMR (125 MHz, $CDCl_3$) δ 148.4, 144.9, 137.8, 128.8, 128.6, 128.3, 128.2, 123.7, 93.2, 72.2, 65.0, 51.3, 45.7, 22.2; FT-IR (KBr) 2962, 2853, 1604, 1520, 1452, 1345, 1109, 1058 cm^{-1}; HRMS (ESI) m/z $[M+H]^+$ calcd for $C_{18}H_{20}N_3O_3$: 326.1499, found: 326.1500.

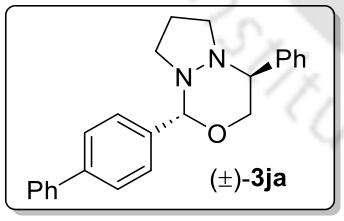

1-([1,1'-Biphenyl]-4-yl)-4-phenyltetrahydro-1H,6H-pyrazolo[1,2-c][1,3,4]oxadiazine 3ja. Analytical TLC on silica gel, 1:19 ethyl acetate/hexane R_f = 0.40; colorless solid; mp 144-144 °C; yield 84% (60 mg); ^{1}H NMR (400 MHz, $CDCl_3$) δ 7.65-7.60 (m, 6H), 7.47-7.43 (m, 4H), 7.38-7.30 (m, 4H), 5.08 (s, 1H), 4.08-4.01 (m, 1H), 3.81-3.75 (m, 2H), 3.03-2.98 (m, 1H), 2.83-2.78 (m, 1H), 2.52-2.44 (m, 2H), 1.91-1.81 (m, 2H); ^{13}C{^{1}H} NMR (125 MHz, $CDCl_3$) δ 141.9, 140.9, 138.2, 137.2, 128.8, 128.7, 128.2, 128.1, 128.0, 127.5, 127.3, 127.2, 95.2, 72.3, 66.5, 51.5, 46.8, 22.0; FT-IR (KBr) 2959, 2853, 1488,

1363, 1107, 1074, 1039 cm^{-1}; HRMS (ESI) m/z $[M+H]^+$ calcd for $C_{24}H_{25}N_2O$: 357.1961, found: 357.1964.

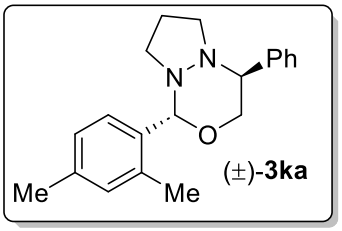

1-(2,4-Dimethylphenyl)-4-phenyltetrahydro-1H,6H-pyrazolo[1,2-c][1,3,4]oxadiazine 3ka. Analytical TLC on silica gel, 1:24 ethyl acetate/hexane R_f = 0.50; colorless liquid; yield 81% (50 mg); ^1H NMR (500 MHz, $CDCl_3$) δ 7.54 (d, *J* = 8.0 Hz, 1H), 7.44-7.43 (m, 2H), 7.36-7.29 (m, 3H), 7.04 (d, *J* = 7.5 Hz, 1H), 6.99 (s, 1H), 5.21 (s, 1H), 4.02-3.96 (m, 1H), 3.78-3.71 (m, 2H), 2.98-2.94 (m, 1H), 2.85-2.80 (m, 1H), 2.48-2.43 (m, 4H), 2.37-2.31 (m, 4H), 1.90-1.73 (m, 2H); $^{13}C\{^1H\}$ NMR (125 MHz, $CDCl_3$) δ 138.3, 138.2, 136.2, 133.4, 131.2, 128.6, 128.3, 128.1, 128.0, 126.7, 92.4, 72.2, 66.7, 51.5, 46.6, 21.9, 21.2, 19.6; FT-IR (neat) 2919, 2851, 1736, 1452, 1113, 1057, 738 cm^{-1}; HRMS (ESI) m/z $[M+H]^+$ calcd for $C_{20}H_{25}N_2O$: 309.1961, found: 309.1972.

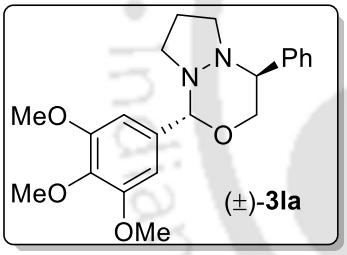

4-Phenyl-1-(3,4,5-trimethoxyphenyl)tetrahydro-1H,6H-pyrazolo[1,2-c][1,3,4]oxadiazine 3la. Analytical TLC on silica gel, 1:4 ethyl acetate/hexane R_f = 0.56; colorless solid; mp 122-123 ºC; yield 83% (61 mg); ^1H NMR (400 MHz, $CDCl_3$) δ 7.43-7.41 (m, 2H), 7.36-7.30 (m, 3H), 6.79 (s, 2H), 4.96 (s, 1H), 4.04-3.97 (m, 1H), 3.89 (s, 6H), 3.84 (s, 3H), 3.75-3.69 (m, 2H), 3.00-2.94 (m, 1H), 2.83-2.78 (m, 1H), 2.51-2.38 (m, 2H), 1.94-1.77 (m, 2H); $^{13}C\{^1H\}$ NMR (125 MHz, $CDCl_3$) δ 153.3, 138.5, 138.2, 133.8, 128.7, 128.24, 128.20, 104.6, 95.3, 72.3, 66.0, 60.9, 56.3, 51.5, 46.6, 22.0; FT-IR (KBr) 2922, 2850, 1593, 1460, 1367, 1232, 1125, 735 cm^{-1}; HRMS (ESI) m/z $[M+H]^+$ calcd for $C_{21}H_{27}N_2O$: 371.1965, found: 371.1975.

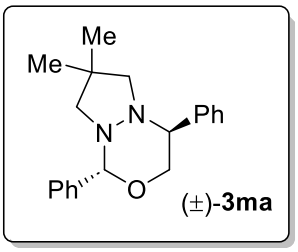

7,7-Dimethyl-1,4-diphenyltetrahydro-1H,6H-pyrazolo[1,2-c][1,3,4]oxadiazine 3ma. Analytical TLC on silica gel, 1:19 ethyl acetate/hexane R_f = 0.45; colorless solid; mp 123-124 ºC; yield 77% (47 mg); ^{1}H NMR (500 MHz, $CDCl_3$) δ 7.55-7.53 (m, 2H), 7.43-7.41 (m, 2H), 7.37-7.29 (m, 6H), 4.80 (s, 1H), 3.99-3.96 (m, 1H), 3.77-3.67 (m, 2H), 2.72 (d, *J* = 9.0 Hz, 1H), 2.40 (d, *J* = 8.5 Hz, 1H), 2.25-2.22 (m, 2H), 1.07 (d, *J* = 14.0 Hz, 6H); ^{13}C{^{1}H} NMR (125 MHz, $CDCl_3$) δ 138.2, 129.2, 128.6, 128.4, 128.1, 128.0, 127.9, 96.6, 72.4, 68.0, 66.9, 63.3, 36.4, 29.1, 28.8; FT-IR (KBr) 2958, 2851, 1738, 1453, 1366, 1119, 1063, 751, 699 cm^{-1}; HRMS (ESI) m/z [M+H]$^+$ calcd for $C_{20}H_{25}N_2O$: 309.1961, found: 309.1966.

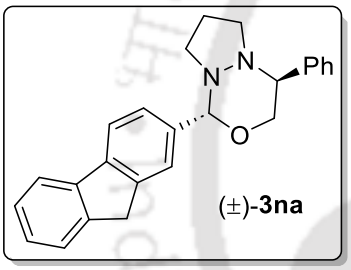

1-(9H-Fluoren-2-yl)-4-phenyltetrahydro-1H,6H-pyrazolo[1,2-c][1,3,4]oxadiazine 3na. Analytical TLC on silica gel, 1:19 ethyl acetate/hexane R_f = 0.46; colorless solid; mp 185-186 ºC ; yield 75% (55 mg); ^{1}H NMR (400 MHz, $CDCl_3$) δ 7.81-7.78 (m, 3H), 7.56 (d, *J* = 7.6 Hz, 2H), 7.47-7.45 (m, 2H), 7.40-7.30 (m, 5H), 5.06 (s, 1H), 4.09-4.02 (m, 1H), 3.93 (s, 2H), 3.82-3.76 (m, 2H), 3.04-2.98 (m, 1H), 2.79-2.73 (m, 1H), 2.51-2.44 (m, 2H), 1.89-1.80 (m, 2H); ^{13}C{^{1}H} NMR (125 MHz, $CDCl_3$) δ 143.7, 143.5, 142.6, 141.4, 138.2, 136.8, 128.7, 128.28, 128.20, 127.0, 126.8, 126.5, 125.2, 124.1, 120.1, 119.7, 96.0, 72.3, 67.0, 51.6, 47.2, 37.0, 21.9; FT-IR (KBr) 2960, 2851, 1453, 1357, 1116, 1073, 1038 cm^{-1}; HRMS (ESI) m/z [M+H]$^+$ calcd for $C_{25}H_{25}N_2O$: 369.1961, found: 369.1961.

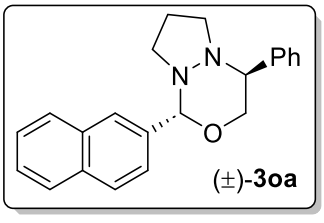

1-(Naphthalen-2-yl)-4-phenyltetrahydro-1H,6H-pyrazolo[1,2-c][1,3,4]oxadiazine 3oa. Analytical TLC on silica gel, 1:19 ethyl acetate/hexane R_f = 0.44; colorless solid; mp 99-100 ºC ; yield 73% (48 mg); ^{1}H NMR (500 MHz, $CDCl_3$) δ 8.02 (s, 1H),

7.90-7.84 (m, 3H), 7.73-7.71 (m, 1H), 7.51-7.47 (m, 4H), 7.39-7.31 (m, 3H), 5.23 (s, 1H), 4.11-4.05 (m, 1H), 3.85-3.80 (m, 2H), 3.04-3.00 (m, 1H), 2.77-2.73 (m, 1H), 2.54-2.44 (m, 2H), 1.89-1.81 (m, 2H); $^{13}C\{^{1}H\}$ NMR (125 MHz, $CDCl_3$) δ 138.2, 135.7, 133.9, 133.2, 128.7, 128.4, 128.3, 128.2, 127.8, 126.9, 126.4, 126.1, 125.2, 95.4, 72.3, 66.4, 51.6, 46.7, 22.0; FT-IR (KBr) 2961, 2850, 1696, 1492, 1452, 1335, 1175, 1117, 1074, 1059 cm^{-1}; HRMS (ESI) m/z $[M+H]^+$ calcd for $C_{22}H_{23}N_2O$: 331.1805, found: 331.1805.

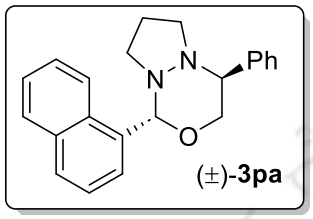

1-(Naphthalen-1-yl)-4-phenyltetrahydro-1H,6H-pyrazolo[1,2-c][1,3,4]oxadiazine 3pa. Analytical TLC on silica gel, 1:19 ethyl acetate/hexane R_f = 0.42; thick liquid; yield 72% (47 mg); ^{1}H NMR (400 MHz, $CDCl_3$) δ 8.69 (d, *J* = 8.4 Hz, 1H), 7.78 (d, *J* = 8 Hz, 2H), 7.70 (d, *J* = 7.2 Hz, 1H), 7.48-7.37 (m, 5H), 7.31-7.22 (m, 3H), 5.62 (s, 1H), 4.05-3.99 (m, 1H), 3.82-3.76 (m, 2H), 2.95-2.89 (m, 1H), 2.67-2.61 (m, 1H), 2.48-2.42 (m, 1H), 2.29-2.22 (m, 1H), 1.80-1.64 (m, 2H); $^{13}C\{^{1}H\}$ NMR (125 MHz, $CDCl_3$) δ 138.3, 133.9, 131.2, 129.4, 128.6, 128.3, 128.2, 128.0, 126.1, 125.9, 125.7, 125.2, 125.1, 93.9, 72.5, 65.9, 51.5, 46.1, 22.0; FT-IR (neat) 2961, 2854, 1510, 1492, 1451, 1171, 1112, 1064 cm^{-1}; HRMS (ESI) m/z $[M+H]^+$ calcd for $C_{22}H_{23}N_2O$: 331.1805, found: 331.1805.

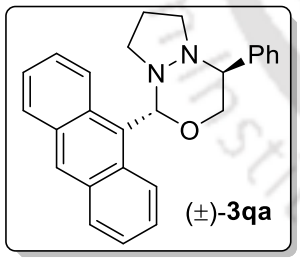

1-(Anthracen-9-yl)-4-phenyltetrahydro-1H,6H-pyrazolo[1,2-c][1,3,4]oxadiazine 3qa. Analytical TLC on silica gel, 1:24 ethyl acetate/hexane R_f = 0.42; yellow thick liquid; yield 68% (52 mg); ^{1}H NMR (500 MHz, $CDCl_3$) δ 9.73 (d, *J* = 8.5 Hz, 1H), 8.67 (d, *J* = 9 Hz, 1H), 8.49 (s, 1H), 8.04-7.98 (m, 2H), 7.59-7.53 (m, 4H), 7.50-7.45 (m, 2H), 7.43-7.40 (m, 2H), 7.37-7.35 (m, 1H), 6.42 (s, 1H), 4.21-4.18 (m, 1H), 4.07-4.05 (m, 1H), 3.98-3.94 (m, 1H), 3.10-3.06 (m, 1H), 2.52-2.45 (m, 2H), 2.41-2.37 (m, 1H), 1.77-1.69 (m, 2H);$^{13}C\{^{1}H\}$ NMR (125 MHz, $CDCl_3$) δ 138.3, 132.1, 131.3, 131.0, 130.5, 129.6, 129.5, 128.9, 128.7, 128.37, 128.32, 128.29, 128.24, 126.3, 125.3, 125.1, 124.6, 123.5, 93.0, 73.0, 69.6, 52.1,

47.7, 21.7; FT-IR (neat) 2960, 2850, 1493, 1450, 1312, 1111, 1068, 1045 cm^{-1}; HRMS (ESI) m/z $[M+H]^+$ calcd for $C_{26}H_{25}N_2O$: 381.1961, found: 381.1961.

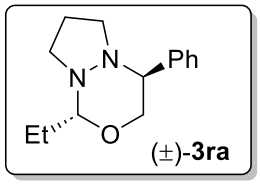

1-Ethyl-4-phenyltetrahydro-1H,6H-pyrazolo[1,2-c][1,3,4]oxadiazine 3ra. Analytical TLC on silica gel, 1:19 ethyl acetate/hexane R_f = 0.55; colorless liquid; yield 80% (37 mg); ^1H NMR (500 MHz, $CDCl_3$) δ 7.37-7.26 (m, 5H), 4.18-4.16 (m, 1H), 3.89-3.83 (m, 1H), 3.60-3.54 (m, 2H), 3.21-3.16 (m, 1H), 2.90-2.85 (m, 1H), 2.62-2.57 (m, 1H), 2.48-2.43 (m, 1H), 2.03-1.94 (m, 1H), 1.92-1.84 (m, 1H), 1.73-1.61 (m, 2H), 1.03 (t, *J* = 7.5 Hz, 3H); $^{13}C\{^1H\}$ NMR (125 MHz, $CDCl_3$) δ 138.5, 128.6, 128.2, 128.0, 93.8, 72.1, 64.3, 51.0, 44.5, 26.5, 22.3, 9.4; FT-IR (neat) 2964, 2829, 1493, 1452, 1378, 1329, 1134, 1059, 1030, 755 cm^{-1}; HRMS (ESI) m/z $[M+H]^+$ calcd for $C_{14}H_{21}N_2O$: 233.1648, found: 233.1642.

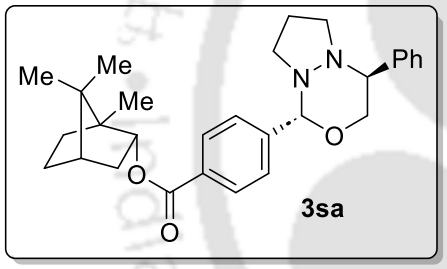

(1*S*,2*R*,4*S*)-1,7,7-Trimethylbicyclo[2.2.1]heptan-2-yl 4-(4-phenyltetrahydro-1H,6H-pyrazolo[1,2-c][1,3,4]oxadiazin-1-yl)benzoate 3sa. Analytical TLC on silica gel, 1:19 ethyl acetate/hexane R_f = 0.48; colorless solid; mp 137-138 ºC; yield 79% (73 mg); ^1H NMR (500 MHz, $CDCl_3$) δ 8.00 (d, *J* = 8.0 Hz, 2H), 7.57 (d, *J* = 8.5 Hz, 2H), 7.36-7.35 (m, 2H), 7.29-7.21 (m, 3H), 5.08-5.04 (m, 2H), 3.97-3.92 (m, 1H), 3.70-3.65 (m, 2H), 2.92-2.88 (m, 1H), 2.68-2.63 (m, 1H), 2.44-2.37 (m, 2H), 2.35-2.30 (m, 1H), 2.09-2.03 (m, 1H), 1.85-1.70 (m, 3H), 1.66 (t, *J* = 4.5 Hz, 1H), 1.37-1.31 (m, 1H), 1.27-1.22 (m, 1H), 1.07-1.04 (m, 1H), 0.90 (s, 3H), 0.84 (s, 6H); $^{13}C\{^1H\}$ NMR (125 MHz, $CDCl_3$) δ 166.6, 142.8, 138.1, 131.5, 129.7, 128.7, 128.27, 128.24, 127.6, 94.3, 80.7, 72.3, 65.5, 51.4, 49.2, 48.0, 46.1, 45.1, 37.0, 28.2, 27.5, 22.1, 19.8, 19.0, 13.7; FT-IR (KBr) 2955, 2929, 1716, 1453, 1363, 1272, 1116, 1076, 1020 cm^{-1}; HRMS (ESI) m/z $[M+H]^+$ calcd for $C_{29}H_{37}N_2O_3$: 461.2799, found: 461.2806.

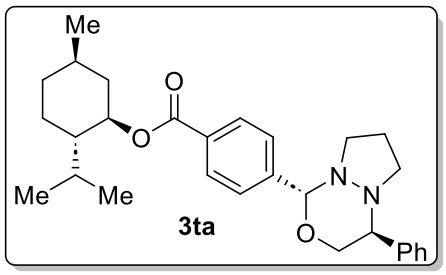

(1*R*,2*S*,5*R*)-2-Isopropyl-5-methylcyclohexyl 4-(4-phenyltetrahydro-1H,6H-pyrazolo[1,2-c][1,3,4]oxadiazin-1-yl)benzoate 3ta. Analytical TLC on silica gel, 1:19 ethyl acetate/hexane R_f = 0.42; yellow thick liquid; yield 75% (69 mg); ^{1}H NMR (500 MHz, $CDCl_3$) δ 8.06 (d, *J* = 8.0 Hz, 2H), 7.63 (d, *J* = 8.0 Hz, 2H), 7.43-7.42 (m, 2H), 7.36-7.29 (m, 3H), 5.15 (s, 1H), 4.96-4.91 (m, 1H), 4.05-3.99 (m, 1H), 3.77-3.72 (m, 2H), 3.00-2.95 (m, 1H), 2.75-2.70 (m, 1H), 2.51-2.46 (m, 1H), 2.42-2.37 (m, 1H), 2.14-2.12 (m, 1H), 1.98-1.92 (m, 1H), 1.89-1.82 (m, 2H), 1.74-1.72 (m, 2H), 1.58-1.54 (m, 2H), 1.17-1.07 (m, 2H), 0.93-0.91 (m, 7H), 0.80 (d, *J* = 7.0 Hz, 3H); ^{13}C{^{1}H} NMR (125 MHz, $CDCl_3$) δ 165.9, 142.7, 138.1, 131.4, 129.7, 128.7, 128.26, 128.24, 127.5, 94.3, 75.0, 72.2, 65.6, 51.4, 47.4, 46.1, 41.1, 34.4, 31.5, 26.6, 23.8, 22.1, 20.8, 16.7; FT-IR (neat) 2956, 2870, 1714, 1453, 1364, 1273, 1114, 1076 cm^{-1}; HRMS (ESI) m/z [M+H]$^+$ calcd for $C_{29}H_{39}N_2O_3$: 463.2955, found: 463.2956.

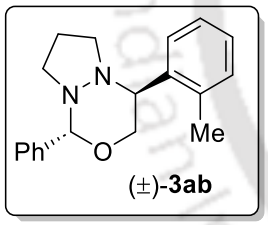

1-Phenyl-4-(*o*-tolyl)tetrahydro-1H,6H-pyrazolo[1,2-c][1,3,4]oxadiazine 3ab. Analytical TLC on silica gel, 1:24 ethyl acetate/hexane R_f = 0.48; thick liquid; yield 68% (40 mg); ^{1}H NMR (600 MHz, $CDCl_3$) δ 7.63 (d, *J* = 7.8 Hz, 1H), 7.57-7.56 (m, 2H), 7.40-7.35 (m, 3H), 7.23-7.21 (m, 1H), 7.20-7.16 (m, 2H), 5.00 (s, 1H), 4.08-4.05 (m, 1H), 4.01-3.99 (m, 1H), 3.65 (t, *J* = 10.8 Hz, 1H), 3.08-3.04 (m, 1H), 2.74-2.71 (m, 1H), 2.45-2.37 (m, 5H), 1.86-1.80 (m, 2H); ^{13}C{^{1}H} NMR (150 MHz, $CDCl_3$) δ 138.2, 136.1, 136.0, 130.5, 129.1, 128.4, 127.7, 127.6, 127.4, 126.3, 95.7, 71.4, 62.0, 51.4, 47.0, 22.0, 19.8; FT-IR (neat) 2961, 2850, 1489, 1455, 1364, 1292, 1113, 1059, 1028 cm^{-1}; HRMS (ESI) m/z [M+H]$^+$ calcd for $C_{19}H_{23}N_2O$: 295.1805, found: 295.1806.

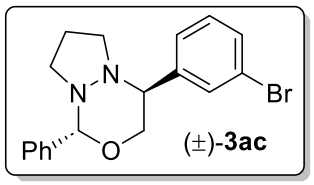

4-(3-Bromophenyl)-1-phenyltetrahydro-1H,6H-pyrazolo[1,2-c][1,3,4]oxadiazine 3ac. Analytical TLC on silica gel, 1:19 ethyl acetate/hexane R_f = 0.46; colorless solid; mp 102-103 ºC; yield 72% (51 mg); ^{1}H NMR (500 MHz, $CDCl_3$) δ 7.61-7.60 (m, 1H), 7.55-7.53 (m, 2H), 7.45-7.43 (m, 1H), 7.39-7.35 (m, 4H), 7.23-7.20 (m, 1H), 4.99 (s, 1H), 4.02-3.96 (m, 1H), 3.72-3.66 (m, 2H), 3.01-2.96 (m, 1H), 2.73-2.69 (m, 1H), 2.46-2.38 (m, 2H), 1.87-1.80 (m, 2H); ^{13}C{^{1}H} NMR (100 MHz, $CDCl_3$) δ 140.6, 138.0, 131.3, 131.1, 130.2, 129.1, 128.5, 127.6, 126.9, 122.8, 95.4, 72.1, 65.9, 51.6, 46.8, 21.9; FT-IR (KBr) 2957, 2853, 1571, 1455, 1367, 1112, 1071 cm^{-1}; HRMS (ESI) m/z $[M+H]^+$ calcd for $C_{18}H_{20}BrN_2O$: 359.0754, found: 359.0750.

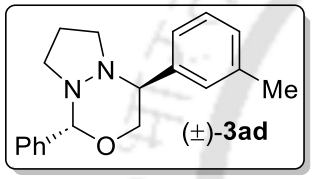

1-Phenyl-4-(*m*-tolyl)tetrahydro-1H,6H-pyrazolo[1,2-c][1,3,4]oxadiazine 3ad. Analytical TLC on silica gel, 1:24 ethyl acetate/hexane R_f = 0.43; colorless solid; mp 96-97 ºC; yield 70% (41 mg); ^{1}H NMR (400 MHz, $CDCl_3$) δ 7.49-7.47 (m, 2H), 7.33-7.29 (m, 3H), 7.17-7.15 (m, 3H), 7.05-7.04 (m, 1H), 4.95 (s, 1H), 3.95-3.92 (m, 1H), 3.70-3.62 (m, 2H), 2.94-2.89 (m, 1H), 2.68-2.63 (m, 1H), 2.43-2.31 (m, 2H), 2.29 (s, 3H), 1.81-1.71 (m, 2H); ^{13}C{^{1}H} NMR (100 MHz, $CDCl_3$) δ 138.3, 138.2, 138.1, 129.1, 128.9, 128.8, 128.5, 128.4, 127.6, 125.4, 95.4, 72.3, 66.4, 51.5, 46.7, 21.9, 21.5; FT-IR (KBr) 2961, 2852, 1608, 1489, 1454, 1365, 1117, 1062, 1039 cm^{-1}; HRMS (ESI) m/z $[M+H]^+$ calcd for $C_{19}H_{23}N_2O$: 295.1805, found: 295.1805.

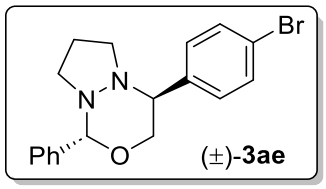

4-(4-Bromophenyl)-1-phenyltetrahydro-1H,6H-pyrazolo[1,2-c][1,3,4]oxadiazine 3ae. Analytical TLC on silica gel, 1:19 ethyl acetate/hexane R_f = 0.42; colorless solid; mp 168-169 ºC; yield 84% (60 mg); ^{1}H NMR (400 MHz, $CDCl_3$) δ 7.55-7.52 (m, 2H), 7.49 (d, J = 8.4 Hz, 2H), 7.40-7.36 (m, 3H), 7.32 (d, J = 8.4 Hz, 2H), 4.99 (s, 1H), 4.02-3.94 (m, 1H), 3.72-3.64 (m, 2H), 2.98-2.93 (m, 1H), 2.74-2.68 (m, 1H), 2.45-2.36 (m, 2H), 1.87-1.78 (m, 2H); ^{13}C{^{1}H} NMR (100 MHz, $CDCl_3$) δ 138.0, 137.2, 131.8, 129.9, 129.1,

128.5, 127.6, 122.0, 95.5, 72.0, 65.8, 51.5, 46.8, 21.9; FT-IR (KBr) 2957, 2828, 1487, 1454, 1363, 1117, 1070, 1010 cm^{-1}; HRMS (ESI) m/z $[M+H]^+$ calcd for $C_{18}H_{20}BrN_2O$: 359.0754, found: 359.0752.

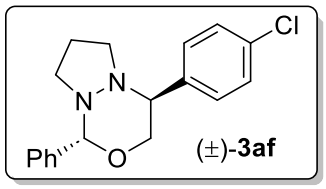

4-(4-Chlorophenyl)-1-phenyltetrahydro-1H,6H-pyrazolo[1,2-c][1,3,4]oxadiazine 3af. Analytical TLC on silica gel, 1:19 ethyl acetate/hexane R_f = 0.48; colorless solid; mp 140-141 ºC; yield 82% (51 mg); ^1H NMR (500 MHz, $CDCl_3$) δ 7.48-7.46 (m, 2H), 7.31-7.29 (m, 5H), 7.26-7.24 (m, 2H), 4.92 (s, 1H), 3.92-3.89 (m, 1H), 3.66-3.58 (m, 2H), 2.91-2.86 (m, 1H), 2.66-2.62 (m, 1H), 2.38-2.30 (m, 2H), 1.82-1.69 (m, 2H); $^{13}C\{^1H\}$ NMR (125 MHz, $CDCl_3$) δ 138.1, 136.7, 133.9, 129.5, 129.1, 128.9, 128.5, 127.6, 95.5, 72.1, 65.8, 51.5, 46.8, 21.9; FT-IR (KBr) 2957, 2853, 1490, 1453, 1369, 1117, 1063, 1040 cm^{-1}; HRMS (ESI) m/z $[M+H]^+$ calcd for $C_{18}H_{20}ClN_2O$: 315.1259, found: 315.1258.

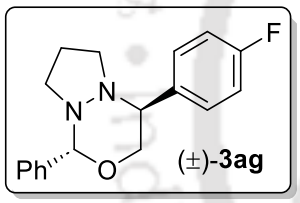

4-(4-Fluorophenyl)-1-phenyltetrahydro-1H,6H-pyrazolo[1,2-c][1,3,4]oxadiazine 3ag. Analytical TLC on silica gel, 1:24 ethyl acetate/hexane R_f = 0.46; thick liquid ; yield 81% (48 mg); ^1H NMR (500 MHz, CDCl3) δ 7.55-7.53 (m, 2H), 7.42-7.36 (m, 5H), 7.05-7.02 (m, 2H), 4.99 (s, 1H), 4.02-3.94 (m, 1H), 3.73-3.66 (m, 2H), 2.96-2.92 (m, 1H), 2.73-2.69 (m, 1H), 2.45-2.37 (m, 2H), 1.89-1.76 (m, 2H); $^{13}C\{^1H\}$ NMR (100 MHz, $CDCl_3$) δ 163.8 (d, $J_{C\text{-}F}$ = 244.7 Hz), 138.0, 133.9 (d, $J_{C\text{-}F}$ = 3.2 Hz), 129.8 (d, $J_{C\text{-}F}$ = 7.9 Hz), 129.1, 128.5, 127.6, 115.7 (d, $J_{C\text{-}F}$ = 21.1 Hz), 95.5, 72.2, 65.7, 51.5, 46.9, 21.9; ^{19}F NMR (471 MHz, $CDCl_3$) δ -114.1; FT-IR (neat) 2957, 2853, 1510, 1456, 1364, 1225, 1063 cm^{-1}; HRMS (ESI) m/z $[M+H]^+$ calcd for $C_{18}H_{20}FN_2O$: 299.1554, found: 299.1553.

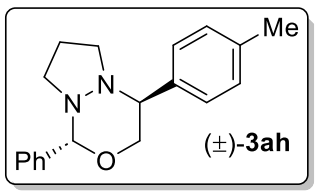

1-Phenyl-4-(*p*-tolyl)tetrahydro-1H,6H-pyrazolo[1,2-c][1,3,4]oxadiazine 3ah. Analytical TLC on silica gel, 1:19 ethyl acetate/hexane R_f = 0.42; colorless solid; mp 97-98 ºC; yield 72% (42 mg); ^1H NMR (500 MHz, $CDCl_3$) δ 7.47-7.46 (m,

2H), 7.30-7.26 (m, 3H), 7.24 (d, *J* = 8 Hz, 2H), 7.08-7.07 (d, *J* = 7.5 Hz, 2H), 4.93 (s, 1H), 3.94-3.88 (m, 1H), 3.67-3.61 (m, 2H), 2.91-2.87 (m, 1H), 2.66-2.62 (m, 1H), 2.40-2.30 (m, 2H), 2.26 (s, 3H), 1.78-1.70 (m, 2H); $^{13}C\{^{1}H\}$ NMR (100 MHz, $CDCl_3$) δ 138.2, 137.8, 135.2, 129.3, 129.0, 128.4, 128.1, 127.6, 95.4, 72.3, 66.2, 51.5, 46.8, 21.9, 21.2; FT-IR (KBr) 2959, 2852, 1514, 1364, 1312, 1112, 1063, 1039 cm^{-1}; HRMS (ESI) m/z $[M+H]^+$ calcd for $C_{19}H_{23}N_2O$: 295.1805, found: 295.1804.

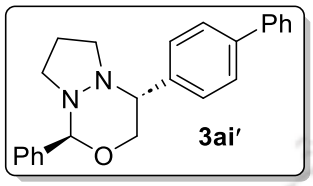

(1S,4R)-4-([1,1'-Biphenyl]-4-yl)-1-phenyltetrahydro-1H,6H-pyrazolo[1,2-c][1,3,4]oxadiazine 3ai'. Analytical TLC on silica gel, 1:19 ethyl acetate/hexane R_f = 0.45; colorless solid; mp 146-147 °C; yield 62% (44 mg); 1H NMR (600 MHz, CDCl3) δ 7.52-7.48 (m, 6H), 7.43 (d, *J* = 8.4 Hz, 2H), 7.38-7.35 (m, 2H), 7.32-7.26 (m, 4H), 4.97 (s, 1H), 4.00-3.96 (m, 1H), 3.73-3.69 (m, 2H), 2.97-2.94 (m, 1H), 2.68-2.64 (m, 1H), 2.45-2.41 (m, 1H), 2.38-2.34 (m, 1H), 1.81-1.74 (m, 2H); $^{13}C\{^{1}H\}$ NMR (150 MHz, $CDCl_3$) δ 141.0, 140.7, 138.0, 137.1, 129.1, 128.9, 128.6, 128.5, 127.5, 127.48, 127.40, 127.1, 95.4, 72.1, 66.1, 51.6, 46.8, 21.9; FT-IR (KBr) 2959, 2852, 1487, 1454, 1364, 1112, 1062, 1039 cm^{-1}; HRMS (ESI) m/z $[M+H]^+$ calcd for $C_{24}H_{25}N_2O$: 357.1961, found: 357.1960. $[\alpha]_D^{21.5}$ = -36 (c = 0.05, $CHCl_3$); HPLC: >96% *ee* [CHIRALCEL OJ-H, hexane/^{i}PrOH = 90:10, flow rate: 1 mL /min, λ = 254 nm, t_R = 18.56 min (minor), 21.78 min (major)].

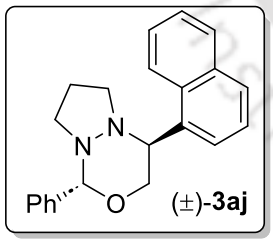

4-(Naphthalen-1-yl)-1-phenyltetrahydro-1H,6H-pyrazolo[1,2-c][1,3,4]oxadiazine 3aj. Analytical TLC on silica gel, 1:19 ethyl acetate/hexane R_f = 0.49; thick liquid; yield 75% (49 mg); ^{1}H NMR (400 MHz, $CDCl_3$) δ 8.30-8.28 (m, 1H), 7.90-7.88 (m, 2H), 7.82 (d, *J* = 8.4 Hz, 1H), 7.63-7.61 (m, 2H), 7.59-7.55 (m, 1H), 7.53-7.49 (m, 2H), 7.44-7.36 (m, 3H), 5.11 (s, 1H), 4.72-4.69 (m, 1H), 4.23-4.21 (m, 1H), 3.79-3.74 (m, 1H), 3.19-3.14 (m, 1H), 2.84-2.79 (m, 1H), 2.54-2.43 (m, 2H), 1.91-1.82 (m, 2H);$^{13}C\{^{1}H\}$ NMR (125 MHz, $CDCl_3$) δ 138.3, 133.9, 131.6, 129.18, 129.13, 128.5, 128.0, 127.7, 126.4, 125.7, 125.6, 122.5, 95.6, 72.2, 60.9, 51.5, 46.9, 22.1; FT-IR (neat) 2962, 2848, 1595, 1511, 1454, 1364,

1111, 1064, 1038 cm^{-1}; HRMS (ESI) m/z $[M+H]^+$ calcd for $C_{22}H_{23}N_2O$: 331.1805, found: 331.1806.

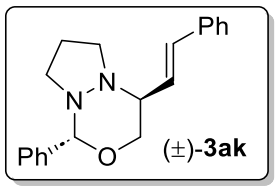

1-Phenyl-4-((E)-styryl)tetrahydro-1H,6H-pyrazolo[1,2-c][1,3,4]oxadiazine 3ak. Analytical TLC on silica gel, 1:24 ethyl acetate/hexane R_f = 0.44; thick liquid; yield 69% (42 mg); ^1H NMR (500 MHz, $CDCl_3$) δ 7.53-7.51 (m, 2H), 7.40-7.31 (m, 7H), 7.27-7.24 (m, 1H), 6.73 (d, *J* = 16.0 Hz, 1H), 6.10-6.05 (m, 1H), 4.87 (s, 1H), 4.02-3.99 (m, 1H), 3.67 (t, *J* = 10.5 Hz, 1H), 3.42-3.37 (m, 1H), 3.26-3.21 (m, 1H), 2.71-2.61 (m, 2H), 2.39-2.34 (m, 1H), 1.90-1.83 (m, 2H); $^{13}C\{^1H\}$ NMR (125 MHz, $CDCl_3$) δ 138.1, 136.5, 134.3, 129.1, 128.8, 128.4, 128.1, 127.6, 126.6, 125.7, 95.6, 70.3, 64.7, 51.8, 46.9, 21.9; FT-IR (neat) 2961, 2851, 1494, 1449, 1365, 1111, 1063, 1028 cm^{-1}; HRMS (ESI) m/z $[M+H]^+$ calcd for $C_{20}H_{23}N_2O$: 307.1805, found: 307.1805.

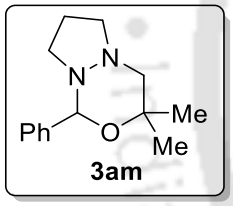

3,3-Dimethyl-1-phenyltetrahydro-1H,6H-pyrazolo[1,2-c][1,3,4]oxadiazine 3am. Analytical TLC on silica gel, 1:4 ethyl acetate/hexane R_f = 0.45; colorless liquid; yield 61% (28 mg); ^1H NMR (500 MHz, $CDCl_3$) δ 7.50-7.49 (m, 2H), 7.34-7.29 (m, 3H), 4.96 (s, 1H), 3.17-3.13 (m, 1H), 2.82 (d, *J* = 11.0 Hz, 1H), 2.58-2.54 (m, 1H), 2.52 (d, *J* = 11.0 Hz, 1H), 2.48-2.42 (m, 1H), 2.35-2.29 (m, 1H), 1.90-1.82 (m, 2H), 1.46 (s, 3H), 1.30 (s, 3H); $^{13}C\{^1H\}$ NMR (125 MHz, $CDCl_3$) δ 138.7, 128.9, 128.4, 127.9, 90.9, 71.7, 62.8, 53.7, 47.2, 28.6, 22.6, 22.1; FT-IR (neat) 2926, 2853, 1737, 1454, 1380, 1198, 1060, 904 cm^{-1}; HRMS (ESI) m/z $[M+H]^+$ calcd for $C_{14}H_{21}N_2O$: 233.1648, found: 233.1652.

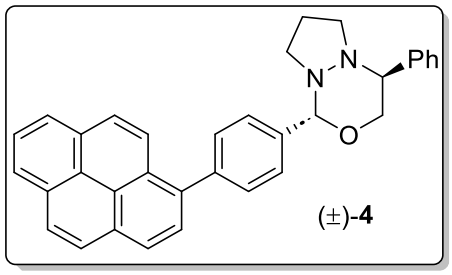

4-Phenyl-1-(4-(pyren-1-yl)phenyl)tetrahydro-1H,6H-pyrazolo[1,2-c][1,3,4]oxadiazine 4. Analytical TLC on silica gel, 1:19 ethyl acetate/hexane

R_f = 0.45; red solid; mp 214-215 °C ; yield 81% (78 mg); ^{1}H NMR (500 MHz, $CDCl_3$) δ 8.15-8.08 (m, 4H), 8.02 (s, 2H), 7.95-7.90 (m, 3H), 7.69 (d, *J* = 7.5Hz, 2H), 7.59 (d, *J* = 8.0 Hz, 2H), 7.41-7.39 (m, 2H), 7.32-7.24 (m, 3H), 5.08 (s, 1H), 4.07-3.98 (m, 1H), 3.78-3.72 (m, 2H), 2.99-2.94 (m, 1H), 2.88-2.83 (m, 1H), 2.52-2.42 (m, 2H), 1.91-1.77 (m, 2H); ^{13}C{^{1}H} NMR (150 MHz, $CDCl_3$) δ 142.0, 138.2, 137.4, 137.2, 131.6, 131.1, 130.8, 130.7, 128.7, 128.6, 128.3, 128.2, 127.7, 127.68, 127.64, 127.62, 127.5, 126.1, 125.3, 125.2, 125.1, 125.03, 125.00, 124.7, 95.5, 72.3, 66.7, 51.6, 47.1, 22.0; FT-IR (KBr) 3037, 2924, 2852, 1602, 1491, 1452, 1115, 1073, 1059 cm^{-1}; HRMS (ESI) m/z $[M+H]^+$ calcd for $C_{34}H_{29}N_2O$: 481.2274, found: 481.2251.

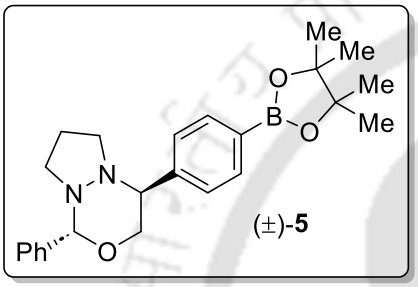

1-Phenyl-4-(4-(4,4,5,5-tetramethyl-1,3,2-dioxaborolan-2-yl)phenyl)tetrahydro-1H,6H-pyrazolo[1,2-c][1,3,4]oxadiazine 5. Analytical TLC on silica gel, 1:19 ethyl acetate/hexane R_f = 0.46; thick liquid; yield 75% (61 mg); ^{1}H NMR (500 MHz, $CDCl_3$) δ 7.75-7.72 (m, 2H), 7.48-7.46 (m, 2H), 7.37 (d, *J* = 6.5Hz, 2H), 7.31-7.26 (m, 3H), 4.95 (s, 1H), 3.95-3.88 (m, 1H), 3.69-3.62 (m, 2H), 2.92-2.87 (m, 1H), 2.66-2.62 (m, 1H), 2.39-2.30 (m, 2H), 1.79-1.70 (m, 2H), 1.26 (s, 12H); ^{13}C{^{1}H} NMR (125 MHz, $CDCl_3$) δ 141.3, 138.2, 135.2, 135.1, 129.0, 128.4, 127.6, 125.4, 95.4, 83.9, 72.2, 66.5, 51.5, 46.7, 25.02, 25.00, 22.0; FT-IR (neat) 2967, 2852, 1612, 1454, 1399, 1358, 1319, 1143, 1088 cm^{-1}; HRMS (ESI) m/z $[M+H]^+$ calcd for $C_{24}H_{32}BN_2O_3$: 407.2500, found: 407.2510.

Crystal Data and Structure Refinement for 3af

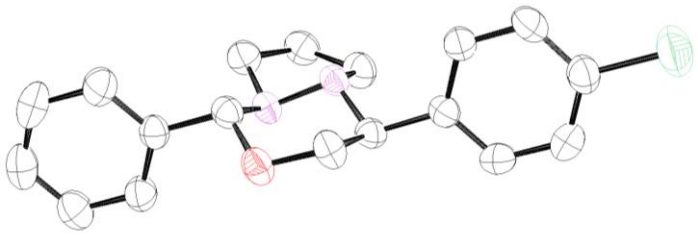

Figure 3. ORTEP diagram of 4-(4-chlorophenyl)-1-phenyltetrahydro-1H,6H-pyrazolo[1,2-c][1,3,4]oxadiazine **3af** (CCDC 2128460) with 50% ellipsoid. H-omitted for clarity.

Identification code	**3af**
Empirical formula	'C18 H19 Cl N2 O'
Formula weight	314.80
Crystal habit, colour	Needle/Colourless
Temperature, *T*/K	296 K
Wavelength, λ/Å	0.71073
Crystal system	'monoclinic'
Space group	'C 2/c'
Unit cell dimensions	a = 23.449(11) Å b = 5.367(3) Å c = 26.573(13) Å α = 90 β = 104.17(3) γ = 90
Volume, *V*/Å^3	3242(3)
Z	8
Calculated density, Mg·m^{-3}	1.290
Absorption coefficient, μ/mm^{-1}	0.239
F(000)	1328
θ range for data collection	1.58 to 25°
Limiting indices	-27 ≤ h ≤ 27, –6 ≤ k ≤ 6, –31 ≤ l ≤ 31
Reflection collected / unique	2862/2287
Refinement method	'SHELXL-2014 (Sheldrick 2014)'
Data / restraints / parameters	2862/0/ 199
Goodness–of–fit on F^2	1.398
Final *R* indices [*I*>2sigma(*I*)]	R1 = 0.0730, wR2 = 0.1947
R indices (all data)	R1 = 0.0924, wR2 = 0.2124

Crystal Data and Structure Refinement for 3ha'

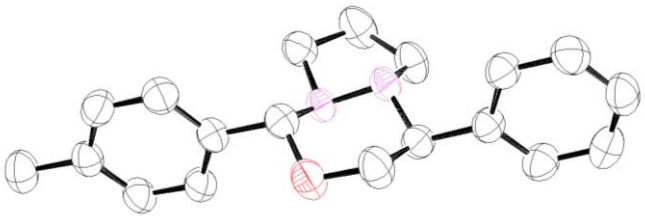

Figure 4. ORTEP diagram of (1R,4S)-4-phenyl-1-(p-tolyl)tetrahydro-1H,6H-pyrazolo[1,2-c][1,3,4]oxadiazine **3ha'** (CCDC 2194308) with 50% ellipsoid. H-omitted for clarity.

Identification code	**3ha'**
Empirical formula	'C19 H22 N2 O'
Formula weight	294.38
Crystal habit, colour	Needle/Colourless
Temperature, *T*/K	298 K
Wavelength, λ/Å	0.71073
Crystal system	'orthorhombic'
Space group	'P 21 21 21'
Unit cell dimensions	a = 5.838(4) Å b = 7.369(5) Å c = 37.97(2) Å α = 90 β = 90 γ = 90
Volume, *V*/Å^3	1633.6(18)
Z	4
Calculated density, Mg·m^{-3}	1.197
Absorption coefficient, μ/mm^{-1}	0.074
F(000)	632
θ range for data collection	2.145 to 27.047°
Limiting indices	-7 ≤ h ≤ 7, –9 ≤ k ≤ 9, –48 ≤ l ≤ 48
Reflection collected / unique	3567/2707
Refinement method	'SHELXL-2019/1 (Sheldrick, 2019)'
Data / restraints / parameters	3567/0/ 200

Goodness−of−fit on F^2	1.132
Final *R* indices [*I*>2sigma(*I*)]	R1 = 0.0484, wR2 = 0.0889
R indices (all data)	R1 = 0.0730, wR2 = 0.0995
Flack parameter	0.0(5)

2.5 References

1. (a) Spreng, M.; Deleforge, J.; Thomas, V.; Boisramé, B.; Drugeon, H. *J. Vet. Pharmacol. Ther*. **1995**, *18*, 284. (b) Ke, S.; Cao, X.; Liang, Y.; Wang, K.; Yang, Z. *Mini-Rev. Med. Chem*. **2011**, *11*, 642.
2. (a) Trost, B. M. *Acc. Chem. Res*. **2002**, *35*, 695. (b) Wender, P. A.; Verma, V. A.; Paxton, T. J.; Pillow, T. H. *Acc. Chem. Res*. **2008**, *41*, 40.
3. For reviews, see: (a) Reissig, H.-U.; Zimmer, R. *Chem. Rev*. **2003**, *103*, 1151. (b) Bach, R. D.; Dmitrenko, O. *J. Am. Chem. Soc*. **2004**, *126*, 4444. (c) Mack, D. J.; Njardarson, J. T. *ACS Catal*. **2013**, *3*, 272. (d) Huang, C.-Y.; Doyle, A. G. *Chem. Rev*. **2014**, *114*, 8153. (e) Schneider, T. F.; Kaschel, J.; Werz, D. B. *Angew. Chem. Int. Ed*. **2014**, *53*, 5504.
4. For reviews, see: (a) Jacobsen, E. N. *Acc. Chem. Res*. **2000**, *33*, 421. (b) He, J.; Ling, J.; Chiu, P. *Chem. Rev*. **2014**, *114*, 8037. (c) Wang, C.; Luo, L.; Yamamoto, H. *Acc. Chem. Res*. **2016**, *49*, 193. (d) Sarkar, T.; Talukdar, K.; Das, B. K.; Shah, T. A.; Debnath, B.; Punniyamurthy, T. *Org. Biomol. Chem*. **2021**, *19*, 3776.
5. (a) Madhushaw, R. J.; Li, C.-L.; Shen, K.-H.; Hu, C.-C.; Liu, R.-S. *J. Am. Chem. Soc*. **2001**, *123*, 7427. (b) Liu, L.; Sun, H. *Angew. Chem., Int. Ed*. **2014**, *53*, 9865. (c) Hu, C.; Song, R.-J.; Hu, M.; Yang, Y.; Li, J.-H.; Luo, S. *Angew. Chem., Int. Ed*. **2016**, *55*, 10423. (d) Hubbell, A. K.; LaPointe, A. M.; Lamb, J. R.; Coates, G. W. *J. Am. Chem. Soc*. **2019**, *141*, 2474.
6. (a) Makhova, N. N.; Shevtsov, A.V.; Petukhova, V. Y. *Russ. Chem. Rev*. **2011**, *80*, 1035. (b) Molchanov, A. P.; Sipkin, D. I.; Koptelov, Y. B.; Kostikov, R. R. *Russ. J. Org. Chem*. **2001**, *37*, 841. (c) Koptelov, Y. B. *Russ. J. Org. Chem*. **2006**, *42*, 1510. (d) Hu, H.; Xu, J.; Wang, F.; Dong, S.; Liu, X.; Feng, X. *Org. Lett*. **2020**, *22*, 93.
7. For reviews, see:(a) Iqbal, J.; Mukhopadhyay, M.; Mandal, A. K. *Synlett* **1997**, 876. (b) Cahiez, G.; Moyeux, A. Cobalt-Catalyzed Cross-Coupling Reactions. *Chem. Rev*. **2010**, *110*, 1435. (c) Moselage, M.; Li, J.; Ackermann, L. *ACS Catal*. **2016**, *6*, 498.
8. Huang, X.-L.; He, L.; Shao, P.-L.; Ye, S. *Angew. Chem., Int. Ed.* **2009**, *48*, 192.

9. Vazquez, J. C.; Davis, J.; Nesterov, V. N.; Wang, H.; Luo, W. *Org. Lett*. **2021**, *23*, 3136.
10. Mishra, M.; Maharana, P. K.; Karjee, P.; Punniyamurthy, T. *Chem. Commun*. **2022**, *58*, 7090.
11. Schmidt, E. Y.; Semenova, N. V.; Ivanova, E. V.; Tatarinova, I. V.; Ushakov, I. A.; Vashchenko, A. V.; Trofimov, B. A. *Chem. Commun*. **2019**, *55*, 2632.
12. Yang, L.; Wang, F.; Lee, R.; Lv, Y.; Huang, K.-W.; Zhong, G. *Org. Lett.* **2014**, *16*, 3872.
13. Morrill, L. C.; Lebl, T.; Slawin, A. M. Z.; Smith, A. D. *Chem. Sci*. **2012**, *3*, 2088.
14. Soeta, T.; Ohgai, T.; Sakai, T.; Fujinami, S.; Ukaji, Y. *Org. Lett.* **2014**, *16*, 4854.
15. Reddy, T. P.; Krishna, A. V.; Ramachary, D. B. *Org. Lett.* **2018**, *20*, 6979.
16. Zuo, H.; Qin, J.; Zhang, W.; Bashir, M. A.; Yu, Q.; Zhao, W.; Wu, G.; Zhong, F. *Org. Lett*. **2020**, *22*, 6911.
17. (a) Murray, S. A.; Liang, M. Z.; Meek, S. J. *J. Am. Chem. Soc*. **2017**, *139*, 14061. (b) Tian, Y.; Jürgens, E.; Kunz, D. *Chem. Commun*. **2018**, *54*, 11340.
18. Guo, H.; Liu, H.; Zhu, F.-L.; Na, R.; Jiang, H.; Wu, Y.; Zhang, L.; Li, Z.; Yu, H.; Wang, B.; Xiao, Y.; Hu, X.-P.; Wang, M. *Angew. Chem. Int. Ed*. **2013**, *52*, 12641.
19. Hoque, E.; Bisht, R.; Haldar, C.; Chattopadhyay, B. *J. Am. Chem. Soc*. **2017**, *139*, 7745.

2.6 HPLC Chromatograms

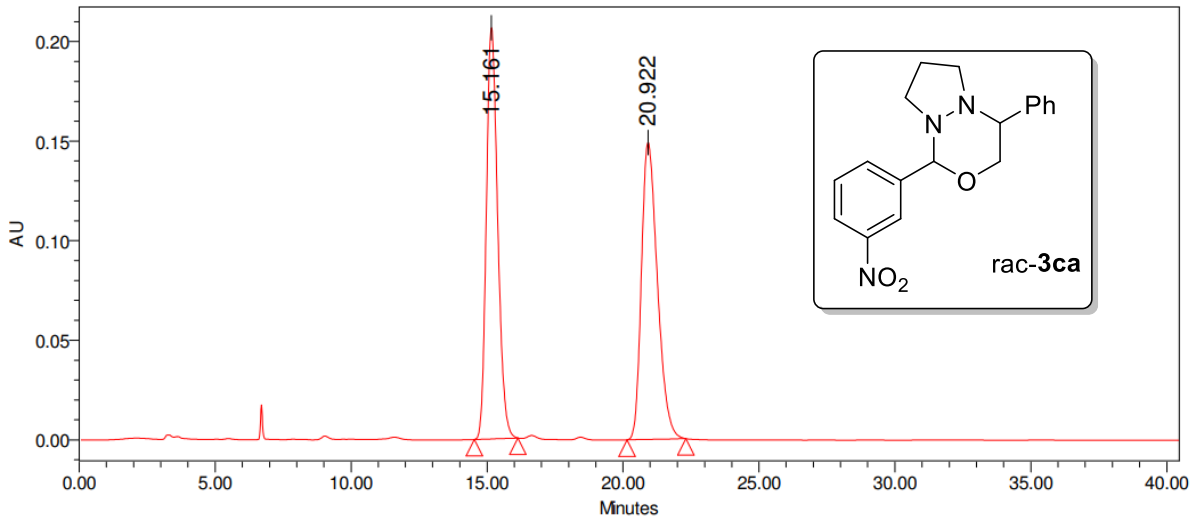

Peak Results

	Start Time (min)	End Time (min)	RT	Height (μV)	% Area
1	14.533	16.133	15.161	206605	49.55
2	20.150	22.317	20.922	149233	50.45

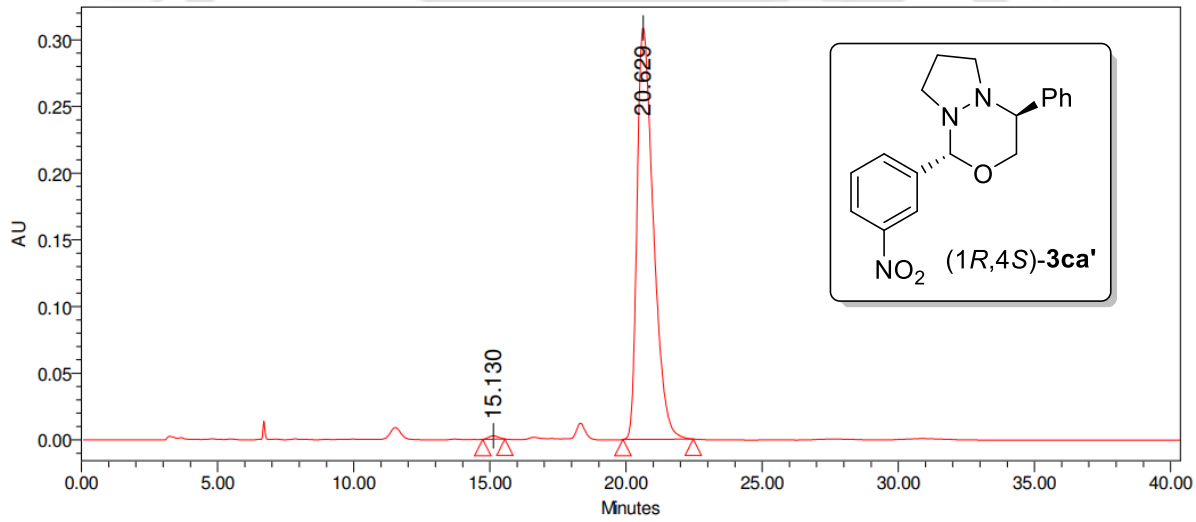

Peak Results

	Start Time (min)	End Time (min)	RT	Height (μV)	% Area
1	14.733	15.550	15.130	2530	0.49
2	19.883	22.467	20.629	308654	99.51

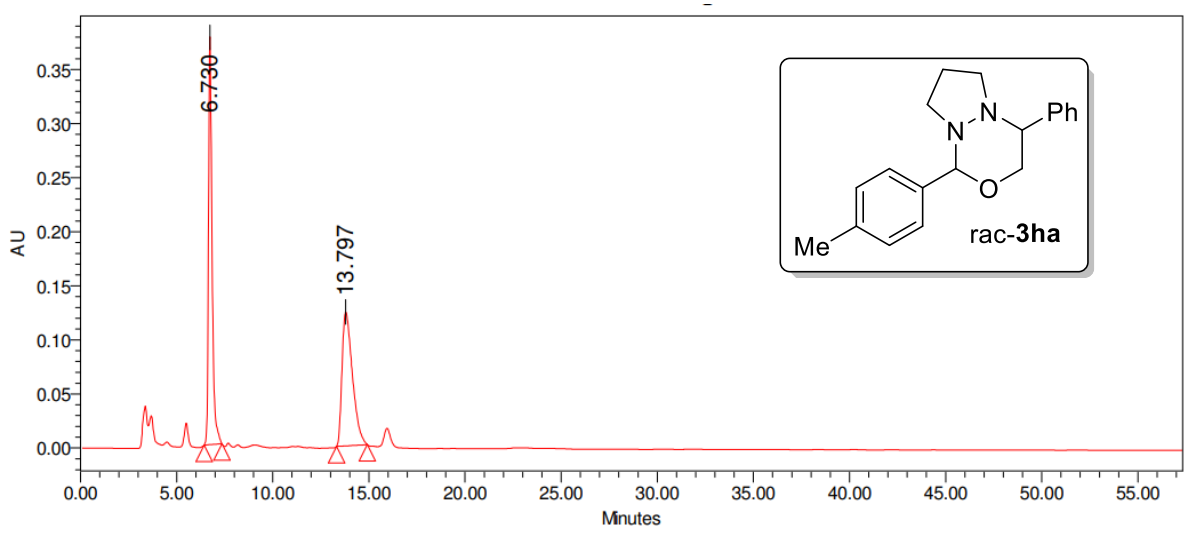

Peak Results

	Start Time (min)	End Time (min)	RT	Height (μV)	% Area
1	6.433	7.350	6.730	377252	51.50
2	13.317	14.917	13.797	123929	48.50

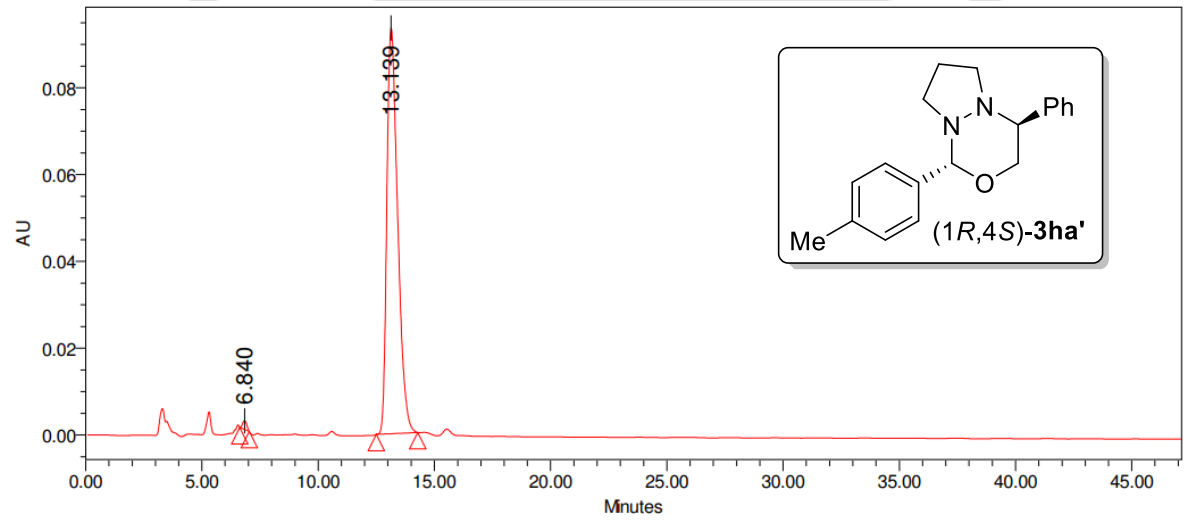

Peak Results

	Start Time (min)	End Time (min)	RT	Height (μV)	% Area
1	6.633	7.033	6.840	2035	0.84
2	12.500	14.283	13.139	93542	99.16

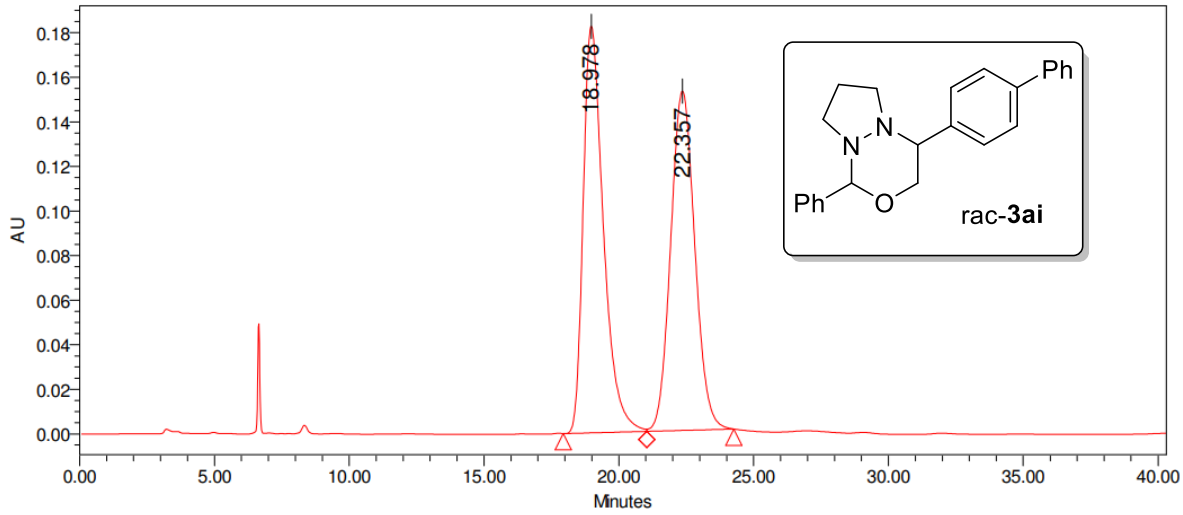

Peak Results

	Start Time (min)	End Time (min)	RT	Height (μV)	% Area
1	17.933	21.033	18.978	182418	50.09
2	21.033	24.267	22.357	152283	49.91

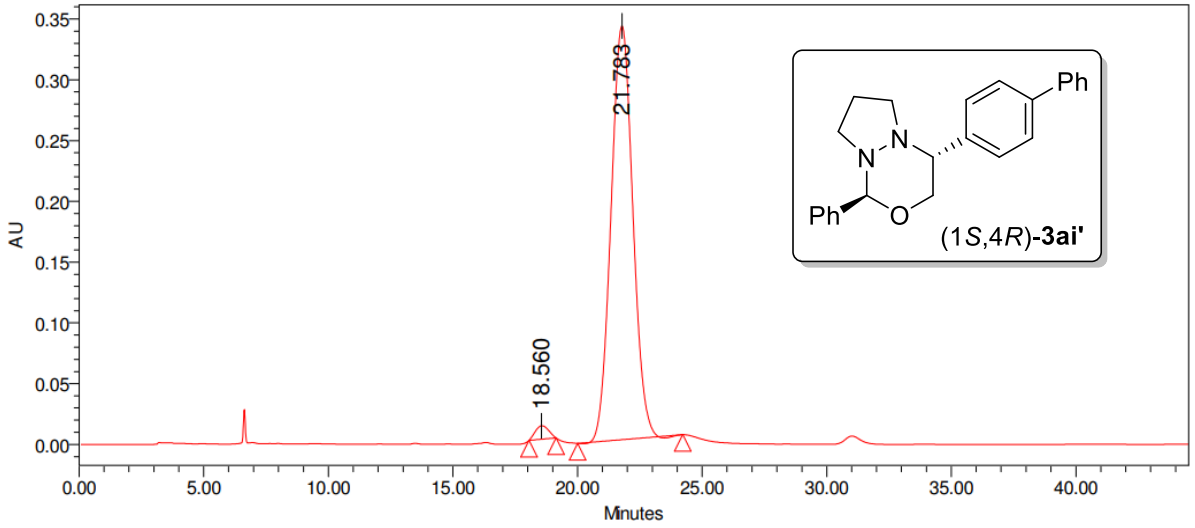

Peak Results

	Start Time (min)	End Time (min)	RT	Height (μV)	% Area
1	18.050	19.133	18.560	11083	1.94
2	20.000	24.217	21.783	340443	98.06

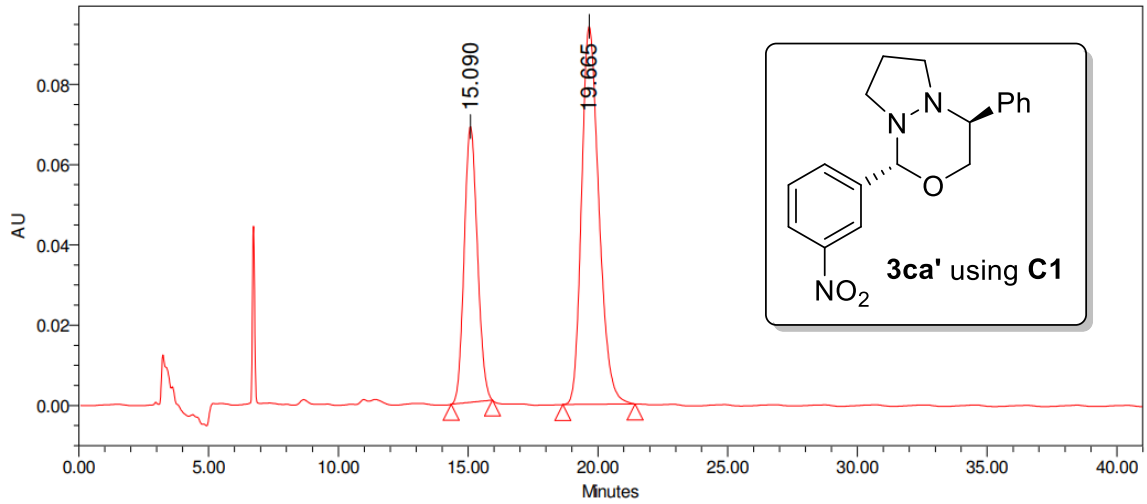

Peak Results

	Start Time (min)	End Time (min)	RT	Height (µV)	% Area
1	14.350	15.933	15.090	68720	35.73
2	18.650	21.433	19.665	94232	64.27

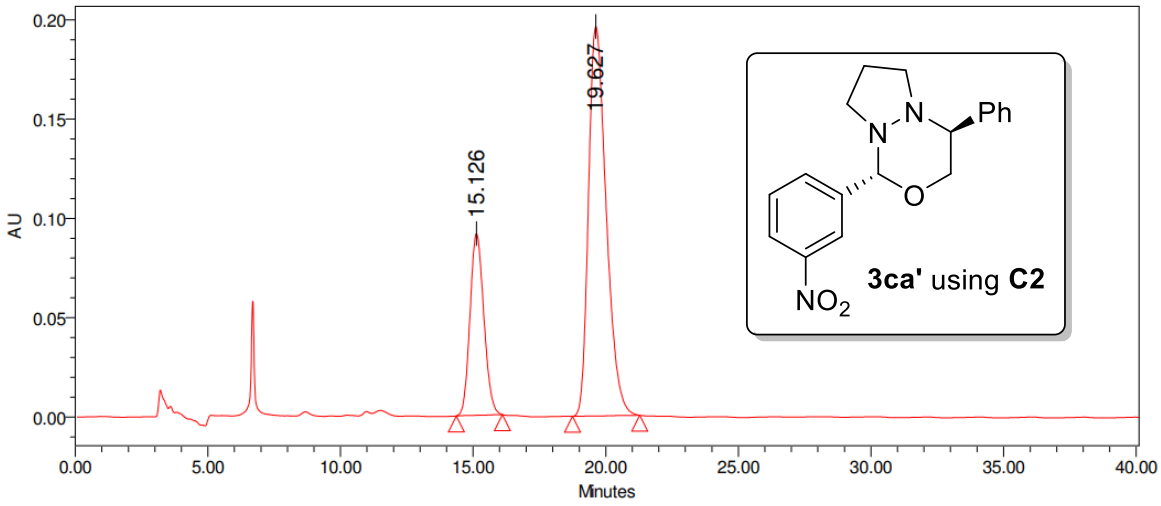

Peak Results

	Start Time (min)	End Time (min)	RT	Height (µV)	% Area
1	14.367	16.100	15.126	91467	26.77
2	18.750	21.283	19.627	196066	73.23

2.7 Selected NMR Spectra

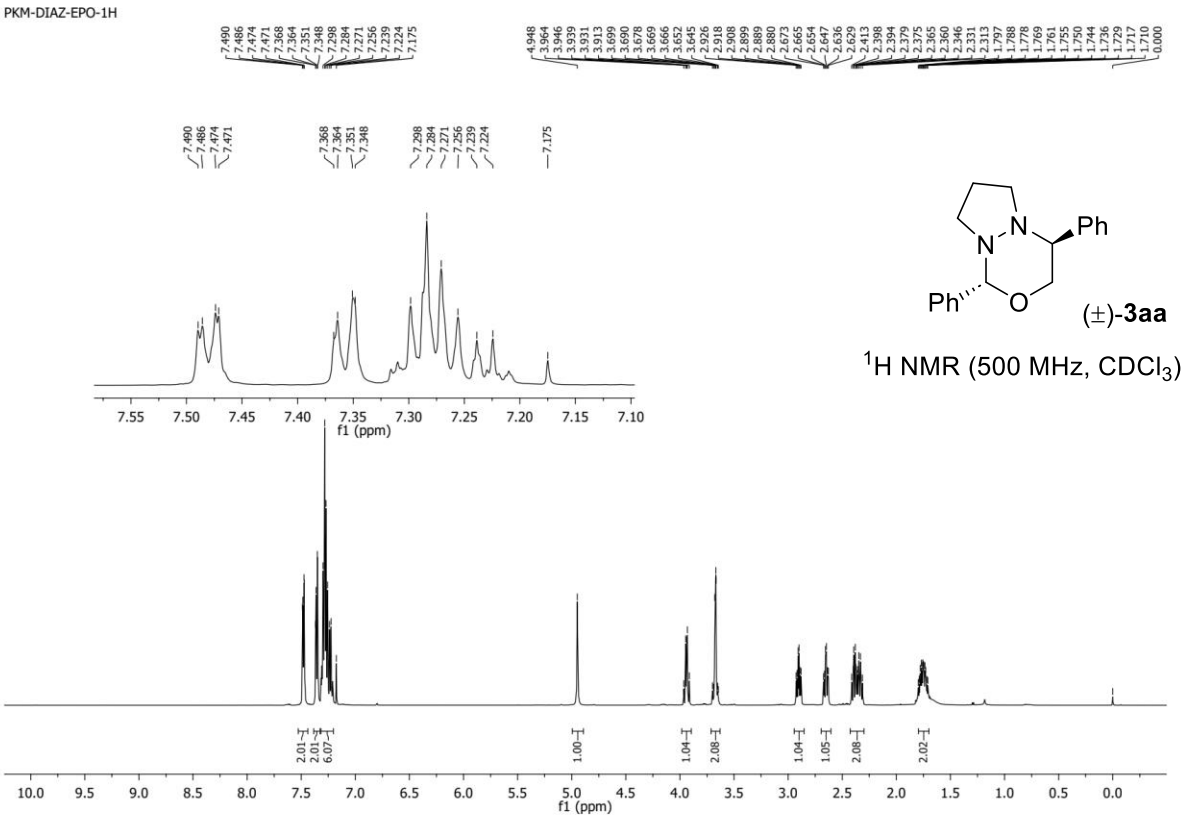

(±)-**3aa**

^{1}H NMR (500 MHz, $CDCl_3$)

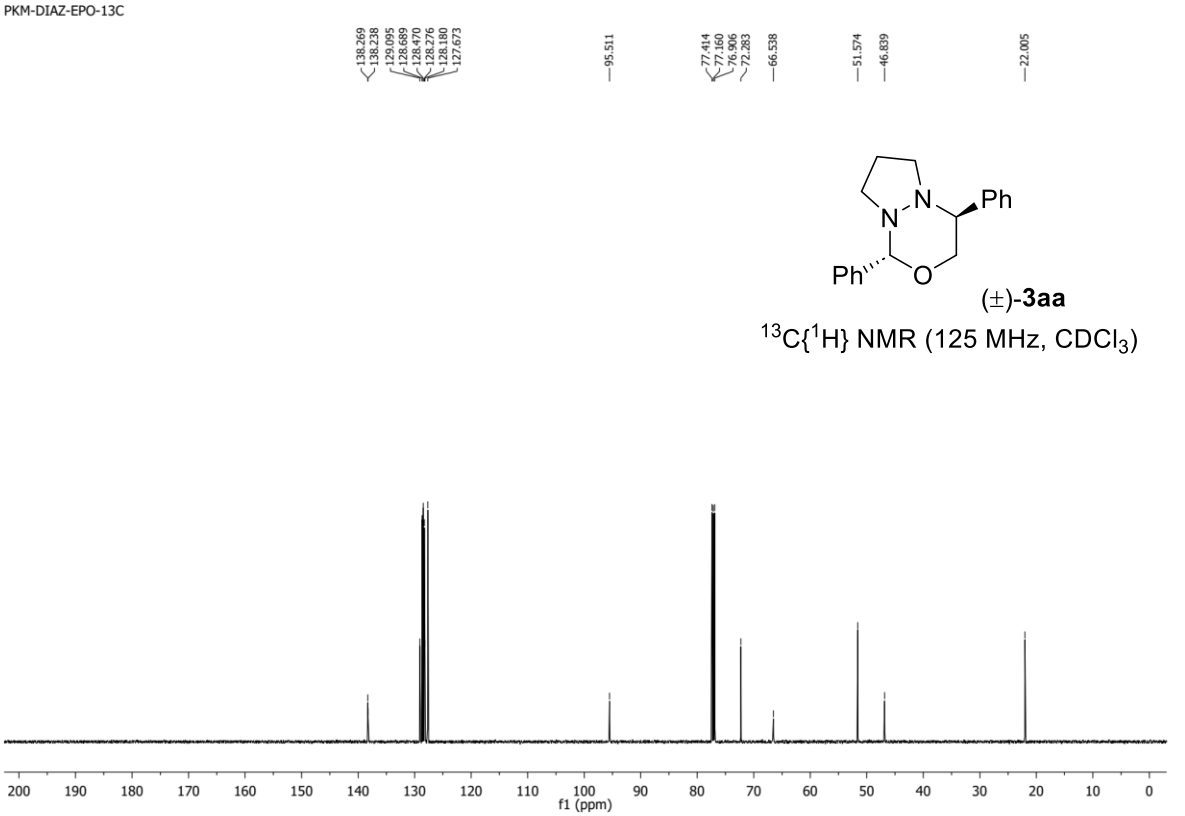

(±)-**3aa**

$^{13}C\{^{1}H\}$ NMR (125 MHz, $CDCl_3$)

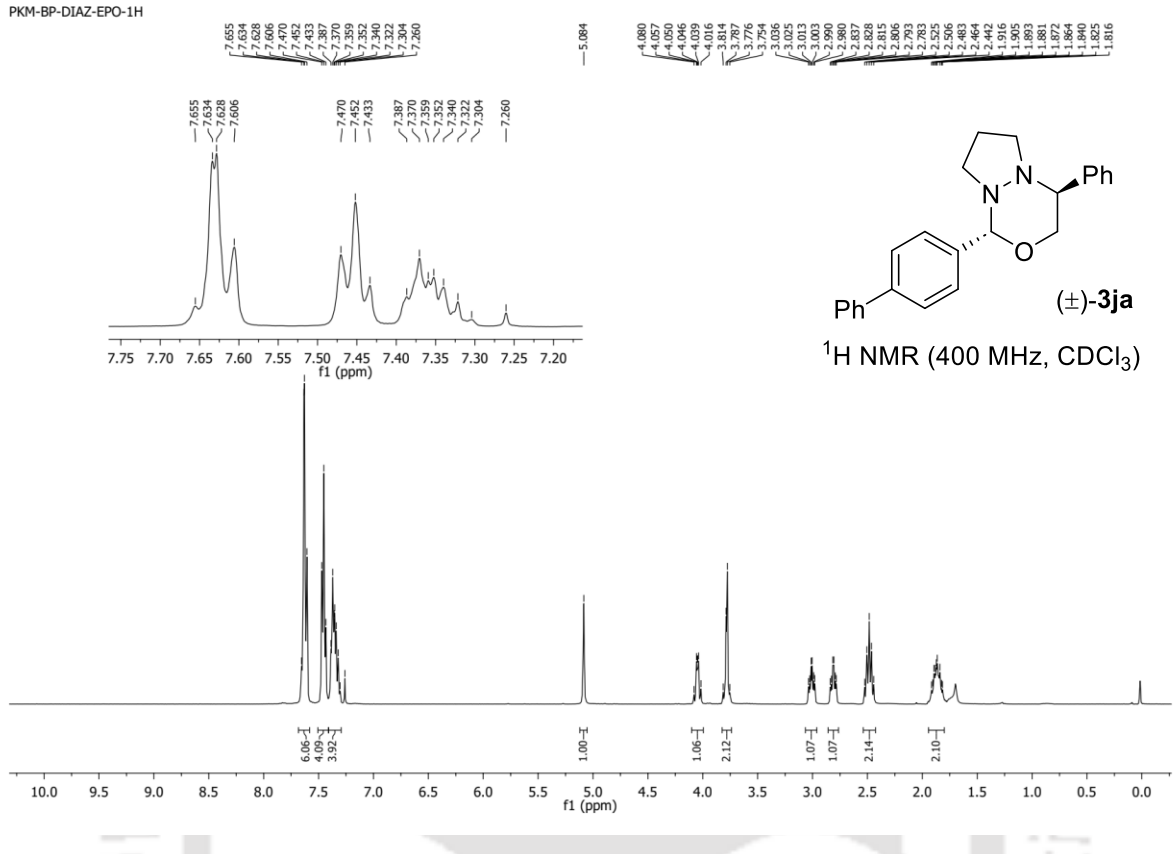

(±)-**3ja**

^{1}H NMR (400 MHz, $CDCl_3$)

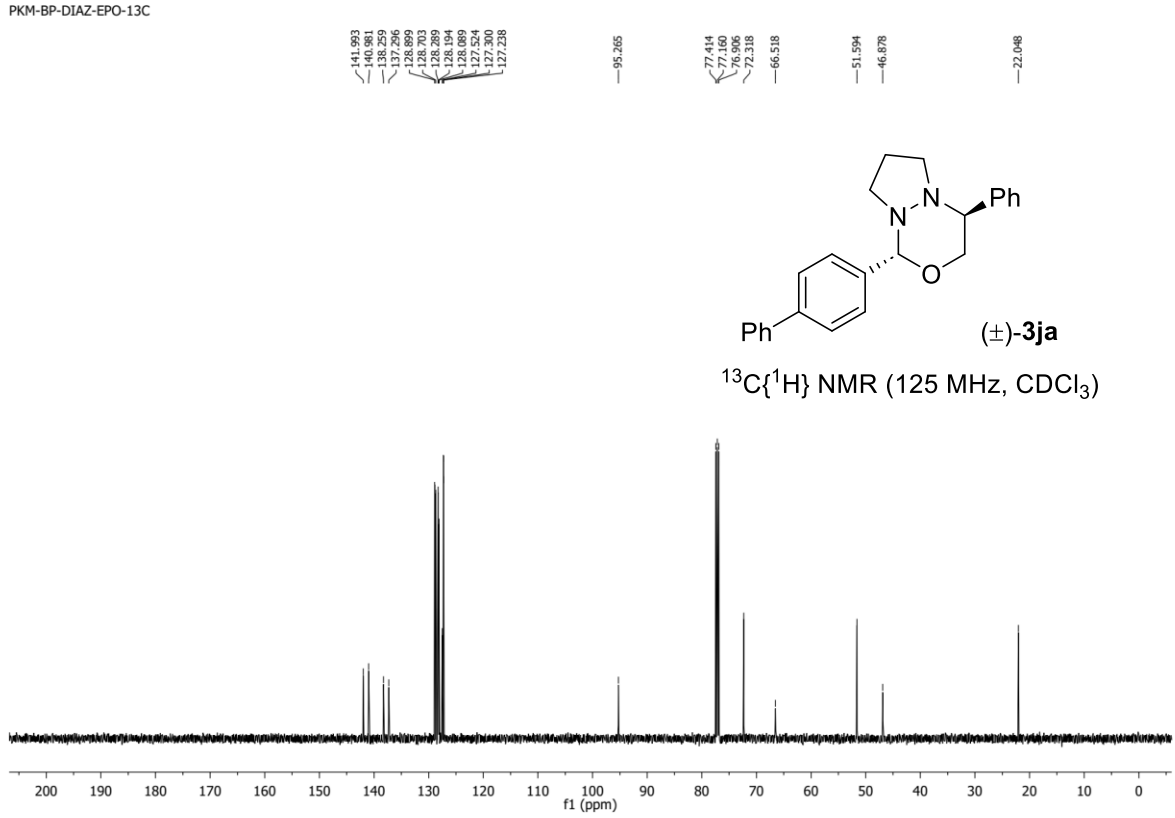

(±)-**3ja**

^{13}C{^{1}H} NMR (125 MHz, $CDCl_3$)

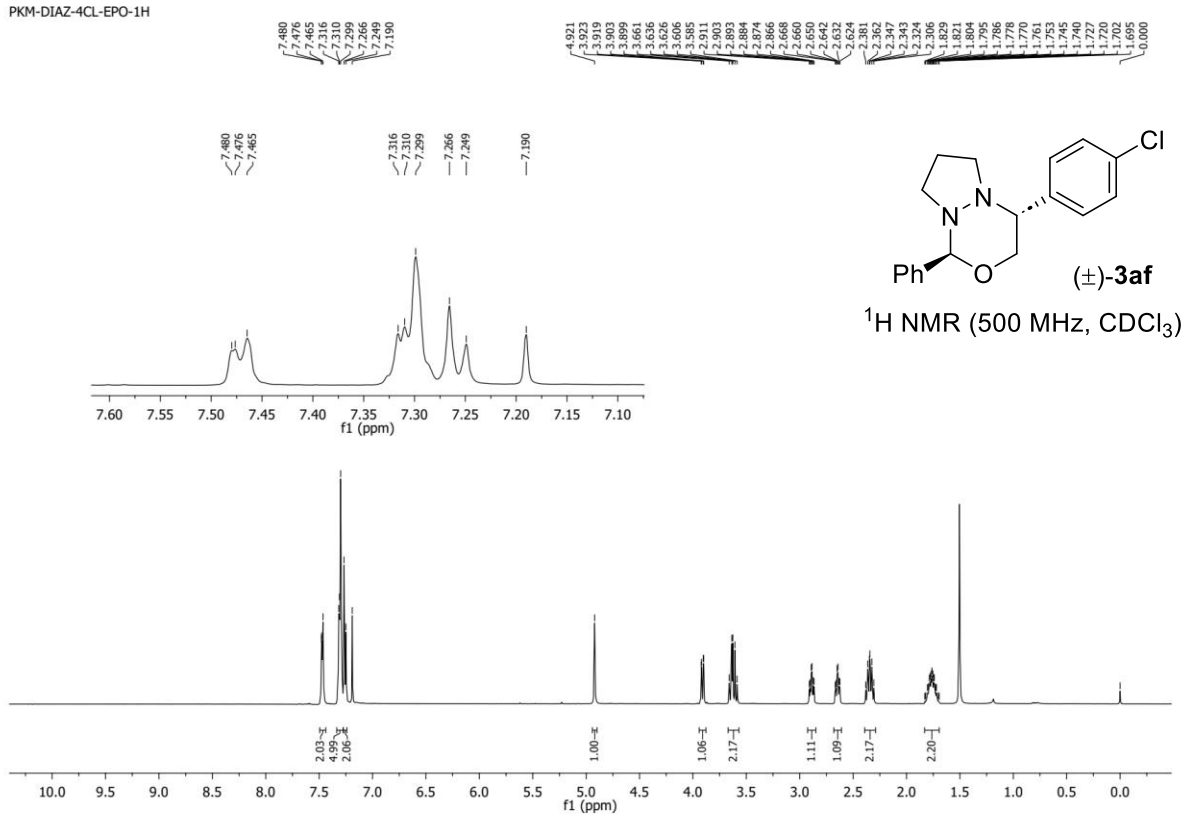

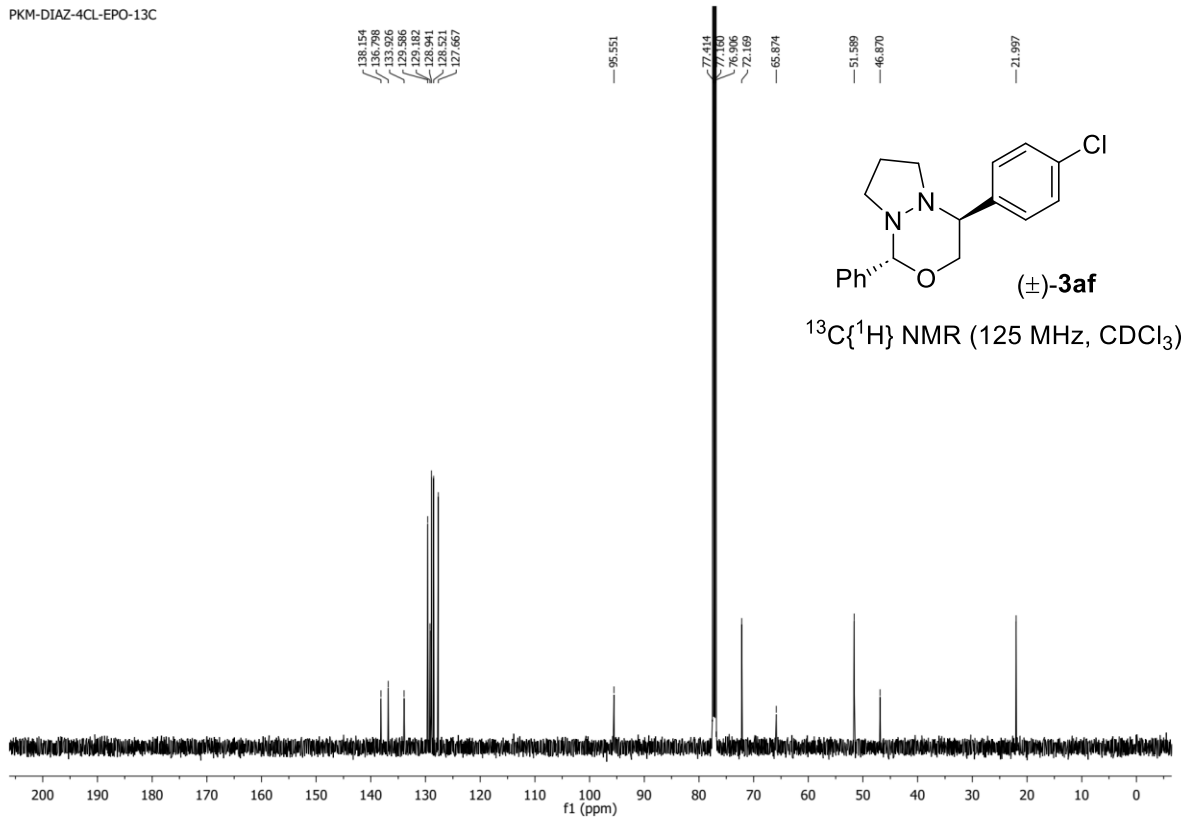

Chapter III

Cu-Catalyzed Cross-Dimerization of Oxaziridines with Aziridines

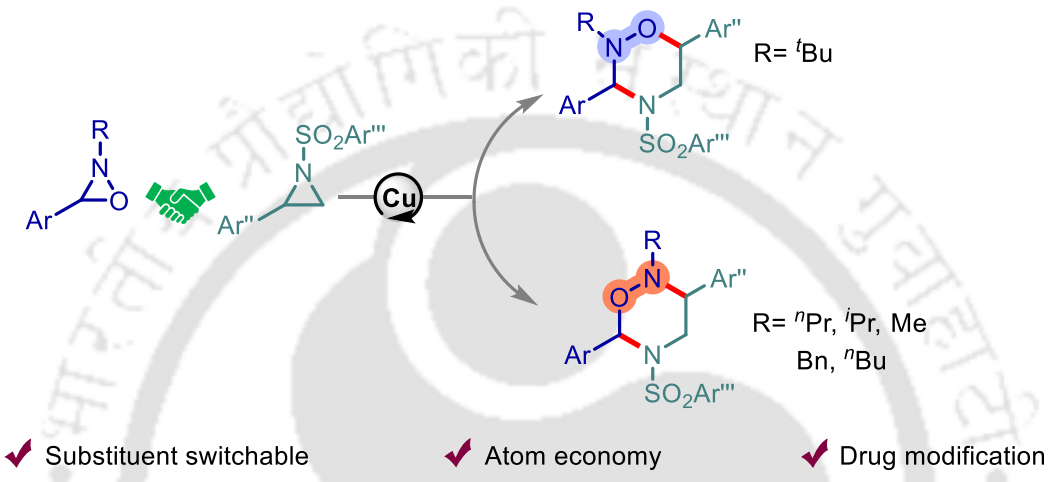

Cu-Catalyzed Cross-Dimerization of Oxaziridines with Aziridines

The rapid expansion of molecular intricacy from simple substrates has always been a mainstay in synthetic organic chemistry. Among the strategies available, transition-metal-catalyzed ring expansion reactions of strained three-membered carbo-/heterocycles represents one of the straight forward approaches towards molecular synthesis.[1] Inherent ring strain associated with these structures render them to undergo ring cleavage to generate dipolar species, which upon selective interception with appropriate dipolarophiles affords cyclized scaffolds.[2] In this context, aziridines, being the smallest azacycles, are recognized for undergoing cycloaddition in the presence of Lewis acids, *via* selective C−C/C−N bond cleavage to afford N-heterocycles.[3] Similarly, oxaziridines, are fascinating strained three-membered rings possessing nitrogen and oxygen in its core structure, offers unmatched advantage owing to their propensity to undergo regioselective C−O, C−N, and N−O bond cleavage to generate diverse dipolar synthons.[4] Of particular note, majority of these cycloadditions involve π-bonded dipolarophiles as coupling partners to furnish larger sized rings from smaller rings. Despite the progress, controlling regioselectivity and ensuring access to precise π-systems, often pushed chemists to seek alternate chemical space. To overcome these deficits, a more general approach involves cross-dimerization of two different strained rings, facilitating the assembly of cyclic scaffolds.[5] To this end, we envisaged that aziridines and oxaziridines can be efficiently cross-dimerized under metal-catalysis to afford functionalized oxadiazines, which are frequently encountered as core motifs in numerous bio-active natural products (Figure 1).[6] In order to streamline this atom-economic strategy, it is important to overcome challenges in averting homo-dimerization, substrate decomposition and undesired mismatch reactions. This chapter focuses on substituent controlled Cu-catalyzed regio-divergent cross-dimerization of oxaziridines with aziridines to synthesize [1,2,4]/[1,2,5]-oxadiazines in good yield.

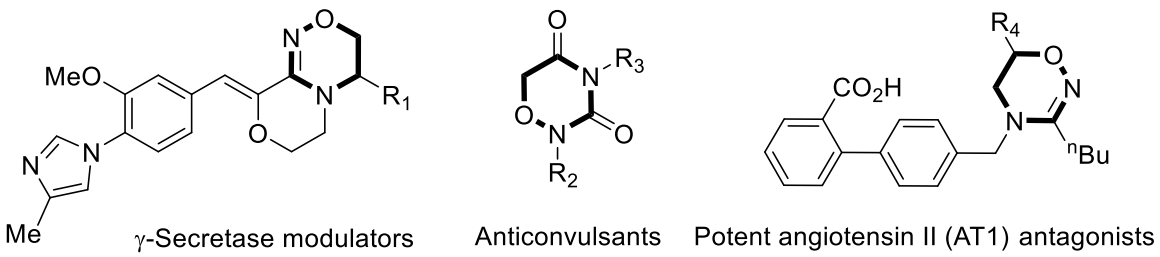

Figure 1. Pharmacologically relevant [1,2,4]-oxadiazines.

3.1 Literature

3.1.1 Reactivity of Oxaziridines

Yoon and co-workers developed a diastereoselective cycloaddition of N-nosyl oxaziridines with styrenes to produce 1,2-isoxazolidines (Scheme 1).[7] This methodology features the intermediacy of elusive N-nosyl nitrones, which resulted from $TiCl_4$-catalyzed rearrangement of N-nosyl oxaziridines. The reaction proceeded in good yield for styrenes with both electron donating as well as withdrawing groups. However, in case of aliphatic olefins, the cycloadduct was isolated in comparatively low yield.

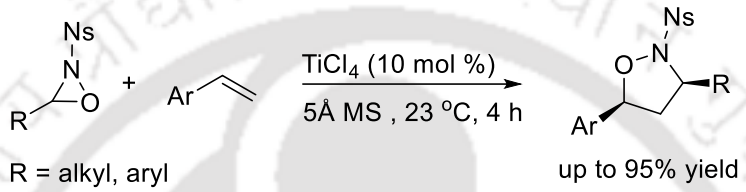

Scheme 1. Cycloaddition of Oxaziridines with Styrenes *via* Nitrone Intermediate

The same group documented a Cu(II)-catalyzed aminohydroxylation of olefins using N-sulfonyl oxaziridines (Scheme 2).[8] Aliphatic olefins and functionally diverse styrenes were tolerated to the reaction conditions. Mechanistically, the reaction involves nucleophilic attack of the styrenes on Lewis acid activated oxaziridines followed by ring closure to afford oxazolidines.

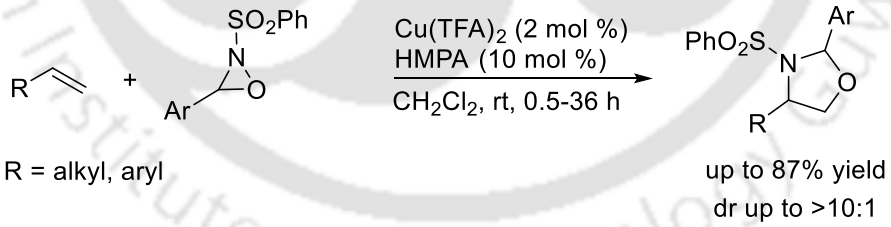

Scheme 2. Aminohydroxylation of Olefins Using N-Sulphonyl Oxaziridines

Zhao group reported a 1,3-dipolar cycloaddition of N-sulphonyl oxaziridines with cyclic allyl alcohols to furnish bicyclic isoxazolidines in good yield (Scheme 3).[9] In presence of stoichiometric amount of $SnCl_4$, oxaziridines gets rearranged to carbonyl imine ylide, which combines with allylic cation to furnish the intended cycloadducts in high diastereoselectivities.

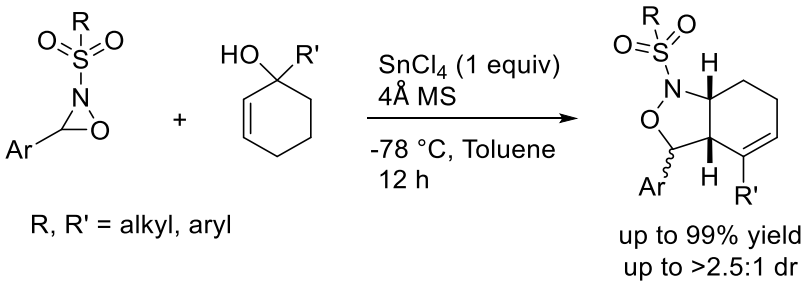

Scheme 3. $SnCl_4$ Promoted Cycloaddition *via* Carbonyl Imine Ylide Intermediate

Larock and co-workers formulated a (3+2)-cycloaddition of arynes with oxaziridines for the synthesis of dihydrobenzisoxazoles (Scheme 4).[10] In presence of CsF and Na_2CO_3 in DME, an *in situ* generated aryne intermediate from silylaryl triflates coupled with oxaziridines to give dihydrobenzisoxazoles in moderate to good yield.

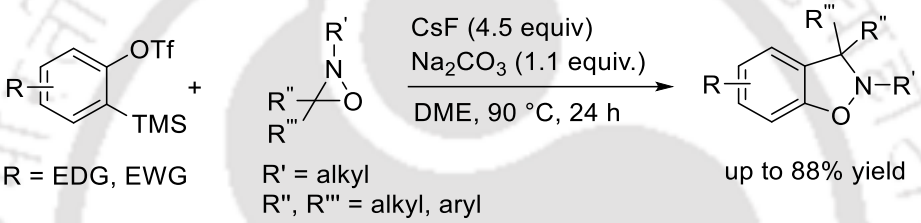

Scheme 4. (3+2)-Cycloaddition of Arynes with Oxaziridines

3.1.2 Reactivity of Aziridines

Our group developed a stereospecific Cu(II)-catalyzed nucleophilic ring opening/cyclization reaction of N-sulfonylaziridines with propargylamines (Scheme 5).[11] The reaction follows hydroamination and isomerization sequence which occurs *via* 6-*exo*-*dig* cyclization to afford functionally diverse piperazines and tetrahydropyarazines. Additionally, the protocol supports reaction of optically active aziridines to yield enantioenriched cycloadduct in high ee values.

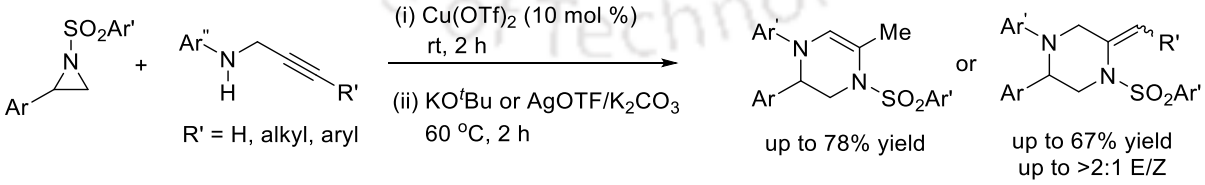

Scheme 5. Cascade Ring Opening/Cyclization of N-Sulfonylaziridines with Propargylamines

Guo group reported a Ni(II)-catalyzed (8+3)-cycloaddition reaction between tropones and N-tosylaziridines to afford fused oxazines (Scheme 6).[12] The reaction tolerates steric as well as

electronic substituents on aziridines to furnish the cycloadducts in good diastereoselective values.

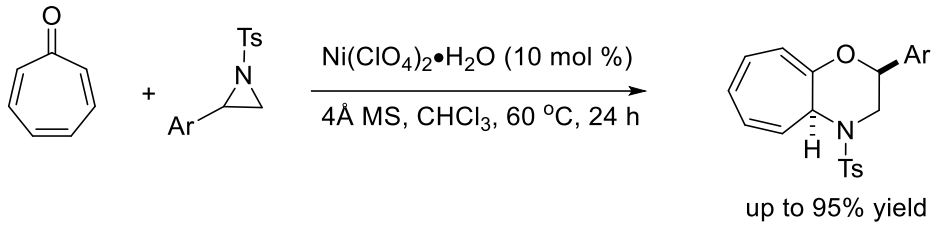

Scheme 6. (8+3)-Cycloaddition of Tropones with Aziridines

3.1.3 Strategies for [1,2,4]/[1,2,5]-Oxadiazine Synthesis

Wang and co-workers documented a DMAP mediated (3+3)-cycloaddition reaction between azaoxyallyl cations and nitrones to furnish [1,2,4]-oxadiazines (Scheme 7).[13] Under mild conditions, the protocol supported a diverse range of nitrones to get the intended cycloadduct in good yields.

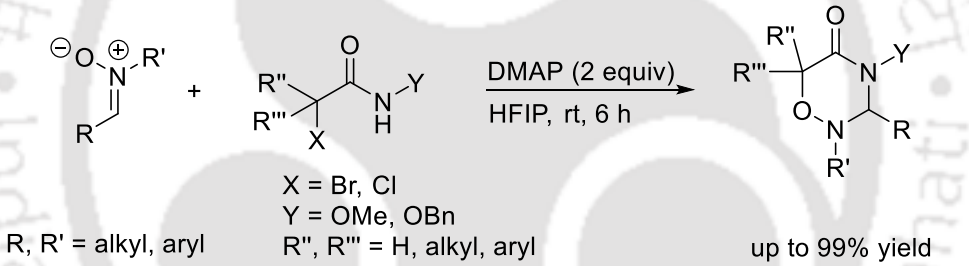

Scheme 7. DMAP Mediated [1,2,4]-Oxadiazine Synthesis

An irreversible condensation reaction of aldehydes and α-aminooxy acetohydrazides under aqueous media to access [1,2,4]-oxadiazines was reported by Trindade and Bode (Scheme 8).[14] The reaction yielded best result when carried out in a mixture of MeCN and acetate buffer at pH 4. Interestingly, aliphatic as well as aromatic aldehydes and isatins proved viable in delivering the desired products in moderate to excellent yields.

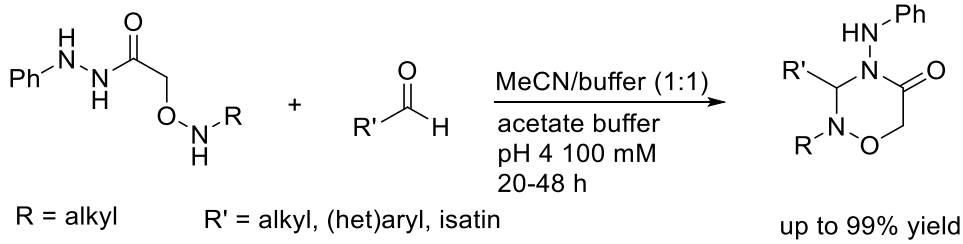

Scheme 8. Condensation of Aldehyde with α-Aminooxy Acetohydrazides in Water

A facile photochemical formal (3+3)-cycloaddition protocol was developed towards the synthesis of [1,2,5]-oxadiazines utilizing nitrone and diaminomethanes as the coupling partners (Scheme 9).[15] Mechanistically, in presence of benzophenone as photo-sensitizer, the reaction proceeds *via* the triplet excited state of the reagents to afford desired product.

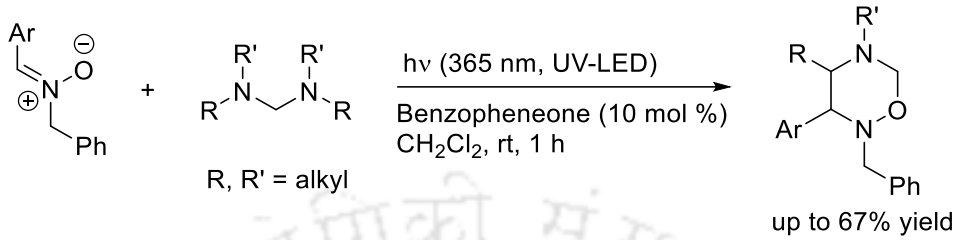

Scheme 9. Photocycloaddition of Nitrones with Diaminomethanes.

3.2 Present Study

Herein we have presented a Cu(II)-catalyzed divergent cross-dimerization strategy of oxaziridines with aziridines to access [1,2,4]/[1,2,5]-oxadiazines. Initially, we commenced the optimization studies taking 2-phenyl-1-tosylaziridine **1a** and 2-tert-butyl-3-phenyloxaziridine **2a** as model substrates in presence of various Lewis acids and solvents (Table 1). Gratifyingly, the cycloadduct **3aa** was formed in 45% yield when the reaction was performed using 10 mol % $Ni(OTf)_2$ in CH_2Cl_2 at 50˚C for 12 h (entry 1). Further screening using $Cu(OTf)_2$ enhanced the yield to 80%, whereas other metal salts such as $Zn(OTf)_2$, $Yb(OTf)_3$ and $Ni(ClO_4)_2•6H_2O$ gave <65% yield (entries 2-5). Further, screening of copper salts such as $Cu(OAc)_2$, $Cu(acac)_2$ and $CuBr_2$ failed to produce the desired outcome (entries 6-8). Solvents such as $(CH_2Cl)_2$, $CHCl_3$, toluene, DMSO, DMF, CH_3CN and THF proved inferior to CH_2Cl_2 (entries 9-15). An increase or decrease in the reaction temperature led to drop in the yield (entries 16-17). In addition, control experiments corresponding to a catalyst-free approach failed to yield the intended cycloadduct, thus emphasizing crucial role of Lewis acids for the cycloaddition (entries 18-19).

With the optimized reaction conditions established, we moved to test the generality of the substrate scope of N-sulfonyl aziridines **2b-p** in presence of oxaziridine **1a** as a representative substrate (Table 2). Aziridine having 2-fluoro substitution at the phenyl ring **2b** afforded the desired product **3ab** in 65% yield. Similarly, functional groups at 4-position of the phenyl ring such as bromo **2c**, chloro **2d**, methyl **2e** and phenyl **2f** proved viable in yielding the cycloadduct **3ac-af** in 69-78% yield. Additionally, 2,4-dimethyl substituted aziridine **2g** and 2-naphthyl **2h** underwent reaction to furnish intended oxadiazines **3ag** and **3ah** in 75% and 79% yield,

Table 1. Optimization of the Reaction Conditions[a]

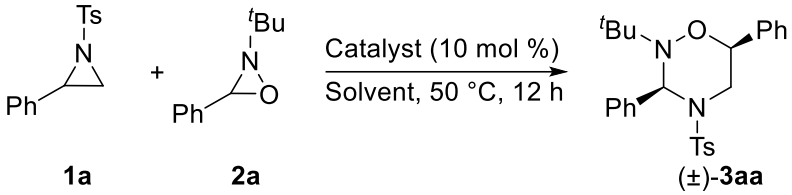

1a **2a** (±)-**3aa**

Entry	Catalyst (10 mol %)	Solvent	Yield [**3aa**, (%)][b]
1	$Ni(OTf)_2$	CH_2Cl_2	45
2	**$Cu(OTf)_2$**	**CH_2Cl_2**	**80**
3	$Zn(OTf)_2$	CH_2Cl_2	54
4	$Yb(OTf)_3$	CH_2Cl_2	65
5	$Ni(ClO_4)_2•6H_2O$	CH_2Cl_2	35
6	$Cu(OAc)_2$	CH_2Cl_2	n.r.
7	$Cu(acac)_2$	CH_2Cl_2	n.r.
8	$CuBr_2$	CH_2Cl_2	n.r.
9	$Cu(OTf)_2$	$(CH_2Cl)_2$	61
10	$Cu(OTf)_2$	$CHCl_3$	42
11	$Cu(OTf)_2$	Toluene	25
12	$Cu(OTf)_2$	DMSO	n.r.
13	$Cu(OTf)_2$	DMF	n.r.
14	$Cu(OTf)_2$	CH_3CN	20
15	$Cu(OTf)_2$	THF	trace
16[c]	$Cu(OTf)_2$	CH_2Cl_2	67
17[d]	$Cu(OTf)_2$	CH_2Cl_2	48
18	-	CH_2Cl_2	n.r.
19[e]	-	$(CH_2Cl)_2$	n.r.

[a]Reaction conditions: **1a** (0.2 mmol), **2a** (0.2 mmol), catalyst (10 mol %), solvent (2 mL), 12 h, 50 ºC. [b]Isolated yield. [c]At 60 ºC. [d]At 40 ºC. [e]At 80 ºC. n.r. = no reaction.

respectively. Further, effect of substituents on the N-sulfonyl aryl ring was verified under the optimized reaction condition. Aziridine bearing N-sulfonylphenyl substituent **2i** reacted to give **3ai** in 70% yield, while 4-methoxy **2j** and 4-nitro **2k** substituent on the aryl ring were tolerated to produce the corresponding heterocycles **3aj**-**ak** in 70-81% yields. Interestingly, 2-naphthyl

2l and heteroarene thiophene **2m** on the N-sulfonyl moiety could afford the intended product in 76% and 73% yields, respectively. To check the versatility of the protocol, aziridines derived from bioactive and drug molecules were subjected to the reaction conditions. For example, aziridine derived from antioxidant carvacrol **2o** successfully yielded the cycloadduct in **3ao** in 78% yield. In a similar manner, non-steroidal anti-inflammatory drug celecoxib **2o** and 1,4-benzodioxane **2p** derived aziridines delivered the intended products **3ao** and **3ap** in 69% and 70% yields, respectively.

Table 3. Substrate Scope of Aziridines [a,b]

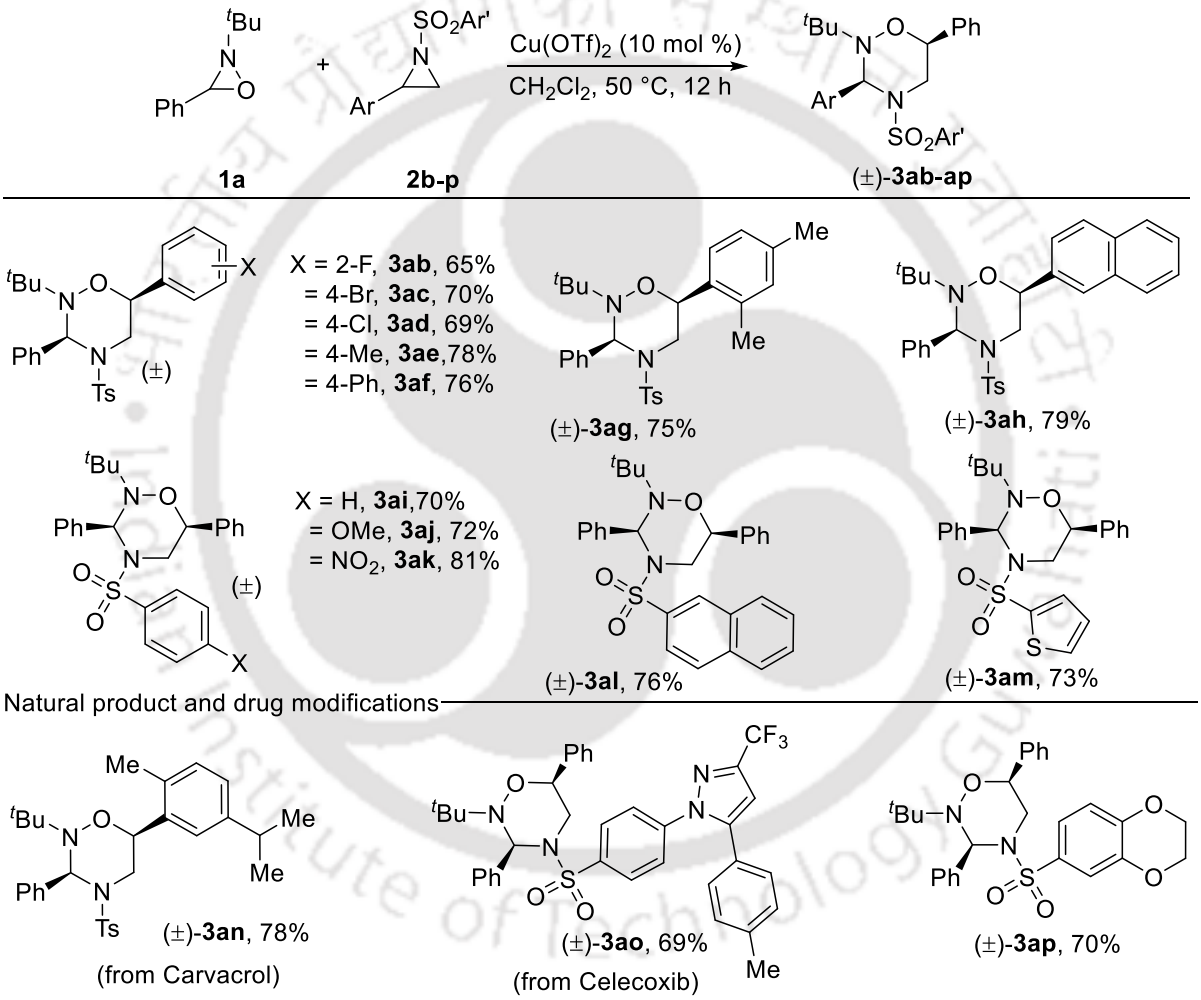

[a]Reaction conditions: **1a** (0.2 mmol), **2b-p** (0.2 mmol), $Cu(OTf)_2$ (10 mol %), CH_2Cl_2 (2 mL), 12 h, 50 ºC. [b]Isolated yield.

Next, we evaluated the scope of substituted N-*tert*-butyl oxaziridines **1b-k** by taking 2-phenyl-1-tosylaziridine **2a** as the model substrate (Table 3). Oxaziridines bearing substitution at 3-position of the aryl ring such as bromo **1b**, methyl **1c** and trifluoromethyl **1d** coupled

efficiently to give **3ba-da** in 65-77% yield. In a similar manner, bromo **1e**, methyl **1f** and *tert*-butyl **1h** at 4-position of the aryl ring participated to yield cycloadducts **3ea-ha** in 75-82% yield, however, strong electron withdrawing NO_2 substituted oxaziridine **1g** produced a trace amount of the product. Further, 2-naphthyl **1i** and 2-furyl **1j** substituted oxaziridine proved viable substrates in yielding the anticipated heterocycles **3ia** and **3ja** in 74% and 85% yields, respectively. The structure of **3ia** was determined using single crystal X-ray analysis. Gratifyingly, oxaziridine derived from naturally occurring cuminaldehyde **1k** furnished the target oxadiazine **3ka** in 76% yield.

Table 3. Substrate Scope of N-*tert*-butyl Oxaziridine[a,b]

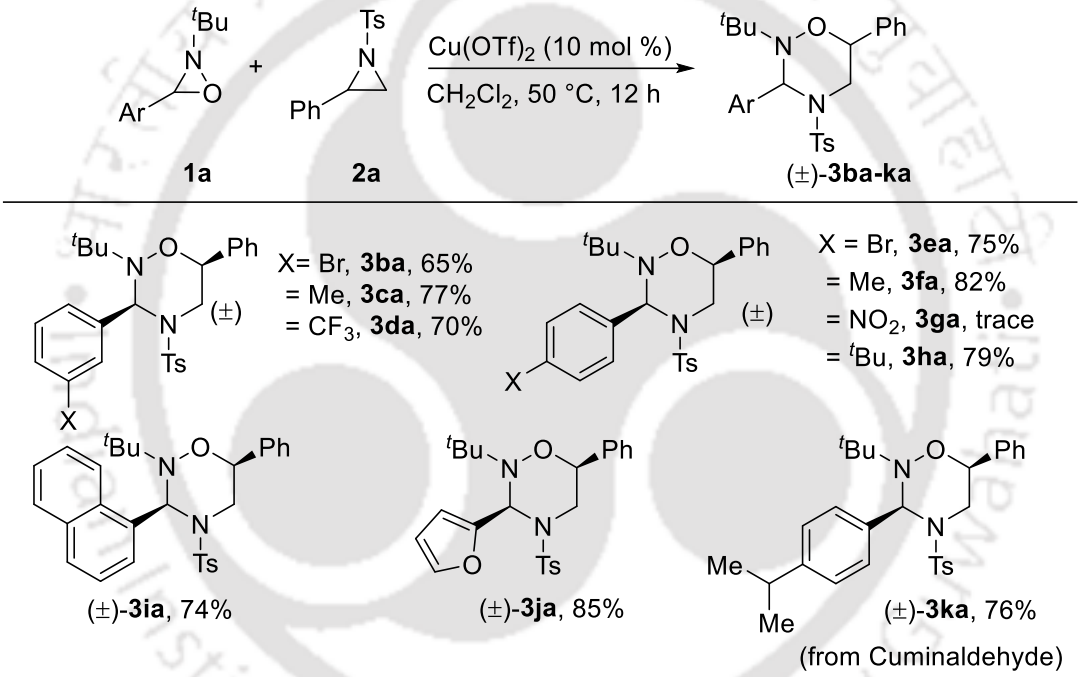

[a]Reaction conditions: **1b-k** (0.2 mmol), **2a** (0.2 mmol), $Cu(OTf)_2$ (10 mol %), CH_2Cl_2 (2 mL), 12 h, 50 ºC. [b]Isolated yield.

Later, we set out to evaluate the effect of different N-alkyl groups of the oxaziridines (Table 4). Interestingly, *iso*-propyl substituted oxaziridine **1l** reacted with **2a** to yield [1,2,5]-oxadiazine **4la** in 65% yield along with a trace amount of [1,2,4]-oxadiazine **3la**. This reversal in regioselectivity motivated us to further screen the effect of N-alkyl groups on the Nitrogen atom of the oxaziridine ring. Gratifyingly, oxaziridines **1m-s** reacted to furnish **4ma-pa** in 67-71% yields. The structure of **4na** was confirmed using single crystal X-ray analysis. This result confers the fact that oxaziridines bearing less sterically hindered N-protecting groups reacted

in a regioselective manner to specifically deliver the respective [1,2,5]-oxadiazines. Further, the reaction of 4-chlorophenyl **1q**, p-tolyl **1r** and 2-naphthyl **1s** derived *N*-propyl oxaziridines produced the cycloadducts **4qa-sa** in 66-70% yields. To further showcase the generality of this

Table 4. Substrate Scope of N-alkyl Oxaziridine[a,b]

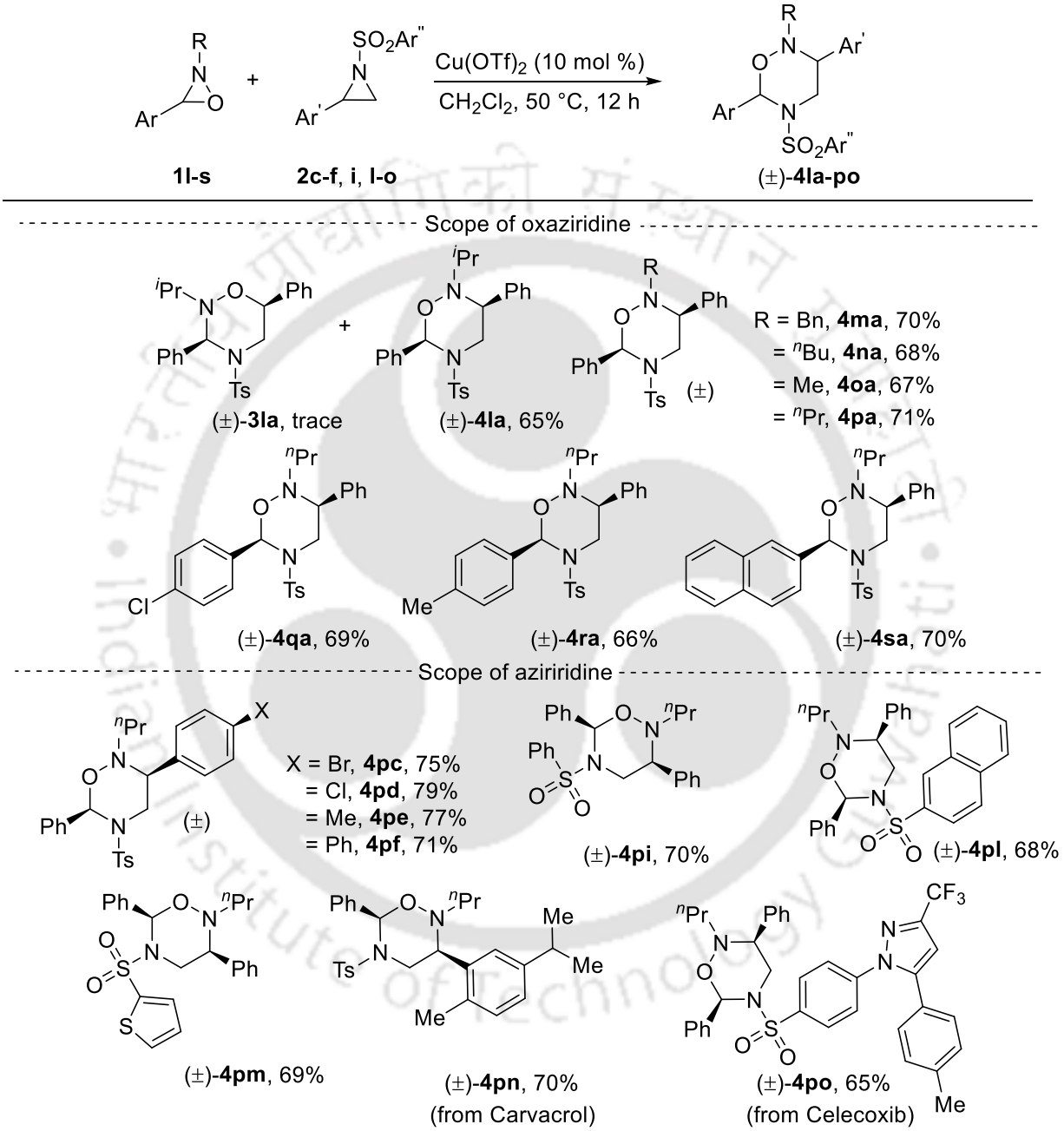

[a]Reaction conditions: **1l-s** (0.2 mmol), **2c-d, i, m-p** (0.2 mmol), $Cu(OTf)_2$ (10 mol %), CH_2Cl_2 (2 mL), 12 h, 50 ºC. [b]Isolated yield.

regioselective transformation, variedly substituted of aziridines were tested by taking 3-phenyl-2-propyl-1,2-oxaziridine **1p** as representative substrate. Substituents on the aryl ring of the

aziridine such as 4-bromo **2c**, 4-chloro **2d**, 4-methyl **2e** and 4-phenyl **2f** were well compatible to furnish the respective oxadiazines **4pc-pf** in 71-79% yields. Moreover, phenylsulfonyl **2i**, naphthalen-2-ylsulfonyl **2l** and thiophen-2-ylsulfonyl **2m** derived aziridines took part to afford **4pi-pm** in 68-70% yields. Gratifyingly carvacrol **2n** and celecoxib **2o** derived aziridines were reacted to produce [1,2,5]-oxadiazines **4pn** and **4po** in 70% and 65% yields, respectively.

a. Radical Trapping Experiment

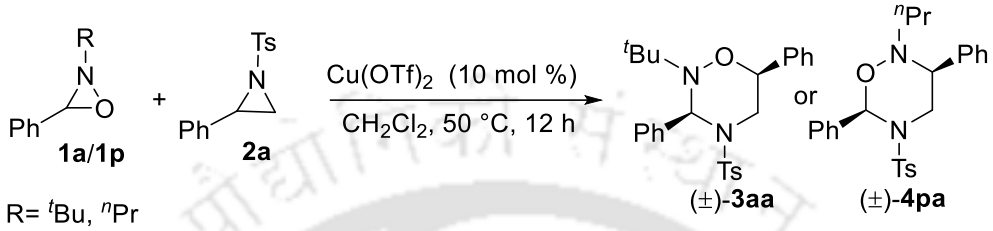

R= ^{t}Bu, ^{n}Pr

Radical scavenger	yield	
	3aa	**4pa**
BHT	70%	65%
TEMPO	62%	63%

b. Reaction of Enantiopure Aziridine

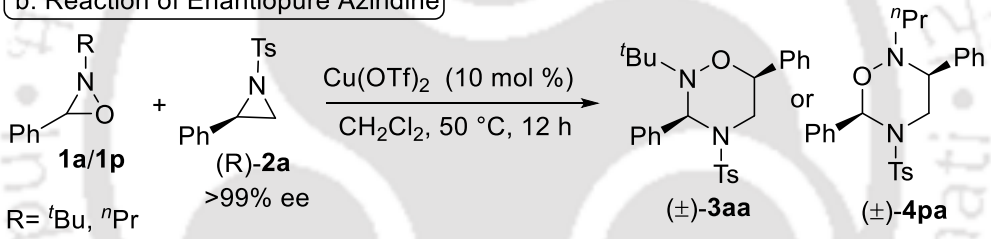

R= ^{t}Bu, ^{n}Pr

Scheme 10. Preliminary Mechanistic Investigation.

To shed light into the reaction pathway, mechanistic experiments were carried out using 2,6-di-*tert*-butyl-4-methylphenol (BHT) and 2,2,6,6-tetramethyl-1-piperidinyloxy (TEMPO). Presence of radical scavengers however did not affect the yield, which ruled out the involvement of radical species (Scheme 10). Further, reaction of enantioenriched aziridine (*R*)-**2a** was carried in presence of oxaziridines **1a** and **1p** independently to check the stereochemical outcome. However, in both the cases, the respective cycloadduct was obtained in racemic form, which suggests that the opening of aziridine may follow the S_N1 pathway. On the basis of these initial findings and literature precedents,[7,9-12,16] a plausible mechanism is described in scheme 11. Initially, in presence of Cu(II), ring opening of **2** occurs to generate intermediate **I**. Consequently, thermal rearrangement of N-*tert*-butyl oxaziridine *via* selective C−O bond cleavage may generate the nitrone intermediate **II,** which subsequently undergoes a nucleophilic attack on **I** to form **III**. Finally, ring closure *via* intramolecular nucleophilic attack accomplishes the [1,2,4]-oxadiazine **3**. On the other hand, presence of sterically less bulkier N-

substituents on **1**, may direct it for a preferential concerted approach in presence of **I** to form the intended [1,2,5]-oxadiazines **4** *via* intermediate **V** and subsequently regenerating the catalyst.

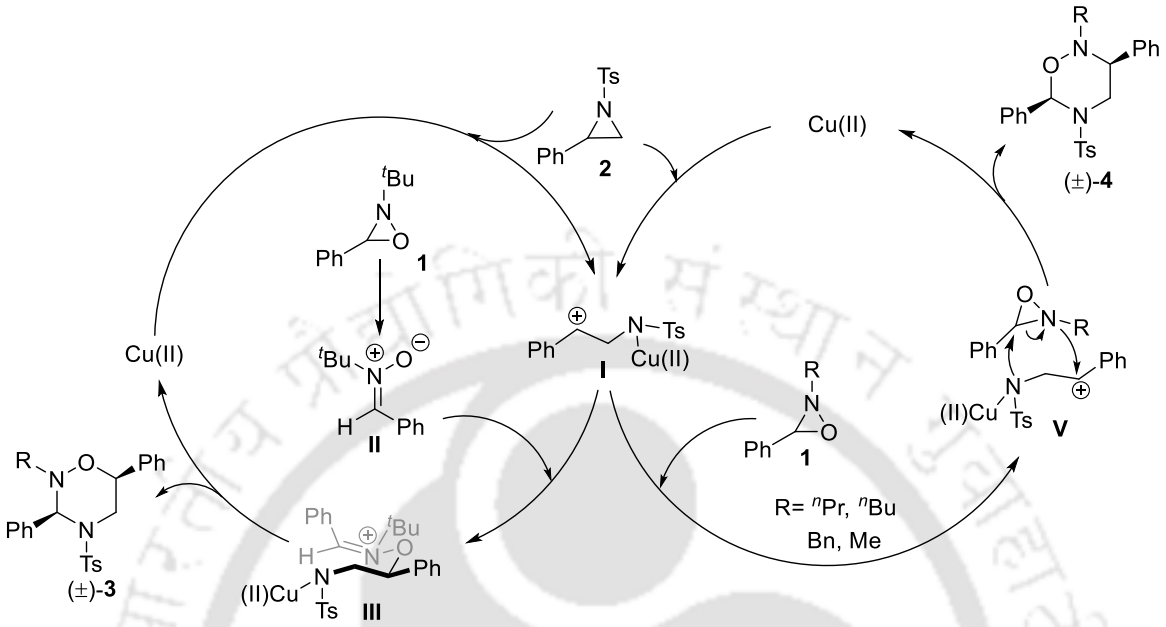

Scheme 11. Plausible Mechanism.

To further showcase the practical utility, scale-up synthesis was carried out by taking **1e** and **2a** as the representative substrates on a 3 mmol scale (Scheme 12a). Gratifyingly, the desired [1,2,4]-oxadiazine **3ea** was obtained in 68% yield. Further, **3ea** was subjected to a series of palladium-catalyzed coupling reactions to afford functionalized products. The oxadiazine **3ea** when treated with pyrene-1-boronic acid undergoes Suzuki coupling to form **5** in 82% yield. Similarly, a Sonagashira coupling in presence of phenylacetylene and borylation using B_2pin_2 afforded the respective coupled products **6** and **7** in 85% and 72% yields, respectively. Later, a separate scale-up synthesis was carried out by taking **1p** (3 mmol) and **2c** (3 mmol) to furnish [1,2,5]-oxadiazine **4pc** in 66% yield (Scheme 12b). Subsequently, **4pc** was subjected to a Suzuki coupling using anti-oxidant sesamol derived boronic acid to furnish **8** in 89% yield.

In conclusion, we have disclosed a Cu(II)-catalyzed divergent synthesis of oxadiazines *via* cross-dimerization of two strained ring systems as reaction partners. This substrate switchable regioselective transformation gives access to functionalized [1,2,4]/[1,2,5]-oxadiazines in moderate to good yields. Mild reaction conditions, substrate scope, natural product/drug modification and post-synthetic transformations are the important practical features.

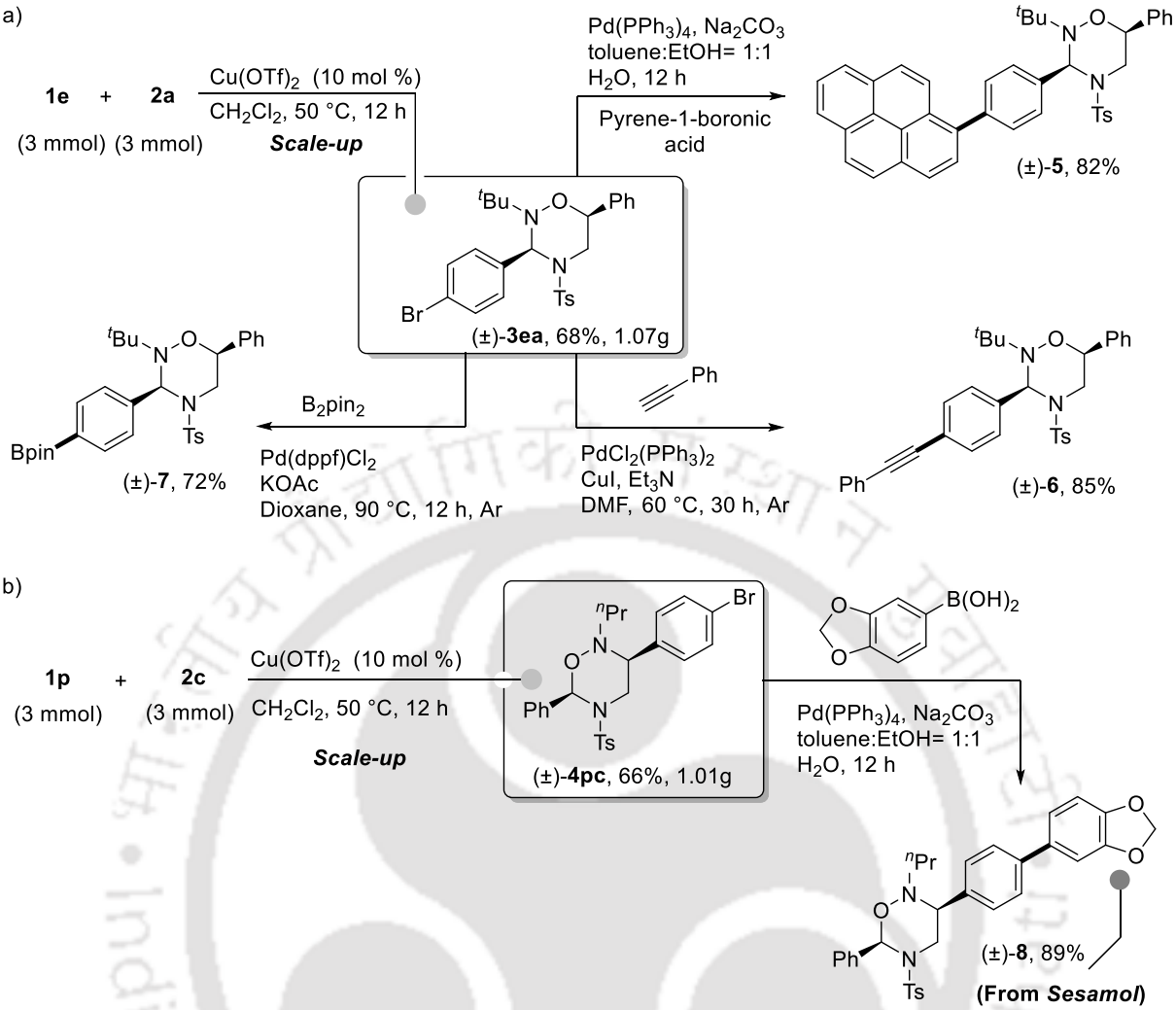

Scheme 12. Synthetic Utilities.

3.3 Experimental Section

General Information. $Ni(OTf)_2$ (96%), $Zn(OTf)_2$ (98%), $Sc(OTf)_3$ (99%), $Cu(OTf)_2$ (98%), $Yb(OTf)_3$ (>99%), $MnCl_2•4H_2O$, $Pd(dppf)Cl_2•CH_2Cl_2$ (>99%), *m*CPBA (≤77%), $Pd(PPh_3)_4$ (99%), and $PdCl_2(PPh_3)_2$ (98%) purchased from Aldrich and used as received. Oxaziridines[10] and Aziridines[11] were prepared according to reported procedure. SRL silica gel G/GF 254 plates were used for analytical TLC and SRL silica gel (100-200 mesh) was used for column chromatography. NMR (^1H, $^{13}C\{^1H\}$, $^{19}F\{^1H\}$) spectra were recorded on Brucker 400, 500 and 600 MHz spectrometer using $CDCl_3$ as solvent and Me_4Si as an internal standard. Chemical shifts (δ) and spin-spin coupling constant (*J*) are reported in ppm and in Hz, respectively, and other data are reported as follows: s = singlet, d = doublet, t = triplet, m = multiplet, q = quartet, dd = doublet of doublet. Melting points were determined using a Büchi B-540 apparatus and are uncorrected. FT-IR spectra were collected on Perkin Elmer IR spectrometer. Q-Tof ESI-

MS (model HAB 273) was used for recording mass spectra. HPLC analysis was carried out using Waters-2489 with Daicel Chiralcel AD-H column utilizing *iso*-propanol and hexane as eluent. Quadrupole time-of-flight electrospray ionization (ESI) mass spectrometer (Agilent 6546) was used for recording HRMS. Single crystal X-ray data was collected on a Bruker SMART APEX equipped with a CCD area detector using Mo/Kα radiation and the structure was solved by direct method using SHELXL 2019/1 and SHELXL 2018/3 (Göttingen, Germany).

General Procedure for the Synthesis of [1,2,4]/[1,2,5]-oxadiazines. Oxaziridine **1** (0.2 mmol, 1.0 equiv), aziridine **2** (0.2 mmol, 1.0 equiv) and $Cu(OTf)_2$ (7.2 mg, 0.02 mmol, 0.1 equiv) were stirred for 12 h in CH_2Cl_2 (2.0 mL, 0.1 M) at 50 ºC under N_2 atmosphere. The reaction mixture was diluted using CH_2Cl_2 (5 mL) and passed through a short pad of celite using CH_2Cl_2 (10 mL). Evaporation of the solvent gave a residue that was purified on silica gel column chromatography using ethyl acetate and hexane as eluent to afford [1,2,4]/[1,2,5]-oxadiazine motifs.

Procedure for Radical Scavenger Experiments. **1a**/**1p** (0.2 mmol, 1 equiv), **2a** (54.6 mg, 0.2 mmol, 1 equiv), $Cu(OTf)_2$ (7.2 mg, 0.02 mmol, 0.1 equiv) and TEMPO/BHT (0.4 mmol, 2 equiv) were stirred for 12 h in CH_2Cl_2 (2 mL, 0.1 M) at 50 ºC under N_2 atmosphere. . The reaction mixture was diluted using CH_2Cl_2 (5 mL) and passed through a short pad of celite using CH_2Cl_2 (10 mL). Evaporation of the solvent gave a residue that was purified on silica gel column chromatography using ethyl acetate and hexane as eluent to afford **3aa**/**4pa**.

Enantiospecific Synthesis of [1,2,4]/[1,2,5]-Oxadiazines. Oxaziridine **1a/1p** (0.2 mmol, 1.0 equiv), (*R*)-**2a** (0.2 mmol, 1.0 equiv) and $Cu(OTf)_2$ (7.2 mg, 0.02 mmol, 0.1 equiv) were stirred for 12 h in CH_2Cl_2 (2.0 mL, 0.1 M) at room temperature (25 ºC) under N_2 atmosphere. The purification was performed as above in general procedure. Then HPLC analysis was carried out using Daicel Chiralcel AD-H column utilizing *iso*-propanol and hexane as eluent.

Scale-up Synthesis of 3ea. 1e (765 mg, 3 mmol, 1.0 equiv), **2a** (819 mg, 3 mmol, 1.0 equiv) and $Cu(OTf)_2$ (108.3 mg, 0.3 mmol, 0.1 equiv) were stirred for 12 h in CH_2Cl_2 (30 mL, 0.1 M) at 50 ºC under N_2 atmosphere. The reaction mixture was diluted with CH_2Cl_2 (20 mL) and passed through a short pad of celite using CH_2Cl_2 (50 mL). Evaporation of the solvent gave a residue that was purified on silica gel column chromatography using ethyl acetate and hexane as an eluent to yield **3ea** in 68% yield (1.07 g).

Synthesis of 5. Compound **3ea** (52 mg, 0.1 mmol, 1.0 equiv), pyrene-1-boronic acid boronic acid (25 mg, 0.1 mmol, 1.0 equiv), $Pd(PPh_3)_4$ (3.5 mg, 0.003 mmol, 0.03 equiv), Na_2CO_3 (11 mg, 0.1 mmol, 1.0 equiv) and H_2O (25 µL) were stirred in toluene: EtOH (1:1, 1 mL) at 100 °C for 12 h under N_2 atmosphere. The reaction mixture was cooled to room temperature and passed through a short pad of celite using CH_2Cl_2 (10 mL). Evaporation of the solvent gave a residue that was purified on silica gel column chromatography to give **5** in 82% yield (53 mg).

Synthesis of 6.[17] Compound **3ea** (52 mg, 0.1 mmol, 1 equiv), phenylacetylene (20.4 mg, 0.1 mmol, 2 equiv,), $PdCl_2(PPh_3)_2$ (7 mg, 0.01 mmol, 0.1 equiv), CuI (1.9 mg, 0.01 mmol, 0.1 equiv) and Et_3N (70 µL, 0.5 mmol, 5 equiv) were stirred in DMF (1 mL) in a pressure at 60 °C for 30 h under argon atmosphere. The resulting mixture was quenched with H_2O and extracted with EtOAc (3 x 10 mL). The combined organic layer was washed with brine (2 x 5 mL) and water (1 x 5 mL). Drying (Na_2SO_4) and evaporation of the solvent gave a residue that was purified on silica gel column chromatography using ethyl acetate/hexane as an eluent to afford **6** in 85% (47 mg) yield.

Synthesis of 7.[17] Compound **3ea** (52 mg, 0.1 mmol, 1.0 equiv), bis(pinacolato)diboron (25 mg, 0.1 mmol, 1.0 equiv), KOAc (20 mg, 0.2 mmol, 2.0 equiv) and $Pd(dppf)Cl_2 \bullet CH_2Cl_2$ (4 mg, 0.005 mmol, 0.05 equiv) were stirred in THF (2 mL) at 100 °C for 4 h in a pressure tube. After completion, the reaction mixture was cooled to room temperature and passed through a short pad of celite using CH_2Cl_2 (15 ml). Evaporation of the solvent gave a residue that was purified on silica gel column chromatography using hexane and ethyl acetate as an eluent to give **7** in 72% yield (42 mg).

Scale-up Synthesis of 4pc. 1p (489 mg, 3 mmol, 1.0 equiv), **2c** (1.05 g, 3 mmol, 1.0 equiv) and $Cu(OTf)_2$ (108.3 mg, 0.3 mmol, 0.1 equiv) were stirred for 12 h in CH_2Cl_2 (30 mL, 0.1 M) at 50 °C under N_2 atmosphere. The reaction mixture was diluted with CH_2Cl_2 (20 mL) and passed through a short pad of celite using CH_2Cl_2 (50 mL). Evaporation of the solvent gave a residue that was purified on silica gel column chromatography using ethyl acetate and hexane as an eluent to yield **4pc** in 66% yield (1.01 g).

Synthesis of 8. Compound **4pc** (51 mg, 0.1 mmol, 1.0 equiv), benzo[d][1,3]dioxol-5-ylboronic acid (17 mg, 0.1 mmol, 1.0 equiv), $Pd(PPh_3)_4$ (3.5 mg, 0.003 mmol, 0.03 equiv), Na_2CO_3 (11 mg, 0.1 mmol, 1.0 equiv) and H_2O (25 µL) were stirred in toluene: EtOH (1:1, 1 mL) at 100 °C in an oil bath for 12 h under N_2 atmosphere. The reaction mixture was cooled to room temperature and passed through a short pad of celite using CH_2Cl_2 (10 mL). Evaporation of the

solvent gave a residue that was purified on silica gel column chromatography to give **8** in 89% yield (50 mg).

3.4 Characterization Data of the Products

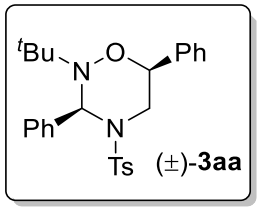

2-(Tert-butyl)-3,6-diphenyl-4-tosyl-1,2,4-oxadiazinane 3aa. Analytical TLC on silica gel, 1:19 ethyl acetate/hexane R_f = 0.45; colorless solid; mp 136-137 ºC; yield 80% (72 mg); ^{1}H NMR (500 MHz, $CDCl_3$) δ 7.74-7.72 (m, 2H), 7.60 (d, *J* = 8.5 Hz, 2H), 7.40-7.37 (m, 2H), 7.35-7.33 (m, 1H), 7.31-7.28 (m, 5H), 7.19 (d, *J* = 8.5 Hz, 2H), 6.06 (s, 1H), 4.74 (dd, *J* = 11.0, 3.0 Hz, 1H), 3.83 (dd, *J* = 14.0, 3.5 Hz, 1H), 3.42-3.37 (m, 1H), 2.38 (s, 3H), 0.98 (s, 9H); ^{13}C{^{1}H} NMR (125 MHz, $CDCl_3$) δ 143.3, 139.0, 138.3, 137.5, 129.7, 129.4, 128.7, 128.4, 128.4, 128.3, 127.7, 125.8, 78.628, 72.3, 58.3, 45.5, 26.8, 21.6; FT-IR (KBr) 2970, 2922, 2856, 1345, 1160, 959, 659 cm^{-1}; HRMS (ESI) m/z $[M+H]^+$ calcd for $C_{26}H_{31}N_2O_3S$: 451.2050, found: 451.2055.

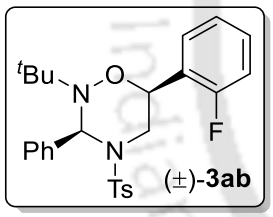

2-(Tert-butyl)-6-(2-fluorophenyl)-3-phenyl-4-tosyl-1,2,4-oxadiazinane 3ab. Analytical TLC on silica gel, 1:19 ethyl acetate/hexane R_f = 0.50; colorless solid; mp 224-225 ºC; yield 65% (61 mg); ^{1}H NMR (500 MHz, $CDCl_3$) δ 7.78-7.76 (m, 2H), 7.71 (d, *J* = 8.5 Hz, 2H), 7.45 (t, *J* = 7.0 Hz,1H), 7.33-7.29 (m, 4H), 7.26-7.24 (m, 2H), 7.20 (t, *J*= 7.0 Hz, 1H), 7.07-7.03 (m, 1H), 6.06 (s, 1H), 4.87 (dd, *J* = 11.0, 2.5 Hz, 1H), 3.94 (dd, *J* = 14.5, 3.0 Hz, 1H), 3.44-3.39 (m, 1H), 2.40 (s, 3H), 0.95 (s, 9H); ^{13}C{^{1}H} NMR (125 MHz, $CDCl_3$) δ 160.6 (d, J_{C-F} = 245.7 Hz), 143.4, 139.0, 137.6, 129.8 (d, J_{C-F} = 8.1 Hz), 129.6, 129.4, 128.4, 128.3, 127.8, 127.0 (d, J_{C-F} = 4.2 Hz), 125.6 (d, J_{C-F} = 14.0 Hz), 124.6 (d, J_{C-F} = 3.5 Hz), 115.7 (d, J_{C-F} = 21.2 Hz), 73.4, 72.5, 58.2, 44.6, 26.7, 21.6; ^{19}F NMR (471 MHz, $CDCl_3$) δ -117.431; FT-IR (KBr) 2922, 1493, 1455, 1345, 1162, 959, 705, 661 cm^{-1}; HRMS (ESI) m/z $[M+H]^+$ calcd for $C_{26}H_{30}FN_2O_3S$: 469.1956, found: 469.1958.

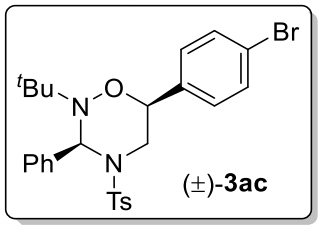

6-(4-Bromophenyl)-2-(tert-butyl)-3-phenyl-4-tosyl-1,2,4-oxadiazinane 3ac. Analytical TLC on silica gel, 1:9 ethyl acetate/hexane R_f = 0.56; colorless solid; mp 168-169 ºC; yield 70% (74 mg); ^{1}H NMR (500 MHz, $CDCl_3$) δ 7.69 (d, *J* = 7.5 Hz, 2H), 7.58 (d, *J* = 8.0 Hz, 2H), 7.52 (d, *J* = 8.0 Hz, 2H), 7.29-7.27 (m, 3H), 7.18-7.17 (m, 4H), 6.04 (s, 1H), 4.70 (dd, *J* = 11.5, 3.0 Hz, 1H), 3.81 (dd, *J* = 14.0, 3.0 Hz, 1H), 3.35-3.30 (m, 1H), 2.38 (s, 3H), 0.97 (s, 9H); ^{13}C{^{1}H} NMR (126 MHz, $CDCl_3$) δ 143.4, 138.8, 137.3, 137.1, 131.9, 129.5, 129.4, 128.5, 128.4, 127.6, 127.5, 122.3, 78.0, 72.2, 58.4, 45.3, 26.7, 21.6; FT-IR (KBr) 2926, 1488, 1343, 1162, 1010, 959, 703 cm^{-1}; HRMS (ESI) m/z $[M+H]^+$ calcd for $C_{26}H_{30}BrN_2O_3S$: 529.1155, found: 529.1158.

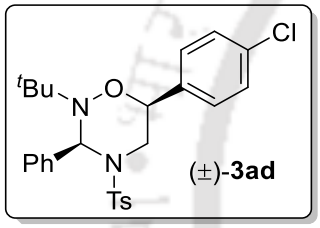

2-(Tert-butyl)-6-(4-chlorophenyl)-3-phenyl-4-tosyl-1,2,4-oxadiazinane 3ad. Analytical TLC on silica gel, 1:9 ethyl acetate/hexane R_f = 0.54; colorless solid; mp 185-186 ºC; yield 69% (67 mg); ^{1}H NMR (500 MHz, $CDCl_3$) δ 7.69-7.68 (m, 2H), 7.59 (d, *J* = 8.5 Hz, 2H), 7.37 (d, *J* = 8.5 Hz, 2H), 7.30-7.28 (m, 3H), 7.24-7.23 (m, 2H), 7.19 (d, *J* = 8.0 Hz, 2H), 6.05 (s, 1H), 4.72 (dd, *J* = 11.5, 3.0 Hz, 1H), 3.81 (dd, *J* = 14.0, 3.0 Hz, 1H), 3.36-3.31 (m, 1H), 2.38 (s, 3H), 0.98 (s, 9H); ^{13}C{^{1}H} NMR (125 MHz, $CDCl_3$) δ 143.4, 138.9, 137.3, 136.6, 134.3, 129.6, 129.4, 129.0, 128.5, 128.4, 127.6, 127.2, 78.0, 72.2, 58.4, 45.4, 26.7, 21.6; FT-IR (KBr) 2924, 1490, 1340, 1162, 959, 814, 656 cm^{-1}; HRMS (ESI) m/z $[M+H]^+$ calcd for $C_{26}H_{30}ClN_2O_3S$: 485.1660, found: 485.1666.

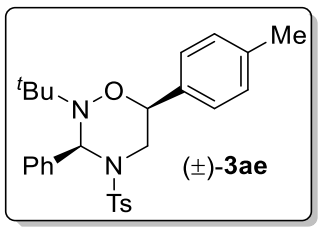

2-(Tert-butyl)-3-phenyl-6-(p-tolyl)-4-tosyl-1,2,4-oxadiazinane 3ae. Analytical TLC on silica gel, 1:9 ethyl acetate/hexane R_f = 0.58; colorless solid; mp 159-160 ºC; yield 78% (73 mg); ^{1}H NMR (500 MHz, $CDCl_3$) δ 7.79-7.78 (m, 2H), 7.66 (d, *J* = 8.0 Hz, 2H), 7.35-7.32 (m, 4H), 7.25-7.23 (m, 5H), 6.10 (s, 1H), 4.76 (dd, *J* = 11.5, 3.0 Hz, 1H),

3.87 (dd, *J* = 14.0, 2.5 Hz, 1H), 3.48-3.43 (m, 1H), 2.44 (s, 3H), 2.42 (s, 3H), 1.03 (s, 9H); $^{13}C\{^{1}H\}$ NMR (126 MHz, $CDCl_3$) δ 143.2, 139.1, 138.2, 137.5, 135.2, 129.7, 129.4, 129.3, 128.4, 128.2, 127.7, 125.9, 78.5, 72.3, 58.3, 45.5, 26.7, 21.6, 21.3; FT-IR (KBr) 2927, 1340, 1162, 959, 702, 659 cm^{-1}; HRMS (ESI) m/z $[M+H]^+$ calcd for $C_{27}H_{33}N_2O_3S$: 465.2206, found: 465.2206.

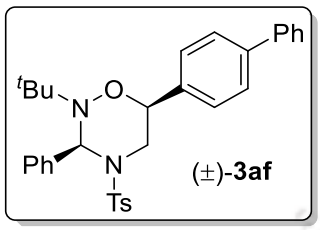

6-([1,1'-Biphenyl]-4-yl)-2-(tert-butyl)-3-phenyl-4-tosyl-1,2,4-oxadiazinane 3af. Analytical TLC on silica gel, 1:9 ethyl acetate/hexane R_f = 0.52; colorless solid; mp 180-181 ºC; yield 76% (80 mg); ^{1}H NMR (500 MHz, $CDCl_3$) δ 7.75-7.74 (m, 2H), 7.62-7.57 (m, 6H), 7.46-7.43 (m, 2H), 7.39-7.36 (m, 3H), 7.30-7.29 (m, 3H), 7.20 (d, *J* = 8.0 Hz, 2H), 6.07 (s, 1H), 4.79 (dd, *J* = 11.0, 3.0 Hz, 1H), 3.88 (dd, *J* = 14.0, 3.0 Hz, 1H), 3.46-3.41 (m, 1H), 2.39 (s, 3H), 1.00 (s, 9H); $^{13}C\{^{1}H\}$ NMR (125 MHz, $CDCl_3$) δ 143.3, 141.4, 140.7, 139.0, 137.4, 137.1, 129.7, 129.4, 129.0, 128.4, 128.3, 127.7, 127.6, 127.5, 127.2, 126.3, 78.4, 72.3, 58.4, 45.5, 26.8, 21.6; FT-IR (KBr) 2924, 1488, 1340, 1162, 959, 761, 664 cm^{-1}; HRMS (ESI) m/z $[M+H]^+$ calcd for $C_{32}H_{35}N_2O_3S$: 527.2363, found: 527.2366.

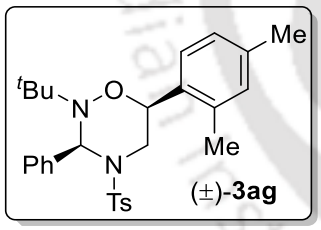

2-(Tert-butyl)-6-(2,4-dimethylphenyl)-3-phenyl-4-tosyl-1,2,4-oxadiazinane 3ag. Analytical TLC on silica gel, 1:9 ethyl acetate/hexane R_f = 0.50; colorless solid; mp 169-170 ºC; yield 75% (72 mg); ^{1}H NMR (500 MHz, $CDCl_3$) δ 7.80-7.78 (m, 2H), 7.65 (d, *J*= 8.0 Hz, 2H), 7.34-7.30 (m, 4H), 7.21 (d, *J* = 8.0 Hz, 2H), 7.08 (d, *J* = 8.0 Hz,1H), 6.98 (s, 1H), 6.10 (s, 1H), 4.85 (dd, *J* = 11.0, 3.0 Hz, 1H), 3.70 (dd, *J* = 14.5, 3.0 Hz, 1H), 3.44-3.39 (m, 1H), 2.39 (s, 3H), 2.31 (s, 3H), 2.14 (s, 3H), 0.97 (s, 9H); $^{13}C\{^{1}H\}$ NMR (125 MHz, $CDCl_3$) δ 143.3, 139.2, 138.1, 137.7, 135.4, 133.3, 131.5, 129.7, 129.3, 128.4, 128.2, 127.9, 127.1, 125.4, 75.9, 72.4, 58.2, 44.5, 26.8, 21.6, 21.1, 19.1; FT-IR (KBr) 2925, 1452, 1344, 1161, 959, 703, 659 cm^{-1}; HRMS (ESI) m/z $[M+H]^+$ calcd for $C_{28}H_{35}N_2O_3S$: 479.2363, found: 479.2367.

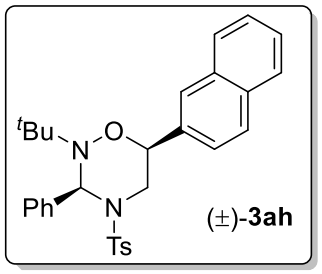

2-(Tert-butyl)-6-(naphthalen-2-yl)-3-phenyl-4-tosyl-1,2,4-oxadiazinane 3ah. Analytical TLC on silica gel, 1:9 ethyl acetate/hexane R_f = 0.48; colorless solid; mp 147-148 ºC; yield 79% (79 mg); ^{1}H NMR (500 MHz, $CDCl_3$) δ 7.87-7.83 (m, 3H), 7.77-7.76 (m, 3H), 7.62 (d, *J* = 8.0 Hz, 2H), 7.52-7.49 (m, 5H), 7.42 (m, 2H), 7.30-7.29 (m, 3H), 7.20 (d, *J* = 8.0 Hz, 2H),), 6.09 (s, 1H), 4.92 (dd, *J* = 11.5, 3.0 Hz, 1H), 3.95 (dd, *J* = 14.0, 3.5 Hz, 1H), 3.51-3.46 (m, 1H), 2.38 (s, 3H), 1.02 (s, 9H); ^{13}C{^{1}H} NMR (125 MHz, $CDCl_3$) δ 143.3, 139.0, 137.4, 135.6, 133.2, 129.7, 129.4, 128.5, 128.4, 128.3, 128.2, 127.9, 127.7, 126.5, 126.4, 124.7, 123.8, 78.6, 72.3, 58.4, 45.5, 26.8, 21.6; FT-IR (KBr) 2975, 2926, 1341, 1161, 957, 815, 660 cm^{-1}; HRMS (ESI) m/z $[M+H]^+$ calcd for $C_{30}H_{33}N_2O_3S$: 501.2206, found: 501.2208.

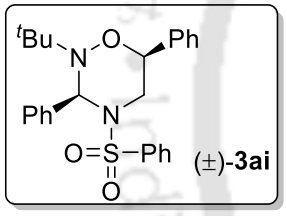

2-(Tert-butyl)-3,6-diphenyl-4-(phenylsulfonyl)-1,2,4-oxadiazinane 3ai. Analytical TLC on silica gel, 1:9 ethyl acetate/hexane R_f = 0.50; colorless solid; mp 172-173 ºC; yield 70% (61 mg); ^{1}H NMR (400 MHz, $CDCl_3$) δ 7.73-7.71 (m, 4H), 7.52-7.48 (m, 1H), 7.41-7.34 (m, 5H), 7.31-7.28 (m, 5H), 6.05 (s, 1H), 4.73 (dd, *J* = 14.0, 3.5 Hz, 1H), 3.87 (dd, *J* = 17.5, 4.0 Hz, 1H), 3.44-3.38 (m, 1H), 0.98 (s, 9H); ^{13}C{^{1}H} NMR (125 MHz, $CDCl_3$) δ 140.2, 138.8, 138.1, 132.5, 129.6, 128.8, 128.4, 128.4, 127.6, 125.9, 78.6, 72.4, 58.3, 45.6, 26.7; FT-IR (KBr) 2924, 1452, 1348, 1164, 959, 735, 696, 594 cm^{-1}; HRMS (ESI) m/z $[M+H]^+$ calcd for $C_{25}H_{29}N_2O_3S$: 437.1893, found: 437.1898.

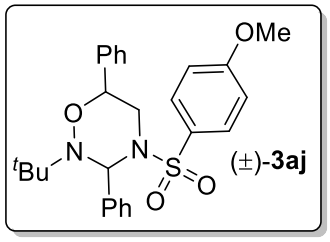

2-(Tert-butyl)-4-((4-methoxyphenyl)sulfonyl)-3,6-diphenyl-1,2,4-oxadiazinane 3aj. Analytical TLC on silica gel, 1:9 ethyl acetate/hexane R_f = 0.42; colorless solid; mp 204-205 ºC; yield 72% (67 mg); ^{1}H NMR (500 MHz, $CDCl_3$) δ 7.73-7.71

(m, 2H), 7.63 (d, *J* = 8.5 Hz, 2H), 7.41-7.38 (m, 2H), 7.35-7.28 (m, 6H), 6.85 (d, *J* = 9.0 Hz, 2H), 6.05 (s, 1H), 4.75 (dd, *J* = 11.5, 3.0 Hz, 1H), 3.83-3.79 (m, 4H), 3.40-3.35 (m, 1H), 0.99 (s, 9H); $^{13}C\{^{1}H\}$ NMR (150 MHz, $CDCl_3$) δ 162.8, 139.0, 138.2, 131.9, 129.7, 128.7, 128.4, 128.3, 128.3, 125.8, 78.5, 72.3, 58.3, 55.7, 45.5, 26.7; FT-IR (KBr) 2972, 2932, 1597, 1495, 1340, 1157, 958, 702 cm^{-1}; HRMS (ESI) m/z $[M+H]^+$ calcd for $C_{26}H_{31}N_2O_4S$: 467.1999, found: 467.2001.

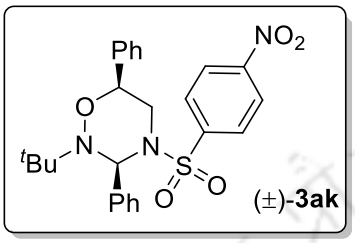

2-(Tert-butyl)-4-((4-nitrophenyl)sulfonyl)-3,6-diphenyl-1,2,4-oxadiazinane 3ak. Analytical TLC on silica gel, 1:9 ethyl acetate/hexane R_f = 0.44; colorless solid; mp 179-180 ºC; yield 81% (78 mg); ^{1}H NMR (500 MHz, $CDCl_3$) δ 8.16 (d, *J* = 8.5 Hz, 2H), 7.76 (d, *J* = 8.5 Hz, 2H), 7.67 (d, *J* = 7.5 Hz, 2H), 7.43-7.40 (m, 2H), 7.38-7.37 (m, 1H), 7.34-7.30 (m, 3H), 7.28-7.26 (m, 2H), 6.03 (s, 1H), 4.89 (dd, *J* = 11.5, 3.0 Hz, 1H), 3.91 (dd, *J* = 13.5, 3.5 Hz, 1H), 3.41-3.36 (m, 1H), 0.99 (s, 9H); $^{13}C\{^{1}H\}$ NMR (125 MHz, $CDCl_3$) δ 149.8, 145.6, 138.2, 137.6, 129.6, 128.9, 128.8, 128.7, 128.66, 128.63, 125.9, 123.8, 78.9, 72.8, 58.7, 45.8, 26.7; FT-IR (KBr) 2975, 2924, 1528, 1350, 1162, 949, 738, 611 cm^{-1}; HRMS (ESI) m/z $[M+H]^+$ calcd for $C_{25}H_{28}N_2O_5S$: 482.1744, found: 482.1748.

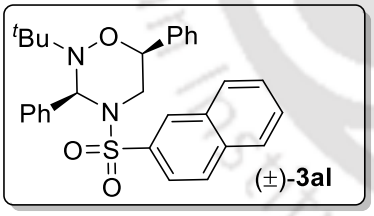

2-(Tert-butyl)-4-(naphthalen-2-ylsulfonyl)-3,6-diphenyl-1,2,4-oxadiazinane 3al. Analytical TLC on silica gel, 1:9 ethyl acetate/hexane R_f = 0.46; colorless solid; mp 131-132 ºC; yield 76% (74 mg); ^{1}H NMR (500 MHz, $CDCl_3$) δ 8.24 (s, 1H), 7.86-7.83 (m, 3H), 7.76-7.74 (m, 2H), 7.69-7.68 (m, 1H), 7.62-7.55 (m, 2H), 7.38-7.35 (m, 2H), 7.33 (d, *J* = 7.0 Hz, 1H), 7.28-7.26 (m, 5H), 6.14 (s, 1H), 4.75 (dd, *J* = 11.0, 3.0 Hz, 1H), 3.92 (dd, *J* = 14.0, 3.5 Hz, 1H), 3.45-3.40 (m, 1H), 0.97 (s, 9H); $^{13}C\{^{1}H\}$ NMR (125 MHz, $CDCl_3$) δ 138.8, 138.1, 137.1, 134.7, 132.1, 129.6, 129.2, 128.95, 128.91, 128.7, 128.48, 128.44, 128.42, 127.9, 127.4, 125.8, 123.0, 78.7, 72.4, 58.4, 45.6, 26.7; FT-IR (KBr) 2972, 2927, 1333, 1160, 960, 702, 657 cm^{-1}; HRMS (ESI) m/z $[M+H]^+$ calcd for $C_{29}H_{31}N_2O_3S$: 487.2050, found: 487.2053.

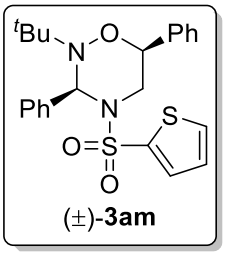

2-(Tert-butyl)-3,6-diphenyl-4-(thiophen-2-ylsulfonyl)-1,2,4-oxadiazinane 3am. Analytical TLC on silica gel, 1:9 ethyl acetate/hexane R_f = 0.45; colorless solid; mp 129-130 °C; yield 73% (65 mg); ^{1}H NMR (400 MHz, $CDCl_3$) δ 7.76-7.74 (m, 2H), 7.51 (dd, *J* = 5.2, 1.2 Hz, 1H), 7.43-7.39 (m, 2H), 7.37-7.34 (m, 4H), 7.31-7.29 (m, 3H), 6.99-6.97 (m, 1H), 6.06 (s, 1H), 4.84 (dd, *J* = 11.6, 3.2 Hz, 1H), 3.93 (dd, *J* = 13.6, 3.2 Hz, 1H), 3.49-3.43 (m, 1H), 1.00 (s, 9H); ^{13}C{^{1}H} NMR (125 MHz, $CDCl_3$) δ 141.0, 138.6, 138.1, 132.3, 131.8, 129.7, 128.8, 128.5, 128.4, 127.1, 125.8, 78.6, 72.6, 58.4, 45.7, 26.7; FT-IR (KBr) 2974, 1453, 1352, 1157, 1014, 959, 732, 666 cm^{-1}; HRMS (ESI) m/z $[M+H]^+$ calcd for $C_{23}H_{27}N_2O_3S_2$: 443.1458, found: 443.1449.

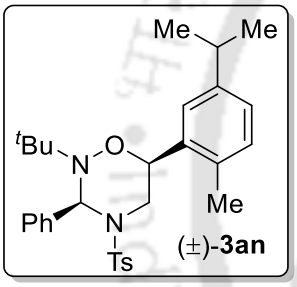

2-(Tert-butyl)-6-(5-isopropyl-2-methylphenyl)-3-phenyl-4-tosyl-1,2,4-oxadiazinane 3an. Analytical TLC on silica gel, 1:9 ethyl acetate/hexane R_f = 0.52; yellow solid; mp 186-187 °C; yield 78% (79 mg); ^{1}H NMR (500 MHz, $CDCl_3$) δ 7.83 (s, 1H), 7.70 (d, *J* = 8.0 Hz, 2H), 7.33-7.32 (m, 4H), 7.23 (d, *J* = 7.5 Hz, 2H), 7.11-7.07 (m, 2H), 6.12 (s, 1H), 4.85 (dd, *J* = 11.0, 3.0 Hz, 1H), 3.72 (dd, *J* = 15.5, 3.5 Hz, 1H), 3.47-3.42 (m, 1H), 2.96-2.88 (m, 1H), 2.40 (s, 3H), 2.14 (s, 3H), 1.27 (d, *J* = 7.0 Hz, 6H), 0.99 (s, 9H); ^{13}C{^{1}H} NMR (125 MHz, $CDCl_3$) δ 146.9, 143.3, 139.2, 137.8, 136.1, 132.6, 130.6, 129.7, 129.3, 128.4, 128.2, 127.9, 126.3, 123.5, 75.9, 72.3, 58.2, 44.4, 33.8, 26.8, 24.2, 24.0, 21.6, 18.7; FT-IR (KBr) 2960, 1457, 1348, 1162, 959, 748, 659 cm^{-1}; HRMS (ESI) m/z $[M+H]^+$ calcd for $C_{30}H_{39}N_2O_3S$: 507.2676, found: 507.2675.

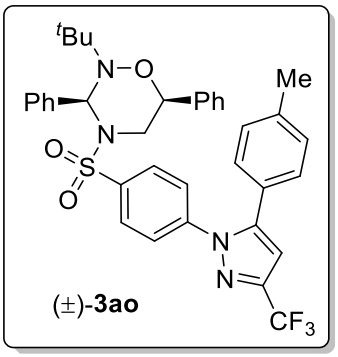

2-(Tert-butyl)-3,6-diphenyl-4-((4-(5-(p-tolyl)-3-(trifluoromethyl)-1H-pyrazol-1-yl)phenyl)sulfonyl)-1,2,4-oxadiazinane 3ao. Analytical TLC on silica gel, 1:9 ethyl acetate/hexane R_f = 0.40; colorless solid; mp 247-248 °C; yield 69% (91 mg); ^{1}H NMR (400 MHz, $CDCl_3$) δ 7.73-7.68 (m, 4H), 7.43-7.34 (m, 5H), 7.30-7.29 (m, 5H), 7.08-7.03 (m, 4H), 6.71 (s, 1H), 6.04 (s, 1H), 4.75 (dd, *J* = 11.6, 3.2 Hz, 1H), 3.84 (dd, *J* = 14.0, 3.2 Hz, 1H), 3.43-3.37 (m, 1H), 2.28 (s, 3H), 0.98 (s, 9H); ^{13}C{^{1}H} NMR (150 MHz, $CDCl_3$) δ 145.2, 144.5 (q, $J_{C\text{-}F}$ = 38.5 Hz), 142.4, 139.83, 139.82, 138.6, 137.8, 129.8, 129.6, 128.9, 128.8, 128.63, 128.60, 128.59, 128.53, 125.89, 125.84, 125.3, 123.8 (q, $J_{C\text{-}F}$ = 267.7 Hz), 106.4, 78.6, 72.6, 58.4, 45.7, 26.7, 21.3; ^{19}F NMR (471 MHz, $CDCl_3$) δ -62.430; FT-IR (KBr) 2927, 1470, 1358, 1236, 1164, 1099, 755 cm^{-1}; HRMS (ESI) m/z $[M+H]^+$ calcd for $C_{36}H_{36}F_3N_4O_3S$: 661.2455, found: 661.2462.

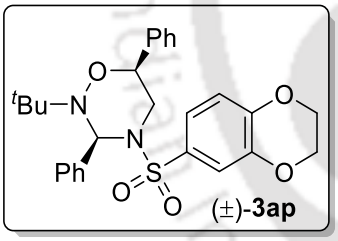

2-(Tert-butyl)-4-((2,3-dihydrobenzo[b][1,4]dioxin-6-yl)sulfonyl)-3,6-diphenyl-1,2,4-oxadiazinane 3ap. Analytical TLC on silica gel, 1:9 ethyl acetate/hexane R_f = 0.42; colorless solid; mp 188-189 °C; yield 70% (69 mg); ^{1}H NMR (500 MHz, $CDCl_3$) δ 7.73-7.71 (m, 2H), 7.41-7.38 (m, 2H), 7.35-7.31 (m, 3H), 7.29-7.28 (m, 3H), 7.26-7.24 (m, 1H), 7.19 (dd, *J* = 8.5, 2.0 Hz, 1H), 6.84 (d, *J* = 8.5 Hz, 1H), 6.02 (s, 1H), 4.76 (dd, *J* = 11.0, 2.5 Hz, 1H), 4.28-4.24 (m, 4H), 3.82 (dd, *J* = 14.0, 3.0 Hz, 1H), 3.41-3.36 (m, 1H), 0.99 (s, 9H); ^{13}C{^{1}H} NMR (125 MHz, $CDCl_3$) δ 147.2, 143.3, 138.9, 138.3, 132.7, 129.7, 128.8, 128.4, 128.38, 128.32, 125.8, 121.3, 117.5, 117.4, 78.5, 72.3, 64.6, 64.2, 58.3, 45.6, 26.7; FT-IR (KBr) 2927, 1494, 1285, 1253, 1155, 958, 699 cm^{-1}; HRMS (ESI) m/z $[M+H]^+$ calcd for $C_{27}H_{31}N_2O_5S$: 495.1948, found: 495.1956.

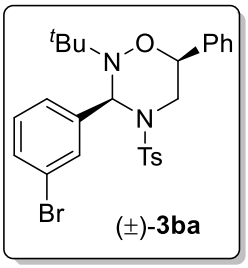

3-(3-Bromophenyl)-2-(tert-butyl)-6-phenyl-4-tosyl-1,2,4-oxadiazinane 3ba. Analytical TLC on silica gel, 1:9 ethyl acetate/hexane R_f = 0.54; colorless solid; mp 174-175 °C; yield 65% (69 mg); ^{1}H NMR (500 MHz, $CDCl_3$) δ 7.86 (s, 1H), 7.70 (d, *J* = 8.0 Hz, 1H), 7.62 (d, *J* = 8.0 Hz, 2H), 7.43-7.38 (m, 3H), 7.36-7.33 (m, 1H), 7.29-7.28 (m, 2H), 7.23-7.21 (d, *J*= 8.0 Hz, 2H), 7.17-7.14 (m, 1H), 5.99 (s, 1H), 4.73 (dd, *J* = 11.0, 3.0 Hz, 1H), 3.85 (dd, *J* = 14.0, 3.5 Hz, 1H), 3.37-3.32 (m, 1H), 2.40 (s, 3H), 1.00 (s, 9H); ^{13}C{^{1}H} NMR (125 MHz, $CDCl_3$) δ 143.5, 141.1, 137.9, 137.2, 132.5, 131.3, 130.0, 129.5, 128.8, 128.5, 128.1, 127.6, 125.9, 122.4, 78.7, 71.4, 58.4, 45.5, 26.8, 21.6; FT-IR (KBr) 2924, 1345, 1162, 959, 748, 659, 583 cm^{-1}; HRMS (ESI) m/z [M+H]$^+$ calcd for $C_{26}H_{30}BrN_2O_3S$: 529.1155, found: 529.1158.

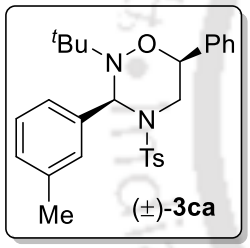

2-(Tert-butyl)-6-phenyl-3-(m-tolyl)-4-tosyl-1,2,4-oxadiazinane 3ca. Analytical TLC on silica gel, 1:9 ethyl acetate/hexane R_f = 0.56; colorless solid; mp 184-185 °C; yield 77% (72 mg); ^{1}H NMR (500 MHz, $CDCl_3$) δ 7.62-7.60 (m, 3H), 7.44 (s, 1H), 7.40-7.37 (m, 2H), 7.35-7.29 (m, 3H), 7.20 (d, *J*= 8.0 Hz, 2H), 7.17-7.14 (m, 1H), 7.11-7.09 (m, 1H), 6.01 (s, 1H), 4.71 (dd, *J* = 11.0, 3.0 Hz, 1H), 3.83 (dd, *J* = 14.5, 3.5 Hz, 1H), 3.43-3.38 (m, 1H), 2.39 (s, 3H), 2.32 (s, 3H), 0.99 (s, 9H); ^{13}C{^{1}H} NMR (150 MHz, $CDCl_3$) δ 143.2, 138.8, 138.3, 137.9, 137.4, 130.3, 129.3, 128.9, 128.7, 128.3, 128.2, 127.7, 126.7, 125.8, 78.5, 72.3, 58.3, 45.6, 26.8, 21.6; FT-IR (KBr) 2978, 2924, 1344, 1161, 964, 744, 661 cm^{-1}; HRMS (ESI) m/z [M+H]$^+$ calcd for $C_{27}H_{33}N_2O_3S$: 465.2206, found: 465.2211.

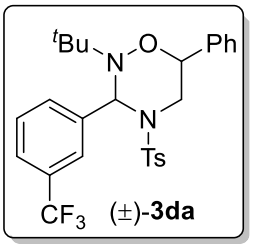

2-(Tert-butyl)-6-phenyl-4-tosyl-3-(3-(trifluoromethyl)phenyl)-1,2,4-oxadiazinane 3da. Analytical TLC on silica gel, 1:9 ethyl acetate/hexane R_f = 0.48; colorless solid; mp 128-129 ºC; yield 70% (73 mg); ^{1}H NMR (400 MHz, $CDCl_3$) δ 8.06 (s, 1H), 7.91 (d, *J* = 7.6 Hz, 1H), 7.61-7.55 (m, 3H), 7.44-7.33 (m, 4H), 7.29-7.27 (m, 2H), 7.21 (d, *J* = 8.4 Hz, 2H), 6.10 (s, 1H), 4.74 (dd, *J* = 11.2, 3.2 Hz, 1H), 3.85 (dd, *J* = 14.0, 3.2 Hz, 1H), 3.35-3.28 (m, 1H), 2.39 (s, 3H), 0.99 (s, 9H); ^{13}C{^{1}H} NMR (125 MHz, $CDCl_3$) δ 143.6, 139.8, 137.8, 137.1, 132.8, 130.7 (q, $J_{C\text{-}F}$ = 32.2 Hz), 129.5, 129.0, 128.9, 128.6, 127.5, 126.3 (q, $J_{C\text{-}F}$ = 4.1 Hz), 125.9, 125.18 (q, $J_{C\text{-}F}$ = 270.7 Hz) 125.10 (q, $J_{C\text{-}F}$ = 3.6 Hz), 78.9, 71.4, 58.4, 45.6, 26.8, 21.6; ^{19}F NMR (377 MHz, $CDCl_3$) δ -62.752; FT-IR (KBr) 2978, 2924, 1329, 1163, 1127, 964, 745, 664 cm^{-1}; HRMS (ESI) m/z $[M+H]^+$ calcd for $C_{27}H_{30}F_3N_2O_3S$: 519.1924, found: 519.1933.

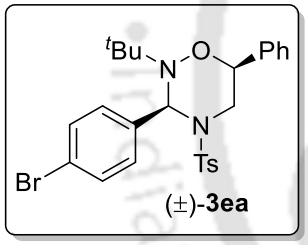

3-(4-Bromophenyl)-2-(tert-butyl)-6-phenyl-4-tosyl-1,2,4-oxadiazinane 3ea. Analytical TLC on silica gel, 1:2 ethyl acetate/hexane R_f = 0.42; colorless solid; mp 149-150 ºC; yield 75% (79 mg); ^{1}H NMR (400 MHz, $CDCl_3$) δ 7.62-7.59 (m, 4H), 7.42-7.32 (m, 5H), 7.28-7.26 (m, 2H), 7.22 (d, *J* = 8.4 Hz, 2H), 6.01 (s, 1H), 4.71 (dd, *J* = 11.6, 3.2 Hz, 1H), 3.85 (dd, *J* = 14.0, 3.2 Hz, 1H), 3.36-3.29 (m, 1H), 2.40 (s, 3H), 0.99 (s, 9H); ^{13}C{^{1}H} NMR (125 MHz, $CDCl_3$) δ 143.5, 138.0, 137.9, 137.2, 131.5, 131.2, 129.5, 128.8, 128.5, 127.6, 125.8, 122.5, 78.5, 71.5, 58.4, 45.4, 26.8, 21.6; FT-IR (KBr) 2978, 1485, 1345, 1161, 959, 745, 659, 585 cm^{-1}; HRMS (ESI) m/z $[M+H]^+$ calcd for $C_{26}H_{30}BrN_2O_3S$: 529.1155, found: 529.1162.

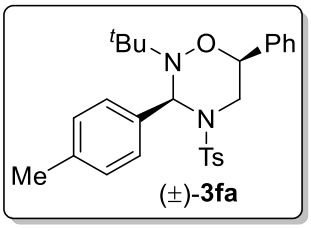

2-(Tert-butyl)-6-phenyl-3-(p-tolyl)-4-tosyl-1,2,4-oxadiazinane 3fa. Analytical TLC on silica gel, 1:9 ethyl acetate/hexane R_f = 0.52; colorless solid; mp 197-198 °C; yield 82% (76 mg); ^{1}H NMR (600 MHz, $CDCl_3$) δ 7.61 (d, *J* = 7.8 Hz, 4H), 7.40-7.37 (m, 2H), 7.34-7.32 (m, 1H), 7.30-7.29 (m, 2H), 7.19 (d, *J* = 7.8 Hz, 2H), 7.09 (d, *J* = 7.8 Hz, 2H), 6.02 (s, 1H), 4.70 (dd, *J* = 11.4, 3.0 Hz, 1H), 3.81 (dd, *J* = 13.8, 3.0 Hz, 1H), 3.40-3.36 (m, 1H), 2.38 (s, 3H), 2.33 (s, 3H), 0.98 (s, 9H); ^{13}C{^{1}H} NMR (150 MHz, $CDCl_3$) δ 143.2, 138.3, 138.0, 137.4, 136.0, 129.5, 129.3, 129.0, 128.7, 128.3, 127.7, 125.8, 78.5, 72.2, 58.2, 45.6, 26.7, 21.6, 21.2; FT-IR (KBr) 2922, 1343, 1161, 959, 750, 659, 593 cm^{-1}; HRMS (ESI) m/z [M+H]$^+$ calcd for $C_{27}H_{33}N_2O_3S$: 465.2206, found: 465.2208.

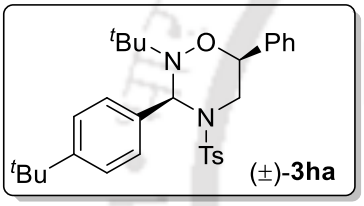

2-(Tert-butyl)-3-(4-(tert-butyl)phenyl)-6-phenyl-4-tosyl-1,2,4-oxadiazinane 3ha. Analytical TLC on silica gel, 1:9 ethyl acetate/hexane R_f = 0.55; colorless solid; mp 164-165 °C; yield 79% (80 mg); ^{1}H NMR (500 MHz, $CDCl_3$) δ 7.62 (d, *J* = 8.0 Hz, 2H), 7.55 (d, *J* = 8.0 Hz, 2H), 7.40-7.38 (m, 2H), 7.35-7.31 (m, 3H), 7.27-7.26 (m, 2H), 7.14 (d, *J* = 8.0 Hz, 2H), 6.02 (s, 1H), 4.77 (dd, *J* = 11.0, 2.5 Hz, 1H), 3.84 (dd, *J* = 13.5, 3.0 Hz, 1H), 3.40-3.35 (m, 1H), 2.35 (s, 3H), 1.30 (s, 9H), 0.98 (s, 9H); ^{13}C{^{1}H} NMR (125 MHz, $CDCl_3$) δ 151.3, 143.0, 138.4, 137.3, 135.7, 129.3, 129.2, 128.7, 128.3, 127.7, 125.8, 125.2, 78.6, 72.2, 58.3, 45.7, 34.6, 31.4, 26.7, 21.5; FT-IR (KBr) 2965, 1346, 1163, 960, 730, 661, 592 cm^{-1}; HRMS (ESI) m/z [M+H]$^+$ calcd for $C_{30}H_{39}N_2O_3S$: 507.2676, found: 507.2686.

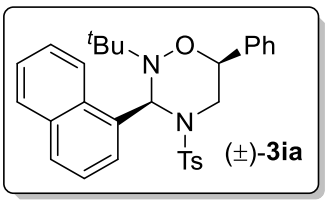

2-(Tert-butyl)-3-(naphthalen-1-yl)-6-phenyl-4-tosyl-1,2,4-oxadiazinane 3ia. Analytical TLC on silica gel, 1:9 ethyl acetate/hexane R_f = 0.48; colorless solid; mp 229-230 °C; yield 74% (74 mg); ^{1}H NMR (500 MHz, $CDCl_3$) δ 8.69 (d, *J* = 8.0 Hz, 2H), 7.88 (d, *J* = 8.0 Hz, 1H), 7.84 (d, *J* = 8.0 Hz, 1H), 7.72 (d, *J* = 7.5 Hz, 2H), 7.67-7.64 (m, 1H), 7.54-7.51 (m, 1H), 7.42-7.31 (m, 6H), 7.20 (d, *J* = 7.5 Hz, 2H), 7.15 (s, 1H), 4.76-4.74

(m, 1H), 3.72-3.69 (m, 1H), 3.58-3.53 (m, 1H), 2.38 (s, 3H), 1.02 (s, 9H); $^{13}C\{^{1}H\}$ NMR (125 MHz, $CDCl_3$) δ 143.6, 138.3, 137.6, 134.2, 134.1, 131.2, 129.4, 129.2, 129.1, 128.9, 128.8, 128.4, 128.1, 127.1, 126.0, 125.7, 124.5, 123.7, 78.4, 65.9, 58.4, 45.4, 27.0, 21.6; FT-IR (KBr) 2974, 1346, 1159, 944, 810, 741, 664 cm^{-1}; HRMS (ESI) m/z $[M+H]^+$ calcd for $C_{30}H_{33}N_2O_3S$: 501.2206, found: 501.2215.

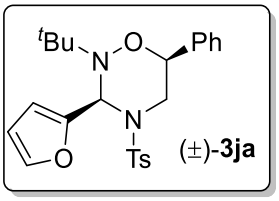

2-(Tert-butyl)-3-(furan-2-yl)-6-phenyl-4-tosyl-1,2,4-oxadiazinane 3ja. Analytical TLC on silica gel, 1:9 ethyl acetate/hexane R_f = 0.48; colorless solid; mp 135-136 °C; yield 85% (75 mg); ^{1}H NMR (500 MHz, $CDCl_3$) δ 7.55 (d, *J* = 7.5 Hz, 2H), 7.38-7.35 (m, 2H), 7.33-7.30 (m, 4H), 7.18 (d, *J* = 8.0 Hz, 2H), 6.336-6.330 (m, 1H), 6.25-6.24 (m, 1H), 6.16 (s, 1H), 4.80 (dd, *J* = 10.5, 1.5 Hz, 1H), 3.81 (dd, *J* = 13.0, 2.5 Hz, 1H), 3.29-3.24 (m, 1H), 2.37 (s, 3H), 0.96 (s, 9H); $^{13}C\{^{1}H\}$ NMR (125 MHz, $CDCl_3$) δ 150.4, 143.2, 141.3, 138.3, 136.7, 129.3, 128.7, 128.4, 127.6, 126.0, 110.6, 110.2, 78.6, 66.0, 58.2, 46.7, 26.0, 21.6; FT-IR (KBr) 2978, 1347, 1223, 1161, 965, 748, 659 cm^{-1}; HRMS (ESI) m/z $[M+H]^+$ calcd for $C_{24}H_{29}N_2O_4S$: 441.1843, found: 441.1847.

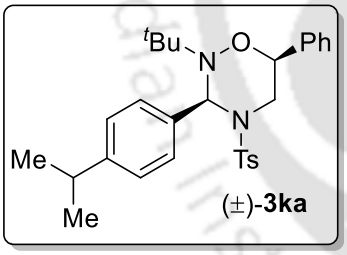

2-(Tert-butyl)-3-(4-isopropylphenyl)-6-phenyl-4-tosyl-1,2,4-oxadiazinane 3ka. Analytical TLC on silica gel, 1:9 ethyl acetate/hexane R_f = 0.50; colorless solid; mp 131-132 °C; yield 76% (75 mg); ^{1}H NMR (400 MHz, $CDCl_3$) δ 7.62 (d, *J* = 8.0 Hz, 2H), 7.55 (d, *J* = 8.4 Hz, 2H), 7.41-7.37 (m, 2H), 7.35-7.30 (m, 3H), 7.15-7.10 (m, 4H), 6.01 (s, 1H), 4.76 (dd, *J* = 11.2, 3.2 Hz, 1H), 3.84 (dd, *J* = 13.6, 3.2 Hz, 1H), 3.39-3.33 (m, 1H), 2.90-2.84 (m, 1H), 2.36 (s, 3H), 1.24 (d, *J* = 7.6 Hz, 6H) 0.97 (s, 9H); $^{13}C\{^{1}H\}$ NMR (125 MHz, $CDCl_3$) δ 149.0, 143.0, 138.4, 137.3, 136.1, 129.6, 129.3, 128.7, 128.3, 127.7, 126.3, 125.8, 78.5, 72.3, 58.3, 45.7, 33.9, 26.7, 24.1, 24.0, 21.6; FT-IR (KBr) 2963, 1345, 1162, 960, 814, 661, 548 cm^{-1}; HRMS (ESI) m/z $[M+H]^+$ calcd for $C_{29}H_{37}N_2O_3S$: 493.2519, found: 493.2519.

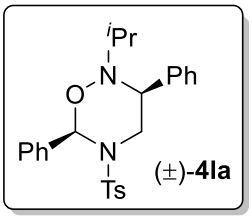

2-Isopropyl-3,6-diphenyl-5-tosyl-1,2,5-oxadiazinane 4la. Analytical TLC on silica gel, 1:15 ethyl acetate/hexane R_f = 0.56; colorless solid; mp 163-164 ºC; yield 65% (57 mg); ^{1}H NMR (500 MHz, $CDCl_3$) δ 7.93 (d, *J* = 8.0 Hz, 2H), 7.59 (d, *J* = 7.5 Hz, 2H), 7.44-7.39 (m, 4H), 7.35-7.32 (m, 1H), 7.18-7.17 (m, 3H), 6.87-6.85 (m, 2H), 6.83 (s, 1H), 3.71-3.65 (m, 1H), 3.44-3.38 (m, 1H), 2.61-2.56 (m, 1H), 2.50 (s, 3H), 1.10 (d, *J* = 6.5 Hz, 3H), 0.57 (d, *J* = 6.5 Hz, 3H); ^{13}C{^{1}H} NMR (125 MHz, $CDCl_3$) δ 143.9, 138.2, 137.7, 129.9, 128.8, 128.3, 128.3, 128.2, 127.8, 127.6, 127.4, 86.0, 61.5, 51.8, 47.5, 21.7, 21.2, 12.2; FT-IR (KBr) 2975, 2932, 1345, 1165, 959, 738, 687 cm^{-1}; HRMS (ESI) m/z $[M+H]^+$ calcd for $C_{25}H_{39}N_2O_3S$: 437.1893, found: 437.1896.

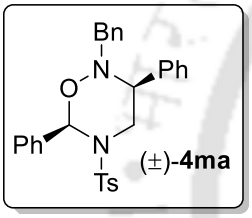

2-Benzyl-3,6-diphenyl-5-tosyl-1,2,5-oxadiazinane 4ma. Analytical TLC on silica gel, 1:15 ethyl acetate/hexane R_f = 0.48; colorless solid; mp 166-167 ºC; yield 70% (68 mg); ^{1}H NMR (400 MHz, $CDCl_3$) δ 7.90 (d, *J* = 8.4 Hz, 2H), 7.41 (d, *J* = 8.0 Hz, 2H), 7.30-7.27 (m, 3H), 7.24-7.18 (m, 6H), 7.10-7.08 (m, 2H), 7.02-7.00 (m, 2H), 6.96-6.94 (m, 2H), 6.72 (s, 1H), 3.73-3.64 (m, 2H), 3.45-3.38 (m, 1H), 3.26 (dd, *J* = 11.2, 3.2 Hz, 1H), 3.21 (d, *J* = 13.6 Hz, 1H), 2.52 (s, 3H); ^{13}C{^{1}H} NMR (125 MHz, $CDCl_3$) δ 144.0, 138.2, 137.7, 137.0, 136.7, 130.2, 129.9, 129.0, 128.5, 128.1, 128.1, 127.9, 127.7, 127.4, 127.2, 86.1, 65.9, 59.7, 47.4, 21.8; FT-IR (KBr) 2927, 1493, 1345, 1165, 1020, 746, 570 cm^{-1}; HRMS (ESI) m/z $[M+H]^+$ calcd for $C_{29}H_{29}N_2O_3S$: 485.1893, found: 485.1894.

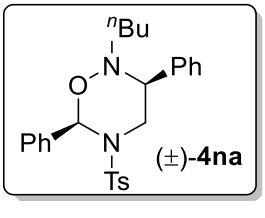

2-Butyl-3,6-diphenyl-5-tosyl-1,2,5-oxadiazinane 4na. Analytical TLC on silica gel, 1:15 ethyl acetate/hexane R_f = 0.52; colorless solid; mp 133-134 ºC; yield 68% (61 mg); ^{1}H NMR (500 MHz, $CDCl_3$) δ 7.92 (d, *J* = 8.0 Hz, 2H), 7.55 (d, *J* = 7.5 Hz, 2H), 7.43-7.39 (m, 4H), 7.35-7.32 (m, 1H), 7.18-7.17 (m, 3H), 6.85-6.82 (m, 3H), 3.68-3.65 (m, 1H), 3.39-3.34 (m, 1H), 3.12 (dd, *J* = 11.0, 3.0 Hz, 1H), 2.51 (s, 3H), 2.38-2.32 (m, 1H), 2.20-2.15

(m, 1H), 1.45-1.37 (m, 1H), 1.22-1.12 (m, 1H), 1.04-0.84 (m, 2H), 0.76 (t, J = 7.5 Hz, 3H); $^{13}C\{^{1}H\}$ NMR (125 MHz, $CDCl_3$) δ 144.0, 138.4, 137.9, 137.7, 129.9, 128.8, 128.3, 128.3, 128.1, 127.9, 127.6, 127.2, 86.1, 66.3, 55.6, 47.4, 28.2, 21.8, 20.3, 13.9; FT-IR (KBr) 2926, 1434, 1346, 1132, 1036, 754, 661 cm^{-1}; HRMS (ESI) m/z $[M+H]^+$ calcd for $C_{26}H_{31}N_2O_3S$: 451.2050, found: 451.2059.

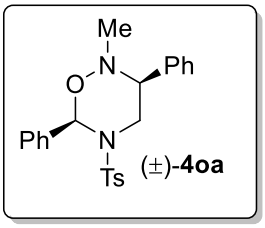

2-Methyl-3,6-diphenyl-5-tosyl-1,2,5-oxadiazinane 4oa. Analytical TLC on silica gel, 1:15 ethyl acetate/hexane R_f = 0.56; colorless solid; mp 165-166 °C; yield 67% (55 mg); ^{1}H NMR (400 MHz, $CDCl_3$) δ 7.92 (, J = 8.0 Hz, 2H), 7.54-7.52 (m, 2H), 7.44-7.40 (m, 4H), 7.36-7.32 (m, 1H), 7.19-7.15 (m, 3H), 6.85-6.83 (m, 2H), 6.80 (s, 1H), 3.68 (dd, J = 14.8, 2.5 Hz, 1H), 3.38-3.31 (m, 1H), 2.99 (dd, J = 11.2, 3.2 Hz, 1H), 2.51 (s, 3H), 2.23 (s, 3H); $^{13}C\{^{1}H\}$ NMR (125 MHz, $CDCl_3$) δ 144.1, 137.9, 137.8, 137.6, 129.9, 128.8, 128.5, 128.1, 127.9, 127.6, 127.1, 86.3, 68.1, 47.1, 43.7, 21.8; FT-IR (KBr) 2922, 1345, 1165, 961, 750, 570 cm^{-1}; HRMS (ESI) m/z $[M+H]^+$ calcd for $C_{23}H_{25}N_2O_3S$: 409.1580, found: 409.1571.

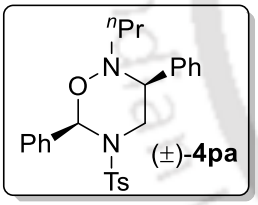

3,6-Diphenyl-2-propyl-5-tosyl-1,2,5-oxadiazinane 4pa. Analytical TLC on silica gel, 1:15 ethyl acetate/hexane R_f = 0.54; colorless solid; mp 124-125 °C; yield 71% (62 mg); ^{1}H NMR (500 MHz, $CDCl_3$) δ 7.91 (d, J = 8.0 Hz, 2H), 7.55 (d, J= 7.5 Hz, 2H), 7.43-7.39 (m, 4H), 7.35-7.32 (m, 1H), 7.18-7.17 (m, 3H), 6.85-6.82 (m, 3H), 3.68 (dd, J = 14.5, 2.0 Hz, 1H), 3.39-3.34 (m, 1H), 3.11 (dd, J = 11.0, 3.0 Hz, 1H), 2.51 (s, 3H), 2.30-2.25 (m, 1H), 2.19-2.14 (m, 1H), 1.57-1.51 (m, 2H), 0.68 (t, J = 7.5 Hz, 3H); $^{13}C\{^{1}H\}$ NMR (125 MHz, $CDCl_3$) δ 144.0, 138.4, 137.8, 137.7, 129.9, 128.8, 128.4, 128.3, 128.1, 127.9, 127.6, 127.2, 86.1, 66.4, 57.8, 47.3, 21.8, 19.4, 11.7; FT-IR (KBr) 2962, 2927, 1488, 1345, 1167, 972, 697 cm^{-1}; HRMS (ESI) m/z $[M+H]^+$ calcd for $C_{25}H_{29}N_2O_3S$: 437.1893, found: 437.1897

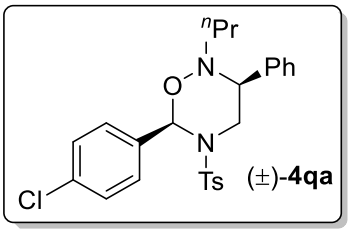

6-(4-Chlorophenyl)-3-phenyl-2-propyl-5-tosyl-1,2,5-oxadiazinane 4qa. Analytical TLC on silica gel, 1:15 ethyl acetate/hexane R_f = 0.52; colorless solid; mp 172-173 ºC; yield 69% (65 mg); ^{1}H NMR (400 MHz, $CDCl_3$) δ 7.90 (d, *J* = 8.4 Hz, 2H), 7.49 (d, *J* = 8.0 Hz, 2H), 7.43 (d, *J* = 8.0 Hz, 2H), 7.38 (d, *J* = 8.4 Hz, 2H), 7.20-7.19 (m, 3H), 6.85-6.82 (m, 2H), 6.77 (s, 1H), 3.67 (dd, *J* = 14.8, 2.0 Hz, 1H), 3.34-3.27 (m, 1H), 3.08 (dd, *J* = 11.2, 3.2 Hz, 1H), 2.51 (s, 3H), 2.31-2.24 (m, 1H), 2.18-2.12 (m, 1H), 1.54-1.47 (m, 2H), 0.68 (t, *J* = 7.2 Hz, 3H); ^{13}C{^{1}H} NMR (125 MHz, $CDCl_3$) δ 144.2, 138.2, 137.7, 136.3, 133.8, 129.9, 128.8, 128.8, 128.6, 128.4, 128.1, 127.5, 85.7, 66.3, 57.8, 47.3, 21.8, 19.4, 11.7; FT-IR (KBr) 2962, 2924, 1488, 1348, 1162, 972, 674 cm^{-1}; HRMS (ESI) m/z $[M+H]^+$ calcd for $C_{25}H_{28}ClN_2O_3S$: 471.1504, found: 471.1504.

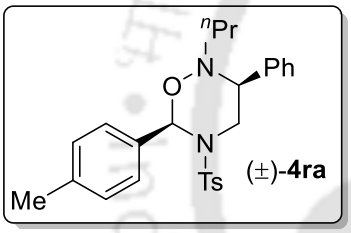

3-Phenyl-2-propyl-6-(p-tolyl)-5-tosyl-1,2,5-oxadiazinane 4ra. Analytical TLC on silica gel, 1:15 ethyl acetate/hexane R_f = 0.56; colorless solid; mp 134-135 ºC; yield 66% (60 mg); ^{1}H NMR (500 MHz, $CDCl_3$) δ 7.91 (d, *J* = 8.0 Hz, 2H), 7.42-7.40 (m, 4H), 7.21-7.16 (m, 5H), 6.86-6.85 (m, 2H), 6.78 (s, 1H), 3.67 (dd, *J* = 15.0, 3.0 Hz, 1H), 3.40-3.35 (m, 1H), 3.11-3.08 (dd, *J* = 11.5, 3.0 Hz, 1H), 2.50 (s, 3H), 2.39 (s, 3H), 2.30-2.24 (m, 1H), 2.18-2.13 (m, 1H), 1.56-1.50 (m, 2H), 0.69 (t, *J* = 7.0 Hz, 3H); ^{13}C{^{1}H} NMR (125 MHz, $CDCl_3$) δ 143.9, 138.5, 137.9, 137.5, 134.6, 129.8, 129.1, 128.7, 128.3, 128.1, 127.6, 127.1, 86.1, 66.5, 57.8, 47.3, 21.8, 21.3, 19.4, 11.7; FT-IR (KBr) 2924, 1254, 1165, 973, 738, 705 cm^{-1}; HRMS (ESI) m/z $[M+H]^+$ calcd for $C_{26}H_{31}N_2O_3S$: 451.2050, found: 451.2056.

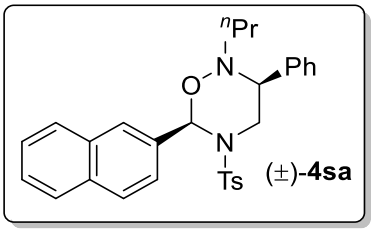

6-(Naphthalen-2-yl)-3-phenyl-2-propyl-5-tosyl-1,2,5-oxadiazinane 4sa. Analytical TLC on silica gel, 1:15 ethyl acetate/hexane R_f = 0.50; colorless solid; mp 189-190 ºC; yield 70% (86 mg); ^{1}H NMR (400 MHz, $CDCl_3$) δ 7.99 (s, 1H), 7.96 (d,

J = 8.4 Hz, 2H), 7.89-7.84 (m, 3H), 7.68-7.65 (m, 1H), 7.52-7.50 (m, 2H), 7.45-7.43 (m, 2H), 7.16-7.12 (m, 3H), 6.97 (s, 1H), 6.81-6.80 (m, 2H), 3.74 (dd, *J* = 14.8, 2.0 Hz, 1H), 3.49-3.42 (m, 1H), 3.13 (dd, *J* = 11.2, 3.2 Hz, 1H), 2.53 (s, 3H), 2.33-2.17 (m, 2H), 1.66-1.59 (m, 2H), 0.68 (t, *J* = 7.6 Hz, 3H); $^{13}C\{^{1}H\}$ NMR (125 MHz, $CDCl_3$) δ 144.1, 138.4, 137.9, 135.3, 133.3, 133.1, 129.9, 128.8, 128.4, 128.3, 128.2, 128.1, 127.7, 127.6, 126.3, 126.2, 126.1, 125.2, 86.3, 66.5, 57.9, 47.5, 21.8, 19.5, 11.8; FT-IR (KBr) 2927, 1343, 1165, 809, 748, 682, 560 cm^{-1}; HRMS (ESI) m/z $[M+H]^+$ calcd for $C_{29}H_{31}N_2O_3S$: 487.2050, found: 487.2056.

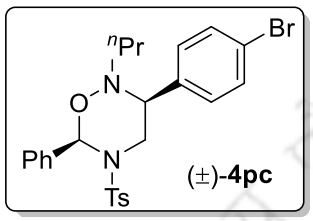

3-(4-Bromophenyl)-6-phenyl-2-propyl-5-tosyl-1,2,5-oxadiazinane 4pc. Analytical TLC on silica gel, 1:15 ethyl acetate/hexane R_f = 0.54; colorless solid; mp 180-181 °C; yield 75% (77 mg); ^{1}H NMR (400 MHz, $CDCl_3$) δ 7.90 (d, *J* = 8.0 Hz, 2H), 7.53 (d, *J* = 7.5 Hz, 2H), 7.42-7.39 (m, 4H), 7.35 (d, *J* = 7.5 Hz, 1H), 7.32 (d, *J* = 8.0 Hz, 2H), 6.81 (s, 1H), 6.74 (d, *J* = 8.5 Hz, 2H), 3.65 (dd, *J* = 15.0, 3.0 Hz, 1H), 3.33-3.29 (m, 1H), 3.11 (dd, *J* = 11.0, 3.0 Hz, 1H), 2.50 (s, 3H), 2.26-2.14 (m, 2H), 1.56-1.51 (m, 2H), 0.69 (t, *J* = 7.0 Hz, 3H); $^{13}C\{^{1}H\}$ NMR (125 MHz, $CDCl_3$) δ 144.1, 137.7, 137.4, 137.4, 132.0, 129.9, 129.2, 128.4, 128.1, 127.9, 127.2, 122.2, 86.1, 65.8, 57.9, 47.1, 21.8, 19.4, 11.7; FT-IR (KBr) 2975, 2924, 1485, 1343, 1162, 959, 661 cm^{-1}; HRMS (ESI) m/z $[M+H]^+$ calcd for $C_{25}H_{28}BrN_2O_3S$: 515.0999, found: 515.1000.

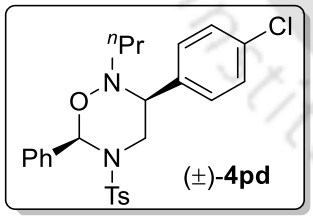

3-(4-Chlorophenyl)-6-phenyl-2-propyl-5-tosyl-1,2,5-oxadiazinane 4pd. Analytical TLC on silica gel, 1:15 ethyl acetate/hexane R_f = 0.52; colorless solid; mp 119-120 °C; yield 79% (74 mg); ^{1}H NMR (400 MHz, $CDCl_3$) δ 7.90 (d, *J* = 8.4 Hz, 2H), 7.53 (d, *J* = 8.0 Hz, 2H), 7.42-7.38 (m, 4H), 7.36-7.32 (m, 1H), 7.17 (d, *J* = 8.4 Hz, 2H), 6.81-6.78 (m, 3H), 3.67-3.62 (m, 1H), 3.34-3.27 (m, 1H), 3.13 (dd, *J* = 11.2, 3.2 Hz, 1H), 2.50 (s, 3H), 2.27-2.13 (m, 2H), 1.55-1.49 (m, 2H), 0.69 (t, *J* = 7.2 Hz, 3H); $^{13}C\{^{1}H\}$ NMR (125 MHz, $CDCl_3$) δ 144.1, 137.8, 137.5, 136.9, 134.1, 129.9, 129.0, 128.9, 128.4, 128.1, 128.0, 127.2, 86.1, 65.8, 57.9, 47.2, 21.8, 19.4, 11.7; FT-IR (KBr) 2963, 1490, 1345, 1167, 1017, 971, 704 cm^{-1}; HRMS (ESI) m/z $[M+H]^+$ calcd for $C_{25}H_{28}ClN_2O_3S$: 471.1504, found: 471.1509.

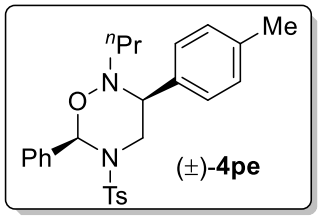

6-Phenyl-2-propyl-3-(p-tolyl)-5-tosyl-1,2,5-oxadiazinane 4pe. Analytical TLC on silica gel, 1:15 ethyl acetate/hexane R_f = 0.53; colorless solid; mp 138-139 °C; yield 77% (69 mg); ^{1}H NMR (400 MHz, $CDCl_3$) δ 7.91 (d, *J* = 8.4 Hz, 2H), 7.55 (d, *J* = 8.0 Hz, 2H), 7.42-7.38 (m, 4H), 7.35-7.31 (m, 1H), 6.99 (d, *J* = 7.6 Hz, 2H), 6.80 (s, 1H), 6.74 (d, *J* = 8.0 Hz, 2H), 3.67-3.62 (m, 1H), 3.38-3.32 (m, 1H), 3.09 (dd, *J* = 11.2, 3.2 Hz, 1H), 2.50 (s, 3H), 2.32-2.25 (m, 4H), 2.18-2.12 (m, 1H), 1.54-1.49 (m, 2H), 0.68 (d, *J* = 7.6 Hz, 3H); ^{13}C{^{1}H} NMR (125 MHz, $CDCl_3$) δ 143.9, 138.1, 137.9, 137.8, 135.4, 129.9, 129.4, 128.4, 128.1, 127.8, 127.5, 127.2, 86.1, 66.2, 57.8, 47.4, 21.8, 21.2, 19.4, 11.7; FT-IR (KBr) 2927, 1345, 1164, 1020, 969, 814, 656 cm^{-1}; HRMS (ESI) m/z [M+H]$^+$ calcd for $C_{26}H_{31}N_2O_3S$: 451.2050, found: 451.2047.

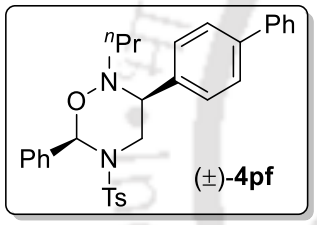

3-([1,1'-Biphenyl]-4-yl)-6-phenyl-2-propyl-5-tosyl-1,2,5-oxadiazinane 4pf. Analytical TLC on silica gel, 1:15 ethyl acetate/hexane R_f = 0.51; colorless solid; mp 149-150 °C; yield 71% (73 mg); ^{1}H NMR (400 MHz, $CDCl_3$) δ 7.93 (d, *J* = 8.4 Hz, 2H), 7.57-7.55 (m, 2H), 7.50-7.48 (m, 2H), 7.44-7.37 (m, 8H), 7.35-7.30 (m, 2H), 6.93 (d, *J* = 8.4 Hz, 2H), 6.84 (s, 1H), 3.37-3.69 (m, 1H), 3.44-3.37 (m, 1H), 3.18 (dd, *J* = 10.8, 3.2 Hz, 1H), 2.52 (s, 3H), 2.38-2.31 (m, 1H), 2.24-2.18 (m, 1H), 1.56-1.53 (m, 2H), 0.71 (t, *J* = 7.6 Hz, 3H); ^{13}C{^{1}H} NMR (125 MHz, $CDCl_3$) δ 144.0, 141.2, 140.5, 137.9, 137.7, 137.4, 129.9, 128.9, 128.4, 128.1, 128.0, 127.9, 127.6, 127.5, 127.2, 127.1, 86.1, 66.2, 57.9, 47.3, 21.8, 19.5, 11.8; FT-IR (KBr) 2927, 1347, 1164, 1019, 971, 695, 569 cm^{-1}; HRMS (ESI) m/z [M+H]$^+$ calcd for $C_{31}H_{33}N_2O_3S$: 513.2206, found: 513.2201.

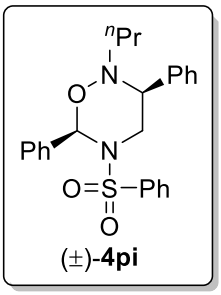

3,6-Diphenyl-5-(phenylsulfonyl)-2-propyl-1,2,5-oxadiazinane 4pi. Analytical TLC on silica gel, 1:15 ethyl acetate/hexane R_f = 0.50; colorless solid; mp 119-120 °C; yield 70% (59 mg); ^{1}H NMR (400 MHz, $CDCl_3$) δ 8.05-8.03 (m, 2H), 7.71-7.62 (m, 3H), 7.56-7.54 (m, 2H), 7.43-7.39 (m, 2H), 7.36-7.32 (m, 1H), 7.18-7.17 (m, 3H), 6.84-6.82 (m, 3H), 3.70-3.65 (m, 1H), 3.42-3.36 (m, 1H), 3.04 (dd, *J* = 11.2, 3.2 Hz, 1H), 2.30-2.23 (m, 1H), 2.17-2.10 (m, 1H), 1.56-1.49 (m, 2H), 0.68 (t, *J* = 7.2 Hz, 3H); ^{13}C{^{1}H} NMR (150 MHz, $CDCl_3$) δ 140.8, 138.3, 137.6, 133.2, 129.3, 128.8, 128.4, 128.3, 128.1, 127.9, 127.6, 127.2, 86.2, 66.4, 57.8, 47.4, 19.4, 11.7; FT-IR (KBr) 2924, 1493, 1348, 1167, 1032, 720, 585 cm^{-1}; HRMS (ESI) m/z $[M+H]^+$ calcd for $C_{24}H_{27}N_2O_3S$: 423.1737, found: 423.1735.

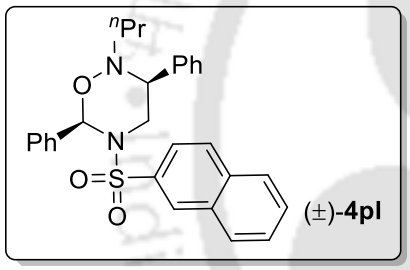

5-(Naphthalen-2-ylsulfonyl)-3,6-diphenyl-2-propyl-1,2,5-oxadiazinane 4pl. Analytical TLC on silica gel, 1:15 ethyl acetate/hexane R_f = 0.48; colorless solid; mp 129-130 °C; yield 68% (64 mg); ^{1}H NMR (500 MHz, $CDCl_3$) δ 8.58 (s, 1H), 8.10-7.98 (m, 4H), 7.72-7.66 (m, 2H), 7.57 (d, *J* = 8.0 Hz, 2H), 7.41 (t, *J* = 7.5 Hz, 2H), 7.36-7.33 (m, 1H), 7.16-7.12 (m, 3H), 6.91 (s, 1H), 6.77 (d, *J* = 7.0 Hz, 2H), 3.77 (dd, *J* = 15.0, 1.5 Hz, 1H), 3.44-3.39 (m, 1H), 3.09 (dd, *J* = 11.0, 2.5 Hz, 1H), 2.24-2.18 (m, 1H), 2.11-2.06 (m, 1H), 1.52-1.45 (m, 2H), 0.63 (t, *J* = 7.5 Hz, 3H); ^{13}C{^{1}H} NMR (125 MHz, $CDCl_3$) δ 138.3, 137.6, 135.1, 132.4, 129.6, 129.4, 129.3, 129.1, 128.7, 128.4, 128.3, 128.1, 127.9, 127.8, 127.6, 127.2, 123.3, 86.2, 66.6, 57.8, 47.4, 19.4, 11.7; FT-IR (KBr) 2924, 1450, 1340, 1165, 1020, 969, 748, 656 cm^{-1}; HRMS (ESI) m/z $[M+H]^+$ calcd for $C_{28}H_{29}N_2O_3S$: 473.1893, found: 473.1888.

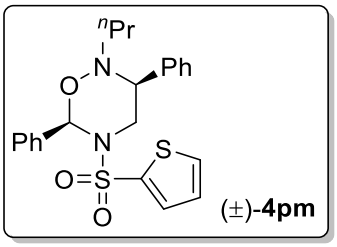

3,6-Diphenyl-2-propyl-5-(thiophen-2-ylsulfonyl)-1,2,5-oxadiazinane 4pm. Analytical TLC on silica gel, 1:15 ethyl acetate/hexane R_f = 0.49; colorless solid; mp 149-150 ºC; yield 69% (59 mg); ^{1}H NMR (500 MHz, $CDCl_3$) δ 7.79-7.78 (m, 1H), 7.73-7.72 (m, 1H), 7.57 (d, *J* = 8.0 Hz, 2H), 7.42 (t, *J* = 7.0 Hz, 2H), 7.36-7.34 (m, 1H), 7.23-7.19 (m, 4H), 6.92-6.90 (m, 2H), 6.82 (s, 1H), 3.80 (dd, *J* = 14.5, 1.5 Hz, 1H), 3.46-3.41 (m, 1H), 3.20 (dd, *J* = 11.5, 3.0 Hz, 1H), 2.35-2.29 (m, 1H), 2.23-2.18 (m, 1H), 1.62-1.57 (m, 2H), 0.70 (t, *J* = 7.0 Hz, 3H); ^{13}C{^{1}H} NMR (125 MHz, $CDCl_3$) δ 141.5, 138.3, 137.4, 133.1, 132.6, 128.8, 128.4, 128.0, 127.9, 127.6, 127.2, 86.3, 66.6, 57.9, 47.6, 19.4, 11.7; FT-IR (KBr) 2924, 1452, 1353, 1160, 1022, 969, 697, 590 cm^{-1}; HRMS (ESI) m/z [M+H]$^+$ calcd for $C_{22}H_{25}N_2O_3S_2$: 429.1301, found: 429.1305.

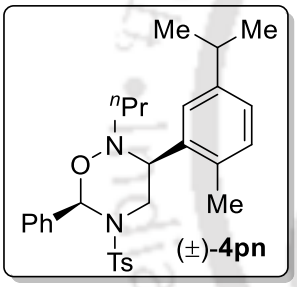

3-(5-Isopropyl-2-methylphenyl)-6-phenyl-2-propyl-5-tosyl-1,2,5-oxadiazinane 4pn. Analytical TLC on silica gel, 1:15 ethyl acetate/hexane R_f = 0.52; colorless solid; mp 124-125 ºC; yield 70% (69 mg); ^{1}H NMR (400 MHz, $CDCl_3$) δ 7.93 (d, *J* = 8.0 Hz, 2H), 7.58 (d, *J* = 7.6 Hz, 2H), 7.44-7.38 (m, 4H), 7.36-7.33 (m, 1H), 6.96-6.90 (m, 2H), 6.87 (s, 1H), 6.65 (s, 1H), 3.60-3.56 (m, 1H), 3.49-3.46 (m, 1H), 3.36-3.30 (m, 1H), 2.66-2.60 (m,1H), 2.48 (s, 3H), 2.31-2.19 (m, 2H), 1.96 (s, 3H), 1.68-1.60 (m, 1H), 1.50-1.42 (m, 1H), 1.01 (t, *J* = 7.6 Hz, 6H), 0.69 (t, *J* = 7.2 Hz, 3H); ^{13}C{^{1}H} NMR (125 MHz, $CDCl_3$) δ 147.1, 143.9, 137.9, 137.8, 136.5, 132.5, 130.3, 129.8, 128.3, 128.2, 127.8, 127.3, 125.5, 125.1, 86.1, 61.4, 57.4, 46.5, 33.5, 24.1, 23.7, 21.7, 19.5, 18.9, 11.9; FT-IR (KBr) 2960, 2927, 1452, 1345, 1162, 1017, 972, 733, 572 cm^{-1}; HRMS (ESI) m/z [M+H]$^+$ calcd for $C_{29}H_{37}N_2O_3S$: 493.2519, found: 493.2502.

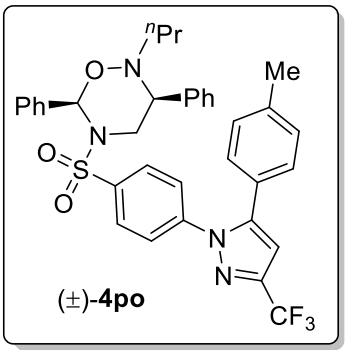

3,6-Diphenyl-2-propyl-5-((4-(5-(p-tolyl)-3-(trifluoromethyl)-1H-pyrazol-1-yl)phenyl)sulfonyl)-1,2,5-oxadiazinane 4po. Analytical TLC on silica gel, 1:15 ethyl acetate/hexane R_f = 0.46; colorless solid; mp 195-196 ºC; yield 65% (84 mg); ^{1}H NMR (500 MHz, $CDCl_3$) δ 8.01 (d, *J* = 9.0 Hz, 2H), 7.60 (d, *J* = 9.0 Hz, 2H), 7.54 (d, *J* = 8.0 Hz, 2H), 7.42 (t, *J* = 7.5 Hz, 2H), 7.37-7.34 (m, 1H), 7.21-7.14 (m, 7H), 6.85 (d, *J* = 6.5 Hz, 2H), 6.80 (s, 1H), 6.77 (s, 1H), 3.71 (dd, *J* = 14.5, 2.5 Hz, 1H), 3.44-3.39 (m, 1H), 3.18 (dd, *J* = 11.0, 3.0 Hz, 1H), 2.36 (s, 3H), 2.34-2.29 (m, 1H), 2.22-2.17 (m, 1H), 1.56-1.53 (m, 2H), 0.71 (t, *J* = 7.5 Hz, 3H); ^{13}C{^{1}H} NMR (125 MHz, $CDCl_3$) δ 145.4, 144.5 (q, $J_{C\text{-}F}$ = 38.6 Hz) 142.8, 140.4, 139.9, 138.1, 137.2, 129.9, 128.98, 128.93, 128.91, 128.5, 128.1, 127.6, 127.1, 126.0, 125.6, 122.2 (q, $J_{C\text{-}F}$ = 267.5 Hz), 106.7, 86.3, 66.7, 57.9, 47.5, 21.4, 19.6, 11.7; ^{19}F NMR (471 MHz, $CDCl_3$) δ -62.409; FT-IR (KBr) 2927, 1470, 1365, 1237, 1165, 1020, 973, 699 cm^{-1}; HRMS (ESI) m/z $[M+H]^+$ calcd for $C_{35}H_{34}F_3N_4O_3S$: 647.2298, found: 647.2295.

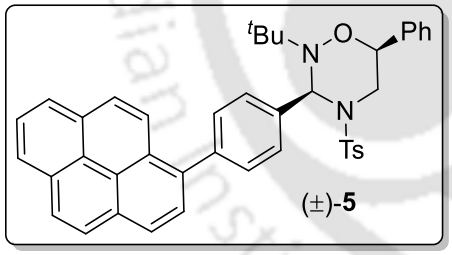

2-(Tert-butyl)-6-phenyl-3-(4-(pyren-1-yl)phenyl)-4-tosyl-1,2,4-oxadiazinane 5. Analytical TLC on silica gel, 1:9 ethyl acetate/hexane R_f = 0.40; brown solid; mp 193-194 ºC; yield 82% (53 mg); ^{1}H NMR (400 MHz, $CDCl_3$) δ 8.24-8.15 (m, 4H), 8.13-8.07 (m, 3H), 8.06-8.00 (m, 2H), 7.96-7.91 (m, 3H), 7.70 (d, *J* = 8.0 Hz, 2H), 7.57 (d, *J* = 8.0 Hz, 2H), 7.43-7.33 (m, 5H), 7.24 (s, 1H), 6.20 (s, 1H), 4.84 (dd, *J* = 10.8, 2.8 Hz, 1H), 3.97 (dd, *J* = 14.0, 3.6 Hz, 1H), 3.57-3.50 (m, 1H), 2.40 (s, 3H), 1.11 (s, 9H); ^{13}C{^{1}H} NMR (125 MHz, $CDCl_3$) δ 143.4, 141.2, 138.2, 137.8, 137.3, 137.2, 131.6, 131.1, 130.8, 130.6, 129.7, 129.4, 128.8, 128.5, 128.4, 127.8, 127.7, 127.6, 127.5, 126.2, 125.8, 125.3, 125.2, 125.1, 125.0, 124.8, 78.6, 72.2, 58.5, 45.7, 26.9, 21.7; FT-IR (KBr) 2967, 2926, 1595, 1344, 1161, 960, 845, 660 cm^{-1}; HRMS (ESI) m/z $[M+H]^+$ calcd for $C_{42}H_{39}N_2O_3S$: 651.2676, found: 651.1677.

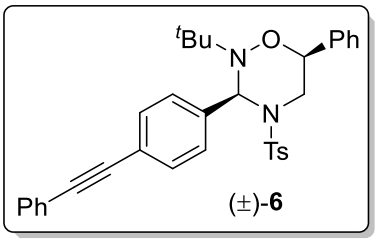

2-(Tert-butyl)-6-phenyl-3-(4-(phenylethynyl)phenyl)-4-tosyl-1,2,4-oxadiazinane 6. Analytical TLC on silica gel, 1:9 ethyl acetate/hexane R_f = 0.42; orange solid; mp 190-191 ºC; yield 85% (47 mg); ^{1}H NMR (500 MHz, $CDCl_3$) δ 7.73 (d, *J* = 8.0 Hz, 2H), 7.63 (d, *J* = 8.0 Hz, 2H), 7.54-7.53 (m, 2H), 7.47 (d, *J* = 8.0 Hz, 2H), 7.42-7.35 (m, 6H), 7.31 (d, *J* = 7.5 Hz, 2H), 7.23 (d, *J* = 8.0 Hz, 2H), 6.07 (s, 1H), 4.75 (dd, *J* = 11.5, 3.5 Hz, 1H), 3.86 (dd, *J* = 14.5, 3.5 Hz, 1H), 3.38 (t, *J* = 12.5 Hz, 1H), 2.40 (s, 3H), 1.01 (s, 9H); ^{13}C{^{1}H} NMR (125 MHz, $CDCl_3$) δ 143.5, 139.0, 138.0, 137.2, 131.7, 131.6, 129.6, 129.4, 128.8, 128.5, 128.4, 127.6, 125.8, 123.3, 123.2, 90.2, 89.0, 78.6, 71.8, 58.3, 45.5, 26.8, 21.6; FT-IR (KBr) 2926, 1496, 1344, 1263, 1162, 1031, 952, 758, 662 cm^{-1}; HRMS (ESI) m/z $[M+H]^+$ calcd for $C_{34}H_{35}N_2O_3S$: 551.2363, found: 551.2347.

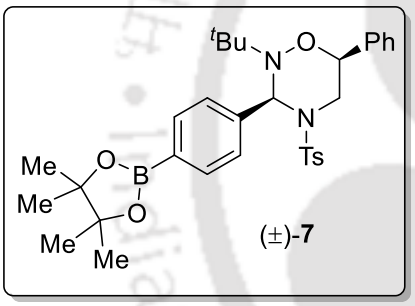

2-(Tert-butyl)-6-phenyl-3-(4-(4,4,5,5-tetramethyl-1,3,2-dioxaborolan-2-yl)phenyl)-4-tosyl-1,2,4-oxadiazinane 7. Analytical TLC on silica gel, 1:9 ethyl acetate/hexane R_f = 0.45; colorless solid; mp 198-199 ºC; yield 72% (42 mg); ^{1}H NMR (500 MHz, $CDCl_3$) δ 7.75-7.71 (m, 4H), 7.60 (d, *J* = 8.0 Hz, 2H), 7.39-7.33 (m, 3H), 7.30-7.28 (m, 2H), 7.18 (d, *J* = 8.0 Hz, 2H), 6.06 (s, 1H), 4.73 (dd, *J* = 11.5, 3.0 Hz, 1H), 3.81-3.78 (m, 1H), 3.37 (t, *J* = 7.0 Hz, 1H), 2.37 (s, 3H), 1.34 (s, 12H), 0.98 (s, 9H); ^{13}C{^{1}H} NMR (125 MHz, $CDCl_3$) δ 143.2, 141.8, 138.2, 137.3, 134.8, 129.4, 129.0, 128.7, 128.4, 127.6, 125.9, 83.9, 78.7, 72.1, 58.3, 45.6, 26.8, 25.0, 24.9, 21.6; FT-IR (KBr) 2924, 1360, 1162, 1094, 961, 662, 544 cm^{-1}; HRMS (ESI) m/z $[M+H]^+$ calcd for $C_{32}H_{42}BN_2O_5S$: 577.2902, found: 577.2887.

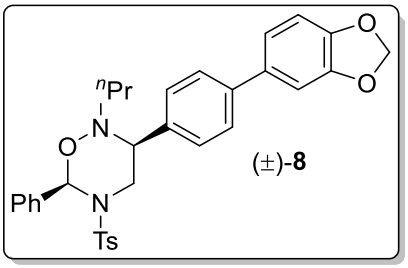

3-(4-(Benzo[d][1,3]dioxol-5-yl)phenyl)-6-phenyl-2-propyl-5-tosyl-1,2,5-oxadiazinane 8. Analytical TLC on silica gel, 1:9 ethyl acetate/hexane R_f = 0.51; colorless solid; mp 156-157 ºC; yield 89% (50 mg); ^{1}H NMR (500 MHz, $CDCl_3$) δ 7.92 (d, *J* = 8.5 Hz, 2H), 7.56 (d, *J* = 8.5 Hz, 2H), 7.43-7.40 (m, 4H), 7.36-7.31 (m, 3H), 6.96-6.94 (m, 2H), 6.89 (d, *J* = 8.5 Hz, 2H), 6.84-6.83 (m, 2H), 5.97 (s, 2H), 3.71-3.67 (m, 1H), 3.42-3.36 (m, 1H), 3.17-3.14 (m, 1H), 2.51 (s, 3H), 2.36-2.30 (m, 1H), 2.22-2.17 (m, 1H), 0.70 (t, *J* = 7.5 Hz, 3H); ^{13}C{^{1}H} NMR (125 MHz, $CDCl_3$) δ 148.1, 147.2, 143.9, 140.8, 137.7, 137.5, 136.9, 134.7, 129.8, 128.3, 128.0, 127.8, 127.7, 127.1, 127.0, 120.5, 108.6, 107.4, 101.1, 86.0, 66.0, 57.7, 47.2, 21.6, 19.3, 11.6; FT-IR (KBr) 2962, 2927, 1480, 1345, 1226, 1038, 806, 740 cm^{-1}; HRMS (ESI) m/z $[M+H]^+$ calcd for $C_{32}H_{33}N_2O_5S$: 557.2105, found: 557.2112.

Crystal Data and Structure Refinement for 3ia

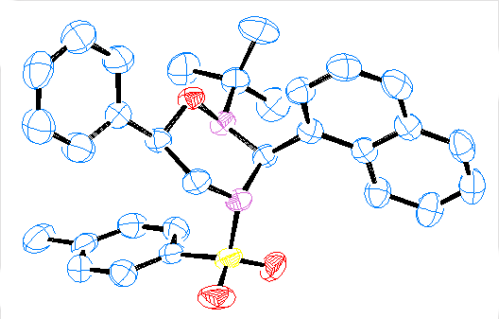

Figure 2. ORTEP diagram of 2-(tert-butyl)-3-(naphthalen-1-yl)-6-phenyl-4-tosyl-1,2,4-oxadiazinane **3af** (CCDC 2426695) with 50% ellipsoid. H-omitted for clarity.

Identification code	**3ia**
Empirical formula	'C30 H32 N2 O3 S'
Formula weight	501.64
Crystal habit, colour	Block/Colourless
Temperature, *T*/K	293 K
Wavelength, *λ*/Å	0.71073
Crystal system	'monoclinic'
Space group	' P 21/c'
Unit cell dimensions	a = 8.1277(10) Å b = 14.3667(13) Å

	c = 22.6619(18) Å α = 90 β = 96.681(9) γ = 90
Volume, V/Å^3	2628.2(5)
Z	4
Calculated density, Mg·m^{-3}	1.268
Absorption coefficient, μ/mm^{-1}	0.157
F(000)	1068
θ range for data collection	2.29 to 28.73°
Limiting indices	-10 ≤ h ≤ 9, –19 ≤ k ≤ 9, –28 ≤ l ≤ 29
Reflection collected / unique	5933/4034
Refinement method	'SHELXL-2019/1 (Sheldrick, 2019)'
Data / restraints / parameters	5933/0/ 330
Goodness–of–fit on F^2	1.041
Final R indices [I>2sigma(I)]	R1 = 0.0571, wR2 = 0.1339
R indices (all data)	R1 = 0.0874, wR2 = 0.1617

Crystal Data and Structure Refinement for 4na

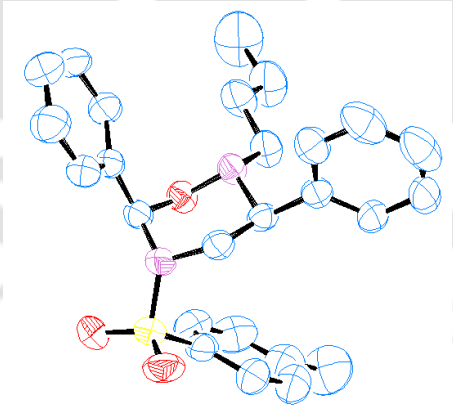

Figure 3. ORTEP diagram of 2-butyl-3,6-diphenyl-5-tosyl-1,2,5-oxadiazinane **4na** (CCDC 2426708) with 50% ellipsoid. H-omitted for clarity.

Identification code	**4na**
Empirical formula	'C26 H30 N2 O3 S'
Formula weight	450.58
Crystal habit, colour	Block/Colourless
Temperature, T/K	296 K

Wavelength, λ/Å	0.71073
Crystal system	'monoclinic'
Space group	'I 1 a 1'
Unit cell dimensions	a = 8.1212(9) Å b = 29.253(3) Å c = 11.1577(11) Å α = 90 β = 110.143(7) γ = 90
Volume, V/Å^3	2488.6(5)
Z	4
Calculated density, Mg·m^{-3}	1.203
Absorption coefficient, μ/mm^{-1}	0.159
F(000)	960
θ range for data collection	1.39 to 25.05°
Limiting indices	-9 ≤ h ≤ 9, –34 ≤ k ≤ 34, –13 ≤ l ≤ 13
Reflection collected / unique	4399/3132
Refinement method	'SHELXL 2018/3 (Sheldrick, 2015)'
Data / restraints / parameters	4399/2/ 292
Goodness–of–fit on F^2	1.013
Final R indices [I>2sigma(I)]	R1 = 0.0350, wR2 = 0.0833
R indices (all data)	R1 = 0.0588, wR2 = 0.0985

3.5 References

1. (a) Nonn, M.; Remete, A. M.; Fülöp, F.; Kiss, L. *Tetrahedron* **2017**, *73*, 5461. (b) Callebaut, G.; Meiresonne, T.; De Kimpe, N.; Mangelinckx, S. *Chem. Rev.* **2014**, *114*, 7954. (c) Ohno, H. *Chem. Rev.* **2014**, *114*, 7784. (d) Wang, C. *Synthesis* **2017**, *49*, 5307. (e) Sarkar, T.; Das, B. K.; Talukdar, K.; Shah, T. A.; Punniyamurthy, T. *ACS Omega* **2020**, *5*, 26316.
2. (a) de Nanteuil, F.; Waser, J. *Angew. Chem. Int. Ed.* **2011**, *50*, 12075. (b) Chakrabarty, S.; Chatterjee, I.; Wibbeling, B.; Daniliuc, C. G.; Studer, A. *Angew. Chem. Int. Ed.* **2014**, *53*, 5964. (c) Liang, Y.-F.; Müller, V.; Liu, W.; Münch, A.; Stalke, D.; Ackermann, L. *Angew. Chem. Int. Ed.* **2017**, *56*, 9415. (d) Xu, P.-W.; Liu, J.-K.; Shen, L.; Cao, Z.-Y.; Zhao, X.-

L.; Yan, J.; Zhou, J. *Nat. Commun.* **2017**, *8*, 1. (e) Satheesh, V.; Vivek Kumar, S.; Punniyamurthy, T. *Chem. Commun.* **2018**, *54*, 11813.

3. (a) Li, L.; Wu, X.; Zhang, J. *Chem. Commun.* **2011**, *47*, 5049. (b) Craig, R. A., II; O'Connor, N. R.; Goldberg, A. F. G.; Stoltz, B. M. *Chemistry* **2014**, *20*, 4806. (c) Bailey, S. J.; Wales, S. M.; Willis, A. C.; Keller, P. A. *Org. Lett.* **2014**, *16*, 4344. (d) Lin, T.-Y.; Wu, H.-H.; Feng, J.-J.; Zhang, J. *Org. Lett.* **2017**, *19*, 6526. (e) Kok, G. P. Y.; Yang, H.; Wong, M. W.; Zhao, Y. *Org. Lett.* **2018**, *20*, 5112. (f) Xu, Y.; Chang, F.; Cao, W.; Liu, X.; Feng, X. *ACS Catal.* **2018**, *8*, 10261.
4. (a) Fabio, M.; Ronzini, L.; Troisi, L. *Tetrahedron* **2008**, *64*, 4979. (b) Michaelis, D. J.; Ischay, M. A.; Yoon, T. P. *J. Am. Chem. Soc.* **2008**, *130*, 6610. (c) Williamson, K. S.; Yoon, T. P. *J. Am. Chem. Soc.* **2010**, *132*, 4570. (d) Williamson, K. S.; Michaelis, D. J.; Yoon, T. P. *Chem. Rev.* **2014**, *114*, 8016. (e) Jang, G. S.; Lee, J.; Seo, J.; Woo, S. K. *Org. Lett.* **2017**, *19*, 6448.
5. (a) Zhao, W.-T.; Gao, F.; Zhao, D. *Angew. Chem. Int. Ed.* **2018**, *57*, 6329. (b) Ghosh, A.; Dey, R.; Banerjee, P. *Chem. Commun.* **2021**, *57*, 5359.
6. (a) Barbarić, M.; Kraljević, S.; Grce, M.; Zorc, B. *Acta Pharm*. **2003**, *53*, 175. (b) Huang, X.; Zhou, W.; Liu, X.; Li, H.; Sun, G.; Mandal, M.; Vicarel, M.; Zhu, X.; Bennett, C.; McCraken, T.; Pissarnitski, D.; Zhao, Z.; Cole, D.; Gallo, G.; Zhu, Z.; Palani, A.; Aslanian, R.; Clader, J.; Czarniecki, M.; Greenlee, W.; Burnett, D.; Cohen-Williams, M.; Hyde, L.; Song, L.; Zhang, L.; Chu, I.; Buevich, A. *ACS Med. Chem. Lett*. **2012**, *3*, 931.
7. Partridge, K. M.; Anzovino, M. E.; Yoon, T. P. *J. Am. Chem. Soc.* **2008**, *130*, 2920.
8. Michaelis, D. J.; Shaffer, C. J.; Yoon, T. P. *J. Am. Chem. Soc.* **2007**, *129*, 1866.
9. Zhao, E.; Zhou, F.; Zhao, Y. *J. Org. Chem.* **2019**, *84*, 4282.
10. Kivrak, A.; Larock, R. C. *J. Org. Chem.* **2010**, *75*, 7381.
11. Das, B. K.; Pradhan, S.; Punniyamurthy, T. *Org. Lett.* **2018**, *20*, 4444.
12. Liu, H.; Jia, H.; Shi, W.; Wang, C.; Zhang, C.; Guo, H. *Org. Lett*. **2018**, *20*, 3570.
13. Jia, Q.; Li, D.; Lang, M.; Zhang, K.; Wang, J. *Adv. Synth. Catal*. **2017**, *359*, 3837.
14. Trindade, A. F.; Bode, J. W. *Org. Lett*. **2016**, *18*, 4210.
15. Itoh, K.; Takashino, A.; Ohtsuka, A.; Kobe, M.; Sawamura, S.; Kato, R.; Hirayama, S.; Karaki, F.; Mizuguchi, T.; Sato, N.; Tokunaga, K.; Toda, Y.; Suga, H.; Ishida, H.; Fujii, H. *ChemPhotoChem* **2020**, *4*, 388.
16. (a) Porter, K. E.; Rzepa, H. S. *J. Chem. Res., Synop*. **1983**, 262. (b) Altmann, J. A.; Rzepa, H. S. *J. Mol. Struct.:THEOCHEM* **1987**, *149*, 33.

17. Chen, C.; Ni, C.; Song, J.-H.; Ding, L.-Y.; Zhang, X.-X.; Guo, H.; Wang, K.; Chen, Z.; Zhu, B. *ACS Catal.* **2024**, *14*, 12181.

3.6 HPLC chromatograms

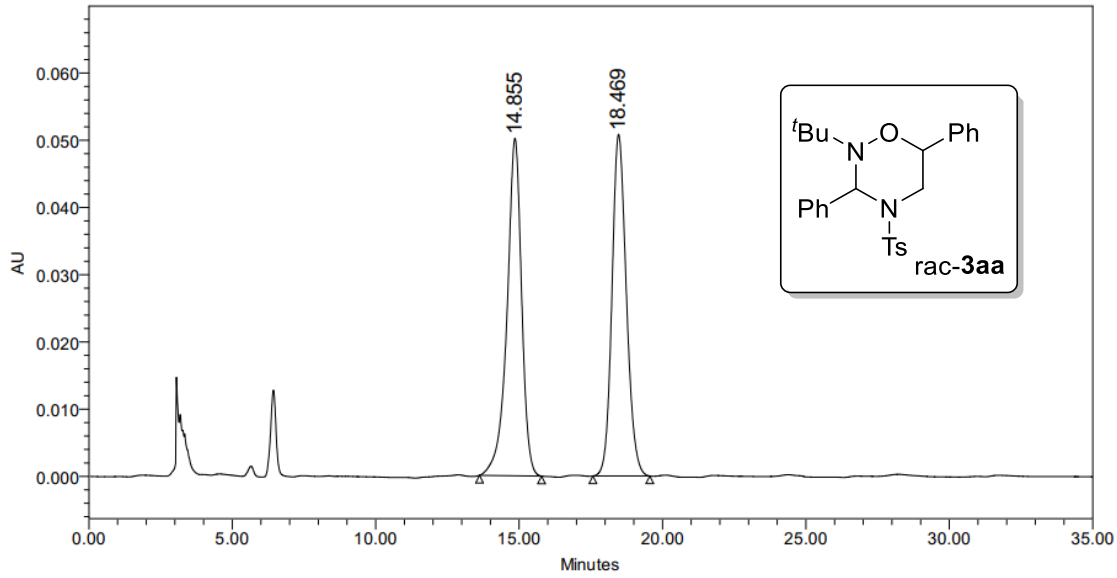

	RT	Area	% Area	Height
1	14.855	1778989	50.06	50207
2	18.469	1774890	49.94	50819

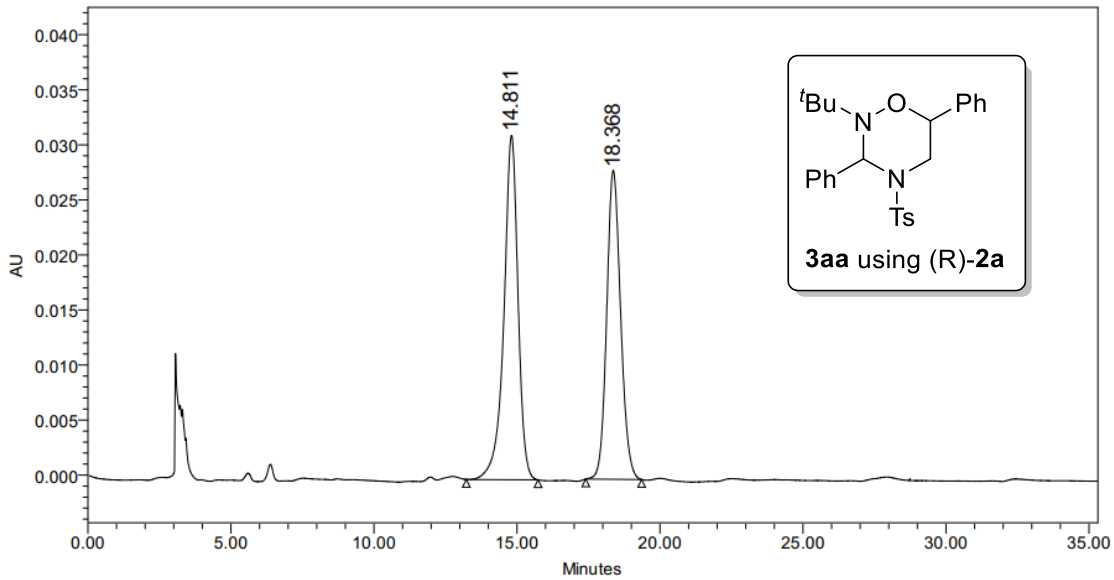

	RT	Area	% Area	Height
1	14.811	1073991	53.09	31283
2	18.368	948977	46.91	28054

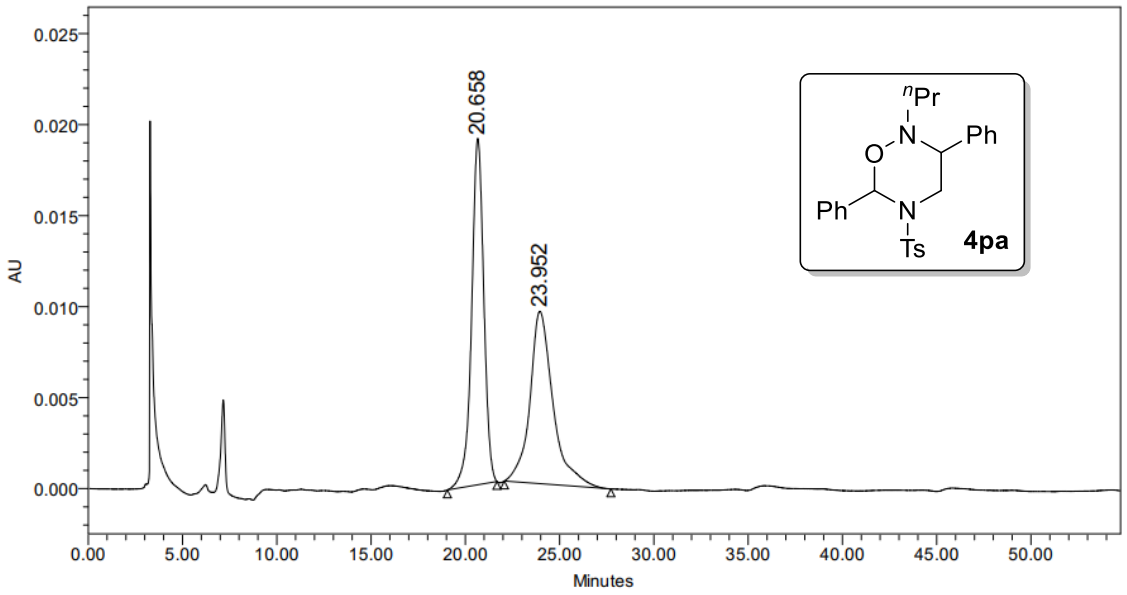

	RT	Area	% Area	Height
1	20.658	853739	51.40	19017
2	23.952	807383	48.60	9471

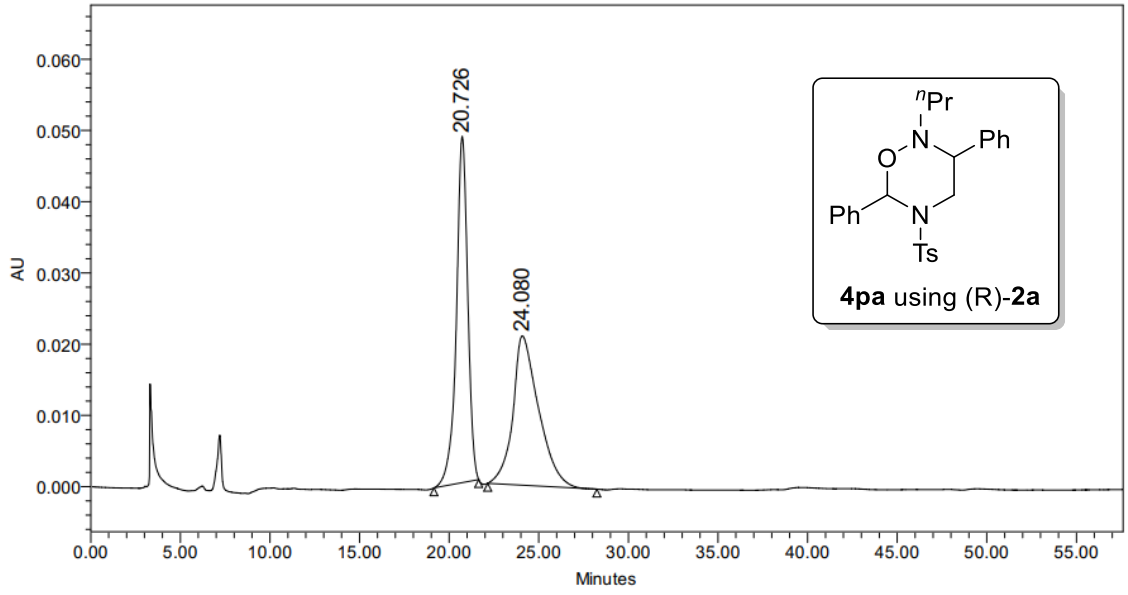

	RT	Area	% Area	Height
1	20.726	2145718	50.63	48586
2	24.080	2092389	49.37	20953

3.7 Selected NMR Spectra

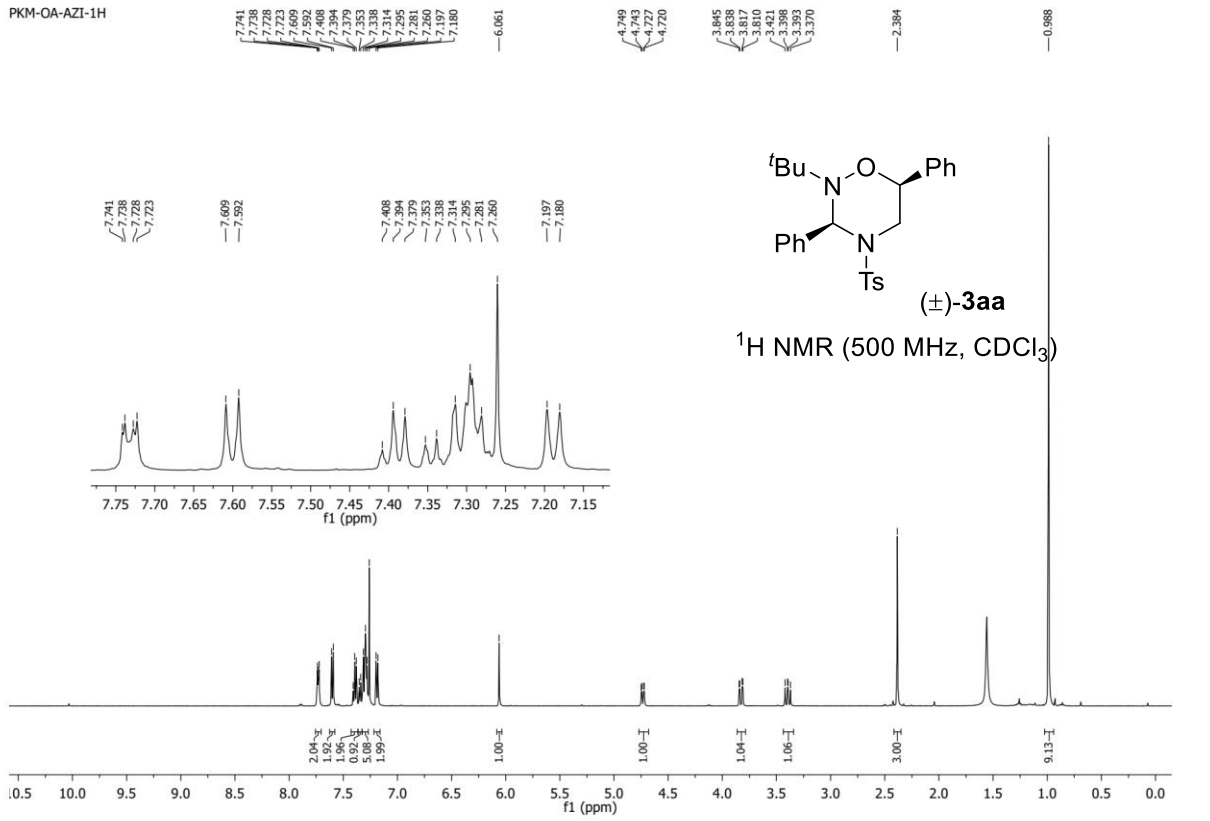

(±)-**3aa**

^{1}H NMR (500 MHz, $CDCl_3$)

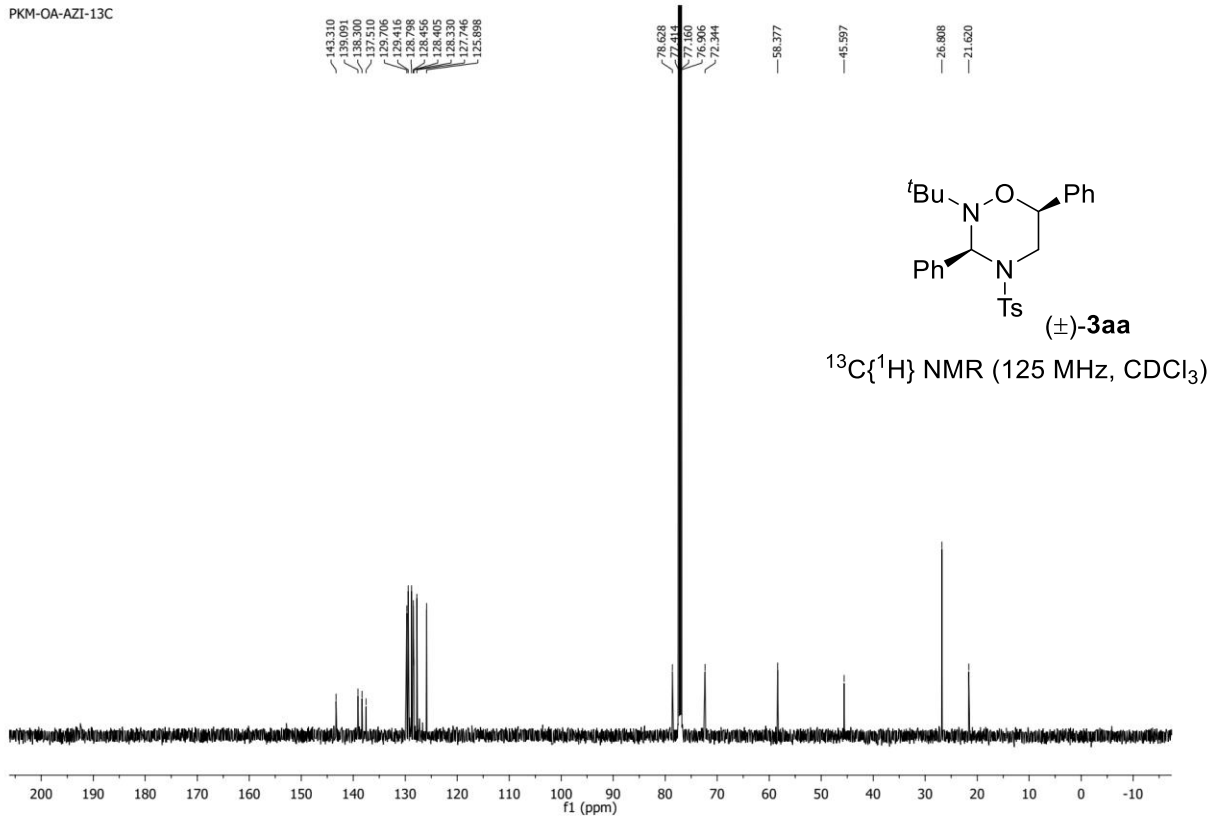

(±)-**3aa**

$^{13}C\{^{1}H\}$ NMR (125 MHz, $CDCl_3$)

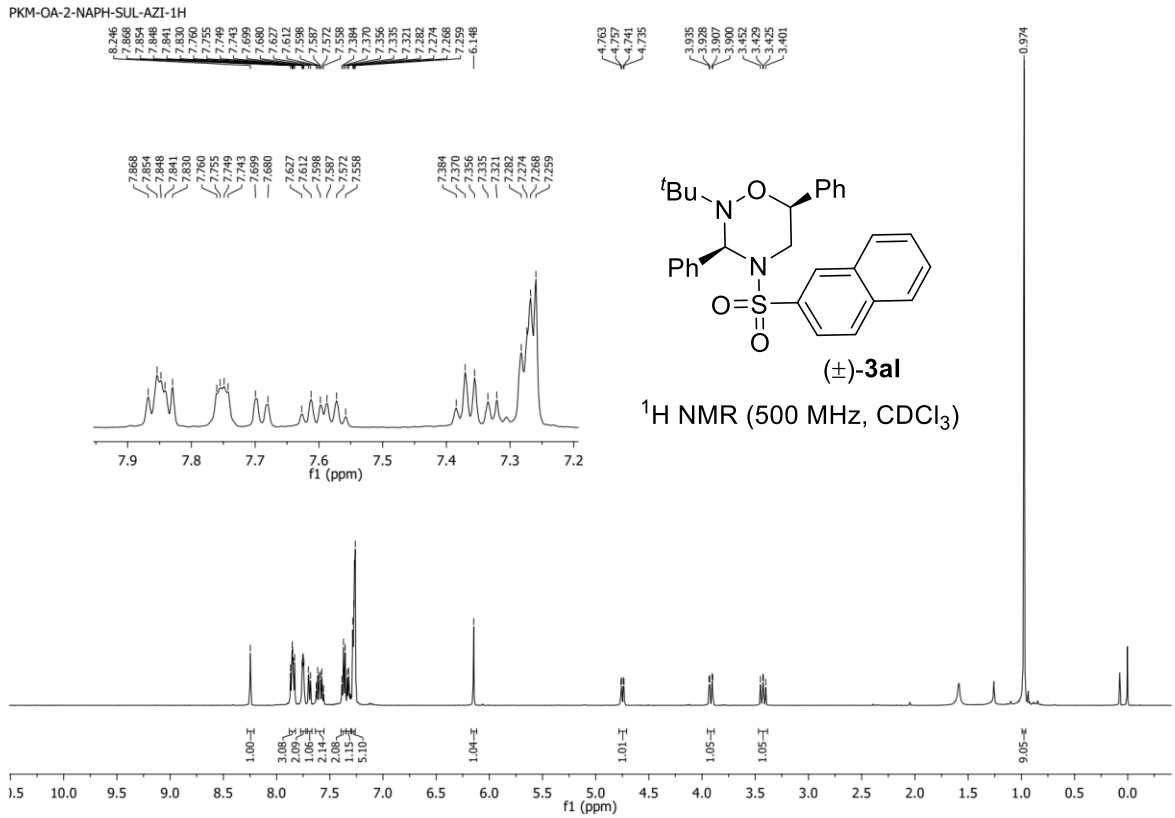

(±)-**3al**

^{1}H NMR (500 MHz, $CDCl_3$)

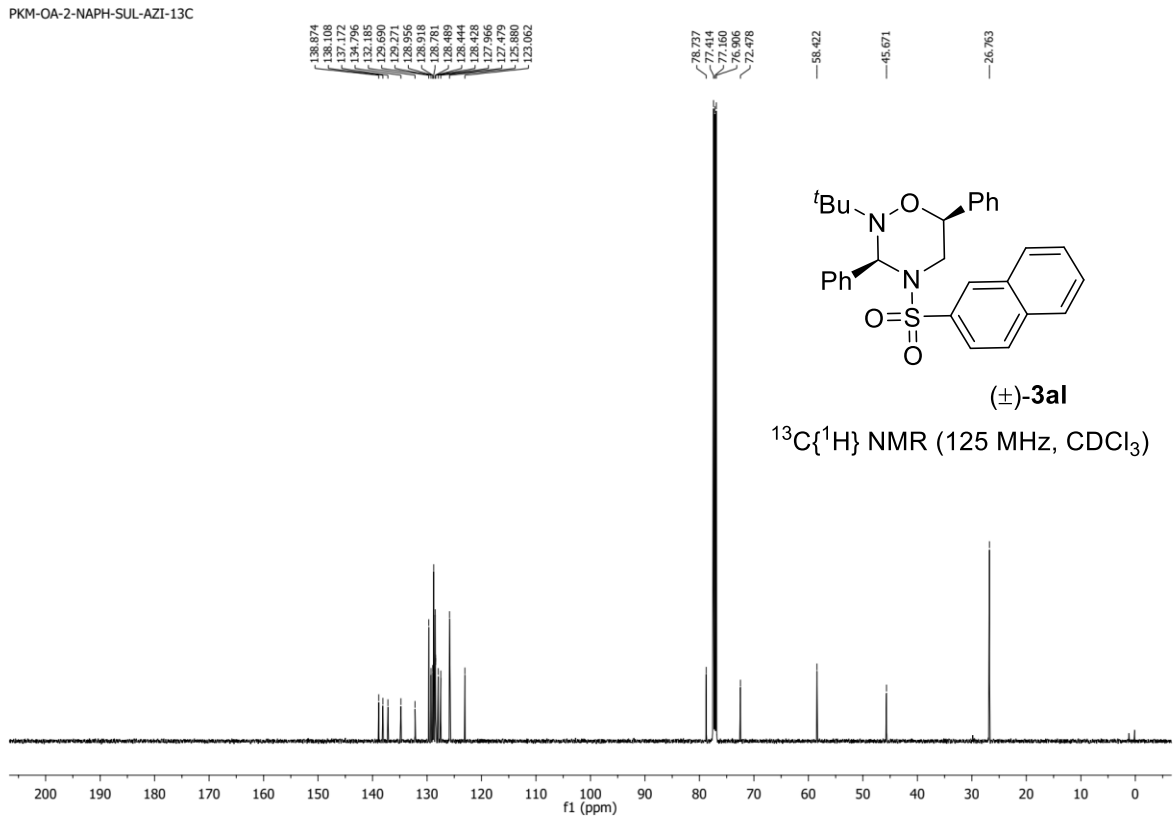

(±)-**3al**

$^{13}C\{^1H\}$ NMR (125 MHz, $CDCl_3$)

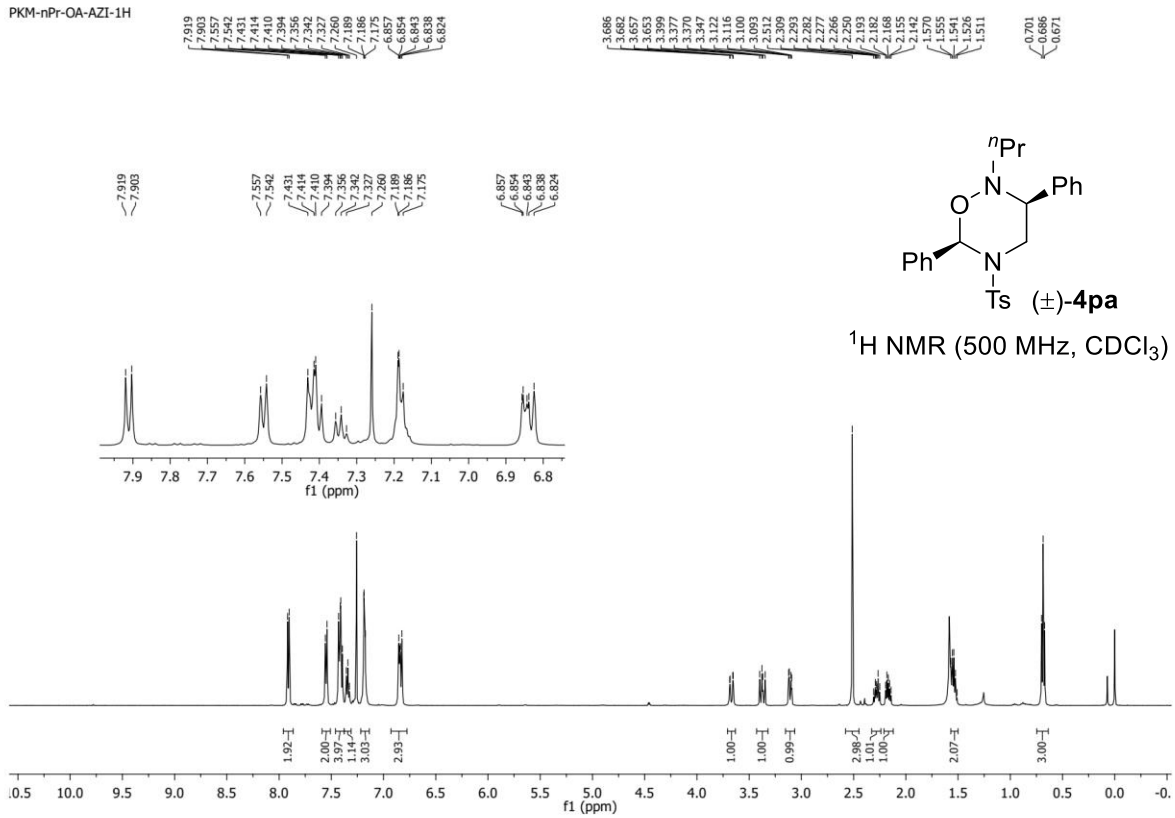

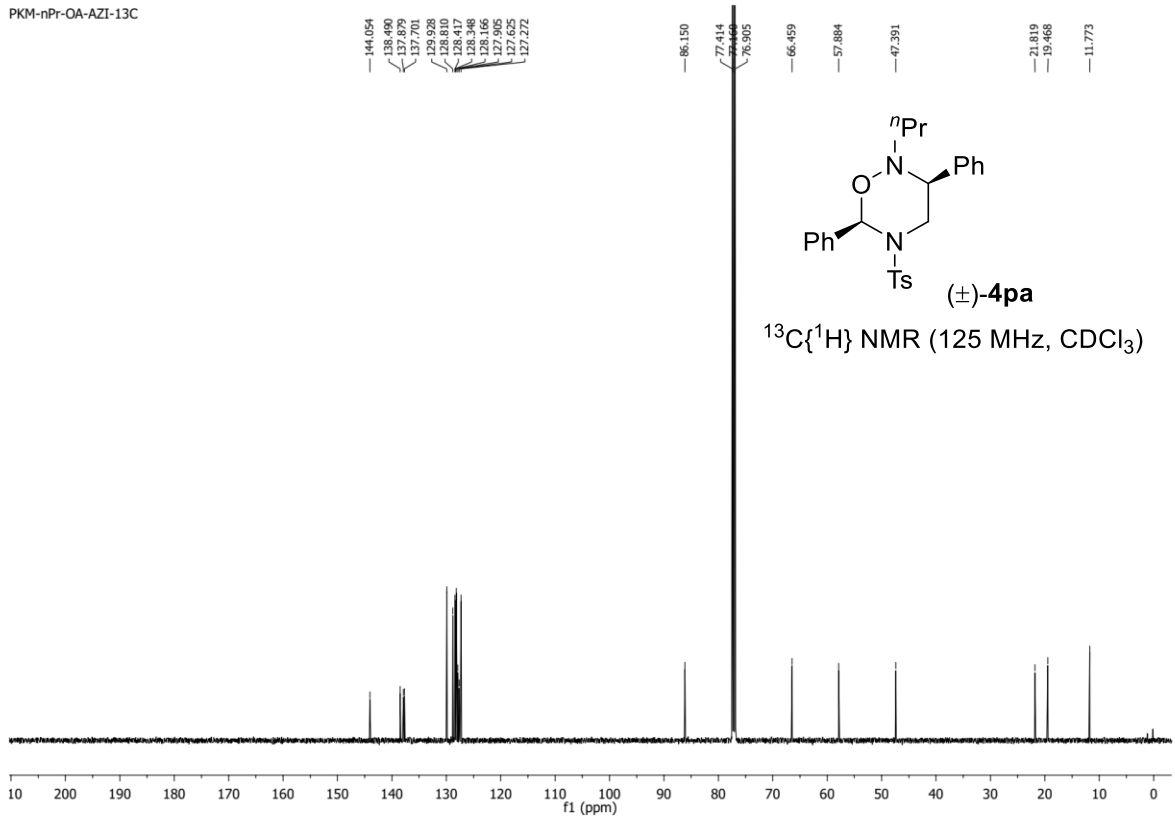

Chapter IV

Rh-Catalyzed C−H Functionalization/Annulation of Arylamides with Maleimides

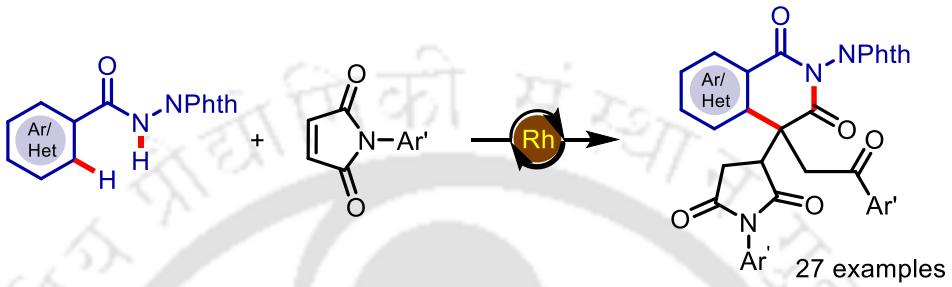

✔ Substrate scope ✔ Cascade transformations ✔ Quarternary carbon

Chem. Commun. **2025**. https://doi.org/10.1039/D5CC02963E.

Rh-Catalyzed C−H Functionalization/Annulation of Arylamides with Maleimides

The rationale of diversity-driven synthesis, aiming at building molecular scaffolds with structural complexity from simple building blocks, holds foremost significance in synthetic organic chemistry. Along this line, transition-metal-catalyzed DG aided C−H functionalization strategy has emerged as a step and atom-economical approach for molecular synthesis due to their ability to site-selectively install appropriate coupling partners across a wide range of substrates.[1] In the realm of target-driven heterocycle synthesis, recent surge in cascade C−H activation/annulation strategies have shown great potential in synthesizing complex organic molecules from simple starting precursors.[2-3] Isoquinoline-1,3-diones and their analogues are commonly occurring N-heterocyclic scaffolds are known for their wide applicability in pharmaceutical domain. For example, representative class of these molecule shows impressive inhibitor activity against tumor cell, aldol reductase and HIV-1 integrase (Figure 1).[4] Accordingly, approaches have thus been developed for the synthesis of such scaffolds and their analogues. Despite the progress, a large number of synthetic routes relied on heavily tailored starting precursors and harsh reaction conditions which limits their potential applications.[5] In this regard, sequential C−H activation and annulative transformation of arylamides have garnered significant attention for accessing N-heterocycles.[6] Further, maleimides being highly electrophilic olefins, positioned them in C−H activation due to their ability to act as an imide coupling partner.[7] In this line, significant efforts towards alkylation, alkenylation and (spiro)annulation of arylamides with maleimides was documented resulting in diverse N-heterocyclic scaffolds with the imide functionality remaining intact.[8] In spite of the advances, sequential alkylation of the arylamide followed by ring scission of the tethered succinimide *via* intramolecular nucleophilic attack of the amide nitrogen, remains elusive, and can serves as a highly step-economic route to access isoquinoline-1,3-diones. This chapter describes a site selective Rh(III)-catalyzed C−H functionalization and nucleophilic ring-opening/Michael addition cascade of arylamides with maleimides to access succinimide-tethered isoquinoline-1,3-diones. The key features include mild conditions, drug/natural product modifications and generation of pharmaceutically relevant all-carbon quaternary center.

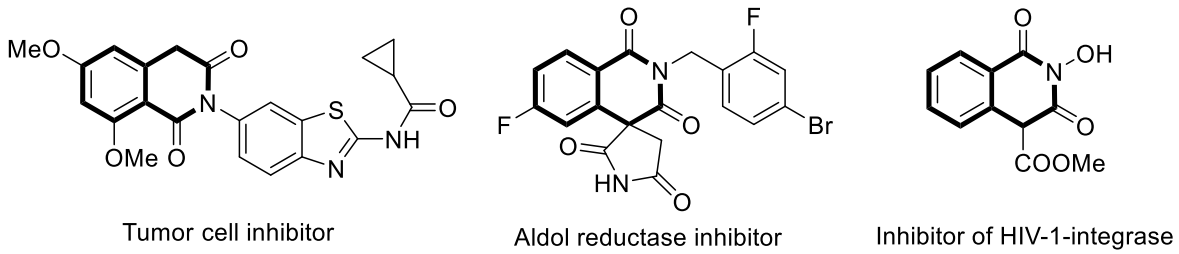

Figure 1. Biologically Important Isoquionoline-1,3-dione scaffolds.

4.1 Literature

4.1.1 Annulation of Arylamides

Rovis group accomplished an oxidative cycloaddition strategy using aryl amides and alkynes to access isoquinolones in good yield (Scheme 1).[9] Under Rh catalysis, the reaction is tolerant to a diverse set of sensitive functional groups *viz*. silyl ether, halides and aldehydes on both the substrates. Interestingly, high regioselectivity was attained in case of unsymmetrical alkynes.

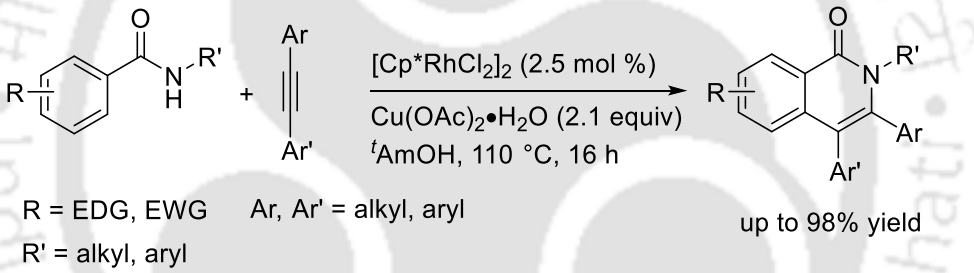

Scheme 1. Rh-Catalyzed Annulation

A dual C−H activation approach towards the synthesis of phenanthridinones was carried out by taking N-methoxyarylamides and arylboronic acids (Scheme 2).[10] This practical cyclization approach proceeded in highly regioselective manner to furnish substituted phenanthridinones in good yield.

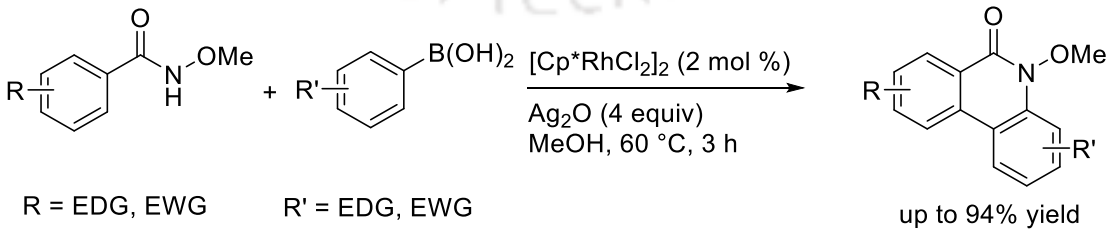

Scheme 2. Rh-Catalyzed Dual C−H Activation/Cyclization

Rh(III)-catalyzed tandem C−H activation/cyclization/condensation procedure towards the synthesis of azepinones was developed using arylamides and α,β-unsaturated aldehydes and

ketones as the coupling partner (Scheme 3).[11] Versatility of this step- economic protocol was exploited towards the efficient total synthesis of homoprotoberberine framework.

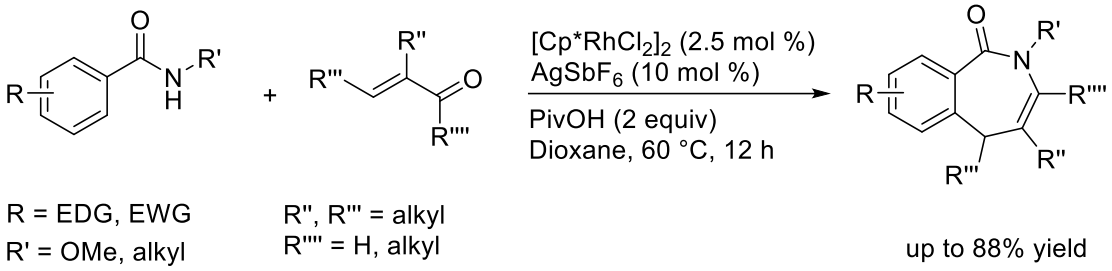

Scheme 3. Rh-Catalyzed Tandem C−H Activation/Cyclization/Condensation

4.1.2 Reactivity of Maleimides

Miura and co-workers reported a Cu-mediated oxidative coupling reaction of benzamides with maleimides to afford a series of spirosuccinamides in good to excellent yield. The reaction proceeds *via* bidentate auxiliary assisted C(sp^2)-H alkenylation followed by intramolecular aza-Michael-addition (Scheme 4).[12]

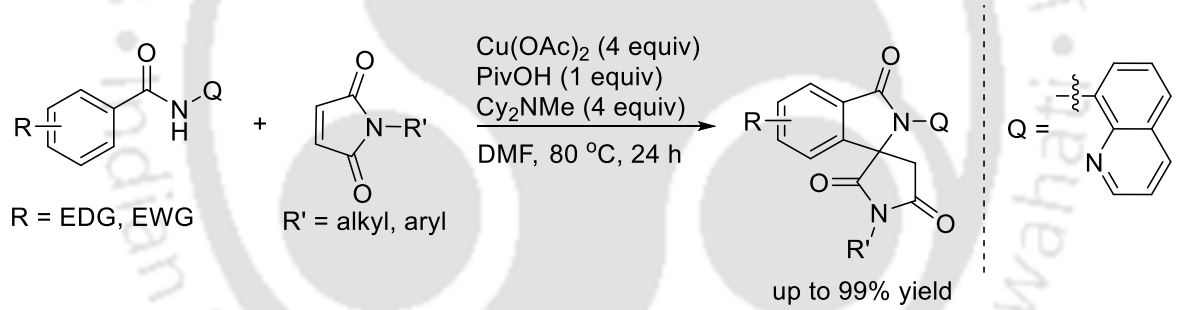

Scheme 4. Cu-Mediated Spiroannulation

Chatani group carried out the alkylation of benzamides using Rh(I) catalysis. Aromatic amides containing 8-aminoquinoline as a bidentate DG successfully converted into alkylated products in presence of a series of N-substituted maleimides (Scheme 5).[13]

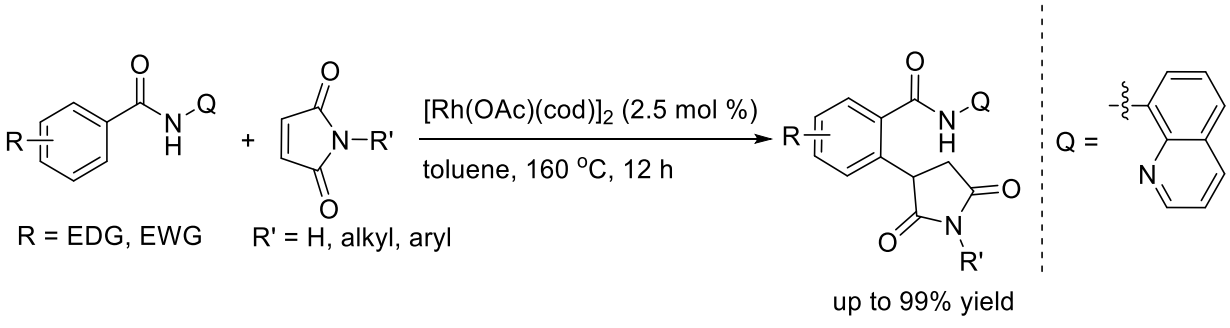

Scheme 5. Rh-Catalyzed Alkylation

Our group documented a dual C(sp^3)−H and C(sp^2)−H activation of 8-methylquinoline N-oxides with maleimides to furnish fused polycyclic quinoline motifs. [3+2]-Annulation, substrates scope and functional group tolerance are the important practical features (Scheme 6).[14]

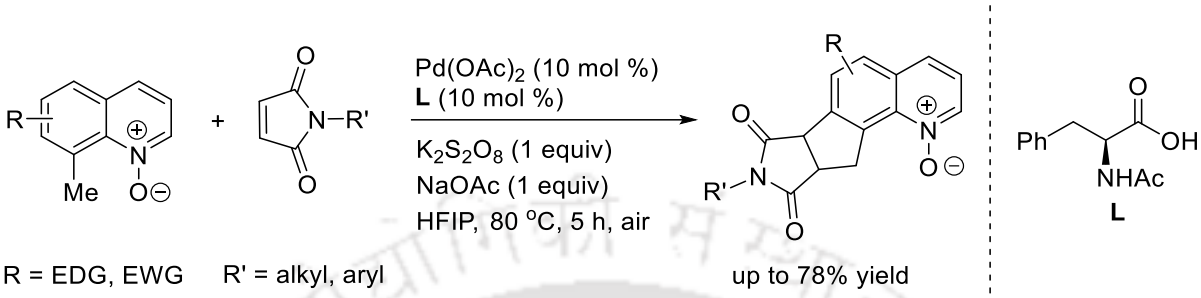

Scheme 6. Pd-Catalyzed [3+2]-Annulation of 8-Methylquinoline N-Oxides with Maleimides

4.1.3 Synthesis of Isoquinoline-1,3-diones

Chatani and co-workers disclosed a bidentate auxiliary assisted ortho C−H carbonylation of arylacetamides under Ru catalysis (Scheme 7).[15] Aryl as well as heteroaryl acetamides with diverse electronic substituents converted to their respective annulated product in good yield. The authors further underscore the use ethylene gas and water is indispensable for completion of the catalytic cycle.

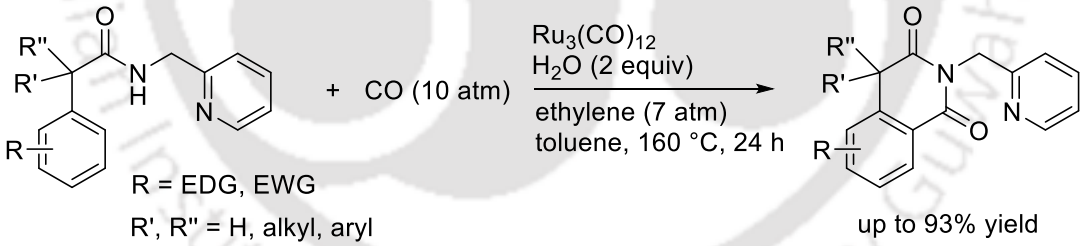

Scheme 7. Ru-Catalyzed *ortho*-C−H Carbonylation of Arylacetamides

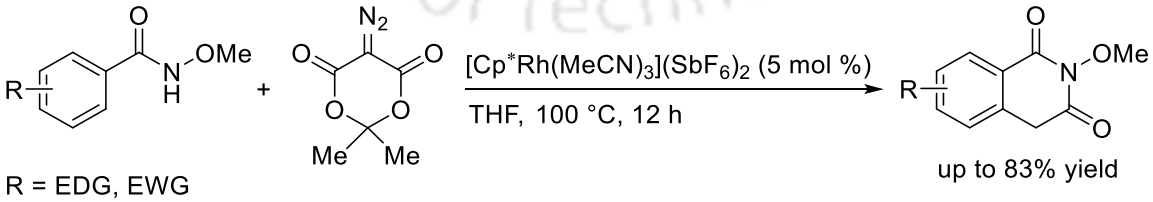

Scheme 8. Cascade C−H Activation/Cyclization of N-Methoxybenzamides with α-Diazotized Meldrum's acid

Yi and co-workers reported a C−H activation/cyclization utilizing N-methoxybenzamides and α-diazotized Meldrum's acid as coupling partner (Scheme 8).[16] Mechanistically, Rh(III)-catalyzed *ortho*-C−H functionalization *via* carbenoid insertion played key role in delivering functionalized isoquinolinediones in good yield.

A Rh(III)-catalyzed tandem functionalization of arylamides towards the synthesis of isoquinolinediones was demonstrated utilizing unsymmetrical 1,4-dicarbonyl derivatives (Scheme 9).[17] This regioselective methodology was utilized for the late-stage synthesis of the pyrrolophenanthridine alkaloid oxoassoanine showcasing its practical utility.

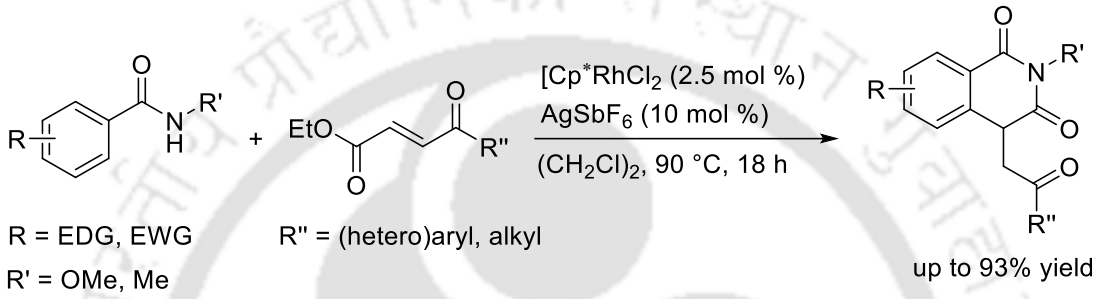

Scheme 9. Rh-catalyzed functionalization of arylamides

4.2 Present Study

This chapter describes a cascade C−H functionalization/annulation of arylamides with maleimides employing Rh(III) catalysis to furnish succinimide tethered isoquinoline-1,3-diones. At the outset, we started the optimization studied by taking *N*-(1,3-dioxoisoindolin-2-yl)benzamide **1a** and 1-phenyl-1*H*-pyrrole-2,5-dione **2a** as the model substrates (Table 1). Delightedly, the annulated product **3aa** was obtained in 77% yield, when both the substrates were stirred in presence of 2 mol % $[Cp^*RhCl_2]_2$, 20 mol % $AgSbF_6$ and 2 equiv NaOAc in $(CH_2Cl)_2$ at 100 ˚C for 16 h (entry 4). Screening of additives revealed that, $AgSbF_6$, was superior to $AgBF_4$ and $AgNTf_2$. Among the bases screened, NaOAc, KOAC, CsOAc, K_2CO_3 and Na_2CO_3, NaOAc afforded best result (entries 1-9). In a set of solvents screened, $(CH_2Cl)_2$ proved superior to TFE, HFIP, THF, PhMe, PhCl and MeOH (entries 10-15). By changing the rhodium source to $[Cp^*Rh(CH_3CN)_3](SbF_6)_2$, a sharp drop in yield was observed, while $[Cp^*Co(CO)I_2]_2$ failed to catalyze the reaction (entries 16-17). In addition, separate control experiments carried out in the absence of either Rh-catalyst, additive and base failed to deliver the desired product. Further, succinimide **1a′**, maleimide **1b′**, *tert*-butyl carbamate **1c′** and tosyl-protected **1d′** benzamides proved ineffective in attaining the desired product.

Table 1. Optimization of the Reaction Conditions.[a]

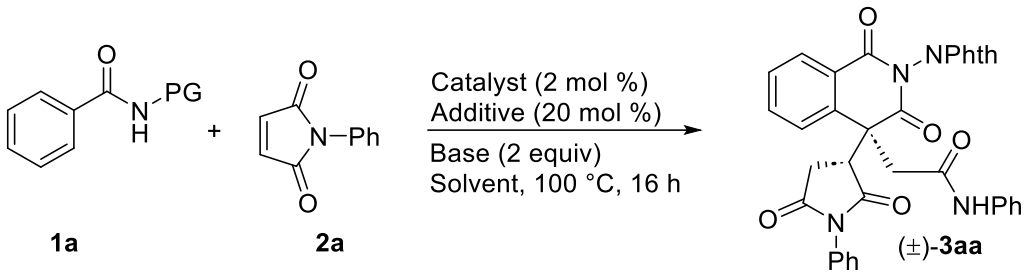

Entry	Catalyst	Additive	Base	Solvent	Yield [**3aa**,(%)][b]
1	$[Cp^*RhCl_2]_2$	$AgSbF_6$	-	$(CH_2Cl)_2$	n.d.
2	$[Cp^*RhCl_2]_2$	$AgSbF_6$	KOAc	$(CH_2Cl)_2$	55
3	$[Cp^*RhCl_2]_2$	$AgSbF_6$	CsOAc	$(CH_2Cl)_2$	48
4	**$[Cp^*RhCl_2]_2$**	**$AgSbF_6$**	**NaOAc**	**$(CH_2Cl)_2$**	**77**
5	$[Cp^*RhCl_2]_2$	$AgSbF_6$	K_2CO_3	$(CH_2Cl)_2$	13
6	$[Cp^*RhCl_2]_2$	$AgSbF_6$	Na_2CO_3	$(CH_2Cl)_2$	16
7	$[Cp^*RhCl_2]_2$	$AgBF_4$	NaOAc	$(CH_2Cl)_2$	trace
8	$[Cp^*RhCl_2]_2$	$AgNTf_2$	NaOAc	$(CH_2Cl)_2$	trace
9	$[Cp^*RhCl_2]_2$	-	NaOAc	$(CH_2Cl)_2$	25
10	$[Cp^*RhCl_2]_2$	$AgSbF_6$	NaOAc	TFE	n.d.
11	$[Cp^*RhCl_2]_2$	$AgSbF_6$	NaOAc	HFIP	n.d.
12	$[Cp^*RhCl_2]_2$	$AgSbF_6$	NaOAc	THF	n.d.
13	$[Cp^*RhCl_2]_2$	$AgSbF_6$	NaOAc	PhMe	trace
14	$[Cp^*RhCl_2]_2$	$AgSbF_6$	NaOAc	PhCl	n.d.
15	$[Cp^*RhCl_2]_2$	$AgSbF_6$	NaOAc	MeOH	n.d.
16	$[Cp^*Rh(CH_3CN)_3](SbF_6)_2]$	-	NaOAc	$(CH_2Cl)_2$	52
17	$[Cp^*Co(CO)I_2]_2$	$AgSbF_6$	NaOAc	$(CH_2Cl)_2$	n.d.
18	-	$AgSbF_6$	NaOAc	$(CH_2Cl)_2$	n.d.
19[c]	$[Cp^*RhCl_2]_2$	$AgSbF_6$	NaOAc	$(CH_2Cl)_2$	40

Unsuccessful Protecting Groups

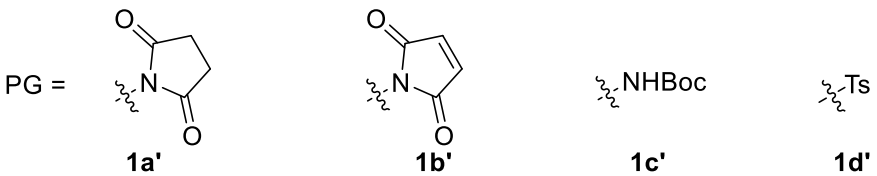

[a]Reaction conditions: **1a** (0.2 mmol), **2a** (0.4 mmol), catalyst (2 mol %), additive (20 mol %), base (2 equiv), solvent (2 mL) at 100 °C, 16 h, N_2. [b]Isolated yield. n.d. = not detected.[c]0.2 mmol **2a** used.

Table 2. Scope of Maleimides[a,b]

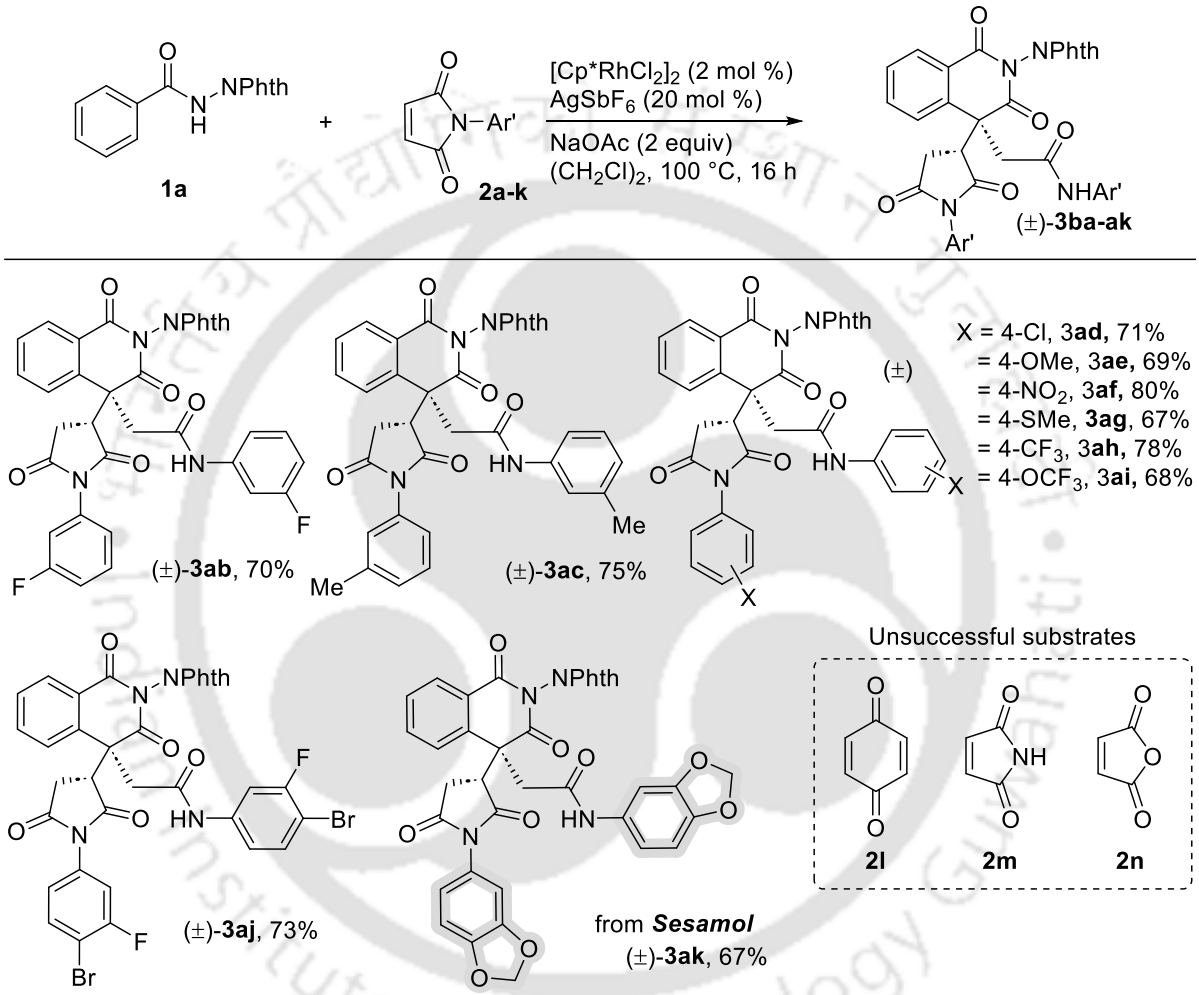

[a]Reaction conditions: **1a** (0.2 mmol), **2b-k** (0.4 mmol), $[Cp^*RhCl_2]_2$ (2 mol %), $AgSbF_6$ (20 mol %), NaOAc (2 equiv), $(CH_2Cl)_2$ (2 mL), 100 °C, 16 h, N_2. [b]Isolated yield. n.d. = not detected.

Table 3. Scope of Arylamides[a,b]

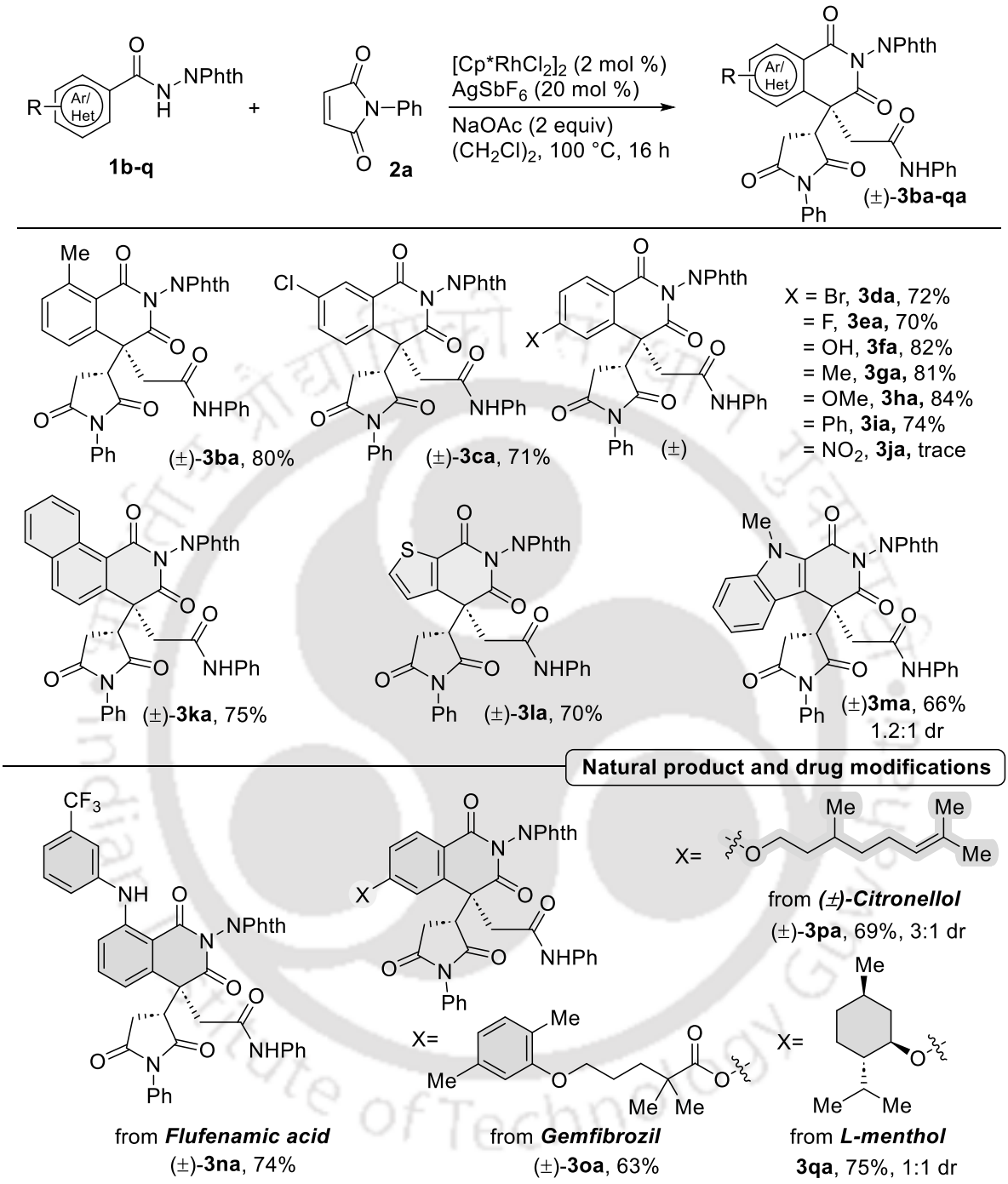

[a]Reaction conditions: **1b-q** (0.2 mmol), **2a** (0.4 mmol), $[Cp^*RhCl_2]_2$ (2 mol %), $AgSbF_6$ (20 mol %), NaOAc (2 equiv), $(CH_2Cl)_2$ (2 mL), 100 °C, 16 h, N_2. [b]Isolated yield. n.d. = not detected.

With optimal reaction conditions, we moved to examine the substrate scope of maleimides by taking *N*-(1,3-dioxoisoindolin-2-yl)benzamide **1a** as the representative substrate (Table 2). As

apparent, regardless of the electronic effect, diverse maleimides smoothly converted into the desired products in good yields. Notably, substituents at 3-position of the *N*-phenyl ring of maleimide such as fluoro **2b** and methyl **2c** could be well tolerated, converting to the desired products **3ab** and **3ac** in 70% and 75% yields, respectively. Similar outcomes were observed with maleimide having substitution at 4-position of the *N*-phenyl ring such as chloro **2d**, methoxy **2e**, nitro **2f**, thiomethyl **2g**, trifluoromethyl **2h** and trifluoromethoxy **2i**, delivering **3ad-ai** in 67-80% yields. Gratifyingly, di-substituted maleimide **2j** delivered the desired **3aj** 73% yield. Pleasingly, anti-oxidant sesamol tethered maleimide **2k** can be tolerated, delivering intended **3ak** in 67% yield. In sharp contrast, electron-deficient substrates such as benzoquinone **2l**, non-substituted maleimide **2m** and maleic anhydride **2n** failed to produce the anticipated outcome.

Next, we shifted the attention to test the generality of the protocol by screening functionally diverse arylamides taking 1-phenyl-1*H*-pyrrole-2,5-dione **2a** as the representative substrate (Table 3). Methyl group on *ortho*-position of the phenyl ring **1b** converted to the desired product **3ba** in 80% yield. In a similar manner, 3-chloro substituted benzamide **1c** afforded **3ca** in 71% yield. Notably, the installation of functional group at 4-position of the phenyl ring such as bromo **1d**, fluoro **1e**, hydroxy **1f**, methyl **1g**, methoxy **1h** and phenyl **1i** transferred into their respective aza-heterocycles **3da-ia** in 72-84% yield, however, in case of nitro **1j** a trace amount of the product was observed. Further, amide derived from 1-naphtyl substituent **1k** took part in the reaction to produce **3ka** in 75% yield. Additionally, heteroaryl derived amide substrates such as thienyl **1l** and indolyl **1m** were proved amenable in delivering respective products **3la** and **3ma** in 70% and 66% (>1.2:1 dr) yields. The structure of **3ma** was determined using single crystal X-ray analysis. Gratifyingly, non-steroidal anti-inflammatory drug flufenamic acid derived benzamide **1n** afforded the annulated **3na** in 74% yield. Further, gemfibrozil tethered benzamide **1o** proved viable partner in delivering **3oa** in 63% yield. Interestingly, naturally occurring monoterpenoids (±)-citronellol **1p** and L-menthol **1q** tethered benzamides were produced the annulated products **3pa** and **3qa** in 69% (3:1 dr) and 75% (1:1 dr), respectively. These outcomes certainly highlight the high potentiality of our protocol.

To shed light into the reaction pathway, mechanistic experiments were carried out (Scheme 10). Firstly, the reaction of **1a** and **2a** was carried out in the presence of BHT and TEMPO. Presence of these radical scavengers in the reaction medium failed to affect the reaction yield, effectively ruling out the involvement of any radical species (Scheme 10a). Further, H/D exchange experiments using CD_3OD as a co-solvent in the absence or presence of **2a** resulted

a) Radical scavenger experiments

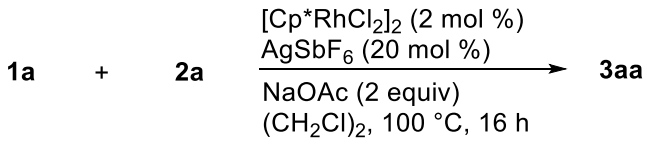

radical scavenger (2 equiv)	yield (**3aa**)
BHT	70%
TEMPO	65%

b) H/D-exchange studies

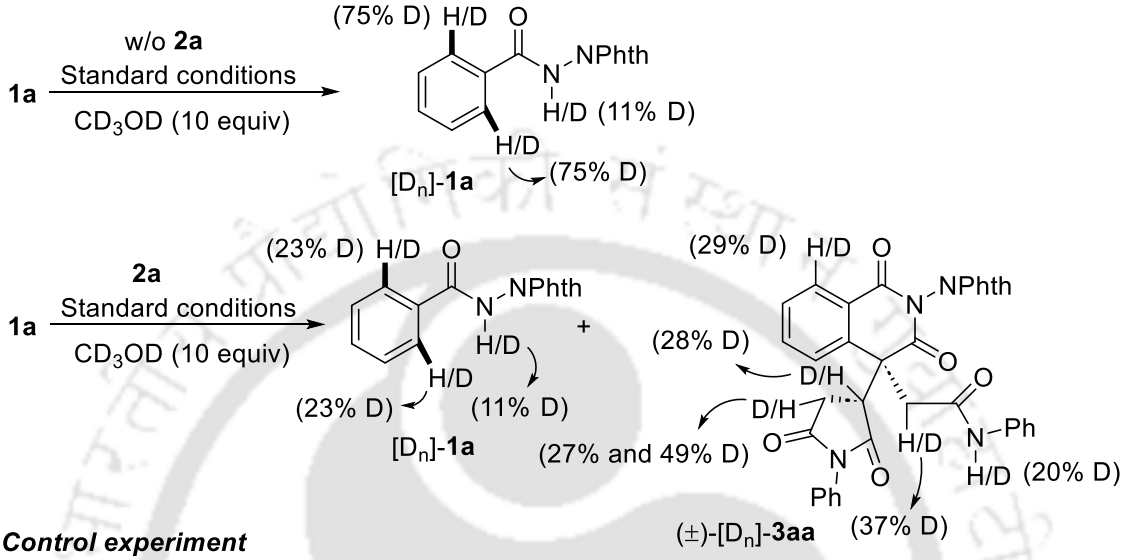

c) Control experiment

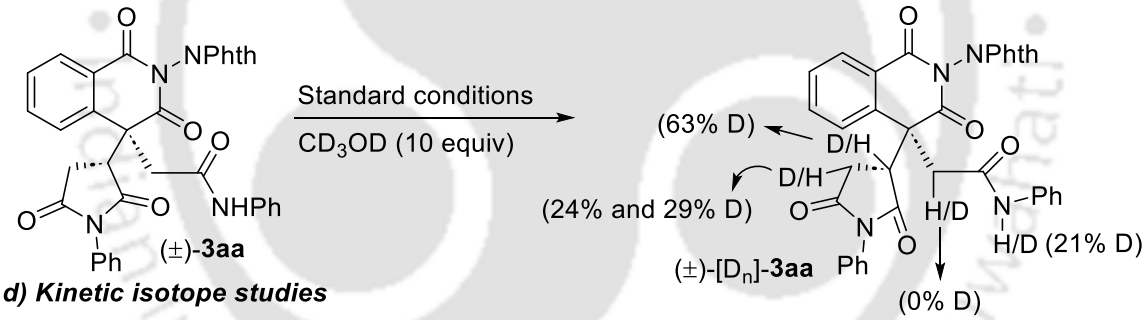

d) Kinetic isotope studies

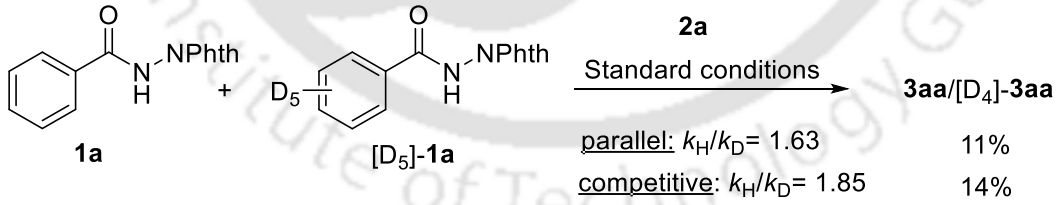

Scheme 10. Preliminary Mechanistic Investigations

in 75% and 23% deuteration at the *ortho*-position of the aryl ring, respectively (Scheme 10b). These outcomes suggest the reversibility in C-H activation process. Additionally, when the H/D exchange was performed in the presence of **2a**, methylene protons of the *N*-phenylacetamide moiety of [Dn]-**3aa** showed 37% of deuteration. Besides, deuteration was not observed at the same protons when a separate control experiment was carried out using **3aa** (Scheme 10c). These findings imply that the reaction may involve protodemetalation. Further, kinetic isotope

experiments using **1a** and [D_5]-**1a** with **2a** yielded k_H/k_D = 1.63 and 1.85 for parallel and competitive experiments, respectively, which indicates the C−H activation step might not be rate determining (Scheme 10d).

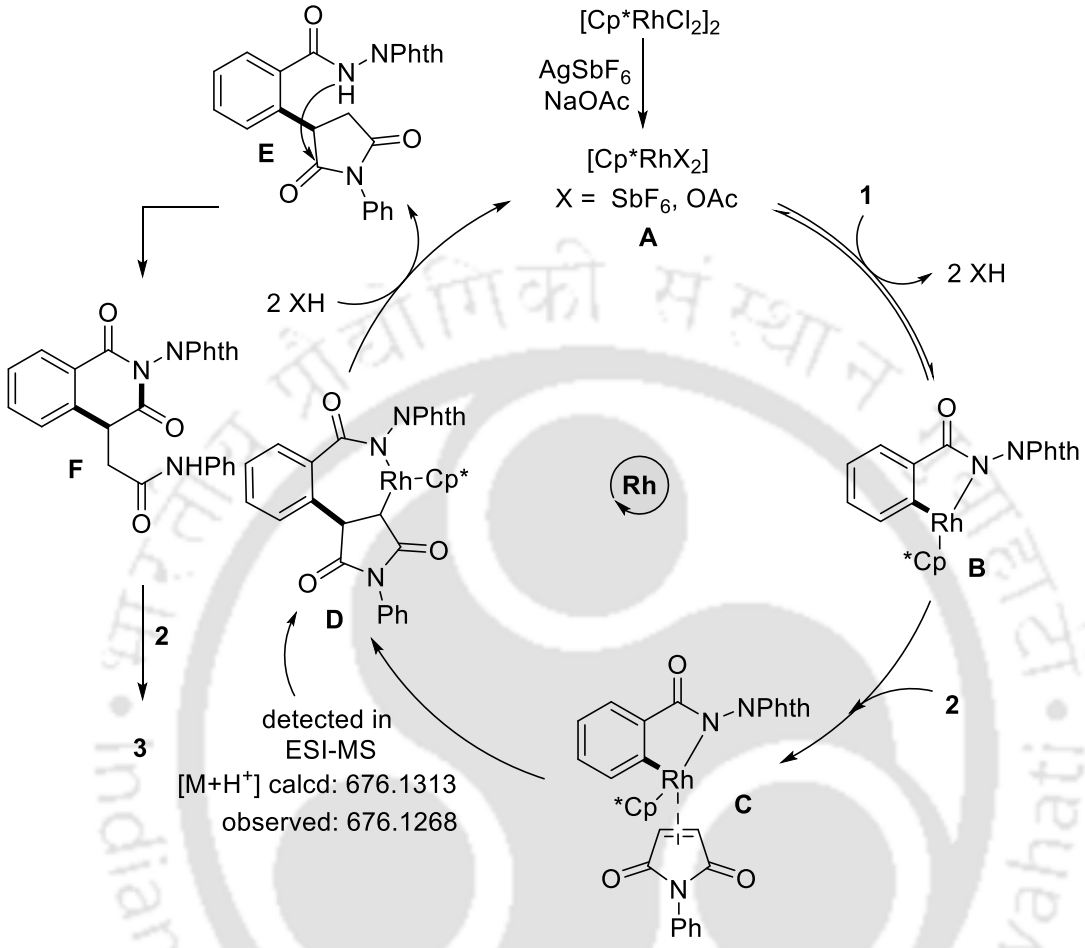

Scheme 11. Plausible Mechanism

On the basis of these mechanistic studies and literature precedents,[18] a plausible mechanism is depicted in Scheme 11. Site selective reversible C−H activation of **1** in presence active Rh-catalyst **A** may form a five-membered rhodacycle **B**. Later, coordination of **2** to intermediate **B** may generate **C**, which upon migratory insertion results in the formation of a seven-member rhodacycle **D**. Protodemetalation generates alkylated species **E** and subsequently regenerates the active Rh(III) catalytic species **A**. Finally, a sequential intramolecular nucleophilic attack followed by intermolecular Michael addition with **2** delivers the desired product **3**.

To showcase practicality of the protocol, scaled-up synthesis was carried out by taking **1a** (2 mmol) with **2a** (4 mmol) as the represenatative substrates (Scheme 12a). The reaction occurred to furnish **3aa** in 63% yield. Further, treatment of the annulated product with electrophilic reagents afford functionalized substrates (Scheme 12b). Interestingly, **3ha** when treated with

propargyl bromide in presence of K_2CO_3 afforded **4** in 80% yield. Moreover, on using allyl bromide, a similar outcome was observed to furnish allyl tethered isoquinoline-1,3-dione **5** in 72% yield.

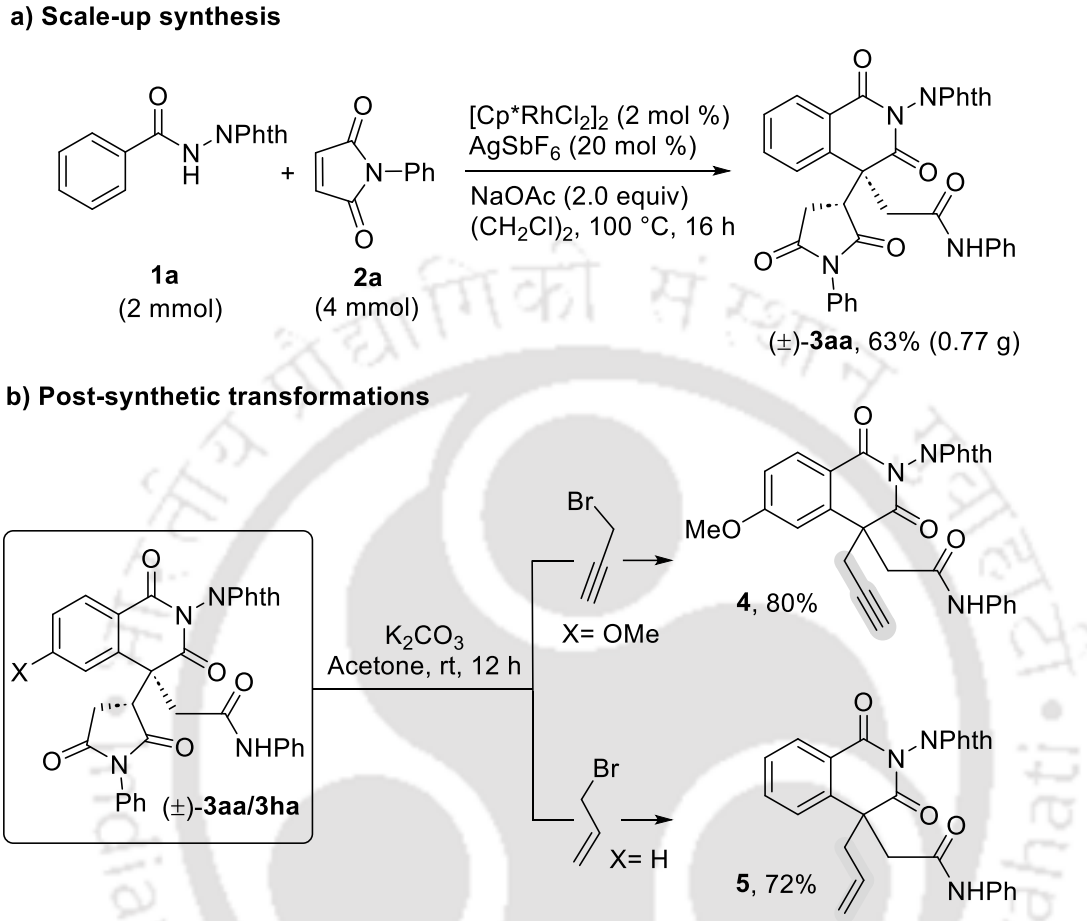

Scheme 12. Synthetic Utilities.

In conclusion, a Rh(III)-catalyzed cascade C−H functionalization/annulation towards the synthesis of isoquinoline-1,3-diones was discussed utilizing arylamides and maleimides as coupling partners. This diastereoselective protocol was performed with broad functional group tolerance. The step-economic operation, generation of quaternary carbon center and drug/natural product modifications are important practical features.

4.3 Experimental Section

General Information. $[Cp^*RhCl_2]_2$ (>97%), $AgSbF_6$ (>98%), $AgNTf_2$ (>97%), $AgBF_4$ (>98%), KOAc, NaOAc, CsOAc, Na_2CO_3, K_2CO_3 2,2,2-trifluoroethanol (TFE) and 1,1,1,3,3,3-hexafluoro-2-propanol (HFIP) of Aldrich and TCI Chemicals were used as received. Tetrahydrofuran (THF), toluene, chlorobenzene, methanol, 1,2-dichloroethane were

dried prior to use according to the standard procedure. Arylamides[19] and maleimides[20] were prepared according to reported procedures. Merck silica gel G/GF 254 plates were used for analytical TLC and SRL silica gel (100-200 mesh) was used for column chromatography. NMR (^{1}H, $^{13}C\{^{1}H\}$ and ^{19}F) spectra were recorded with Bruker Avance III 600, 500 and 400 MHz spectrometers using $CDCl_3$, DMSO-d_6 as solvent and Me_4Si as an internal standard. Chemical shifts (δ) and spin-spin coupling constant (*J*) are reported in ppm and in Hz, respectively, and peak patterns are reported as follows: s = singlet, d = doublet, t = triplet, m = multiplet, q = quartet, dd = doublet of doublets. Melting points were determined using a Büchi B-540 apparatus and are uncorrected. FT-IR spectra were collected on Perkin Elmer IR spectrometer. Quadrupole time-of-flight electrospray ionization (ESI) mass spectrometer (Agilent 6546) was used for recording HRMS. Single crystal X-ray data was collected on a Bruker SMART APEX equipped with a CCD area detector using Mo/Kα radiation and the structure was solved by direct method using SHELXL 2019/3 and SHELXL 2018/3 (Göttingen, Germany).

General Procedure for Rh-Catalyzed C−H Functionalization/Annulation of Benzamides with Maleimides. Substrate **1** (0.2 mmol, 1 equiv), maleimide **2** (0.4 mmol, 2 equiv), $[RhCp^*Cl_2]_2$ (0.004 mmol, 0.02 equiv, 2.5 mg), $AgSbF_6$ (0.04 mmol, 0.02 equiv, 13.7 mg) and NaOAc (0.4 mmol, 2 equiv, 32.8 mg) were stirred in $(CH_2Cl)_2$ (2 mL) at 100 °C for 16 h in pressure tube under N_2 atmosphere. After completion, the mixture was diluted with CH_2Cl_2 (10 mL), and passed through a short pad of celite using CH_2Cl_2 (2 x 10 mL). Evaporation of the solvent gave a residue that was purified on silica gel column chromatography using EtOAc/hexane as an eluent to afford **3**.

Radical Scavenger Experiments. To a solution of **1a** (0.2 mmol, 1 equiv), **2a** (0.4 mmol, 2 equiv), $[RhCp^*Cl_2]_2$ (0.004 mmol, 0.02 equiv, 2.5 mg), $AgSbF_6$ (2.5 mg, 0.004 mmol, 0.02 equiv) and NaOAc (, 0.4 mmol, 2 equiv) in $(CH_2Cl)_2$, TEMPO/BHT (0.4 mmol, 2 equiv) was added and the resulting mixture was stirred at 100 °C for 16 h. The mixture was diluted with CH_2Cl_2 (10 mL), and passed through a short pad of celite using CH_2Cl_2 (2 x 10 mL) . Evaporation of the solvent gave a residue that was purified on silica gel column chromatography using EtOAc/hexane as an eluent.

H/D Exchange Experiment of 1a with CD_3OD in Absence of 2a. *N*-(1,3-Dioxoisoindolin-2-yl)benzamide **1a** (0.2 mmol, 1 equiv, 53.2 mg), $[RhCp^*Cl_2]_2$ (0.004 mmol, 0.02 equiv, 2.5 mg), $AgSbF_6$ (0.004 mmol, 0.2 equiv, 13.7 mg), NaOAc (0.4 mmol, 2 equiv, 32.8 mg) and CD_3OD (2 mmol, 10 equiv, 41 μL) were stirred in $(CH_2Cl)_2$ (2 mL) at 100 °C for 16 h in pressure tube

under N_2 atmosphere. After completion, the resulting mixture was diluted with CH_2Cl_2 (10 mL), and passed through a short pad of celite using CH_2Cl_2 (2 x 10 mL). Evaporation of the solvent gave a residue that was purified on silica gel column chromatography using EtOAc/hexane as an eluent to afford [D_n]-**1a**.

H/D Exchange Experiment of 1a with CD_3OD in Presence of 2a. *N*-(1,3-Dioxoisoindolin-2-yl)benzamide **1a** (0.2 mmol, 1 equiv, 53.2 mg), 1-phenyl-1H-pyrrole-2,5-dione **2a** (0.4 mmol, 2 equiv, 69.2 mg), $[RhCp^*Cl_2]_2$ (0.004 mmol, 0.02 equiv, 2.5 mg), $AgSbF_6$ (0.004 mmol, 0.2 equiv, 13.7 mg), NaOAc (0.4 mmol, 2 equiv, 32.8 mg) and CD_3OD (2 mmol, 10 equiv, 41 µL) were stirred in $(CH_2Cl)_2$ (2 mL) at 100 °C for 16 h in pressure tube under N_2 atmosphere. After completion, the mixture was diluted with CH_2Cl_2 (10 mL), and passed through a short pad of celite using CH_2Cl_2 (2 x 10 mL). Evaporation of the solvent gave a residue that was purified on silica gel column chromatography using EtOAc/hexane as an eluent to afford [D_n]-**3aa**.

H/D Exchange of 3aa with CD_3OD. Product **3aa** (0.1 mmol, 1 equiv, 61.2 mg), $[RhCp^*Cl_2]_2$ (0.002 mmol, 0.02 equiv, 1.25), $AgSbF_6$ (0.02 mmol, 0.2 equiv, 6.8 mg), NaOAc (0.2 mmol, 2 equiv, 16.4 mg) and CD_3OD (1 mmol, 10 equiv, 21 µL) were stirred in $(CH_2Cl)_2$ (1 mL) at 100 °C for 4 h in a pressure tube N_2 atmosphere. After completion, the mixture was diluted with CH_2Cl_2 (10 mL), and passed through a short pad of celite using CH_2Cl_2 (2 x 10 mL) . Evaporation of the solvent gave a residue that was purified on silica gel column chromatography using EtOAc/hexane as an eluent to afford [D_n]-**3aa**.

Parallel Kinetic Isotope Experiment. Two pressures tubes were separately charged with *N*-(1,3-dioxoisoindolin-2-yl)benzamide **1a** (0.1 mmol, 26.6 mg) or *N*-(1,3-dioxoisoindolin-2-yl)benzamide-2,3,4,5,6-d_5 [D_5]-**1a** (0.1 mmol, 27.1 mg), 1-phenyl-1H-pyrrole-2,5-dione **2a** (0.2 mmol, 34.6 mg), $[RhCp^*Cl_2]_2$ (0.002 mmol, 1.25 mg), $AgSbF_6$ (0.02 mmol, 6.8 mg) and NaOAc (0.2 mmol, 16.4 mg) were stirred in $(CH_2Cl)_2$ (1 mL) at 100 °C for 2 h N_2 atmosphere. After completion, both the reaction mixtures were combined and passed through a short pad of celite using CH_2Cl_2 (2 x 10 mL). Evaporation of the solvent gave a residue that was purified on silica gel column chromatography using EtOAc/hexane as an eluent The KIE value was determined to be k_H/k_D = 1.63 based on the ^1H NMR analysis of **3aa**/[D_4]-**3aa**.

Competitive Kinetic Isotope Experiment. *N*-(1,3-Dioxoisoindolin-2-yl)benzamide **1a** (0.1 mmol, 26.6 mg), *N*-(1,3-dioxoisoindolin-2-yl)benzamide-2,3,4,5,6-d_5 **[D_5]-1a** (0.1 mmol, 27.1 mg), 1-phenyl-1H-pyrrole-2,5-dione **2a** (0.4 mmol, 69.2 mg), $[RhCp^*Cl_2]_2$ (0.004 mmol, 2.5

mg), $AgSbF_6$ (0.04 mmol, 13.6 mg) and NaOAc (0.4 mmol, 32.8 mg) were stirred in $(CH_2Cl)_2$ (2 mL) at 100 °C for 2 h in pressure tube N_2 atmosphere. After completion, the mixture was diluted with CH_2Cl_2 (10 mL), and passed through a short pad of celite using CH_2Cl_2 (2 x 10 mL) . Evaporation of the solvent gave a residue that was purified on silica gel column chromatography using EtOAc/hexane as an eluent. The KIE value was determined to be k_H/k_D = 1.85 based on the ^1H NMR analysis of **3aa**/[D_4]-**3aa**.

Scale-up Experiment. *N*-(1,3-Dioxoisoindolin-2-yl)benzamide **1a** (2 mmol, 1 equiv, 532 mg), 1-phenyl-1H-pyrrole-2,5-dione **2** (4 mmol, 2 equiv, 692 mg), $[RhCp^*Cl_2]_2$ (0.04 mmol, 0.02 equiv, 25 mg), $AgSbF_6$ (0.4 mmol, 0.02 equiv, 137.2 mg) and NaOAc (4 mmol, 2 equiv, 328 mg) were stirred in $(CH_2Cl)_2$ (20 mL) at 100 °C for 16 h in pressure tube N_2 atmosphere. After completion, the mixture was then diluted with CH_2Cl_2 (50 mL), and passed through a short pad of celite using CH_2Cl_2 (2 x 50 mL). Evaporation of the solvent gave a residue that was purified on silica gel column chromatography using EtOAc/hexane as an eluent to afford **3aa** (63%, 0.77g).

Synthesis of 4.[21] To a stirred solution of **3ha** (0.1 mmol, 1 equiv,) in acetone (1 mL) propargyl bromide (0.3 mmol, 3 equiv, 36 mg), K_2CO_3 (0.5 mmol, 5 equiv, 70 mg) were added. The resultant mixture was stirred at room temperature for 12 h. After completion, the resultant mixture was diluted with EtOAc (10 mL) and passed through a short pad of celite using EtOAc (2 x 10 mL). Evaporation of the solvent gave a residue that was purified on silica gel column chromatography using EtOAc/hexane as an eluent to afford **4**.

Synthesis of 5. To a stirred solution of **3aa** (0.1 mmol, 1 equiv,) and allyl bromide (0.1 mmol, 3 equiv, 36.3 mg) in acetone (1 mL), K_2CO_3 (0.5 mmol, 5 equiv, 70 mg) was added. The resultant mixture was stirred at room temperature for 12 h. After completion, the resultant mixture was diluted with EtOAc (10 mL) and passed through a short pad of celite using EtOAc (2 x 10 mL). Evaporation of the solvent gave a residue that was purified on silica gel column chromatography using EtOAc/hexane as an eluent to afford **5**.

4.4 Characterization Data of the Products

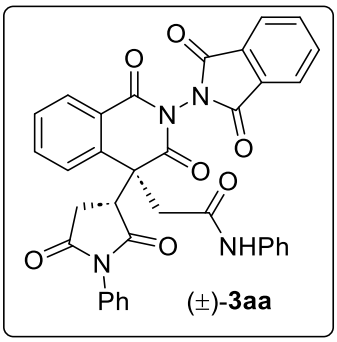

2-(4-(2,5-Dioxo-1-phenylpyrrolidin-3-yl)-2-(1,3-dioxoisoindolin-2-yl)-1,3-dioxo-1,2,3,4-tetrahydroisoquinolin-4-yl)-N-phenylacetamide 3aa. Analytical TLC on silica gel, 1:2 ethyl acetate/hexane R_f = 0.48; colorless solid; mp 235-236 °C; yield 77% (94 mg); ^{1}H NMR (500 MHz, $CDCl_3$) δ 8.38 (d, *J* = 8.0 Hz, 1H), 7.97-7.93 (m, 2H), 7.83-7.79 (m, 2H), 7.64 (t, *J* = 7.5 Hz, 1H), 7.55-7.51 (m, 2H), 7.46-7.38 (m, 4H), 7.32 (d, *J* = 8.0 Hz, 2H), 7.18 (t, *J* = 7.5 Hz, 2H), 7.08 (d, *J* = 7.5 Hz, 2H), 7.00 (t, *J* = 7.5 Hz, 1H), 4.33 (d, *J* = 16.5 Hz, 1H), 3.91 (d, *J* = 16.5 Hz, 1H), 3.73 (dd, *J* = 9.0, 5.5 Hz, 1H), 3.25 (dd, *J* = 19.0, 9.5 Hz, 1H), 2.75 (dd, *J* = 18.5, 5.0 Hz, 1H); ^{13}C{^{1}H} NMR (125 MHz, $CDCl_3$) δ 175.6, 173.2, 171.1, 166.3, 164.0, 162.9, 160.4, 137.3, 136.9, 135.2, 135.1, 134.8, 131.4, 131.0, 130.5, 130.2, 129.4, 129.3, 129.1, 129.0, 126.5, 126.2, 125.2, 124.6, 124.5, 124.3, 119.8, 52.3, 48.9, 44.5, 31.2; FT-IR (KBr) 2924, 1745, 1711, 1385, 1191, 880, 755 cm^{-1}; HRMS (ESI) m/z $[M+H]^+$ calcd for $C_{35}H_{25}N_4O_7$: 613.1718, found: 613.1728.

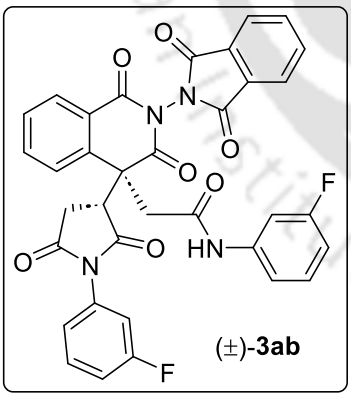

2-(2-(1,3-Dioxoisoindolin-2-yl)-4-(1-(3-fluorophenyl)-2,5-dioxopyrrolidin-3-yl)-1,3-dioxo-1,2,3,4-tetrahydroisoquinolin-4-yl)-N-(3-fluorophenyl)acetamide 3ab. Analytical TLC on silica gel, 1:2 ethyl acetate/hexane R_f = 0.48; colorless solid; mp 294-295 °C; yield 70% (91 mg); ^{1}H NMR (500 MHz, DMSO-d_6) δ ^{1}H NMR (400 MHz, DMSO-d_6) δ 10.47 (s, 1H), 8.22 (d, *J* = 8.0 Hz, 1H), 8.11-8.10 (m, 2H), 8.06-8.02 (m, 2H), 7.88 (t, *J* = 7.5 Hz, 1H), 7.73 (d, *J* = 8.0 Hz, 1H), 7.63 (t, *J* = 7.5 Hz, 1H), 7.57-7.52 (m, 1H), 7.34-7.25 (m, 3H), 7.13 (d, *J* = 8.0 Hz, 1H), 7.08-7.06 (m, 2H), 6.83 (t, *J* = 7.0 Hz,

1H), 4.14 (d, J = 17.0 Hz, 1H), 3.94 (dd, J = 9.0, 5.5 Hz, 1H), 3.76 (d, J = 17.5 Hz, 1H), 3.15 (dd, J = 18.0, 9.0 Hz, 1H), 2.82 (dd, J = 18.0, 5.0 Hz, 1H); $^{13}C\{^1H\}$ NMR (125 MHz, DMSO-d_6) δ 174.3, 173.2, 170.3, 167.3, 163.7, 162.9 (d, J_{C-F} = 240.0 Hz), 162.69, 162.68 (d, J_{C-F} = 243.0 Hz),160.7, 140.1 (d, J_{C-F} = 11.0 Hz), 139.0, 136.2, 136.0, 135.6, 133.2 (d, J_{C-F} = 10.5 Hz), 130.7 (d, J_{C-F} = 9.0 Hz), 130.4 (d, J_{C-F} = 9.3 Hz), 129.1, 129.0, 128.8, 128.7, 125.5, 125.2, 124.5, 123.1 (d, J_{C-F} = 2.8 Hz), 115.7 (d, J_{C-F} = 20.2 Hz), 114.77, 114.75, 114.1 (d, J_{C-F} = 23.8 Hz), 110.0 (d, J_{C-F} = 20.8 Hz), 105.8 (d, J_{C-F} = 26.0 Hz), 50.5, 48.9, 43.9, 31.1; ^{19}F NMR (471 MHz, DMSO-d_6) δ -112.00; FT-IR (KBr) 2923, 1748, 1715, 1492, 1317, 1190, 710 cm^{-1}; HRMS (ESI) m/z $[M+H]^+$ calcd for $C_{35}H_{23}F_2N_4O_7$: 649.1529, found: 649.1530.

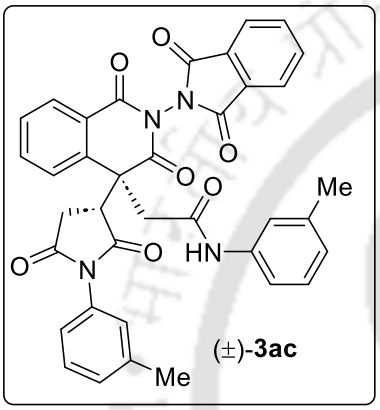

(±)-**3ac**

2-(4-(2,5-Dioxo-1-(m-tolyl)pyrrolidin-3-yl)-2-(1,3-dioxoisoindolin-2-yl)-1,3-dioxo-1,2,3,4-tetrahydroisoquinolin-4-yl)-N-(m-tolyl)acetamide 3ac. Analytical TLC on silica gel, 1:2 ethyl acetate/hexane R_f = 0.45; colorless solid; mp 289-290 °C; yield 75% (96 mg); ^1H NMR (400 MHz, $CDCl_3$) δ 8.39 (d, J = 7.6 Hz, 1H), 7.98-7.92 (m, 2H), 7.83-7.79 (m, 2H), 7.66-7.63 (m, 1H), 7.56-7.52 (m, 2H), 7.36-7.31 (m, 2H), 7.21 (d, J = 7.2 Hz, 1H), 7.13-7.04 (m, 3H), 6.87-6.81 (m, 3H), 4.33 (d, J = 17.2 Hz, 1H), 3.90 (d, J = 16.4 Hz, 1H), 3.72 (dd, J = 8.8, 5.2 Hz, 1H), 3.24 (dd, J = 18.8, 9.2 Hz, 1H), 2.74 (dd, J = 18.8, 5.2 Hz, 1H), 2.37 (s, 3H), 2.23 (s, 3H); $^{13}C\{^1H\}$ NMR (150 MHz, $CDCl_3$) δ 175.7, 173.4, 171.1, 166.3, 164.0, 162.9, 160.4, 139.5, 138.9, 137.2, 136.9, 135.2, 135.0, 134.8, 131.2, 131.0, 130.5, 130.2, 130.0, 129.3, 129.2, 128.8, 127.1, 126.2, 125.34, 125.32, 124.6, 124.2, 123.5, 120.3, 116.9, 52.3, 48.9, 44.5, 31.2, 21.5, 21.4; FT-IR (KBr) 3358, 2929, 1746, 1712, 1491, 1382, 1317, 1191, 711 cm^{-1}; HRMS (ESI) m/z $[M+H]^+$ calcd for $C_{37}H_{29}N_4O_7$: 641.2031, found: 641.2010.

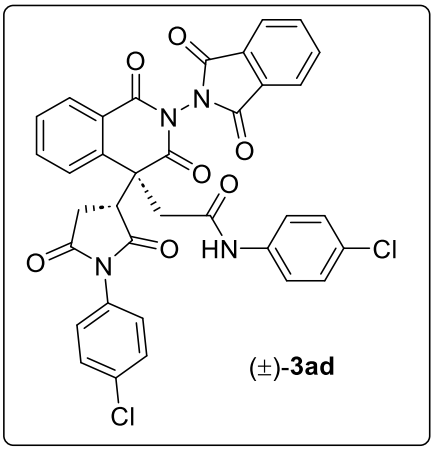

N-(4-Chlorophenyl)-2-(4-(1-(4-chlorophenyl)-2,5-dioxopyrrolidin-3-yl)-2-(1,3-dioxoisoindolin-2-yl)-1,3-dioxo-1,2,3,4-tetrahydroisoquinolin-4-yl)acetamide 3ad. Analytical TLC on silica gel, 1:2 ethyl acetate/hexane R_f = 0.42; colorless solid; mp 278-279 ºC; yield 71% (96 mg); ^{1}H NMR (500 MHz, $CDCl_3$) δ 8.39 (d, *J* = 7.5 Hz, 1H), 7.97-7.92 (m, 2H), 7.84-7.80 (m, 2H), 7.64 (t, *J* = 7.5 Hz, 1H), 7.55 (t, *J* = 8.0 Hz, 1H), 7.49-7.47 (m, 2H), 7.42 (d, *J* = 8.5 Hz, 2H), 7.27-7.26 (m, 2H), 7.13 (d, *J* = 8.5 Hz, 2H), 7.05 (d, *J* = 8.5 Hz, 2H), 4.29 (d, *J* = 16.5 Hz, 1H), 3.89 (d, *J* = 16.5 Hz, 1H), 3.73 (dd, *J* = 9.0, 5.5 Hz, 1H), 3.25 (dd, *J* = 19.0, 9.0 Hz, 1H), 2.76 (dd, *J* = 19.0, 5.0 Hz, 1H); ^{13}C{^{1}H} NMR (125 MHz, $CDCl_3$) δ 175.2, 172.9, 171.0, 166.4, 164.0, 163.0, 160.3, 136.8, 135.8, 135.3, 135.1, 135.0, 134.9, 131.1, 130.4, 130.1, 129.7, 129.6, 129.55, 129.51, 129.0, 127.7, 126.2, 125.1, 124.6, 124.3, 121.0, 52.1, 48.9, 44.5, 31.2; FT-IR (KBr) 2925, 1746, 1714, 1493, 1317, 1190, 1092, 711 cm^{-1}; HRMS (ESI) m/z $[M+H]^+$ calcd for $C_{35}H_{23}Cl_2N_4O_7$: 681.0938, found: 681.0937.

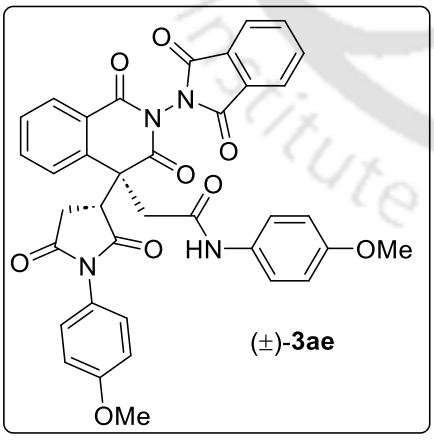

2-(2-(1,3-Dioxoisoindolin-2-yl)-4-(1-(4-methoxyphenyl)-2,5-dioxopyrrolidin-3-yl)-1,3-dioxo-1,2,3,4-tetrahydroisoquinolin-4-yl)-N-(4-methoxyphenyl)acetamide 3ae. Analytical TLC on silica gel, 1:1 ethyl acetate/hexane R_f = 0.55; colorless solid; mp 230-231 ºC; yield 69% (93 mg); ^{1}H NMR (400 MHz, $CDCl_3$) δ 8.36 (d, *J* = 7.6 Hz, 1H), 7.96-7.91 (m, 2H), 7.81-7.79 (m, 2H), 7.63 (t, *J* = 7.2 Hz, 1H), 7.53-7.49

(m, 2H), 7.40 (s, 1H), 7.20 (d, J = 8.8 Hz, 2H), 7.00-6.91 (m, 4H), 6.70 (d, J = 8.8 Hz, 2H),4.27 (d, J = 16.4 Hz, 1H), 3.85-3.69 (m, 5H), 3.69 (s, 3H), 3.21 (dd, J = 18.8, 9.2 Hz, 1H), 2.74 (dd, J = 19.2, 5.2 Hz, 1H); $^{13}C\{^1H\}$ NMR (125 MHz, $CDCl_3$) δ 175.8, 173.6, 171.1, 166.1, 164.0, 162.9, 160.4, 159.9, 156.5, 137.1, 135.1, 135.0, 134.8, 131.0, 130.58, 130.52, 130.2, 129.3, 127.7, 126.2, 125.3, 124.5, 124.2, 123.9, 121.6, 114.7, 114.1, 55.6, 55.5, 52.3, 48.9, 44.4, 31.2; FT-IR (KBr) 3356, 2927, 1745, 1710, 1603, 1499, 1316, 1025, 709 cm^{-1};HRMS (ESI) m/z $[M+H]^+$ calcd for $C_{37}H_{29}N_4O_9$: 673.1929, found: 673.1923.

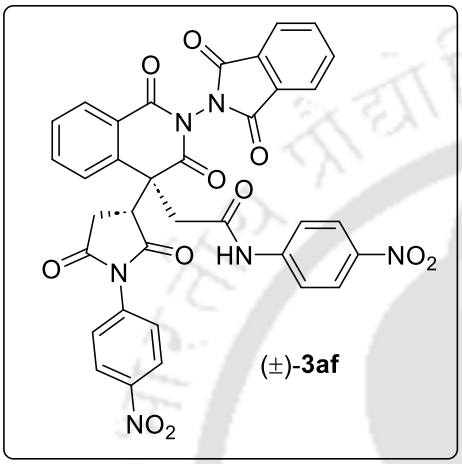

2-(2-(1,3-Dioxoisoindolin-2-yl)-4-(1-(4-nitrophenyl)-2,5-dioxopyrrolidin-3-yl)-1,3-dioxo-1,2,3,4-tetrahydroisoquinolin-4-yl)-N-(4-nitrophenyl)acetamide 3af. Analytical TLC on silica gel, 1:1 ethyl acetate/hexane R_f = 0.45; colorless solid; mp 190-191 ºC; yield 80% (112 mg); ^1H NMR (500 MHz, DMSO-d_6) δ 10.88 (s, 1H), 8.37 (d, J = 8.5 Hz, 2H), 8.23 (d, J = 7.5 Hz, 1H), 8.16 (d, J = 9.0 Hz, 2H), 8.10-8.09 (m, 2H), 8.047-8.040 (m, 2H), 7.87 (t, J = 7.5 Hz, 1H), 7.76 (d, J = 8.0 Hz, 1H), 7.64-7.61 (m, 3H), 7.55 (d, J = 8.5 Hz, 2H), 4.21 (d, J = 17.0 Hz, 1H), 4.00 (dd, J = 8.5, 6.0 Hz, 1H), 3.84 (d, J = 17.5 Hz, 1H), 3.21 (dd, J = 18.5, 9.5 Hz, 1H), 2.91 (dd, J = 18.0, 4.5 Hz, 1H), $^{13}C\{^1H\}$ NMR (125 MHz, DMSO-d_6) δ 173.4, 172.3, 170.3, 168.2, 163.6, 162.5, 160.5, 146.7, 144.4, 142.3, 140.0, 137.6, 136.1, 136.0, 129.1, 129.0, 128.9, 128.7, 127.7, 126.2, 124.9, 124.6, 124.5, 124.4, 124.2, 118.8, 52.2, 47.7, 44.7, 31.4; FT-IR (KBr) 2919, 1746, 1719, 1510, 1343, 1177, 853, 711 cm^{-1}; HRMS (ESI) m/z $[M+Na]^+$ calcd for $C_{35}H_{22}N_6NaO_{11}$: 725.1239, found: 725.1225.

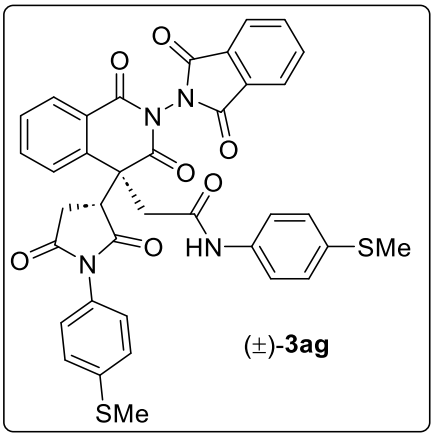

2-(2-(1,3-Dioxoisoindolin-2-yl)-4-(1-(4-(methylthio)phenyl)-2,5-dioxopyrrolidin-3-yl)-1,3-dioxo-1,2,3,4-tetrahydroisoquinolin-4-yl)-N-(4-(methylthio)phenyl)acetamide 3ag. Analytical TLC on silica gel, 1:1 ethyl acetate/hexane R_f = 0.52; colorless solid; mp 224-225 °C; yield 67% (94 mg); ^{1}H NMR (400 MHz, $CDCl_3$) δ 8.39 (d, *J* = 6.8 Hz, 1H), 7.98-7.92 (m, 2H), 7.84-7.81 (m, 2H), 7.66-7.62 (m, 1H), 7.56-7.48 (m, 2H), 7.42 (s, 1H), 7.30-7.25 (m, 4H), 7.11 (d, *J* = 8.4 Hz, 2H), 7.01 (d, *J* = 8.4 Hz, 2H), 4.32 (d, *J* = 16.8 Hz, 1H), 3.90 (d, *J* = 16.4 Hz, 1H), 3.71 (dd, *J* = 9.2, 5.6 Hz, 1H), 3.24 (dd, *J* = 19.2, 9.6 Hz, 1H), 2.74 (dd, *J* = 18.8, 5.2 Hz, 1H), 2.48 (s, 3H), 2.39 (s, 3H); ^{13}C{^{1}H} NMR (100 MHz, $CDCl_3$) δ 175.5, 173.3, 171.1, 166.3, 164.0, 163.0, 160.4, 140.4, 136.9, 135.2, 135.1, 134.97, 134.93, 133.7, 131.0, 130.4, 130.1, 129.3, 128.0, 127.9, 126.78, 126.73, 126.2, 125.2, 124.6, 124.3, 120.3, 52.2, 48.9, 44.4, 31.2, 16.7, 15.6; FT-IR (KBr) 2922, 1744, 1712, 1497, 1318, 1190, 709 cm^{-1}; HRMS (ESI) m/z $[M+H]^+$ calcd for $C_{37}H_{29}N_4O_7S_2$: 705.1472, found: 705.1438.

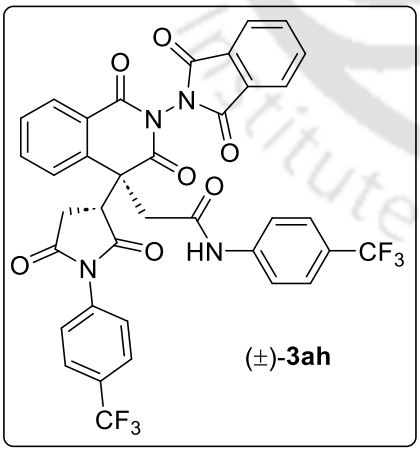

2-(4-(2,5-Dioxo-1-(4-(trifluoromethyl)phenyl)pyrrolidin-3-yl)-2-(1,3-dioxoisoindolin-2-yl)-1,3-dioxo-1,2,3,4-tetrahydroisoquinolin-4-yl)-N-(4-(trifluoromethyl)phenyl)acetamide 3ah. Analytical TLC on silica gel, 1:2 ethyl acetate/hexane R_f = 0.40; colorless solid; mp 285-286 °C; yield 78% (117 mg); ^{1}H NMR (400 MHz, DMSO-d_6) δ 10.63 (s, 1H), 8.23 (d, *J* = 7.6 Hz, 1H), 8.11-8.03 (m, 4H), 7.90-7.85 (m,

3H), 7.74 (d, J = 8.0 Hz, 1H), 7.64-7.58 (m, 5H), 7.47 (d, J = 8.0 Hz, 2H), 4.19 (d, J = 17.6 Hz, 1H), 3.97 (dd, J = 8.4, 5.2 Hz, 1H), 3.81 (d, J = 17.2 Hz, 1H), 3.19 (dd, J = 18.0, 9.2 Hz, 1H), 2.87 (dd, J = 18.4, 4.4 Hz, 1H); $^{13}C\{^{1}H\}$ NMR (125 MHz, DMSO-d_6) δ 174.2, 173.2, 170.2, 167.6, 163.6, 162.6, 160.6, 141.9, 138.9 (q, J_{C-F} = 4.0 Hz), 136.1, 136.0, 135.6, 135.3, 129.1, 129.0, 128.8, 128.7, 128.6, 127.6, 126.0 (q, J_{C-F} = 4.3 Hz), 125.4, 125.3, 125.2, 124.9, 124.5 (q, J_{C-F} = 4.0 Hz), 123.5, 123.3, 123.1, 122.7, 118.9 (q, J_{C-F} = 4.3 Hz), 50.6, 49.0, 43.8, 31.2. ^{19}F NMR (471 MHz, DMSO-d_6) δ -60.39, -61.14; FT-IR (KBr) 3355, 2928, 1749, 1717, 1324, 1177, 1124, 1067, 709 cm^{-1}; HRMS (ESI) m/z $[M+H]^+$ calcd for $C_{37}H_{25}F_6N_4O_7$: 749.1465, found: 749.1488.

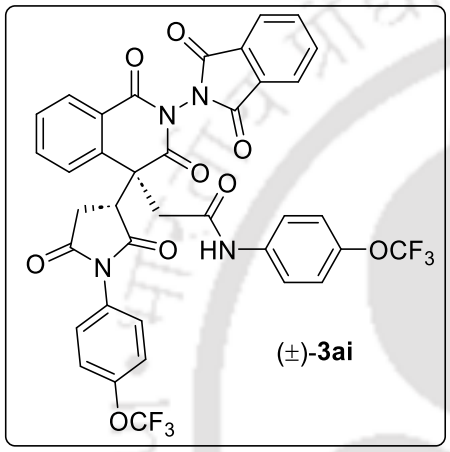

2-(4-(2,5-Dioxo-1-(4-(trifluoromethoxy)phenyl)pyrrolidin-3-yl)-2-(1,3-dioxoisoindolin-2-yl)-1,3-dioxo-1,2,3,4-tetrahydroisoquinolin-4-yl)-N-(4-(trifluoromethoxy)phenyl)acetamide 3ai. Analytical TLC on silica gel, 1:1 ethyl acetate/hexane R_f = 0.52; colorless solid; mp 280-281 ºC; yield 68% (106 mg); ^{1}H NMR (400 MHz, DMSO-d_6) δ 10.45 (s, 1H), 8.22 (d, J = 7.6 Hz, 1H), 8.11-8.09 (m, 2H), 8.05-8.02 (m, 2H), 7.87 (t, J = 7.2 Hz, 1H), 7.72 (d, J = 8.0 Hz, 1H), 7.62 (t, J = 7.6 Hz, 1H), 7.52-7.47 (m, 4H), 7.36 (d, J = 8.8 Hz, 2H), 7.25 (d, J = 8.8 Hz, 2H), 4.15 (d, J = 16.8 Hz, 1H), 3.94 (dd, J = 8.8, 5.2 Hz, 1H), 3.77 (d, J = 17.2 Hz, 1H), 3.17 (dd, J = 18.0, 9.2 Hz, 1H), 2.83 (dd, J = 18.0, 4.8 Hz, 1H); $^{13}C\{^{1}H\}$ NMR (125 MHz, DMSO-d_6) δ 174.4, 173.4, 170.3, 167.1, 163.7, 162.6, 160.7, 147.8 (q, J_{C-F} = 1.8 Hz), 143.6 (q, J_{C-F} = 1.8 Hz), 139.0, 137.6, 136.2, 136.0, 135.6, 130.7, 129.1(q, J_{C-F} = 3.6 Hz), 128.9, 128.8, 128.7, 128.5, 126.4, 125.5, 125.2, 124.6 (q, J_{C-F} = 4.0 Hz), 124.1 (q, J_{C-F} = 11.0 Hz), 121.6, 121.1 (q, J_{C-F} = 254.0 Hz), 121.0 (q, J_{C-F} = 255.0 Hz) 120.3, 50.6, 48.9, 43.7, 31.1;^{19}F NMR (471 MHz, DMSO) δ -56.87, -57.12; FT-IR (KBr) 2925, 1747, 1715, 1510, 1260, 1212, 881, 711 cm^{-1}; HRMS (ESI) m/z $[M+H]^+$ calcd for $C_{37}H_{23}F_6N_4O_9$: 781.1364, found: 781.1332.

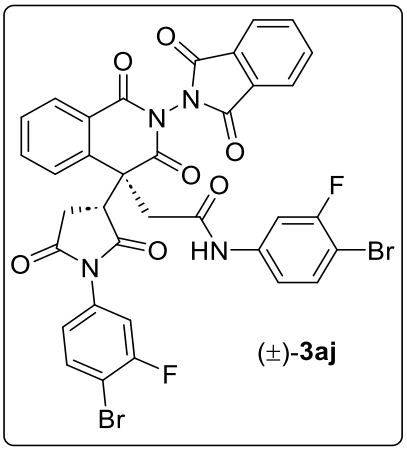

N-(4-Bromo-3-fluorophenyl)-2-(4-(1-(4-bromo-3-fluorophenyl)-2,5-dioxopyrrolidin-3-yl)-2-(1,3-dioxoisoindolin-2-yl)-1,3-dioxo-1,2,3,4-tetrahydroisoquinolin-4-yl)acetamide 3aj. Analytical TLC on silica gel, 1:2 ethyl acetate/hexane R_f = 0.45; colorless solid; mp 291-292 °C; yield 73% (117 mg); ^{1}H NMR (500 MHz, DMSO-d_6) δ 10.59 (s, 1H), 8.21 (d, J = 8.0 Hz, 1H), 8.11-8.08 (m, 2H), 8.04-8.03 (m, 2H), 7.87 (t, J = 8.5 Hz, 2H), 7.73 (d, J = 8.0 Hz, 1H), 7.62 (t, J = 7.5 Hz, 1H), 7.56 (t, J = 8.5 Hz, 1H), 7.49 (dd, J = 11.5, 2.0 Hz, 1H), 7.28 (dd, J = 9.5, 2.0 Hz, 1H), 7.12 (dd, J = 9.0, 2.0 Hz, 1H), 7.07 (dd, J = 8.0, 1.0 Hz, 1H), 4.11 (d, J = 17.0 Hz, 1H), 3.94 (dd, J = 9.0, 5.5 Hz, 1H), 3.75 (d, J = 17.0 Hz, 1H), 3.15 (dd, J = 18.0, 9.0 Hz, 1H), 2.86 (dd, J = 18.0, 5.0 Hz, 1H); ^{13}C{^{1}H} NMR (125 MHz, DMSO-d_6) δ 174.0, 172.9, 170.2, 167.5, 163.7, 162.6, 160.6, 158.9 (d, J_{C-F} = 241.3 Hz), 158.8 (d, J_{C-F} = 243.7 Hz), 139.5 (d, J_{C-F} = 10.2 Hz), 136.2, 136.0, 135.6, 133.7, 133.4, 132.4 (d, J_{C-F} = 22.1 Hz), 129.09, 129.03, 128.8, 128.7, 125.5, 125.2, 124.57, 124.53, 116.35, 116.32, 115.3 (d, J_{C-F} = 25.0 Hz), 108.2, 108.1, 107.0 (d, J_{C-F} = 26.7 Hz), 101.0 (d, J_{C-F} = 21.1 Hz), 50.4, 48.9, 43.9, 31.1; ^{19}F NMR (471 MHz, DMSO-d_6) δ -106.271, -106.757; FT-IR (KBr) 2925, 1746, 1719, 1489, 1259, 712 cm^{-1}; HRMS (ESI) m/z [M+H]$^+$ calcd for $C_{35}H_{21}Br_2F_2N_4O_7$: 804.9740, found: 804.9737.

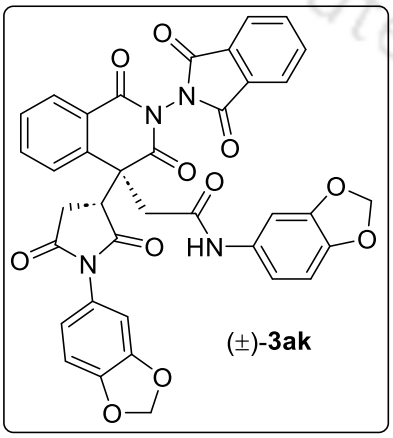

N-(Benzo[d][1,3]dioxol-5-yl)-2-(4-(1-(benzo[d][1,3]dioxol-5-yl)-2,5-dioxopyrrolidin-3-yl)-2-(1,3-dioxoisoindolin-2-yl)-1,3-dioxo-1,2,3,4-

tetrahydroisoquinolin-4-yl)acetamide 3ak. Analytical TLC on silica gel, 1:1 ethyl acetate/hexane R_f = 0.52; colorless solid; mp 229-230 °C; yield 67% (94 mg); ^{1}H NMR (500 MHz, DMSO-d_6) δ 10.13 (s, 1H), 8.22 (d, *J* = 7.5 Hz, 1H), 8.10-8.09 (m, 2H), 8.04-8.00 (m, 2H), 7.87 (t, *J* = 8.0 Hz, 1H), 7.67-7.61 (m, 2H), 7.05-6.99 (m, 2H), 6.77-6.75 (m, 2H), 6.70 (s, 1H), 6.62 (d, *J* = 8.5 Hz, 1H), 6.08 (s, 2H), 5.93 (s, 2H), 4.10 (d, *J* = 17.0 Hz, 1H), 3.86 (dd, *J* = 9.0, 5.0 Hz, 1H), 3.69 (d, *J* = 17.0 Hz, 1H), 3.10 (dd, *J* = 18.0, 9.0 Hz, 1H), 2.72 (dd, *J* = 20.5, 5.0 Hz, 1H); ^{13}C{^{1}H} NMR (125 MHz, DMSO-d_6) δ 174.7, 173.6, 170.4, 166.5, 163.7, 162.6, 160.6, 147.3, 147.2, 146.9, 142.9, 136.1, 135.9, 135.5, 132.8, 129.0, 128.8, 128.7, 125.57, 125.56, 125.2, 125.2, 124.5, 120.6, 111.8, 108.1, 107.9, 107.7, 101.8, 101.1, 100.9, 50.8, 48.7, 43.7, 40.4, 31.0; FT-IR (KBr) 2919, 2850, 1746, 1711, 1489, 1351, 1037, 712 cm^{-1}; HRMS (ESI) m/z [M+H]$^+$ calcd for $C_{37}H_{25}N_4O_{11}$: 701.1514, found: 701.1483.

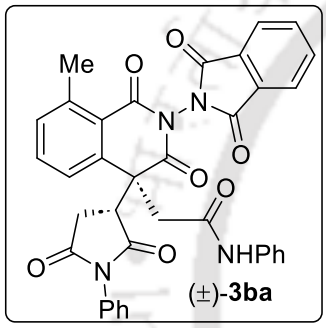

(±)-**3ba**

2-(4-(2,5-Dioxo-1-phenylpyrrolidin-3-yl)-2-(1,3-dioxoisoindolin-2-yl)-8-methyl-1,3-dioxo-1,2,3,4-tetrahydroisoquinolin-4-yl)-N-phenylacetamide 3ba. Analytical TLC on silica gel, 1:2 ethyl acetate/hexane R_f = 0.46; colorless solid; mp 231-232 °C; yield 80% (100 mg); ^{1}H NMR (500 MHz, $CDCl_3$) δ 7.95-7.90 (m, 2H), 7.80-7.78 (m, 2H), 7.58 (s, 1H), 7.46-7.42 (m, 3H), 7.40-7.36 (m, 2H), 7.31 (d, *J* = 8.0 Hz, 3H), 7.15 (t, *J* = 7.0 Hz, 2H), 7.06 (d, *J* = 7.5 Hz, 2H), 6.98 (t, *J* = 7.5 Hz, 1H), 4.30 (d, *J* = 16.5 Hz, 1H), 3.89 (d, *J* = 16.5 Hz, 1H), 3.71 (dd, *J* = 9.0, 5.5 Hz, 1H), 3.25 (dd, *J* = 19.0, 9.5 Hz, 1H), 2.79-2.75 (m, 4H); ^{13}C{^{1}H} NMR (125 MHz, $CDCl_3$) δ 175.7, 173.5, 170.8, 166.5, 164.1, 163.1, 160.3, 145.4, 138.3, 137.4, 135.0, 134.8, 134.0, 133.4, 131.4, 130.5, 130.2, 129.3, 129.1, 128.9, 126.5, 124.5, 124.3, 124.2, 124.1, 123.4, 119.8, 52.2, 49.1, 44.6, 31.3, 24.1; FT-IR (KBr) 2928, 1745, 1712, 1499, 1443, 1384, 1194, 881, 754, 695 cm^{-1}; HRMS (ESI) m/z [M+H]$^+$ calcd for $C_{36}H_{27}N_4O_7$: 627.1874, found: 627.1856.

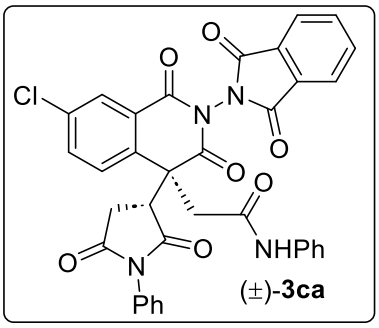

2-(7-Chloro-4-(2,5-dioxo-1-phenylpyrrolidin-3-yl)-2-(1,3-dioxoisoindolin-2-yl)-1,3-dioxo-1,2,3,4-tetrahydroisoquinolin-4-yl)-N-phenylacetamide 3ca. Analytical TLC on silica gel, 1:2 ethyl acetate/hexane R_f = 0.42; colorless solid; mp 295-296 °C; yield 71% (92 mg); ^{1}H NMR (500 MHz, $CDCl_3$) δ 8.34 (d, *J* = 1.5 Hz, 1H), 7.97-7.93 (m, 2H), 7.83-7.81 (m, 2H), 7.59 (dd, *J* = 8.5, 1.5 Hz, 1H), 7.47 (t, *J* = 8.5 Hz, 3H), 7.43-7.40 (m, 2H), 7.32 (d, *J* = 7.5 Hz, 2H), 7.20 (t, *J* = 7.5 Hz, 2H), 7.11 (d, *J* = 7.5 Hz, 2H), 7.02 (t, *J* = 7.0 Hz, 1H), 4.31 (d, *J* = 16.5 Hz, 1H), 3.90 (d, *J* = 17.0 Hz, 1H), 3.73 (dd, *J* = 9.0, 6.0 Hz, 1H), 3.26 (dd, *J* = 19.0, 9.5 Hz, 1H), 2.74 (dd, *J* = 19.0, 5.0 Hz, 1H); ^{13}C{^{1}H} NMR (125 MHz, $CDCl_3$) δ 175.4, 173.0, 170.6, 166.2, 163.8, 162.8, 159.5, 137.2, 135.9, 135.4, 135.2, 135.1, 134.9, 131.3, 130.7, 130.5, 130.1, 129.49, 129.43, 129.2, 129.1, 127.9, 126.9, 126.4, 124.6, 124.3, 119.8, 52.0, 48.8, 44.6, 31.2; FT-IR (KBr) 2922, 1747, 1713, 1502, 1383, 1310, 1191, 752 cm^{-1}; HRMS (ESI) m/z $[M+H]^+$ calcd for $C_{35}H_{24}ClN_4O_7$: 647.1328, found: 647.1297.

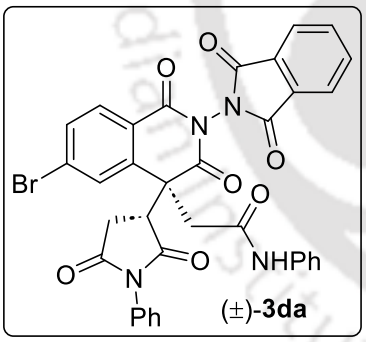

2-(6-Bromo-4-(2,5-dioxo-1-phenylpyrrolidin-3-yl)-2-(1,3-dioxoisoindolin-2-yl)-1,3-dioxo-1,2,3,4-tetrahydroisoquinolin-4-yl)-N-phenylacetamide 3da. Analytical TLC on silica gel, 1:2 ethyl acetate/hexane R_f = 0.48; colorless solid; mp 278-279 °C; yield 72% (99 mg); ^{1}H NMR (400 MHz, $CDCl_3$) δ 10.22 (s, 1H), 8.12-8.08 (m, 3H), 8.04-8.02 (m, 2H), 7.84 (dd, *J* = 8.4, 1.6 Hz, 1H), 7.49 (t, *J* = 7.2 Hz, 3H), 7.44 (d, *J* = 7.6 Hz, 1H), 7.40 (d, *J* = 8.0 Hz, 2H), 7.26-7.23 (m, 4H), 7.01 (t, *J* = 7.2 Hz, 1H), 4.11 (d, *J* = 16.8 Hz, 1H), 4.05-4.01 (m, 1H), 3.71 (d, *J* = 16.8 Hz, 1H), 3.14 (dd, *J* = 18.0, 9.2 Hz, 1H), 2.92 (dd, *J* = 18.0, 5.6 Hz, 1H); ^{13}C{^{1}H} NMR (125 MHz, DMSO-d_6) δ 174.5, 173.5, 169.8, 166.8, 163.5, 162.5, 160.2, 141.8, 138.3, 136.1, 136.0, 131.88, 131.81, 130.7, 129.7, 129.0, 128.8, 128.7, 128.6, 128.5, 127.0, 126.8, 124.66, 124.60, 124.5, 123.5, 119.1, 50.4, 48.8, 43.9, 31.1; FT-IR

(KBr) 2920, 2851, 1744, 1712, 1543, 1464, 1315, 695 cm^{-1} ; HRMS (ESI) m/z $[M+H]^+$ calcd for $C_{35}H_{24}BrN_4O_7$: 691.0823, found: 691.0828.

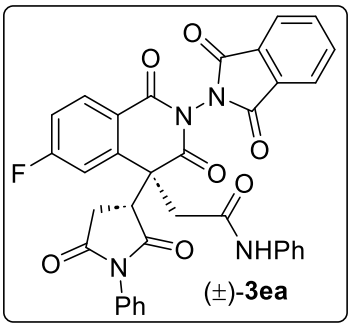

2-(4-(2,5-Dioxo-1-phenylpyrrolidin-3-yl)-2-(1,3-dioxoisoindolin-2-yl)-6-fluoro-1,3-dioxo-1,2,3,4-tetrahydroisoquinolin-4-yl)-N-phenylacetamide 3ea. Analytical TLC on silica gel, 1:2 ethyl acetate/hexane R_f = 0.44; colorless solid; mp 286-287 °C; yield 70% (88 mg); ^{1}H NMR (500 MHz, $CDCl_3$) δ 8.40-8.37 (m, 1H), 7.94-7.90 (m, 2H), 7.80-7.78 (m, 2H), 7.59 (s, 1H), 7.45 (t, *J* = 7.5 Hz, 2H), 7.39 (t, *J* = 7.5 Hz, 1H), 7.30 (d, *J* = 7.5 Hz, 2H), 7.26-7.25 (m, 1H), 7.21 (t, *J* = 8.5 Hz, 1H), 7.16 (t, *J* = 7.5 Hz, 2H), 7.10 (d, *J* = 7.5 Hz, 2H), 6.99 (t, *J* = 7.0 Hz, 1H), 4.23 (d, *J* = 17.0 Hz, 1H), 3.88 (d, *J* = 17.0 Hz, 1H), 3.70 (dd, *J* = 8.5, 5.5 Hz, 1H), 3.24 (dd, *J* = 19.0, 9.5 Hz, 1H), 2.76 (dd, *J* = 18.5, 5.0 Hz, 1H); ^{13}C{^{1}H} NMR (125 MHz, $CDCl_3$) δ 175.3, 173.1, 170.6, 167.8 (d, J_{C-F} = 257.1 Hz), 166.2, 163.9, 162.9, 159.6, 140.4, 137.2, 135.1, 134.9, 134.0 (d, J_{C-F} = 9.75 Hz), 131.2, 130.4, 130.1, 129.4, 129.2, 129.0, 126.5, 124.6, 124.5, 124.3, 122.8, 119.8, 117.1 (d, J_{C-F} = 21.8 Hz), 112.8 (d, J_{C-F} = 24.1 Hz), 52.1, 48.8, 44.5, 31.1; ^{19}F NMR (471 MHz, $CDCl_3$) δ -99.70; FT-IR (KBr) 2921, 1746, 1713, 1499, 1384, 1197, 755, 693 cm^{-1} ; HRMS (ESI) m/z $[M+H]^+$ calcd for $C_{35}H_{24}FN_4O_7$: 631.1624, found: 631.1607.

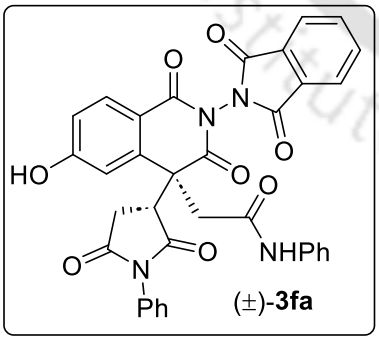

2-(4-(2,5-dioxo-1-phenylpyrrolidin-3-yl)-2-(1,3-dioxoisoindolin-2-yl)-6-hydroxy-1,3-dioxo-1,2,3,4-tetrahydroisoquinolin-4-yl)-N-phenylacetamide 3fa. Analytical TLC on silica gel, 1:1 ethyl acetate/hexane R_f = 0.40; colorless solid; mp 263-264 °C; yield 82% (103 mg); ^{1}H NMR (500 MHz, DMSO-d_6) δ 11.06 (S, 1H), 10.28 (s, 1H), 8.11-8.03 (m, 5H), 7.50 (t, *J* = 7.5 Hz, 2H), 7.45-7.41 (m, 3H), 7.24 (t, *J* = 8.0 Hz, 2H), 7.16 (d, *J* = 7.5 Hz, 2H), 7.01-6.99 (m, 2H), 6.96-6.95 (m, 1H), 4.21 (d, *J* =

17.0 Hz, 1H), 3.76 (dd, *J* = 9.5, 4.5 Hz, 1H), 3.73 (d, *J* = 17.0 Hz, 1H), 3.14 (dd, *J* = 18.5, 9.5 Hz, 1H), 2.62 (dd, *J* = 18.5, 4.0 Hz, 1H); $^{13}C\{^{1}H\}$ NMR (125 MHz, DMSO-d_6) δ 174.9, 173.7, 170.9, 166.9, 163.9, 163.8, 162.7, 160.0, 140.7, 138.5, 136.1, 135.9, 132.0, 131.8, 129.1, 128.9, 128.8, 128.7, 126.9, 124.4, 123.3, 118.9, 116.3, 116.2, 111.9, 51.2, 48.7, 43.6, 31.2; FT-IR (KBr) 2925, 1745, 1711, 1499, 1318, 1198, 757, 696 cm^{-1} ; HRMS (ESI) m/z $[M+H]^+$ calcd for $C_{35}H_{25}N_4O_8$: 629.1667, found: 629.1642.

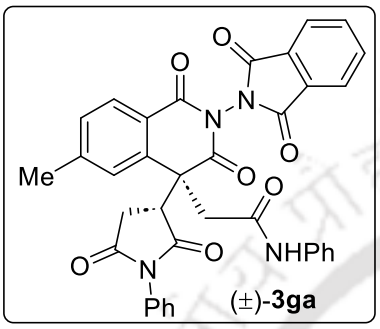

2-(4-(2,5-Dioxo-1-phenylpyrrolidin-3-yl)-2-(1,3-dioxoisoindolin-2-yl)-6-methyl-1,3-dioxo-1,2,3,4-tetrahydroisoquinolin-4-yl)-N-phenylacetamide 3ga. Analytical TLC on silica gel, 1:2 ethyl acetate/hexane R_f = 0.45; colorless solid; mp 236-237 °C; yield 81% (101 mg); ^{1}H NMR (500 MHz, $CDCl_3$) δ 8.25 (d, *J* = 8.0 Hz, 1H), 7.94-7.89 (m, 2H), 7.80-7.76 (m, 2H), 7.58 (s, 1H), 7.44 (t, *J* = 7.5 Hz, 2H), 7.40 (d, *J* = 7.5 Hz, 1H), 7.32-7.30 (m, 4H), 7.14 (t, *J* = 7.5 Hz, 2H), 7.06 (d, *J* = 7.5 Hz, 2H), 6.97 (t, *J* = 7.0 Hz, 1H), 4.27 (d, *J* = 17.0 Hz, 1H), 3.88 (d, *J* = 16.5 Hz, 1H), 3.72 (dd, *J* = 9.5, 5.5 Hz, 1H), 3.19 (dd, *J* = 19.0, 9.5 Hz, 1H), 2.76 (dd, *J* = 19.0, 5.0 Hz, 1H), 2.35 (s, 3H); $^{13}C\{^{1}H\}$ NMR (125 MHz, $CDCl_3$) δ 175.7, 173.4, 171.2, 166.4, 164.0, 163.0, 160.4, 146.6, 137.4, 137.1, 135.0, 134.8, 131.3, 130.9, 130.5, 130.3, 130.1, 129.3, 129.1, 128.9, 126.4, 125.6, 124.5, 124.3, 124.2, 123.6, 119.6, 52.1, 48.9, 44.4, 31.2, 22.2; FT-IR (KBr) 3357, 1746, 1712, 1543, 1443, 1318, 1244, 881, 755, 695 cm^{-1}; HRMS (ESI) m/z $[M+H]^+$ calcd for $C_{36}H_{27}N_4O_7$: 627.1874, found: 627.1858.

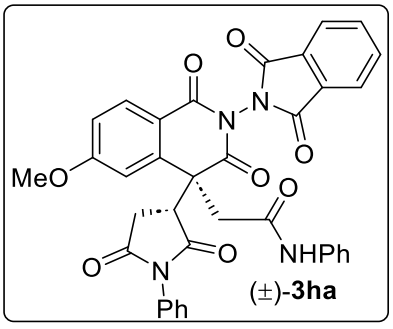

2-(4-(2,5-Dioxo-1-phenylpyrrolidin-3-yl)-2-(1,3-dioxoisoindolin-2-yl)-6-methoxy-1,3-dioxo-1,2,3,4-tetrahydroisoquinolin-4-yl)-N-phenylacetamide 3ha. Analytical TLC on silica gel, 1:1 ethyl acetate/hexane R_f = 0.55;

colorless solid; mp 210-211 °C; yield 84% (108 mg); ^{1}H NMR (500 MHz, $CDCl_3$) δ 8.32 (d, *J* = 9.0 Hz, 1H), 7.97-7.92 (m, 2H), 7.82-7.78 (m, 2H), 7.48 (s, 1H), 7.44 (t, *J* = 7.5 Hz, 2H), 7.39 (t, *J* = 7.0 Hz, 2H), 7.34 (d, *J* = 8.0 Hz, 2H), 7.18 (t, *J* = 8.0 Hz, 2H), 7.10 (d, *J* = 7.5 Hz, 2H), 7.02-6.98 (m, 2H), 4.28 (d, *J* = 16.5 Hz, 1H), 3.89 (d, *J* = 16.5 Hz, 1H), 3.75 (s, 3H), 3.71 (dd, *J* = 9.0, 5.0 Hz, 1H), 3.21 (dd, *J* = 19.0, 9.5 Hz, 1H), 2.78 (dd, *J* = 18.5, 4.5 Hz, 1H); ^{13}C{^{1}H} NMR (125 MHz, $CDCl_3$) δ 175.8, 173.4, 171.2, 166.3, 165.1, 164.1, 163.1, 159.9, 139.1, 137.4, 135.0, 134.8, 133.4, 131.4, 130.6, 130.2, 129.3, 129.1, 129.0, 126.6, 124.5, 124.4, 124.2, 119.7, 118.8, 114.1, 111.6, 55.8, 52.3, 48.9, 44.5, 31.2; FT-IR (KBr) 3355, 2930, 1746, 1711, 1603, 1499, 1317, 1025, 881, 756 cm^{-1}; HRMS (ESI) m/z $[M+H]^+$ calcd for $C_{36}H_{27}N_4O_8$: 643.1823, found: 643.1806.

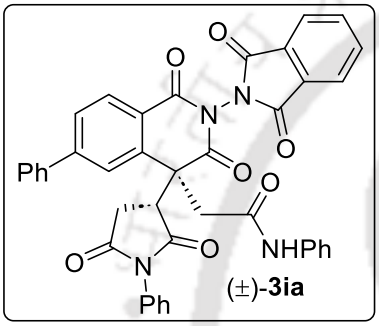

(±)-**3ia**

2-(4-(2,5-Dioxo-1-phenylpyrrolidin-3-yl)-2-(1,3-dioxoisoindolin-2-yl)-1,3-dioxo-6-phenyl-1,2,3,4-tetrahydroisoquinolin-4-yl)-N-phenylacetamide 3ia. Analytical TLC on silica gel, 1:2 ethyl acetate/hexane R_f = 0.45; colorless solid; mp 200-201 °C; yield 74% (102 mg); ^{1}H NMR (400 MHz, $CDCl_3$) δ 8.44 (d, *J* = 8.4 Hz, 1H), 7.94-7.91 (m, 2H), 7.80-7.75 (m, 4H), 7.58 (s, 1H), 7.46-7.44 (m, 2H), 7.39-7.36 (m, 3H), 7.29 (t, *J* = 8.0 Hz, 3H), 7.23 (t, *J* = 8.0 Hz, 2H), 7.14 (t, *J* = 7.2 Hz, 2H), 6.97 (t, *J* = 6.8 Hz, 1H), 6.89 (d, *J* = 7.2 Hz, 2H), 4.30 (d, *J* = 16.4 Hz, 1H), 3.94 (d, *J* = 16.8 Hz, 1H), 3.77 (dd, *J* = 8.4, 5.2 Hz, 1H), 3.25 (dd, *J* = 18.8, 9.2 Hz, 1H), 2.83 (dd, *J* = 19.2, 4.8 Hz, 1H); ^{13}C{^{1}H} NMR (125 MHz, $CDCl_3$) δ 175.9, 173.4, 171.1, 166.4, 164.0, 163.0, 160.3, 148.1, 138.6, 137.5, 137.3, 135.0, 134.8, 131.6, 131.2, 130.5, 130.2, 129.2, 129.1, 129.0, 128.9, 127.8, 127.5, 127.1, 126.6, 124.7, 124.5, 124.4, 124.2, 123.8, 119.8, 52.4, 49.0, 44.6, 31.3; FT-IR (KBr) 2918, 1744, 1712, 1606, 1318, 1193, 755, 696 cm^{-1}; HRMS (ESI) m/z $[M+H]^+$ calcd for $C_{41}H_{29}N_4O_7$: 689.2031, found: 689.2019.

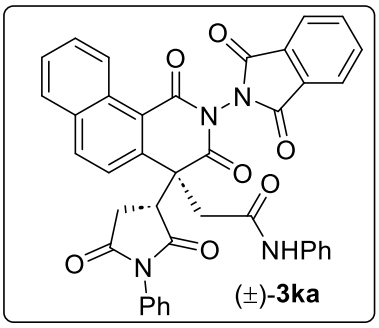

2-(4-(2,5-Dioxo-1-phenylpyrrolidin-3-yl)-2-(1,3-dioxoisoindolin-2-yl)-1,3-dioxo-1,2,3,4-tetrahydrobenzo[h]isoquinolin-4-yl)-N-phenylacetamide 3ka. Analytical TLC on silica gel, 1:2 ethyl acetate/hexane R_f = 0.40; colorless solid; mp 221-222 °C; yield 75% (99 mg); ^{1}H NMR (400 MHz, $CDCl_3$) δ 9.63 (d, *J* = 8.8 Hz, 1H), 8.11 (d, *J* = 8.8 Hz, 1H), 8.00-7.95 (m, 2H), 7.86-7.81 (m, 3H), 7.72 (t, *J* = 7.6 Hz, 1H), 7.64-7.59 (m, 2H), 7.46-7.37 (m, 4H), 7.30 (d, *J* = 7.6 Hz, 2H), 7.14 (t, *J* = 7.6 Hz, 2H), 7.08 (d, *J* = 7.2 Hz, 2H), 6.96 (t, *J* = 7.2 Hz, 1H), 4.46 (d, *J* = 16.4 Hz, 1H), 4.01 (d, *J* = 16.8 Hz, 1H), 3.80 (dd, *J* = 9.2, 6.0 Hz, 1H), 3.30 (dd, *J* = 18.8, 9.2 Hz, 1H), 2.83 (dd, *J* = 18.8, 5.6 Hz, 1H); ^{13}C{^{1}H} NMR (125 MHz, $CDCl_3$) δ 175.6, 173.2, 170.6, 166.2, 164.1, 163.2, 160.6, 139.2, 137.2, 136.9, 135.1, 134.9, 133.4, 132.1, 131.4, 130.6, 130.4, 130.2, 129.4, 129.1, 128.9, 128.7, 127.8, 127.3, 126.5, 124.6, 124.4, 124.3, 121.4, 120.9, 119.8, 52.7, 48.8, 44.3, 31.2; FT-IR (KBr) 3358, 2924, 1745, 1712, 1499, 1379, 1189, 754, 695 cm^{-1}; HRMS (ESI) m/z $[M+H]^+$ calcd for $C_{39}H_{27}N_4O_7$: 663.1874, found: 663.1857.

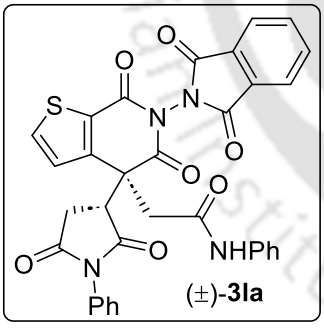

2-(4-(2,5-Dioxo-1-phenylpyrrolidin-3-yl)-6-(1,3-dioxoisoindolin-2-yl)-5,7-dioxo-4,5,6,7-tetrahydrothieno[2,3-c]pyridin-4-yl)-N-phenylacetamide 3la. Analytical TLC on silica gel, 1:2 ethyl acetate/hexane R_f = 0.42; colorless solid; mp 201-202 °C; yield 70% (87 mg); ^{1}H NMR (500 MHz, $CDCl_3$) δ 7.96-7.92 (m, 2H), 7.82-7.79 (m, 3H), 7.48-7.44 (m, 3H), 7.41 (t, *J* = 7.0 Hz, 1H), 7.36 (d, *J* = 8.0 Hz, 2H), 7.20 (t, *J* = 7.5 Hz, 2H), 7.12-7.10 (m, 3H), 7.02 (t, *J* = 7.0 Hz, 1H), 4.21 (d, *J* = 16.5 Hz, 1H), 3.75-3.72 (m, 2H), 3.21 (dd, *J* = 18.5, 9.0 Hz, 1H), 2.83 (dd, *J* = 18.5, 5.5 Hz, 1H); ^{13}C{^{1}H} NMR (125 MHz, $CDCl_3$) δ 175.5, 173.2, 171.5, 166.0, 164.0, 163.0, 155.9, 143.5, 137.3, 136.8, 135.1, 134.9, 131.3, 130.4, 130.1, 130.0, 129.4, 129.2, 129.0, 126.5, 125.5, 124.6, 124.5, 124.3, 119.8, 51.6, 48.2,

44.8, 31.2; FT-IR (KBr) 2925, 1744, 1712, 1599, 1501, 1386, 1321, 1189, 879 cm^{-1}; HRMS (ESI) m/z $[M+H]^+$ calcd for $C_{33}H_{23}N_4O_7S$: 619.1282, found: 619.1283.

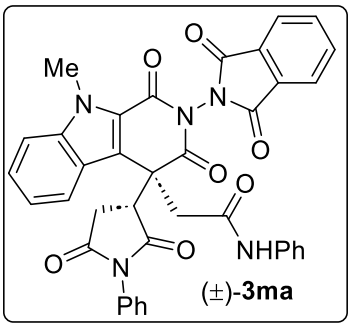

2-(4-(2,5-dioxo-1-phenylpyrrolidin-3-yl)-2-(1,3-dioxoisoindolin-2-yl)-9-methyl-1,3-dioxo-2,3,4,9-tetrahydro-1H-pyrido[3,4-b]indol-4-yl)-N-phenylacetamide 3ma. Analytical TLC on silica gel, 1:1 ethyl acetate/hexane R_f = 0.52; orange solid; mp 237-238 ºC; yield 66% (88 mg); 1.2:1 mixture of diastereomers; ^1H NMR (400 MHz, DMSO-d_6) δ 10.88 (s, 0.84H), 10.23 (s, 1H), 8.61 (d, J = 7.6 Hz, 0.86H), 8.13-8.10 (m, 2H), 8.07-8.04 (m, 1.87H), 8.00-7.96 (m, 3.0H), 7.93 (d, J = 8.4 Hz, 1H), 7.75 (d, J = 8.4 Hz, 1H), 7.54 (t, J = 7.2 Hz, 3H), 7.50-7.45 (m, 3.74H), 7.37-7.33 (m, 8H), 7.20-7.15 (m, 3H), 6.95 (t, J = 7.6 Hz, 2H), 6.83 (d, J = 7.6 Hz, 1H), 6.79-6.77 (m, 2H), 6.72-6.70 (m, 1.85H), 4.73 (d, J = 8.0 Hz, 0.85H), 4.54 (d, J = 17.2 Hz, 1H), 4.18 (dd, J = 8.0, 6.0 Hz, 1H), 4.13 (s, 3H), 3.88-3.75 (m, 3.56H), 3.64 (d, J = 5.6 Hz, 1H), 3.18 (s, 2.6H), 3.14-3.12 (m, 1H), 2.86 (dd, J = 17.6, 4.8 Hz, 1H); $^{13}C\{^1H\}$ NMR (125 MHz, $CDCl_3$) δ 175.7, 174.8, 174.4, 172.8, 172.3, 172.2, 167.4, 165.8, 165.7, 164.5, 163.3, 163.3, 156.2, 156.0, 146.6, 140.9, 138.9, 136.6, 136.4, 136.15, 136.14, 135.9, 132.7, 132.2, 131.1, 129.66, 129.61, 129.5, 129.3, 129.2, 129.1, 129.0, 128.99, 128.97, 128.4, 127.37, 127.32, 127.2, 126.7, 124.9, 124.5, 123.7, 123.5, 122.87, 122.86, 122.81, 122.4. 122.1, 121.7, 120.46, 120.40, 119.3, 118.3, 114.2, 112.3, 108.5, 75.8, 50.7, 48.6, 44.0, 43.0, 41.7, 32.2, 31.7, 29.6; FT-IR (KBr) 2924, 1745, 1712, 1497, 1386, 1189, 747, 696 cm^{-1}; HRMS (ESI) m/z $[M+H]^+$ calcd for $C_{38}H_{28}N_5O_7$: 666.1983, found: 666.1965.

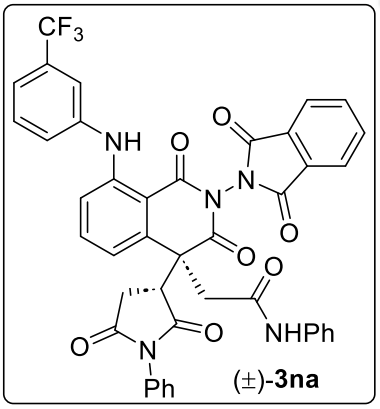

2-(4-(2,5-Dioxo-1-phenylpyrrolidin-3-yl)-2-(1,3-dioxoisoindolin-2-yl)-1,3-dioxo-8-((3-(trifluoromethyl)phenyl)amino)-1,2,3,4-

tetrahydroisoquinolin-4-yl)-N-phenylacetamide 3na. Analytical TLC on silica gel, 1:1 ethyl acetate/hexane R_f = 0.50; colorless solid; mp 227-228 °C; yield 74% (114 mg); ^{1}H NMR (400 MHz, $CDCl_3$) δ 10.33 (s, 1H), 7.98-7.92 (m, 2H), 7.81-7.79 (m, 2H), 7.62 (s, 1H), 7.50 (s, 1H), 7.47-7.37 (m, 7H), 7.35 (s, 1H), 7.30-7.29 (m, 1H,), 7.16 (t, *J* = 7.6 Hz, 2H), 7.10 (d, *J* = 8.0 Hz, 3H), 6.99 (t, *J* = 7.2 Hz, 1H), 6.79 (d, *J* = 7.6 Hz, 1H), 4.30 (d, *J* = 16.8 Hz, 1H), 3.91 (d, *J* = 16.8 Hz, 1H), 3.70 (dd, *J* = 9.2, 5.2 Hz, 1H), 3.29 (dd, *J* = 18.8, 9.2 Hz, 1H), 2.92 (dd, *J* = 19.2, 5.2 Hz, 1H); ^{13}C{^{1}H} NMR (125 MHz, $CDCl_3$) δ 175.6, 173.7, 170.8, 166.8, 164.1, 163.1, 163.0, 150.0, 139.8, 139.1, 137.5, 135.6, 135.1, 134.9, 132.2 (q, J_{C-F} = 32.3 Hz), 131.4, 130.4, 130.2, 130.0, 129.4, 129.1, 129.0, 127.5, 126.5, 124.9 (q, J_{C-F} = 270.8 Hz), 124.5, 124.3, 124.2, 121.8 (q, J_{C-F} = 3.6 Hz), 121.0 (q, J_{C-F} = 3.6 Hz), 119.7, 114.4, 113.8, 107.6, 52.2, 49.3, 44.8, 31.3; ^{19}F NMR (471 MHz, CDCl3) δ -62.74; FT-IR (KBr) 2921, 1746, 1715, 1456, 1377, 1331, 1175, 801, 696 cm^{-1}; HRMS (ESI) m/z $[M+H]^+$ calcd for $C_{42}H_{29}F_3N_5O_7$: 772.2014, found: 772.2003.

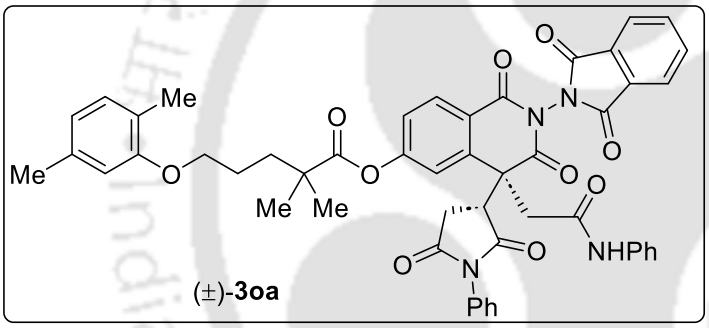

(±)-**3oa**

4-(2,5-Dioxo-1-phenylpyrrolidin-3-yl)-2-(1,3-dioxoisoindolin-2-yl)-1,3-dioxo-4-(2-oxo-2-(phenylamino)ethyl)-1,2,3,4-tetrahydroisoquinolin-6-yl 5-(2,5-dimethylphenoxy)-2,2-dimethylpentanoate 3oa. Analytical TLC on silica gel, 1:1 ethyl acetate/hexane R_f = 0.46; colorless solid; mp 301-302 °C; yield 63% (108 mg); ^{1}H NMR (500 MHz, DMSO-d_6) δ 10.22 (s, 1H), 8.27 (d, *J* = 8.5 Hz, 1H), 8.12-8.09 (m, 2H), 8.06-8.03 (m, 2H), 7.47-7.44 (m, 4H), 7.41-7.35 (m, 3H), 7.23 (t, *J* = 7.5 Hz, 2H), 7.19 (d, *J* = 7.5 Hz, 2H), 7.00 (t, *J* = 7.5 Hz, 1H), 6.92 (d, *J* = 7.5 Hz, 1H), 6.69 (s, 1H), 6.62 (d, *J* = 7.0 Hz, 1H), 4.15 (d, *J* = 17.5 Hz, 1H), 3.99-3.92 (m, 3H), 3.72 (d, *J* = 17.0 Hz, 1H), 3.14 (dd, *J* = 18.0, 9.5 Hz, 1H), 2.76 (dd, *J* = 18.0, 3.0 Hz, 1H), 2.23 (s, 3H), 2.01 (s, 3H), 1.84-1.81 (m, 2H), 1.75-1.72 (m, 2H), 1.31 (d, *J* = 4.5 Hz, 6H); ^{13}C{^{1}H} NMR (125 MHz, DMSO- d_6) δ 175.0, 174.6, 173.4, 170.2, 166.8, 163.6, 162.6, 159.9, 156.4, 156.0, 138.4, 136.1, 136.05, 136.01, 131.8, 130.9, 130.0, 129.0, 128.8, 128.8, 128.66, 128.60, 126.9, 124.5, 123.4, 122.8, 122.6, 122.4, 120.5, 119.1, 118.7, 112.0, 67.2, 50.8, 48.8, 43.9, 42.0, 36.2, 31.1, 24.58, 24.52, 21.0, 15.4; FT-IR (KBr) 2924, 1746, 1712, 1443, 1314, 1193, 1101, 755, 694 cm^{-1}; HRMS (ESI) m/z $[M+H]^+$ calcd for $C_{50}H_{45}N_4O_{10}$: 861.3130, found: 861.3117.

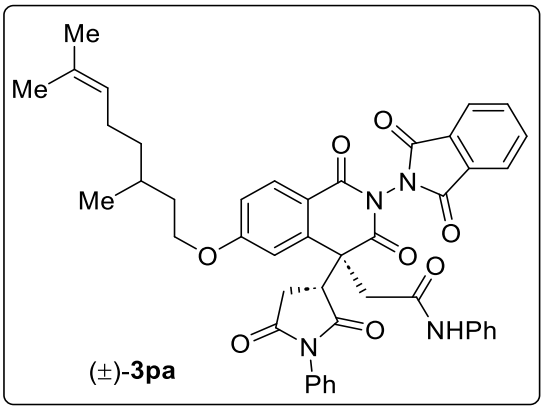

2-(6-((3,7-Dimethyloct-6-en-1-yl)oxy)-4-(2,5-dioxo-1-phenylpyrrolidin-3-yl)-2-(1,3-dioxoisoindolin-2-yl)-1,3-dioxo-1,2,3,4-tetrahydroisoquinolin-4-yl)-N-phenylacetamide 3pa. Analytical TLC on silica gel, 1:1 ethyl acetate/hexane R_f = 0.55; colorless solid; mp 235-236 ºC; yield 69% (106 mg); 3:1 mixture of diastereomer; ^{1}H NMR (600 MHz, DMSO-d_6) δ 10.19 (s, 1H), 10.08 (s, 0.27H), 8.16 (d, J = 8.4 Hz, 0.69H), 8.09-8.01 (m, 5H), 7.52-7.39 (m, 8H), 7.35-7.32 (m, 0.68H), 7.29-7.26 (m, 0.33H), 7.29-7.21 (m, 3H), 7.15-7.11 (m, 2.32H), 7.08 (s, 1H), 6.99 (t, J = 7.2 Hz, 1.32H), 5.08-5.05 (m, 1.33H), 4.33 (d, J = 17.4 Hz, 0.36H), 4.22 (d, J = 16.2 Hz, 1.68H), 4.13-4.08 (m, 1.33H), 4.03-3.99 (m, 1.33H), 3.87-3.83 (m, 1.32H), 3.71 (d, J = 16.8 Hz, 1H), 3.15 (dd, J = 18.6, 9.0 Hz, 1H), 2.78-2.69 (m, 1.39H), 1.98-1.92 (m, 3H), 1.80-1.72 (m, 2.32H), 1.62 (s, 4H), 1.57-1.54 (m, 4H), 1.38-1.29 (m, 1.69H), 1.23-1.13 (m, 2.33H), 1.00-0.95 (m, 1H), 0.93-0.86 (m, 3H); ^{13}C{^{1}H} NMR (125 MHz, DMSO-d_6) δ 174.9, 173.6, 170.6, 167.0, 164.0, 163.8, 162.7, 160.05, 160.00, 138.5, 136.1, 135.9, 131.7, 130.6, 130.5, 129.28, 129.22, 129.1, 128.9, 128.8, 128.6, 128.4, 126.8, 126.7, 124.5, 124.4, 123.3, 119.0, 118.9, 117.6, 116.7, 115.2, 114.7, 114.6, 111.73, 111.71, 111.66, 111.65, 66.8, 66.7, 52.5, 51.2, 48.8, 47.6, 43.7, 36.5, 36.4, 35.2, 31.2, 28.9, 28.8, 25.4, 24.9, 24.8, 19.2, 19.1, 17.5. FT-IR (KBr) 2924, 1749, 1712, 1603, 1499, 1316, 1196, 882, 755, 697 cm^{-1}; HRMS (ESI) m/z $[M+H]^+$ calcd for $C_{45}H_{43}N_4O_8$: 767.3075, found: 767.3039.

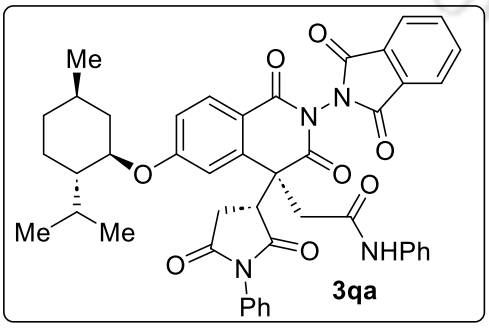

2-(4-(2,5-Dioxo-1-phenylpyrrolidin-3-yl)-2-(1,3-dioxoisoindolin-2-yl)-6-(((1R,2S,5R)-2-isopropyl-5-methylcyclohexyl)oxy)-1,3-dioxo-1,2,3,4-tetrahydroisoquinolin-4-yl)-N-phenylacetamide 3qa. Analytical TLC on silica gel,

1:1 ethyl acetate/hexane R_f = 0.52; colorless solid; mp 258-259 ºC; yield 75% (115 mg); ^{1}H NMR (500 MHz, DMSO-d_6) δ 10.27 (d, J = 10.0 Hz, 1H), 8.13-8.05 (m, 4H), 7.51-7.44 (m, 4H), 7.38-7.33 (m, 2H), 7.22-7.19 (m, 3H), 7.13-7.12 (m, 3H), 6.98 (t, J = 7.5 Hz, 1H), 4.84 (d, J = 30.5 Hz, 1H), 4.29 (d, J = 16.0 Hz, 1H), 3.87-3.84 (m, 1H), 3.70 (d, J = 16.5 Hz, 1H), 3.16 (dd, J = 18.0, 9.0 Hz, 1H), 2.75-2.69 (m, 1H), 1.84 (t, J = 15.0 Hz, 1H), 1.72-1.67 (m, 2H), 1.48-1.40 (m, 3H), 1.07-0.97 (m, 2H), 0.93-0.86 (m, 2H), 0.83-0.79 (m, 3H), 0.64 (d, J = 16.5 Hz, 1H), 0.57-0.52 (m, 4H); ^{13}C{^{1}H} NMR (125 MHz, DMSO-d_6) δ 174.7, 173.6, 170.5, 170.4, 167.0, 166.9, 163.8, 163.5, 163.5, 162.72, 162.71, 159.9, 159.8, 138.4, 138.3, 136.0, 135.9, 131.9, 131.8, 131.7, 129.1, 128.8, 128.78, 128.76, 128.6, 128.58, 128.52, 126.7, 126.6, 124.4, 123.35, 123.34, 119.1, 119.0, 117.2, 115.6, 112.5, 74.3, 74.0, 51.3, 48.7, 48.6, 46.58, 46.55, 43.4, 43.3, 36.9, 36.8, 34.1, 31.3, 28.7, 25.7, 25.6, 24.2, 21.8, 21.6, 20.7, 20.6, 20.3, 20.2; FT-IR (KBr) 2924, 1749, 1713, 1605, 1318, 1200, 754 cm^{-1}; HRMS (ESI) m/z [M+H]$^+$ calcd for $C_{45}H_{43}N_4O_8$: 767.3075, found: 767.3051.

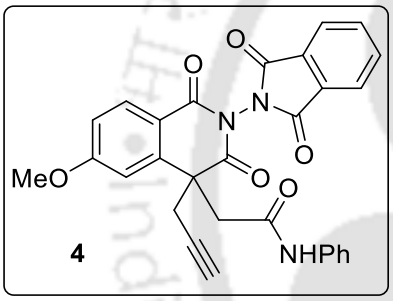

4

2-(2-(1,3-Dioxoisoindolin-2-yl)-6-methoxy-1,3-dioxo-4-(prop-2-yn-1-yl)-1,2,3,4-tetrahydroisoquinolin-4-yl)-N-phenylacetamide **4**. Analytical TLC on silica gel, 1:1 ethyl acetate/hexane R_f = 0.45; colorless solid; mp 273-274 ºC; yield 80% (41 mg); ^{1}H NMR (400 MHz, DMSO-d_6) δ 10.08 (s, 1H), 8.09-8.01 (m, 5H), 7.41 (d, J = 7.6 Hz, 2H), 7.30 (d, J = 2.0 Hz, 1H), 7.23 (t, J = 7.6 Hz, 2H), 7.14 (dd, J = 8.4, 2.0 Hz, 1H), 6.99 (t, J = 6.8 Hz, 1H), 3.90 (s, 3H), 3.61-3.49 (m, 2H), 3.06-3.02 (m, 1H), 2.94 (t, J = 2.4 Hz, 1H), 2.90-2.85 (m, 1H); ^{13}C{^{1}H} NMR (100 MHz, DMSO-d_6) δ 171.6, 167.0, 164.5, 163.2, 163.0, 160.4, 143.6, 138.6, 135.96, 135.90, 131.0, 129.1, 129.0, 128.7, 124.3, 124.2, 123.2, 118.9, 117.1, 113.8, 111.2, 77.6, 75.9, 55.9, 50.2, 44.5, 32.4; FT-IR (KBr) 3355, 2923, 2203, 1746, 1601, 1304, 1029, 712 cm^{-1}; HRMS (ESI) m/z [M+H]$^+$ calcd for $C_{29}H_{22}N_3O_6$: 508.1503, found: 508.1500.

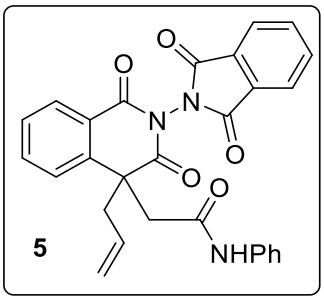

2-(4-Allyl-2-(1,3-dioxoisoindolin-2-yl)-1,3-dioxo-1,2,3,4-tetrahydroisoquinolin-4-yl)-N-phenylacetamide 5. Analytical TLC on silica gel, 1:2 ethyl acetate/hexane R_f = 0.52; colorless solid; mp 258-259 ºC; yield 72% (34 mg); ^{1}H NMR (400 MHz, DMSO-d_6) δ 10.08 (s, 1H), 8.12-8.02 (m, 5H), 7.83 (t, J = 7.6 Hz, 1H), 7.78 (d, J = 8.0 Hz, 1H), 7.54 (t, J = 7.6 Hz, 1H), 7.38 (d, J = 8.0 Hz, 2H), 7.21 (t, J = 7.6 Hz, 2H), 6.98 (t, J = 7.2 Hz, 1H), 5.72-5.62 (m, 1H), 4.99-4.96 (m, 1H), 4.87-4.82 (m, 1H), 3.61-3.51 (m, 2H), 2.79-2.70 (m, 2H); ^{13}C{^{1}H} NMR (100 MHz, DMSO-d_6) δ 172.1, 167.3, 163.7, 162.9, 161.0, 142.2, 138.5, 136.1, 135.9, 135.3, 130.5, 129.1, 128.9, 128.7, 128.5, 127.7, 125.6, 124.47, 124.44, 124.1, 123.2, 120.6, 118.9, 50.9, 47.3, 44.9; FT-IR (KBr) 2921, 1713, 1496, 1386, 1257, 1187, 694 cm^{-1}; HRMS (ESI) m/z [M+H]$^+$ calcd for $C_{28}H_{22}N_3O_5$: 480.1554, found: 480.1530.

Crystal Data and Structure Refinement for 3aa

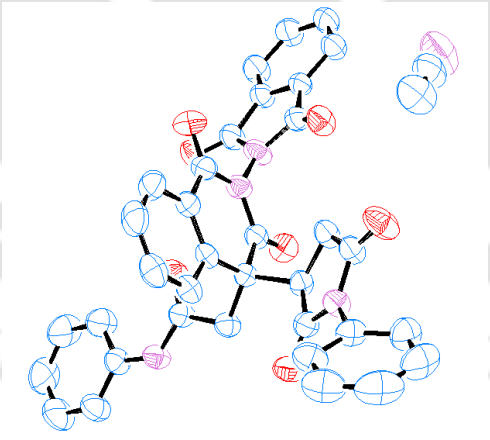

Figure 2. ORTEP diagram of 2-(4-(2,5-Dioxo-1-phenylpyrrolidin-3-yl)-2-(1,3-dioxoisoindolin-2-yl)-1,3-dioxo-1,2,3,4-tetrahydroisoquinolin-4-yl)-*N*-phenylacetamide **3aa** (CCDC 2421512) with 50% ellipsoid. H-omitted for clarity.

Identification code	**3aa**
Empirical formula	'C35 H24 N4 O7, C2 H3 N'
Formula weight	653.63
Crystal habit, colour	Block/Colourless

Temperature, *T*/K	293 K
Wavelength, *λ*/Å	0.71073
Crystal system	'orthorhombic'
Space group	'P n a 21'
Unit cell dimensions	a = 12.0923(14) Å b = 11.9690(14) Å c = 21.896(3) Å α = 90 β = 90 γ = 90
Volume, *V*/Å^3	3169.0(6)
Z	4
Calculated density, Mg·m^{-3}	1.370
Absorption coefficient, *μ*/mm^{-1}	0.097
F(000)	1360
θ range for data collection	2.39 to 25.04°
Limiting indices	-14 ≤ h ≤ 14, –14 ≤ k ≤ 14, –26 ≤ l ≤ 26
Reflection collected / unique	5580/4923
Refinement method	'SHELXL 2019/3 (Sheldrick, 2015)'
Data / restraints / parameters	5580/1/444
Goodness–of–fit on F^2	1.097
Final *R* indices [*I*>2sigma(*I*)]	R1 = 0.0348, wR2 = 0.0777
R indices (all data)	R1 = 0.0454, wR2 = 0.0892

Crystal Data and Structure Refinement for 3ma

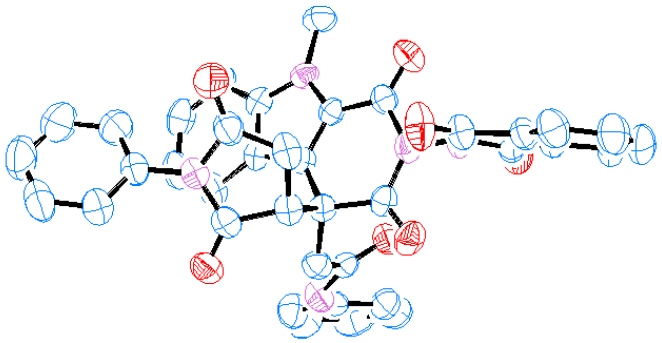

Figure 3. ORTEP diagram of 2-(4-(2,5-Dioxo-1-phenylpyrrolidin-3-yl)-2-(1,3-dioxoisoindolin-2-yl)-9-methyl-1,3-dioxo-2,3,4,9-tetrahydro-1H-pyrido[3,4-b]indol-4-yl)-N-phenylacetamide **3ma** (CCDC 2421514) with 50% ellipsoid. H-omitted for clarity.

Identification code	**3ma**
Empirical formula	2(C38 H27 N5 O7), 3[C2H6SO]
Formula weight	1565.67
Crystal habit, colour	Clear light orange
Temperature, *T*/K	295 K
Wavelength, λ/Å	0.71073
Crystal system	'triclinic'
Space group	'P -1'
Unit cell dimensions	a = 15.0035(15) Å b = 15.2445(15) Å c = 19.376(2) Å α = 79.425(3) β = 72.534(3) γ = 64.120(3)
Volume, *V*/Å^3	3796.3(7)
Z	2
Calculated density, Mg·m^{-3}	1.370
Absorption coefficient, μ/mm^{-1}	0.176
F(000)	1636
θ range for data collection	1.48 to 25.36°
Limiting indices	-18 ≤ h ≤ 18, –18 ≤ k ≤ 18, –23 ≤ l ≤ 23
Reflection collected / unique	13757/9344
Refinement method	'SHELXL 2018/3 (Sheldrick, 2015)'
Data / restraints / parameters	13757/865/911
Goodness–of–fit on F^2	1.060
Final *R* indices [*I*>2sigma(*I*)]	R1 = 0.0669, wR2 = 0.1412
R indices (all data)	R1 = 0.1003, wR2 = 0.1606

4.5 References

1. For reviews, see: (a) Colby, D. A.; Bergman, R. G.; Ellman, J. A. *Chem. Rev.* **2010**, *110*, 624. (b) Gensch, T.; Hopkinson, M. N.; Glorius, F.; Wencel-Delord, J. *Chem. Soc. Rev.* **2016**, *45*, 2900. (c) Lam, N. Y. S.; Wu, K.; Yu, J.-Q. *Angew. Chem. Int. Ed.* **2021**, *60*, 15767. (d) Zhao, B.; Prabagar, B.; Shi, Z. *Chem* **2021**, *7*, 2585. (e) Guillemard, L.; Kaplaneris, N.; Ackermann, L.; Johansson, M. J. *Nat. Rev. Chem.* **2021**, *5*, 522. (f) Docherty, J. H.; Lister, T. M.; Mcarthur, G.; Findlay, M. T.; Domingo-Legarda, P.; Kenyon, J.; Choudhary, S.; Larrosa, I. *Chem. Rev.* **2023**, *123*, 7692.
2. (a) Ackermann, L. *Acc. Chem. Res.* **2014**, *47*, 281. (b) Gulías, M.; Mascareñas, J. L. *Angew. Chem. Int. Ed.* **2016**, *55*, 11000. (c) Song, L.; Van der Eycken, E. V. *Chem. Eur. J.* **2021**, *27*, 121.
3. (a) Lu, Q.; Greßies, S.; Cembellín, S.; Klauck, F. J. R.; Daniliuc, C. G.; Glorius, F. *Angew. Chem. Int. Ed.* **2017**, *56*, 12778. (b) Park, H.; Yu, J.-Q. *J. Am. Chem. Soc.* **2020**, *142*, 16552. (c) Wu, Y.-J.; Chen, J.-H.; Teng, M.-Y.; Li, X.; Jiang, T.-Y.; Huang, F.-R.; Yao, Q.-J.; Shi, B.-F. *J. Am. Chem. Soc.* **2023**, *145*, 24499. (d) Yang, J.-M.; Lin, Y.-K.; Sheng, T.; Hu, L.; Cai, X.-P.; Yu, J.-Q. *Science* **2023**, *380*, 639. (e) Li, Y.; Xu, J.; Oliveira, J. C. A.; Scheremetjew, A.; Ackermann, L. *ACS Catal.* **2024**, *14*, 8160.
4. (a) Malamas, M. S.; Hohman, T. C.; Millen, J. *J. Med. Chem.* **1994**, *37*, 2043. (b) Hill, R. A.; Rudra, S.; Peng, B.; Roane, D. S.; Bounds, J. K.; Zhang, Y.; Adloo, A.; Lu, T. *Bioorg. Med. Chem*. **2003**, *11*, 2099. (c) Kang, B.-R.; Wang, J.; Li, H.; Li, Y.; Mei, Q.-B.; Zhang, S.-Q. *Med. Chem. Res.* **2014**, *23*, 1340. (d) Billamboz, M.; Bailly, F.; Lion, C.; Touati, N.; Vezin, H.; Calmels, C.; Andréola, M.-L.; Christ, F.; Debyser, Z.; Cotelle, P. *J. Med. Chem.* **2011**, *54*, 1812.
5. (a) Hasegawa, N.; Charra, V.; Inoue, S.; Fukumoto, Y.; Chatani, N. *J. Am. Chem. Soc.* **2011**, *133*, 8070. (b) Kong, W.; Casimiro, M.; Fuentes, N.; Merino, E.; Nevado, C. *Angew. Chem. Int. Ed.* **2013**, *52*, 13086. (c) Zhang, Z.; Jia, C.; Kong, X.; Hussain, M.; Liu, Z.; Liang, W.; Jiang, L.; Jiang, H.; Ma, J. *ACS Sustainable Chem. Eng.* **2020**, *8*, 16463. (d) Niu, Y. N.; Xia, X. F. Recent Developments in the Synthesis of the Isoquinoline-1,3(2H,4H)-Dione by Radical Cascade Reaction. *Org. Biomol. Chem*. **2022**, 20, 7861.
6. (a) Yu, D.; de Azambuja, F.; Glorius, F. *Angew. Chem. Int. Ed.* **2014**, *53*, 2754. (b) Hyster, T. K.; Dalton, D. M.; Rovis, T. *Chem. Sci.* **2015**, *6*, 254. (c) Lu, Y.; Wang, H.-W.; Spangler, J. E.; Chen, K.; Cui, P.-P.; Zhao, Y.; Sun, W.-Y.; Yu, J.-Q. *Chem. Sci.*

2015, *6*, 1923. (d) Su, B.; Wei, J.-B.; Wu, W.-L.; Shi, Z.-J. *ChemCatChem* **2015**, *7*, 2986. (e) Huang, H.; Nakanowatari, S.; Ackermann, L. *Org. Lett.* **2017**, *19*, 4620. (f) Xu, Y.; Lin, Y.; Homölle, S. L.; Oliveira, J. C. A.; Ackermann, L. *J. Am. Chem. Soc.* **2024**, *146*, 24105.

7. (a) Kumar, N. Y. P.; Rogge, T.; Yetra, S. R.; Bechtoldt, A.; Clot, E.; Ackermann, L. *Chem. Eur. J.* **2017**, *23*, 17449. (b) Manoharan, R.; Jeganmohan, M. *Asian J. Org. Chem.* **2019**, *8*, 1949. (c) Vivek Kumar, S.; Banerjee, S.; Punniyamurthy, T. *Org. Chem. Front.* **2020**, *7*, 1527. (d) Chowdhury, D.; Dana, S.; Maity, S.; Baidya, M. *Org. Lett.* **2020**, *22*, 6760.(e) Aslam, M.; Mohandoss, S.; Lee, Y. R. *Org. Lett.* **2021**, *23*, 6206. (f) Zhou, Q.; Li, B.; Zhang, X.; Fan, X. *Org. Biomol. Chem.* **2024**, *22*, 2324. (g) Aslam, M.; Akhtar, M. S.; Lim, H. N.; Seo, J. H.; Lee, Y. R. *Org. Biomol. Chem.* **2025**, *23*, 269.
8. (a) Muniraj, N.; Prabhu, K. R. *Org. Lett.* **2019**, *21*, 1068. (b) Zhao, H.; Wang, T.; Qing, Z.; Zhai, H. *Chem. Commun.* **2020**, *56*, 5524. (c) Liu, S.-L.; Ye, C.; Wang, X. *Org. Biomol. Chem.* **2022**, *20*, 4837.
9. Hyster, T. K.; Rovis, T. *J. Am. Chem. Soc.* **2010**, *132*, 10565.
10. Karthikeyan, J.; Haridharan, R.; Cheng, C.-H. *Angew. Chem. Int. Ed.* **2012**, *51*, 12343.
11. Shi, Z.; Grohmann, C.; Glorius, F. *Angew. Chem. Int. Ed.* **2013**, *52*, 5393.
12. Miura, W.; Hirano, K.; Miura, M. *Org. Lett*. **2015**, *17* , 4034.
13. He, Q.; Yamaguchi, T.; Chatani, N. *Org. Lett*. **2017**, *19*, 4544.
14. Mandal, S.; Barman, M.; Debnath, B.; Punniyamurthy, T. *Org. Lett*. **2024**, *26*, 7560.
15. Shibata, K.; Hasegawa, N.; Fukumoto, Y.; Chatani, N. *ChemCatChem* **2012**, *4*, 1733.
16. Shi, J.; Zhou, J.; Yan, Y.; Jia, J.; Liu, X.; Song, H.; Xu, H. E.; Yi, W. *Chem. Commun.* **2015**, *51*, 668.
17. Weinstein, A. B.; Ellman, J. A. *Org. Lett.* **2016**, *18*, 3294.
18. (a) Yang, W.; Dong, J.; Wang, J.; Xu, X. *Org. Lett.* **2017**, *19*, 616. (b) Zheng, G.; Duan, X.; Chen, L.; Sun, J.; Zhai, S.; Li, X.; Jing, J.; Li, X. *J. Org. Chem.* **2020**, *85*, 4543. (c) Guo, S.; Liu, Y.; Wang, Y.; Zhang, X.; Fan, X. *J. Org. Chem.* **2020**, *85*, 8910.
19. Han, X.; Zhu, X.; Zhu, S.; Wei, L.; Hong, Z.; Guo, L.; Chen, H.; Chi, B.; Liu, Y.; Feng, L.; Ren, Y.; Wan, J. *J. Chem. Inf. Model.* **2016**, *56*, 73.
20. Long, L.; Wang, W.; Zhu, Y.; Luo, W.; Zhang, Y.; Chen, J.; Wei, Y.; Chen, Z. *Org. Lett.* **2023**, *25*, 7775.
21. Zhang, R.-L.; Liu, B.; Qiu, K.-X.; Li, H.-T.; Zhang, H.-N.; Shen, B.-C.; Sun, Z.-W. *Org. Lett*. **2023**, *25*, 1711.

4.6 Selected NMR Spectra

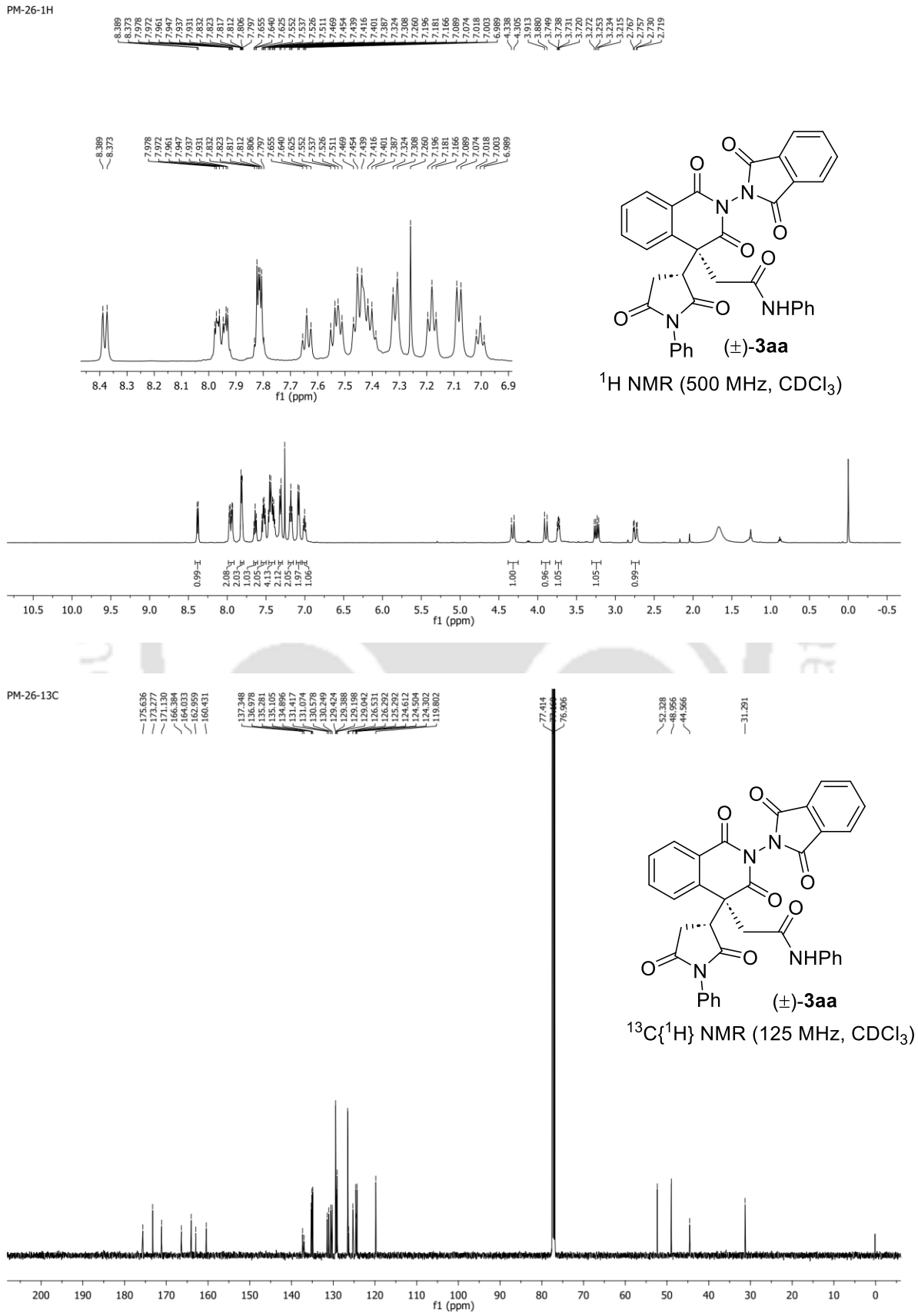

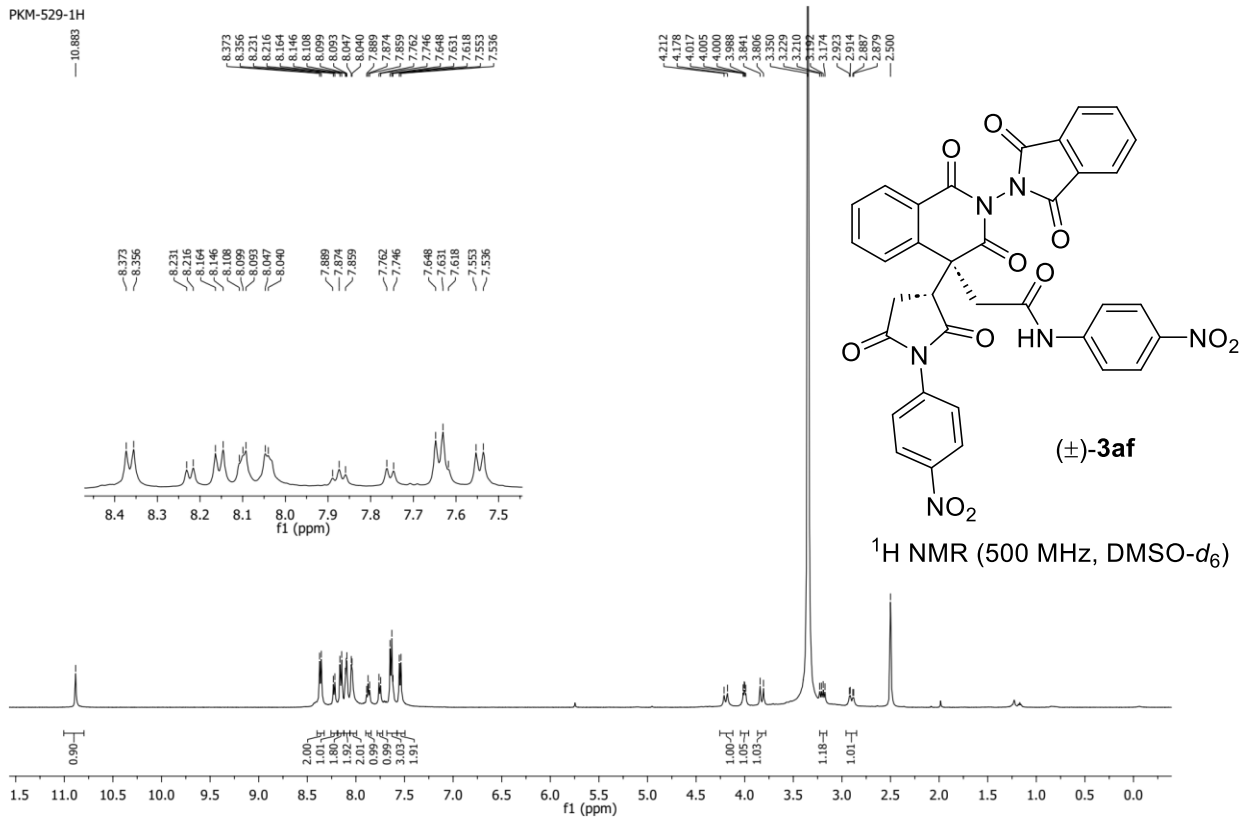

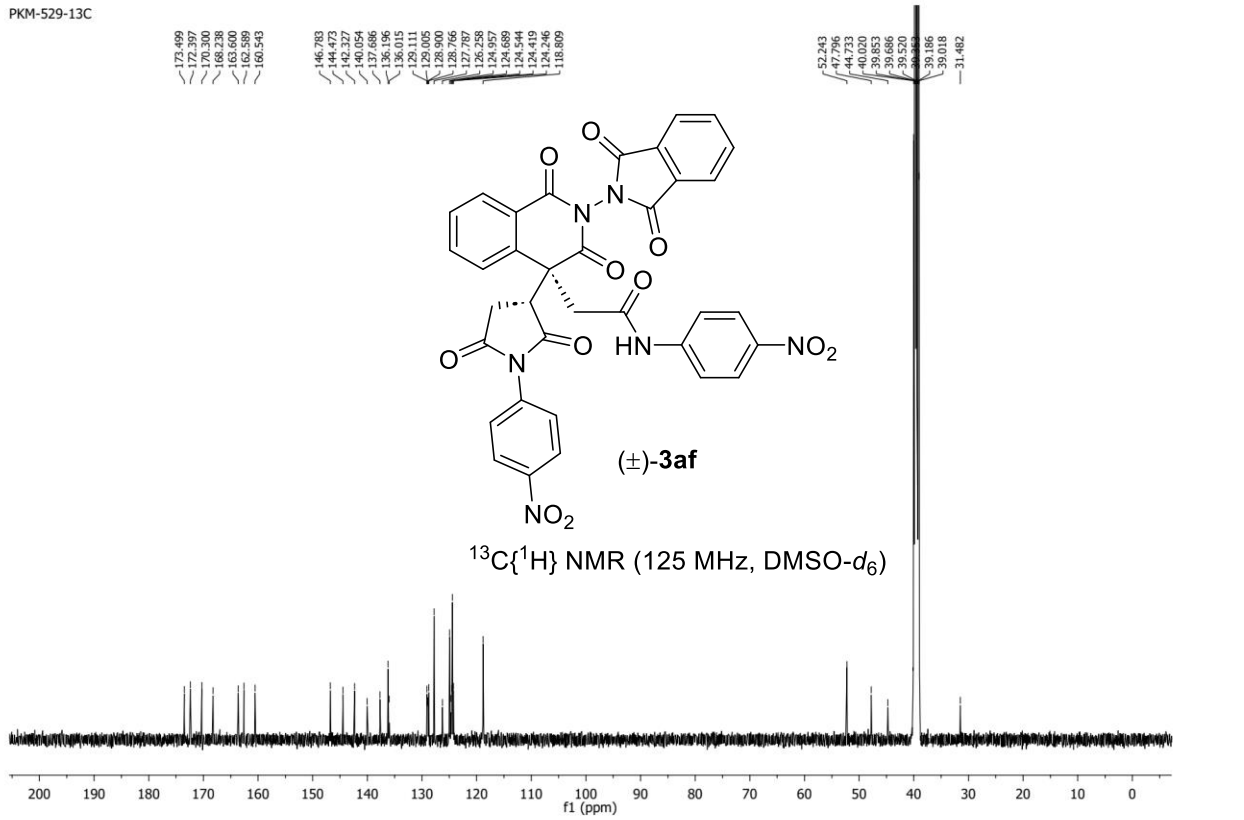

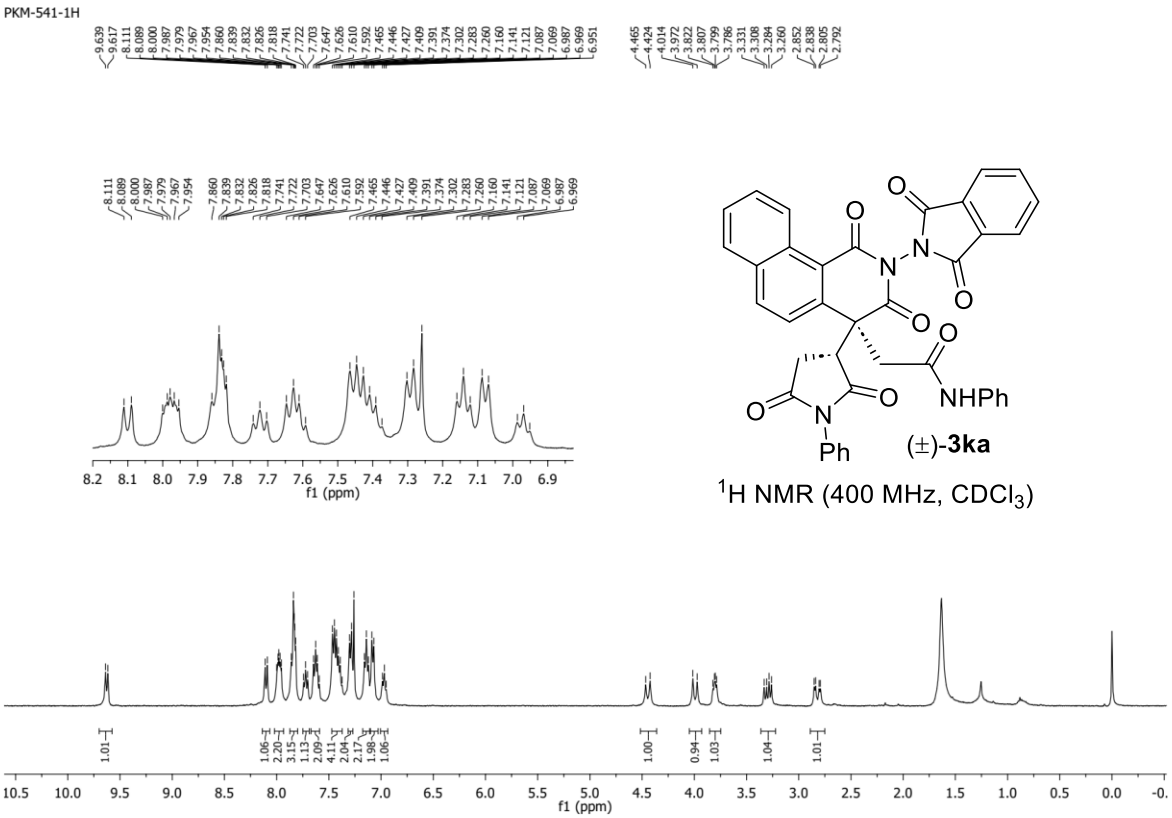

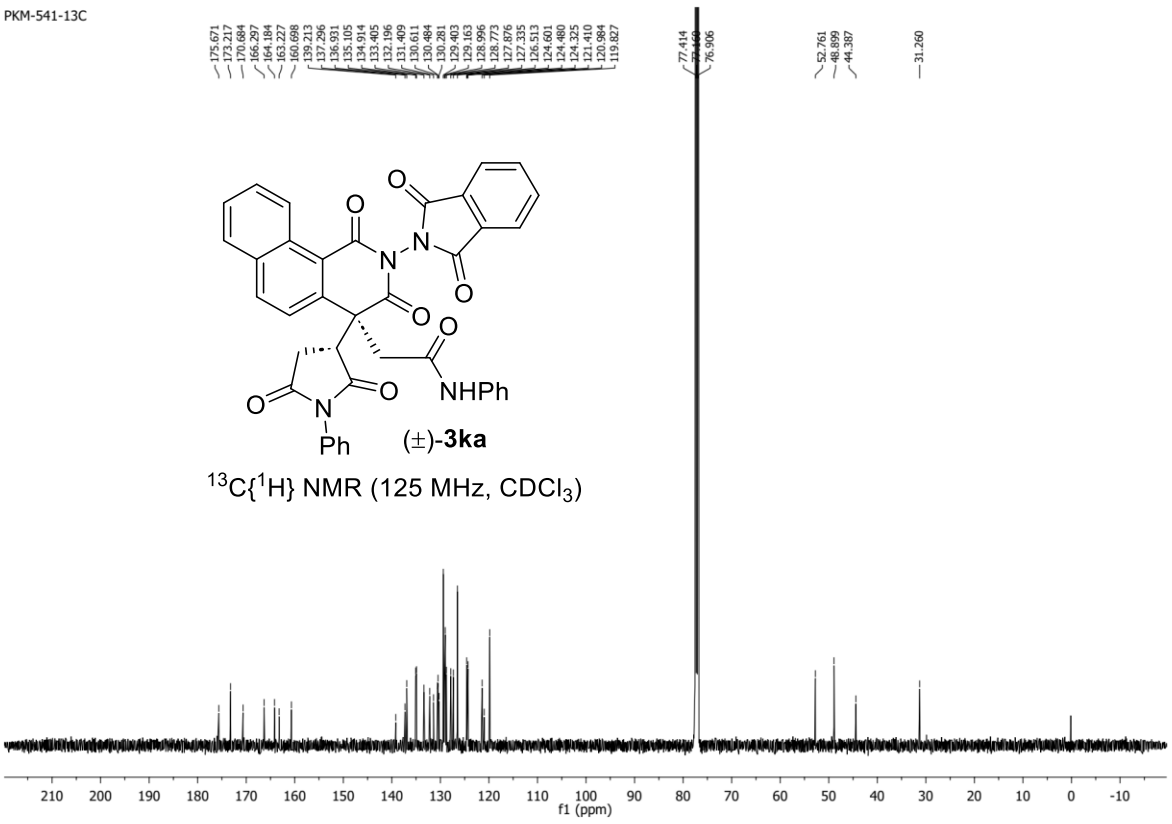

Thesis Overview

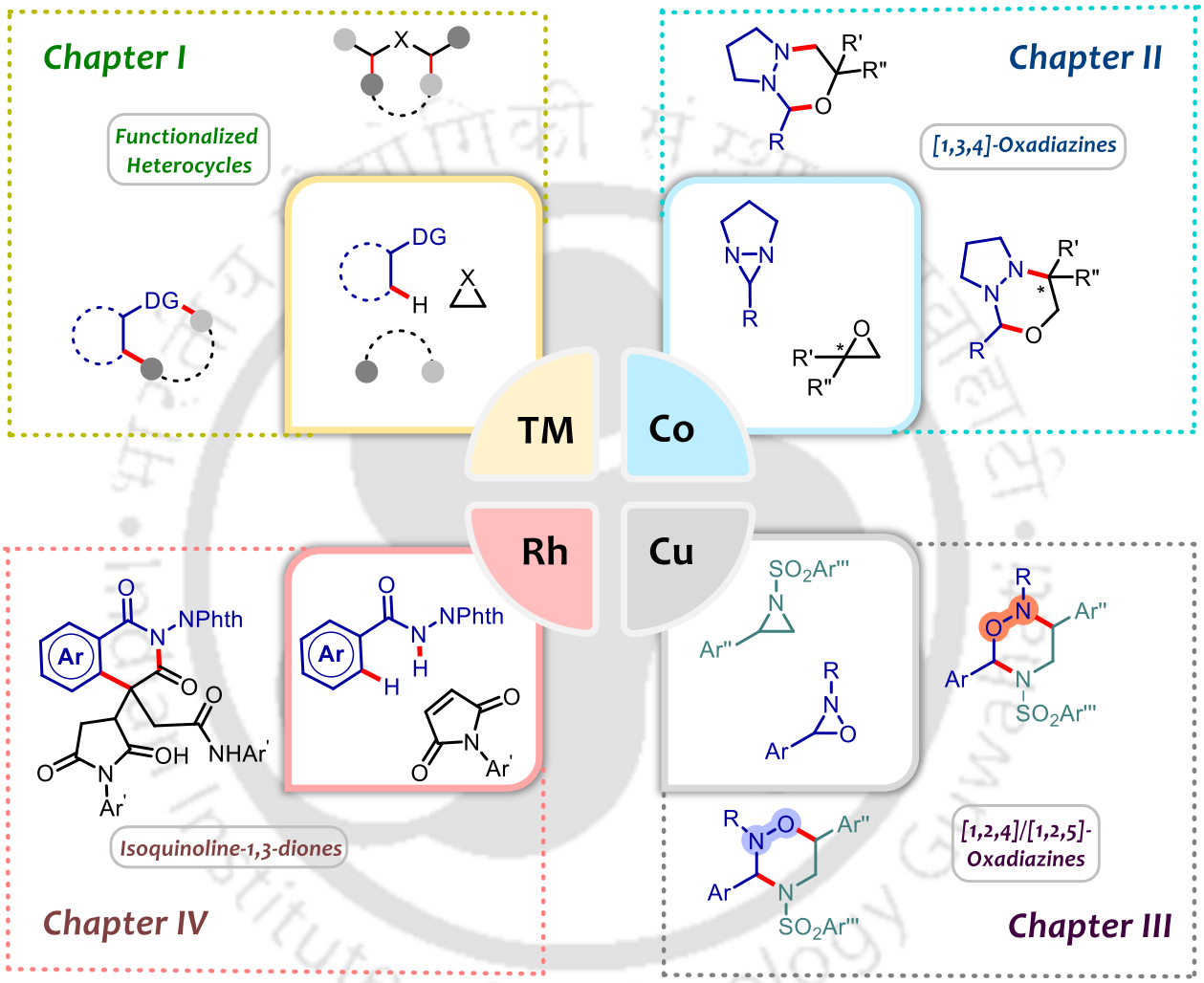

Summary

Functionalized heterocycles are the core structural components in numerous bioactive-natural products and hold paramount importance in modern drug discovery. Development of efficient synthetic strategies for synthesis of heterocycles has thus invited significant attention in recent times.

Chapter I covers a transition-metal-catalyzed strain driven ring expansion of three-membered rings to synthesize diverse heterocycles. The discussed methodologies showed good functional group tolerance in delivering functionalized heterocycles in stereo/regioselective manner. Additionally, cascade C−H functionalization/annulation strategy showcased potentiality in synthesizing fused heterocycles with improved site-selectivity.

Chapter II describes a C−N/C−O bonds formation of oxiranes with diaziridines under Co-catalysis to synthesize functionalized 1,3,4-oxadiazines. A broad range of diaziridines as well as oxiranes proved competent substrates in delivering the desired heterocycles. Gratifyingly, enantioenriched oxiranes were reacted in stereospecific manner to yield oxadiazines in optically pure form.

Chapter III focuses on a Cu-catalyzed cross-dimerization using oxaziridines and aziridines to access varied oxadiazines. This substituent dependent regio-divergent strategy allowed access to [1,2,4]/[1,2,5]-oxadiaiznes in good yields under mild conditions. Functional group tolerance, drug and natural product modification and synthetic transformations are the important practical features.

Chapter IV illustrates a Rh-catalyzed sequential C−H functionalization/annulation of benzamides with maleimides to access succinimide tethered isoquinoline-1,3-diones. This protocol was extended to heteroaryl as well as drug/natural product derived amides to furnish annulated products in good yield. The practical aspects of the methodology include the substrate scope, broad functional group tolerance and access to quaternary carbon center.

List of Publications

1. Sarkar, T.; Shah, T. A.; **Maharana, P. K.**; Talukdar, K.; Das, B. K.; Punniyamurthy, T. Transition-metal-catalyzed Directing Group Assisted (Hetero)Aryl C−H Functionalization: Construction of C−C/C−heteroatom Bonds. *Chem. Rec*. **2021**, *21*, 3758.

2. Talukdar, K.; Shah, T. A.; Sarkar, T.; Roy, S.; **Maharana, P. K.**; Punniyamurthy, T. Pd-Catalyzed Bidentate Auxiliary Assisted Remote C(sp^3)H Functionalization. *Chem. Commun*. **2021**, *57*, 13221.

3. Sarkar, T.; Kar, S.; **Maharana, P. K.**; Shah, T. A.; Punniyamurthy, T. Transition Metal-catalyzed C-H Functionalization of Benzofused Azoles with Two or More Heteroatoms. Transition-Metal-Catalyzed C−H Functionalization of Heterocycles. Wiley March 25, 2023, pp 319-356.

4. Sarkar, T.; **Maharana, P. K**.; Roy, S.; Punniyamurthy, T. Expedient Ni-Catalyzed C−H/C−H Cross-Dehydrogenative Coupling of Aryl Amides with Azoles. *Chem. Commun*. **2022**, *58*, 5980.

5. Mishra, M.; **Maharana, P. K**.; Karjee, P.; Punniyamurthy, T. Expedient Cobalt-Catalyzed Stereospecific Cascade C−N and C−O Bond Formation of Styrene Oxides with Hydrazones. *Chem. Commun*. **2022**, *58*, 7090.

6. Sarkar, T.; Shah, T. A.; **Maharana, P. K**.; Debnath, B.; Punniyamurthy, T. Dual Metallaphotoredox-catalyzed Directed C(sp^2)−H Functionalization: Access to C−C/C−heteroatom Bonds. *Eur. J. Org. Chem*. **2022**, *2022*, e202200541.

7. Kar, S.; Sarkar, T.; **Maharana, P. K**.; Guha, A. K.; Punniyamurthy, T. Bi-Catalyzed 1,2-Reactivity of Spirocyclopropyl Oxindoles with Dithianediol: Access to Spiroheterocycles. *Org. Lett*. **2022**, *24*, 4965.

8. Punniyamurthy, T.; Basak, S.; Paul, T.; **Maharana, P. K**.; Debnath, B. Transition-Metal-Catalyzed Directing-Group-Assisted C_4−H Carbon-Carbon Bond Formation of Indole. *Synlett* **2023**, *34*, 759.

9. Das, B.K.; Sarkar, T.; **Maharana, P.K**.; Kar, S.; Punniyamurthy, T. Cascade Zinc- and Silver Catalyzed Stereospecific C-O and C-N Bond Formations. *Eur. J. Org. Chem*. **2022**, *2022*, e202201237.

10. **Maharana, P. K**.; Sarkar, T.; Kar, S.; Purkayastha, S. K.; Guha, A. K.; Punniyamurthy, T. Cobalt-Catalyzed Stereospecific C−N/C−O Bond Formation of Oxiranes with Diaziridines. *J. Org. Chem*. **2023**, *88*, 9447.

11. Verma, K.; Mishra, M.; **Maharana, P. K**.; Bhattacharyya, H.; Saha, S.; Punniyamurthy, T. $Sc(OTf)_3$-Catalyzed Domino C−C/C−N Bond Formation of Aziridines with Quinones via Radical Pathway. *Org. Lett*. **2023**, *25*, 7933.

12. Shah, T. A.; Sarkar, T.; Kar, S.; **Maharana, P. K**.; Talukdar, K.; Punniyamurthy, T. Transition-metal-catalyzed Directed C−H Functionalization in/on Water. *Chem. Asian J*. **2024**, *19*, e202300815.

13. Kar, S.; **Maharana, P. K**.; Punniyamurthy, T.; Trivedi, V. Tandem (4 + 3)-Annulation of Aziridines: Stereoselective Access to Fused Azepinoindoles. *Org. Lett*. **2023**, *25*, 8850.

14. Samantaray, S.; **Maharana, P. K**.; Kar, S.; Saha, S.; Punniyamurthy, T. Redox-Neutral Zinc-Catalyzed Cascade [1,4]-H Shift/Annulation of Diaziridines with Donor-Acceptor Aziridines. *Chem. Commun*. **2024**, *60*, 3441.

15. Kar, S.; **Maharana, P. K**.; Maity, S.; Trivedi, V.; Punniyamurthy, T. Copper-Catalyzed (4+3)-Cycloaddition of 4-Indolylcarbinols with Aziridines: Stereoselective Synthesis of Azepinoindoles. *Chem. Commun*. **2024**, *60*, 12008.

16. **Maharana, P. K.;** Muthuraja, P.; Kar, S.; Veerappan, T.; Punniyamurthy, T. Cascade C-H Functionalization/Annulation of Arylamides: Access to Succinimide-Tethered Isoquinoline-1,3-Diones. *Chem. Commun*. 2025. https://doi.org/10.1039/D5CC02963E.

17. **Maharana, P. K**.; Kar, S.; Punniyamurthy, T. Copper Catalyzed Cross Dimerization of Oxaziridines with Aziridines: Diastereoselective Access to Oxadiazines. (*Manuscript under preparation*).

Conference Attended

Poster Presentation

1. **Prabhat Kumar Maharana ,** Tanumay Sarkar and Tharmalingam Punniyamurthy, "Cobalt-Catalyzed Stereospecific Synthesis of [1,3,4]-Oxadiazine form Diaziridines and Oxiranes" CRSI-NSC-28, IIT Guwahati, Guwahati, March 25-27th, 2022.

2. **Prabhat Kumar Maharana,** Tanumay Sarkar, Subhradeep Kar, Sidhartha Purkayastha, Ankur kanti Guha and Tharmalingam Punniyamurthy, "Cobalt-Catalyzed Stereospecific C−N/C−O Bond Formation of Oxiranes with Diaziridines" RIC-2023, IIT Guwahati, Guwahati, May 14-16th, 2023.

3. **Prabhat Kumar Maharana,** Tanumay Sarkar, Subhradeep Kar, Sidhartha Purkayastha, Ankur kanti Guha and Tharmalingam Punniyamurthy, "Cobalt-Catalyzed Stereospecific C−N/C−O Bond Formation of Oxiranes with Diaziridines" XVIII-JNOST-2023, IISER Pune, Pune, October 10-12th, 2023.

4. **Prabhat Kumar Maharana,** Tanumay Sarkar, Subhradeep Kar, Sidhartha Purkayastha, Ankur kanti Guha and Tharmalingam Punniyamurthy, "Cobalt-Catalyzed Stereospecific C−N/C−O Bond Formation of Oxiranes with Diaziridines" CRSI-NSC-32, BITS Pilani, Pilani, February 2-4th, 2024.

5. **Prabhat Kumar Maharana,** Tanumay Sarkar, Subhradeep Kar, Sidhartha Purkayastha, Ankur kanti Guha and Tharmalingam Punniyamurthy, "Cobalt-Catalyzed Stereospecific C−N/C−O Bond Formation of Oxiranes with Diaziridines" FICS-2024, IIT Guwahati, Guwahati, December 2-4th, 2024.